THE REFLECTION EFFECT

in

CLOSE BINARY SYSTEMS

ProQuest LLC.
789 East Eisenhower Parkway
P.O. Box 1346
Ann Arbor, MI 48106 – 1346

C O N T E N T S

INTRODUCTORY REMARKS: HISTORICAL PERSPECTIVE

1. According to KUIPER, about 70% of all stars in the solar neighbourhood belong to double or multiple systems: double stars are therefore one of the commoner phenomena in the Galaxy. And amongst these, close binary systems are frequently observed in the form of eclipsing or spectroscopic binaries. Light curves are available for about a quarter of the 4,000 or so eclipsing variables which have been discovered. A similar number of spectroscopic binaries are known, largely amongst the brighter stars, and for these stars velocity curves are available. The proportion of stars observed which turn out to be spectroscopic binaries is in the region of 20%, a figure which is doubled for stars of spectral type B.

Apart from their numerical importance, close binary systems are our only source of information about the masses of early-type stars and therefore of the upper part of the empirical mass-spectral type relationship; they provide a test of the theories

of the internal constitution of the stars through their apsidal motions and the ellipticities of their components; and they are of inherent interest in that they raise questions about their origin and evolution, and the nature of their mutual interactions. The importance of the systems is further enhanced by the recent discoveries that several novae and explosive variables consist of close pairs, often with orbital periods of only a few hours. Explosive variables tend to be intrinsically faint, so that although few are known, their space density may be high.

2. The periodicity of the light variations of Algol was first announced in 1782 by GOODRICKE, although, as is well known, the name suggests that Algol's variability was known to the Arabs long before. It was not until 1889, however, that the eclipsing nature of the star was finally established: VOGEL found Algol to be a spectroscopic binary whose conjunctions coincide with the minima of light. The first spectroscopic binary, namely the brighter component of Mizar in the Great Bear, had been discovered earlier that year by PICKERING.

Although at that time only a few stars were

known to be close binary systems, the number of discoveries increased rapidly in the closing decades of the nineteenth century and in the early part of the twentieth century; and methods were soon developed by means of which it is possible to extract the discoverable elements of a close binary from the light or velocity curves. In four papers published in 1912, RUSSELL and SHAPLEY divulged the first general method of discussing eclipsing variables. Basically they considered spherical stars with linear but otherwise arbitrary limb-darkening. In comparing their model with real stars, it is necessary to 'rectify' the observed light curve, that is, to remove the variations due to complications arising from the fact that close stars cannot be regarded simply as limb-darkened spheres. The authors derived approximate expressions for the bolometric effects of oblateness and reflection. In 1915, SHAPLEY published the elements of 90 eclipsing systems derived by the new method.

3. With the development of modern photoelectric photometry it has been found that RUSSELL's graphical method is not powerful enough to handle

light curves whose individual observations are measured to within a few thousandths of a magnitude. An analytical method was developed by KOPAL over the period 1941 - 50 which is applicable to binaries which do not depart greatly from the idealised model of a pair of spherical, arbitrarily limb-darkened stars unaffected by proximity effects.

However, most systems of this sort undergo mutual interactions. Two types of interaction manifest themselves in the light variations and spectra of close binaries, these being due to the tidal distortions and mutual heating of the stars, the latter being known as the reflection effect. KOPAL's method is not therefore applicable in general, as these effects are often large.

With the increasing availability of electronic computers, it appears that a third stage of development in the study of binary systems is arising. Papers have been published by TABACHNIK and SHULBERG† (1965), and KITAMURA* (1965), describing methods for the determination of the orbital elements of eclipsing binaries by means of computers. The method of KITAMURA is useful in

† Soviet Astronomy 9, no3, 467

* Advances in Astronomy and Astrop
Vol 3, p. 27. (Edit. by Z. Kopal)

the study of light curves with shallow minima: the ratio of the depths of the minima, used in earlier analyses, is often an uncertain quantity, whereas the ratio of the areas, used by KITAMURA, can be found more accurately.

The difficulty remains that the light variations of close binaries outside eclipse are not theoretically understood. A résumé of the investigations of these variations to date follows in the sections below:-

4. Photometric Effects of Distortion. The theory of the form of distorted bodies is largely classical and was developed in the nineteenth century by CLAIRAUT, LEGENDRE and LAPLACE. It was early recognised that the prolateness of the component stars is at least one cause of the light variability outside eclipse. As already stated, a preliminary attempt was made by RUSSELL and SHAPLEY to estimate the bolometric consequences of this, but as gravity-darkening had not then been discovered their result was not generally valid. The latter effect was discovered independently by MILNE† and VON ZEIPEL* in 1924, but it was not until 1934 that

† *M.N. 84, 665, 684 and 702.

the influence of this darkening on the photometry of close systems was investigated, by TAKEDA†, who adopted a Roche model: a restriction which was removed in 1941 by STERNE*. A further discussion on the photometric effects of ellipticity was given by RUSSELL in 1945‡. A more exact investigation of the mutual distortion of binary components has been published by KOPAL, but the investigations of 1941 and 1945 are adequate to deal with the most refined photometry.

5. The Bolometric Reflection Effect. The effect was discovered by DUGAN in 1908, in the Algol system. The first theoretical treatment is due to RUSSELL and SHAPLEY who assumed simply that the inner hemispheres of the components were uniformly brighter than the outer hemispheres. They found that the variation of brightness between eclipses could be represented by a $\cos\theta$ term (where θ is a phase angle), which is easily identified with the corresponding term arising from a Fourier expansion of the light variation outside eclipse. Thereafter the existence of a 'reflection' term was noted in many systems. It was not until 1926, however, that the first fully quantitative treatment was published, by EDDINGTON.

† Kyoto Mem. A 17, 197 * Proc. U.S. Nat. Acad. Sci., 27, 99 ‡ Ap. J. 102, 1.

The basis of EDDINGTON's† argument was that the rate of re-emission of 'reflected' energy equals the rate at which energy is incident on any area of the stellar surface. In 1926 also, the transfer equation for reflected radiation was approximately solved by MILNE.* A phase function for reflected light was derived by him, subject to a number of physical approximations. In particular, the incident radiation was taken to be parallel; and he did not discuss the change in quality of radiation which will in general take place, that is, a spectral re-distribution of the incident energy. However, MILNE confirmed the result that a $\cos\theta$ term is a sufficiently good representation of the bolometric effect of reflection.

SHU‡, twenty-two years later, generalised EDDINGTON's discussion to the extent of considering the illuminating star as a point source at a finite distance from the reflecting star. The restriction that the irradiating star be a point source was removed by KOPAL' in 1954: the finite size of the illuminating star manifests itself by virtue of a penumbral zone and secondary reflection. However, observations of eclipsing binaries, which have

† M.N. 86, 320, 1926. * M.N. 87, 43. ‡ Proc. U.S. Nat. Acad. Sci., 34, 311, 1948.
' M.N. 114, 101

accumulated rapidly since SEN's work, are not usually in good agreement with the theoretical expectations. For instance the phenomenon of 'negative reflection' is commonly observed, that is the coefficient of $\cos\Theta$ in the Fourier expansion has the wrong sign. It is argued later in the thesis that the treatment of the bolometric reflection effect to date has not been satisfactory, largely due to the slow convergence of various series which have been developed by these authors.

6. Photometric Reflection. The light changes due to reflection occurring in a discrete range of wavelength have usually been discussed in the literature in terms of a 'luminous efficiency factor', whose value is calculated on the assumption that each part of the reflecting atmosphere radiates like a black body. SOBIESKI† (1965) has solved the transfer equation for grey and non-grey atmospheres on the assumption that the irradiating flux is a parallel beam. His results apply to Algol-type systems and disagree with the observations of several such systems.

† Ap. J. Supp. No 109, 12, 263.
ibid. 109, 12, 276.

7. The determination of the elements of a close system from the velocity curves is a relatively elementary matter. The geometrical centre of the stellar disc is taken to coincide with the projected centre of gravity of each star, an assumption which was examined by KOPAL in 1943, who found it to be justified. He also concluded that departures due to reflection would be small.

8. The Spectroscopic Reflection Effect. In his 1926 paper, EDDINGTON pointed out that reflection must have an effect on the velocity curves of spectroscopic binaries. This effect has been comparatively neglected. KOPAL's investigation of 1943 involved the adoption of a point source of illumination at a finite distance from the primary reflecting star.

The spectroscopic reflection effect has been noted in only a few close binaries. One of these is 60 Cygni which was discussed by OVENDEN† in 1954. This author came to the conclusion that the spectroscopic reflection effect had a considerable influence on the estimated masses of the stars,

† M.N. 114, 569.

factors of 2 and 3 being involved, in contradiction to the theoretical view that only a small influence on the velocity curves was to be expected. OVENDEN's paper inspired a further treatment of the effect by BATTEN†, published in 1957. BATTEN made use of KOPAL's 1954 bolometric theory. His conclusion was that only rarely, in the case of some very close pairs, would the effect reach the importance indicated for 60 Cygni.

In 1963, OVENDEN* published a further paper on the spectroscopic reflection effect in which he revealed a conceptual fallacy inherent in all previous treatments of the effect. The paper also included observations of the spectroscopic binary 57 Cygni, which indicated that in this system also the effect is larger by a least an order of magnitude than previous theories would indicate.

In view of the aforementioned fallacy, and of the observations of 57 Cygni, it is clear that the spectroscopic reflection effect also requires to be completely re-discussed.

9. The present thesis arises from an attempt to provide a theoretical interpretation of the observations of 57 Cygni in terms of the spectroscopic reflection effect.

† M.N. 117, 521 * M.N. 126, 77.

In Chapter I the 1963 paper of M.W.OVENDEN is summarised. A first attempt is made to interpret the observations, and two difficulties are met with. Neither difficulty can be resolved in terms of the simple model of the stars adopted.

Chapter II consists of a discussion of these difficulties.

In Chapter III I attempt to find a completely general solution to the problem of constructing a model of 57 Cygni from the observations. In the event only broad constraints can be placed on the temperature distributions over the inner hemispheres. But it is possible to show that the axes of rotation of the stars and their axis of revolution are all parallel in space, with an uncertainty of only a few degrees. Evidence of surface circulatory currents is found; these currents are probably a secondary consequence of the reflection effect.

The first three chapters almost fulfill the initial purpose of the research. However, in the course of studying KOPAL's 1954 bolometric theory of the reflection effect (as a prelude to BATTEN's 1957 spectroscopic theory) a number of algebraic errors became apparent. It was therefore decided to

pursue this point.

The first part of Chapter IV consists of a discussion of KOPAL's theory. In the event the algebraic errors do not affect the final result. The second part is a critique of some concepts and assumptions underlying the theory. These are found to be dubious and I conclude that KOPAL's theory is inapplicable to systems whose radii are comparable with the distance apart of their closest points.

In Chapter V the bolometric reflection effect is treated from a different point of view. The problem is regarded formally as that of solving a partial differential equation, the transfer equation, subject to appropriate boundary conditions. The brightness distribution over the reflecting star turns out to differ significantly from that derived from KOPAL's theory.

Acknowledgements. I am grateful to Professor P.A. Sweet for a number of discussions on some mathematical points, particularly relating to the integral equation formulation of Chapter III and some integrals occurring in Chapter IV. I am particularly indebted to my supervisor, Dr. M.W.Ovenden,

who suggested the problem, and with whom I have and many invaluable discussions on all aspects of the reflection effect.

The investigation was pursued at Glasgow University, and was supported by a grant from the Science Research Council.

William McD. Napier

P A R T I

Spectroscopic Reflection Effect

Chapter I. PRELIMINARY ANALYSIS

As the starting-point of this research is the paper by M.W. OVENDEN (1963) I shall begin by summarising its contents.

1. The author points out that in eclipsing system 60 Cygni which he had studied some years ago (1954)†, for which photometric and spectroscopic observations were available, the effect of reflection on the determination of the stellar masses was considerable. He states that "The relative brightness of the secondary was essentially equal to the amount of reflected light (calculated from Eddington's formula), and the assumption that the secondary spectrum was a result of reflection, the spectrum coming from a 'hotspot' close to the primary star, served to reconcile the deduced masses with the general mass-spectral type relationship, and the observed mass-ratio with the observed ellipticity of the component stars. The corrected masses, on this hypothesis, were approximately 3 and 2 times the uncorrected masses, for the primary and secondary

† M.N. 114, 569.

components respectively."

This result was contrary to what would be expected from the early theoretical investigations of Z. KOPAL et al., which implied that the mass-distortion due to the spectroscopic reflection effect should be small. However, the earlier work involved some approximations. In the light of this paradox, A.H.BATTEN(1957)† further pursued the analytical problem. As the bolometric theory of KOPAL*(1954) was by now available, and as this was considered to supersede the previous work, BATTEN was able to calculate a mass-distortion which was more accurate (in the context of the theoretical ideas used) than before. The procedure was to calculate the 'distortion' velocity due to reflection by means of the formula

$$\rho = \frac{\iint_{\Sigma} V I \, d\sigma}{\iint_{\Sigma} I \, d\sigma} \qquad (1)$$

where the domain of integration Σ is the projected area of the visible disc of the reflecting star, σ is an element of area, V the radial velocity, and I the brightness at any point of the disc. I is

† M.N. 117, 521 * M.N. 114, 101.

obtained from KOPAL's formula. BATTEN found that the mass-distortion would only rarely, in the case of some very close pairs, be as large as was indicated for 60 Cygni.

However, it was noted by OVENDEN that a conceptual fallacy exists in the treatment of the spectroscopic reflection effect by BATTEN as well as by the earlier workers in the field. To illustrate this, consider a spectral line which is so temperature-sensitive that it can appear only at the hottest point of the surface of the reflecting star, that is, at the sub-primary point. Then when the system is in the nodes such a line is shifted from the undisplaced position by the maximum possible amount, although the φ evaluated by (1) might be small. The use of the bolometric radiation I as the weight factor is thus seen to be irrelevant to the problem.

The illustration quoted above indicates that the size of the reflection effect should depend on the physical behaviour of the spectrum line considered, and OVENDEN decided to investigate empirically whether in a close binary system, this was so.

2. The star chosen from a short-list of twenty was

57 Cygni (HD 199081), apparent magnitude 4.7, period $2^{d}.954822$, with a spectral type given as B3 in the Henry Draper catalogue and B5V in the MKK catalogue. Most of the observational results were obtained from a series of plates taken in 1938 by J.A.PEARCE† with the 73-inch Victoria telescope.

The author (i.e., M.W. Ovenden) supposed that at any point on the reflecting star there would be an effective spectral type depending on the position of the point; the closer a small area of atmosphere to the sub-stellar point, the hotter the area would be and therefore the earlier its effective spectral type. In that case the size of the reflection term for a given spectral line will depend on the temperature at which the given line reaches its maximum strength, in the sense that the greater T_{max}, the larger the reflection term. T_{max} is the temperature at which an absorption line reaches maximum strength on the main sequence. Table I lists the lines used by OVENDEN, the spectral type at which each line reaches its maximum equivalent width, and the range of spectral type to half the maximum equivalent width, this data being taken from various authors.

† Pub. Amer. Ast. Soc. 9, 268, 1939.

TABLE I

Ion	Adopted wavelength	Spectral type for max e.w.	Spectral range to ½ max. e.w.
Hγ	4340.466		
Hδ	4101.738	Later than A0	
Hε	3970.075		
CaII	3968.465	Later than A0	B7-
	3933.664		
SiII	4130.876	Later than A0	B6-
	4128.051		
SiIII	4574.777		
	4567.872	B1	O 9.5-B3
	4552.654		
SiIV	4116.103	B0	O 8.5-B1.5
	4088.862		
NII	3994.996	B 1.5	B 1-B 2.5
NIII	4103.394	O 9	O 7.5-B 0
	4097.330		
CII	4267.160	B3	B 0-B 7
OII	4416.975		
	4414.904		
	4349.428		
	4319.635		
	4317.144	B 1	O 9-B 2.5
	4119.221		
	4075.868		
	4072.162		
	4069.794		
MgII	4481.228	Later than A0	B6-
HeI(^{1}D)	4387.928		
	4143.759	B 2	B 0-B 4
	4009.270		
HeI(^{3}D)	4471.477	B 3	O 9-B 7.5
	4026.189		
HeI	4437.549		
HeI	4120.812	?	?
HeI	3964.727		

TABLE 2

Elements from the least-squares solutions of the velocity-difference observations.

Ion	γ	K_A	e_A	ω_A	B_A
			0.126 ± 0.020	$113^\circ \pm 10^\circ$	0.193 ± 0.026
MgII	+0.0±3.5	244.6±5.2	139	121 14	215 032
CaII	+6.5 4.2	218.4 6.4	027	121 14	215 032
SiII	+3.1 4.3	205.0 6.7	029	110 14	189 039
CII	+0.9 3.6	222.1 5.1	023	89 13	132 036
HeI(^{3}D)	+4.0 3.5	232.6 5.3	022	113 9	195 025
HeI(^{1}D)	+2.6 2.9	214.7 4.3	019	116 10	202 026
MII	+6.6 4.1	187.6 6.2	030	107 19	175 051
OII	+5.5 4.2	205.1 6.2	029	102 12	168 032
SiIII	+6.8 5.7	252.1 8.9	031	101 18	164 050
SiIV	+1.0 3.9	183.1 6.1	029	111 14	186 037
NIII	+4.1 3.7	160.2 5.6	033	108 19	185 052
Hδ	+0.9 3.4	230.7 4.9	021	106 12	175 033
Hϵ	+5.1 3.8	213.6 5.9	025	123 14	224 038
Hθ	-5.6 3.5	188.8 7.0	030	141 10	267 028
HeI(4437)	+5.2 4.1	218.8 5.8	026	98 19	160 052
HeI(4120)	+0.5 3.6	221.0 5.8	024	115 8	198 020
HeI(3964)	+0.4 4.0	176.9 6.5	032	137 13	259 035

TABLE 3

Ion	Star	γ (km/sec)	K (km/sec)	e	ω	B	$a \sin i$ $\times 10^6$ km	$m \sin^3 i$ $\odot$
Mg II	1	-15.5±2.9	113.6±4.2	0.094±0.036	133°±22°	0.245[P]±0.061	4.44	2.27
	2	-15.4 2.6	131.3 4.0	164 028	284 10	172 028	5.08	1.96
Ca II	1	-9.3 3.6	99.4 5.4	163 050	106 19	178 051	3.85	1.44
	2	-11.6 4.7	112.5 7.4	158 058	342 22	318 060	4.36	1.27
Si II	1	-10.2 3.2	91.6 4.7	063 049	*	*	3.59	1.35
	2	-14.5 2.6	112.2 3.9	158 032	293 12	191 034	4.35	1.10
C II	1	-16.9 2.7	106.7 3.9	068 036	131 31	247 056	4.18	1.66
	2	-18.1 2.9	115.5 4.1	135 035	256 15	098 041	4.49	1.53
He I(^{3}D)	1	- 9.4 3.0	108.7 4.5	124 039	117 19	210 051	4.09	1.55
	2	-13.5 2.0	123.7 3.0	158 023	292 9	191 023	4.40	1.45
He I(^{1}D)	1	-12.8 2.8	104.9 4.1	104 038	107 21	183 058	4.24	1.92
	2	- 9.8 2.2	112.6 3.3	166 027	297 10	195 026	4.80	1.69
N II	1	- 7.3 4.3	9214 6.9	162 067	137 24	265 064	3.58	0.98
	2	-16.3 3.7	96.0 5.6	131 055	238 25	357 067	3.74	0.94
O II	1	- 6.2 3.1	95.9 4.5	116 046	89 24	141 064	3.74	1.30
	2	-12.7 2.6	108.8 3.8	177 034	291 11	158 030	4.20	1.15
Si III	1	- 6.3 5.2	126.3 7.5	007 062	*	*	4.96	2.43
	2	-13.5 4.0	131.0 6.6	265 041	298 10	194 026	4.96	2.35
Si IV	1	-10.9 3.1	91.3 4.9	115 050	148 25	299 067	3.56	0.88
	2	-10.5 2.9	91.8 4.5	197 042	279 14	146 038	3.53	0.87
N III	1	- 6.7 3.0	76.3 4.3	065 055	113 51	202 141	2.99	0.69
	2	-11.1 3.7	88.2 5.4	175 057	280 21	161 056	3.41	0.60
H γ	1	-17.9 3.0	110.1 4.4	138 039	104 17	178 045	4.28	1.89
	2	-18.6 2.5	121.2 3.6	072 029	281 24	158 066	4.75	1.72
H δ	1	-12.1 3.4	102.5 4.9	089 047	112 31	206 085	4.01	1.49
	2	-16.5 3.1	111.4 4.7	108 039	305 21	217 058	4.35	1.37
H ϵ	1	- 1.0 4.8	89.8 8.8	203 061	97 24	165 063	3.45	1.17
	2	+ 0.9 4.7	107.4 8.7	179 063	335 19	298 052	4.15	0.98
He I(4437)	1	-12.1 4.1	108.5 6.1	129 052	128 25	253 068	4.22	1.58
	2	-17.2 3.4	112.2 4.9	110 044	235 22	262 062	4.38	1.53
He I(4120)	1	- 6.8 3.0	100.3 4.5	161 042	109 16	181 042	3.93	1.65
	2	- 7.7 2.8	119.5 4.4	204 033	298 10	206 026	4.59	1.38
He I(3964)	1	- 8.6 3.5	85.7 5.3	058 058	179 55	389 153	3.36	0.90
	2	- 9.8 4.1	95.7 7.2	218 062	314 17	239 044	3.67	0.80
Pearce	1	-19.1 0.5	114.6 0.95	140 006	102 3	173 ...	4.46	2.08

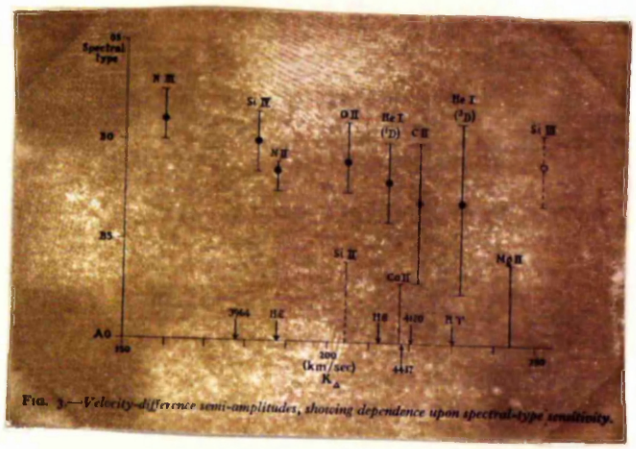

FIG. 3.—*Velocity-difference semi-amplitudes, showing dependence upon spectral-type sensitivity.*

Figure 1

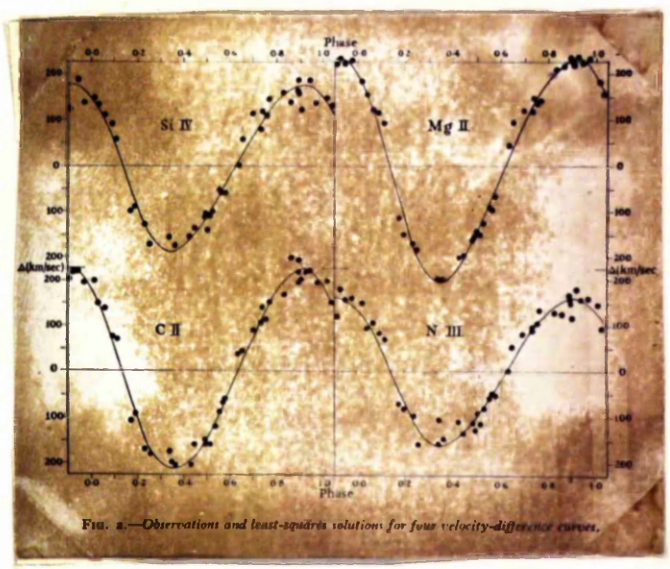

FIG. 2.—*Observations and least-squares solutions for four velocity-difference curves.*

Figure 2

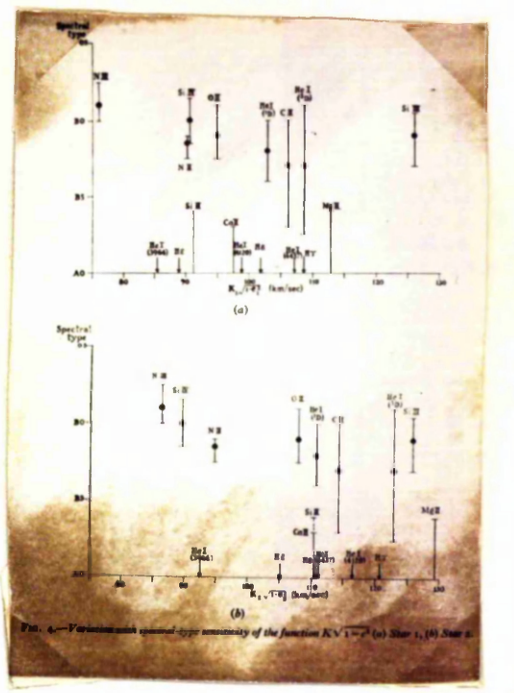

(a)

(b)

Figure 3

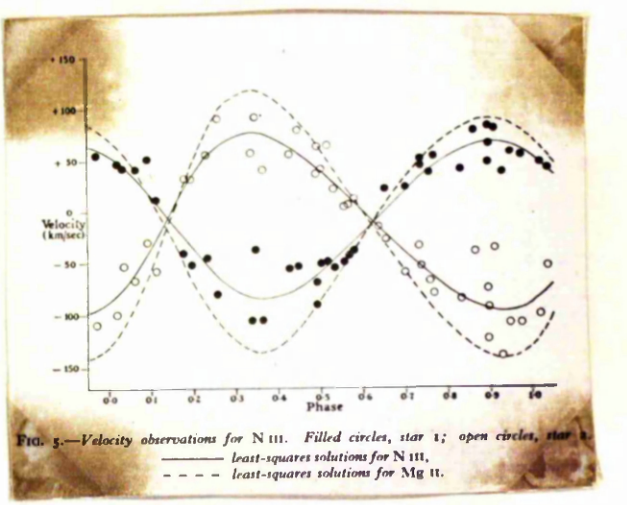

FIG. 5.—*Velocity observations for* N III. *Filled circles, star 1; open circles, star 2.*
——— *least-squares solutions for* N III,
- - - - *least-squares solutions for* Mg II.

Figure 4

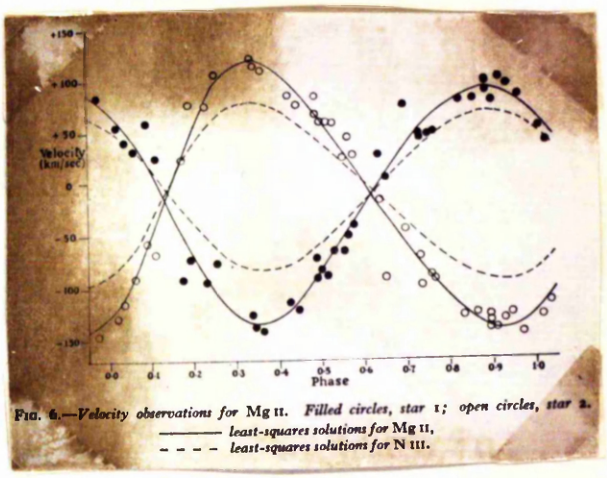

FIG. 6.—*Velocity observations for* Mg II. *Filled circles, star 1; open circles, star 2.*
——— *least-squares solutions for* Mg II,
- - - - *least-squares solutions for* N III.

Figure 5

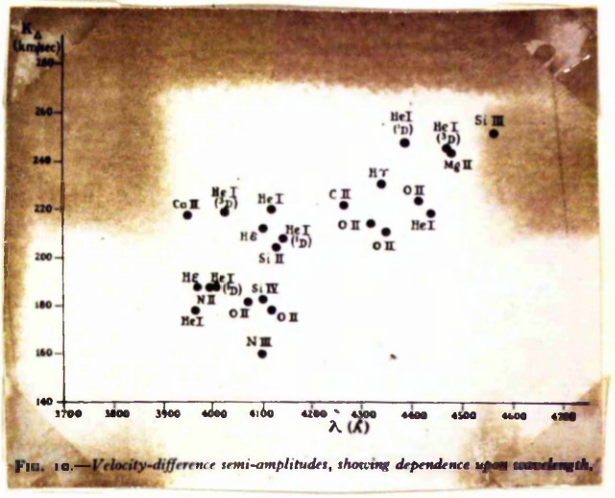

FIG. 10.—*Velocity-difference semi-amplitudes, showing dependence upon wavelength.*

Figure 6

Velocity-difference curves were represented by

$$\Delta = \gamma + K_2[\cos(\nu + \omega) + e\cos\omega] \qquad (2)$$

in the usual symbolism .

The systemic velocity γ is zero for a normal velocity-difference curve, but as the curves being analysed are distorted by reflection, (2) will in general only be an approximate fit to the observations and the presence of reflection may produce a pseudo-γ .

The results along with standard errors of the elements are given in Table 2. Figure 1 illustrates the variation of semi-amplitude K_2 from one group of lines to another, and in figure 2 four velocity-difference curves of the form (2) are plotted along with the observations.

A similar procedure was carried out for the individual velocity curves. The elements derived are given in Table 3, where the component stars are arbitrarily designated 1 and 2. Variations of $K_1(1-e^2)^{\frac{1}{2}}$ and $K_2(1-e^2)^{\frac{1}{2}}$ are shown in figures 3a and 3b. The velocity curves and individual observations of the extreme cases NIII and MgII are shown in figures 4 and 5. These observations cannot be reconciled with a single velocity curve. It is noticeable however, that the fit of each line on to a curve of the

type (2) is quite close.

A number of checks on the reality of the effect were made, including independent measurements of some of the plates by R.M.PETRIE. The possibilities of an artefact of measurement or of some sort of systematic blending of lines were also discussed, and rejected. The effect was thus established as a property of the binary system.

3. A qualitative discussion of the effect was finally given by the author, and a correlation predicted which turned out, in fact, to hold.

In the first place, it might be that the star has different angular velocities of rotation at different depths. If in addition the centre of illumination of each star was displaced from the geometrical centre, by a reflection effect which might be quite small, then weaker lines, formed at greater depths, would have systematically larger or smaller reflection effects depending on the vertical velocity gradient in the atmosphere.

Another possibility is that different effective centres of illumination produce the various displacements. Then we expect the lines corresponding to the higher temperatures to be displaced towards

the sub-stellar points. If the stars rotate in such a way that the same hemispheres always face inwards, or even if their rotation is only approximately of this form, then the high-temperature lines on this model correspond to the velocity curves with smaller semi-amplitude K, which is what we observe.

An inspection of figures 3a and 3b suggests that the SiII, SiIII and CaII lines, and possibly the NII line also, may be anomalous. However, OVENDEN demonstrates that the lines form a two-parameter system, figures 3 illustrating the relationship with only one of the parameters, namely T_{max}. The other parameter is the wavelength λ, and figure 6 demonstrates this correlation. The anomalies mentioned above are then seen to disappear.

This second correlation was predicted by the author on the assumption that the hypothesis of reflection holds. An absorption line is due to the removal of energy from the continuum at some wavelength, the amount of energy removed being $W\ B_\lambda(T)$, where W is the equivalent width of the line and $B_\lambda(T)$ is the Planck function corresponding to some temperature T. The displacement of a line

from the geometrical centre therefore depends on the variation of $W B_\lambda(T)$ over the stellar surface; in general, the steeper the rise of $B_\lambda(T)$ from the outwards facing hemisphere towards the sub-stellar point, the greater the displacement of a line. But at the temperatures prevailing in a B-type star and for the range of wavelength within which the observed lines are found, the Planck function is steeper at the shorter wavelengths. We thus expect lines of shorter wavelengths to be more displaced from the non-reflecting position, and this is what is demonstrated in figure 6, again on the assumption that the velocities of rotation and revolution are comparable and in the same sense. (This has been found to be the case for systems with period less than 10 days or so from a statistical analysis of line broadening in spectroscopic binaries).

The conclusions of this analysis are that in the system 57 Cygni:-

(i) different lines give different velocity curves, the semi-amplitude K in particular varying considerably from line to line.

(ii) the difference is correlated with the spectral-type at which the lines reach their maximum strength on the main sequence, and with wavelength

(iii) the theories of BATTEN and earlier workers are inadequate to explain the observations, both as to the size and the behaviour of the effect

(iv) the reflection effect, corrected for the conceptual fallacy previously discussed of the above theories, provides a qualitative explanation of the line behaviour

(v) the effect is a large one (larger than the author himself had anticipated) so that the calculated mass-function, if not corrected for reflection, might be considerably in error (see the final column in Table 3)

A Model for 57 Cygni

4. The two components of 57 Cygni have almost identical spectra, this being one of the features necessary for the inclusion of a system in the short-list mentioned in section 2. Occasionally star 1 was observed to have a marginally stronger absorption line than 2, which suggests that star 1 is slightly more luminous than 2; which is consistent

with the fact that $K_1 \geq K$. However for the purpose of the present model it is sufficient to take the phases as identical.

Hγ and MgII were particularly strong lines in the spectrum of 57 Cygni, which suggests that they occur over most of the stellar surface. An examination of figure 12 indicates that, unlike most other absorption lines, MgII should be weaker at spectral types earlier than B3. As the binary has type B3 or thereabouts on the Harvard system, then lines such as those of HeI(^{3}D) will be displaced towards the opposite star, while MgII, due to its weakness over the inner hemisphere, must be displaced in the opposite direction. It follows that the position of zero displacement must correspond to a position somewhere between MgII and HeI(^{3}D), and we can take $K_0 = 110$ km/sec. This argument will be modified somewhat by the Planck function. $\rho = K - K_0$ for any line immediately follows from Table 3 or, if $(1-e^2)^{\frac{1}{2}}$ is neglected, from figure 3.

From ALLEN's 'Astrophysical Quantities' a star of Harvard type B3 has mass $M = 6.6\odot$. Taking the orbit to be circular we have that the radius of the system is a, where

$$\frac{a^3}{P^2} = 2M$$

where a is measured in astronomical units, period P in years, and M is in units of the solar mass. Since P = 2.856 days we have $a = 0.093$ a.u. But a star of type B3 has radius $R = 5\odot$, again from AQ. Then the separation of the sub-stellar points is 0.046 a.u., or a stellar diameter. Prolateness of the components will tend to reduce this separation, but it is shown in Chapter II that the components have longest axes only a few percent longer than their polar axes.

If the circular velocity of one component (with the other as origin) is V, then

$$V = \frac{2\pi a}{P}$$

and V = 357 km/sec. As $K_0 = \frac{1}{2}V \sin i$, where the inclination i is measured from the plane perpendicular to the observer's line of sight, we find $i = 38^\circ$.

More generally,

$$M \sin^3 i = K_0^3 P/2\pi^3$$

if T is measured in years and K in a.u./year. Thus

$$M \sin^3 i = 1.56$$

on our model.

The masses of early-type stars are largely derived from the velocity curves of spectroscopic binaries, which curves may be affected by reflection to a greater extent than has been previously thought. It is possible that the masses of the early-type stars are thus underestimated. If we set an upper limit of 2 to the factor by which the masses are underestimated, and if we also suppose that each component star is unlikely to have $M < 4.4\odot$, then (figure 7)

$$30^\circ < i < 45^\circ$$

and from Kepler's equation

$$0.081 \text{ a.u.} < a < 0.117 \text{ a.u.}$$

In figure 9 the stars have their minimum separation in the apparent orbit. p and d are the projected separations of the centres and closest points of the stellar discs respectively. In an eclipsing system, $d < 0$. We have

$$d = p - 2R = a \cos i - 2R = 0.026 \text{ a.u.}$$

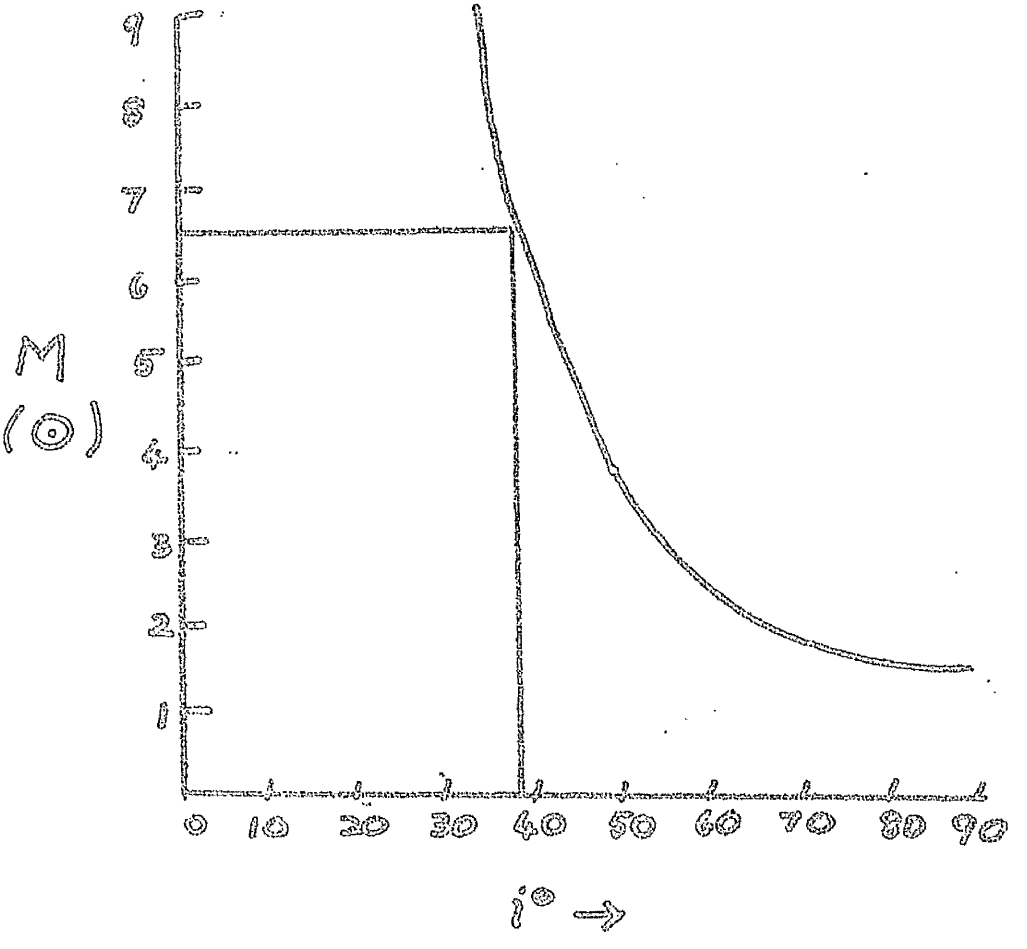

Inclination of 57 Cygni against Mass of each Component.

Figure 7

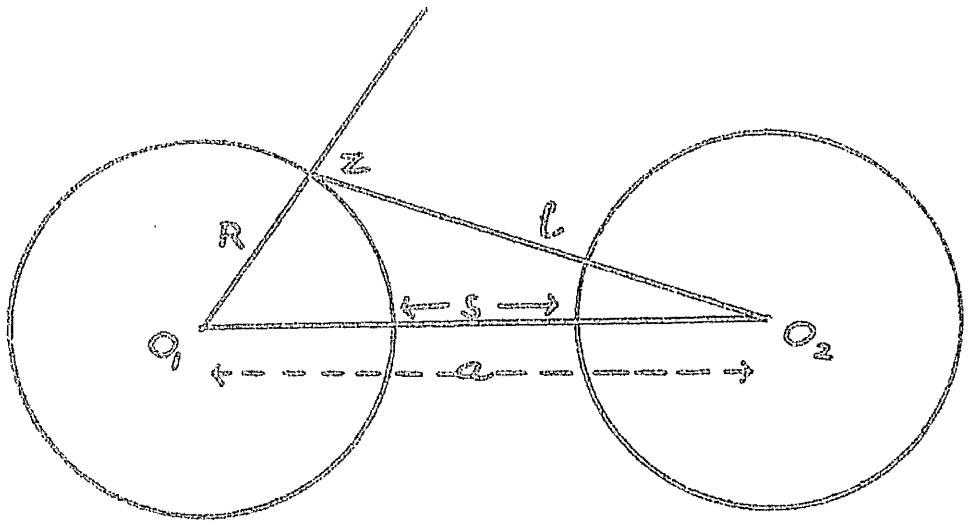

Figure 8

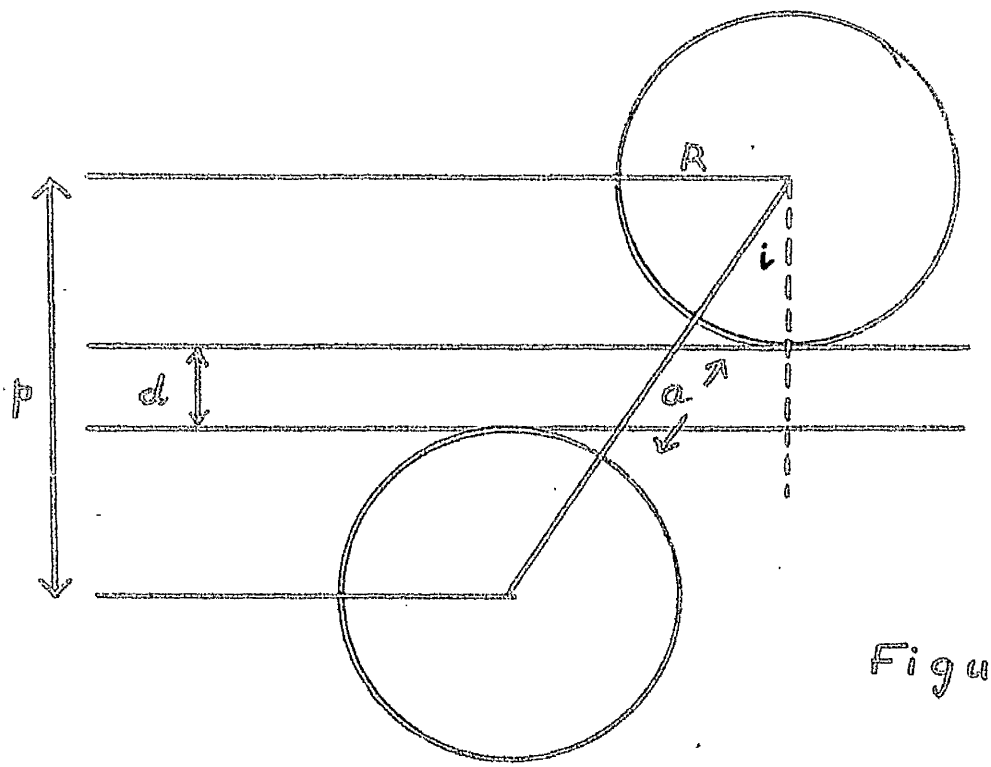

Figure 9

which is consistent with the fact that 57 Cygni is not an eclipsing system. Suppose $d = 0$, corresponding to a marginally eclipsing binary. Then

$$i_{crit} = \cos^{-1}(2R/a) = 60^{\circ}$$

5. Suppose the effective temperature on the outer hemispheres is T_e, and neglect prolateness, limb- and gravity-darkening. Over the inward-facing hemispheres there will be a fully lit zone, where the companion star appears entirely above the horizon to an observer on the other star, and a penumbral zone. KOPAL† (1954) has shown that over the fully-lit zone, the radiation received on each square centimetre from the adjacent star is equivalent to that from a point source of the same luminosity and zenith distance. Thus the energy emitted from a square centimetre at an arbitrary point is

$$\sigma T^4 = \sigma T_e^4 + \sigma T_e^4 (R/\ell)^2 \cos z$$

where (R, ℓ, z) are defined in figure 8. Then from Stefan's law, if T_s is the effective temperature of the sub-stellar point,

$$T_s = \left[T_e^4 + T_e^4 (R/\ell)^2 \right]^{\frac{1}{4}}$$

† M.N. 114, 101.

$\ell = s + R$, s the separation of the sub-stellar points.

$$\therefore \frac{T_s}{T_e} = \left[1 + \frac{1}{(s/R)+1}\right]^{\frac{1}{4}} \quad \text{with} \quad T_e = 20,000^{\circ}.$$

s/R	T_s/T_e	T_s
0	1.20	24,000
$\frac{1}{2}$	1.10	22,000
1	1.06	21,200
$1\frac{1}{2}$	1.04	20,800
2	1.02(5)	20,500

Table 4.

As in our model s/R = 2, the rise in temperature due to the reflection effect is only 500° or so even if we assume $T_e = 20,000^{\circ}$, a rather high value compared with most estimates in the literature. Since it is unlikely that $a < 0.08$ l a.u. then S/R > $1\frac{1}{2}$ and a temperature rise $(T_s - T_e)$ of more than 5%, or $1,000^{\circ}$, is unlikely (figure 10). KOPAL's theory (presented in Chapter IV) neglects the effect of multiple reflections. According to the theory presented in Chapter V, these are only of consequence when the stars are separated by less than a stellar radius.

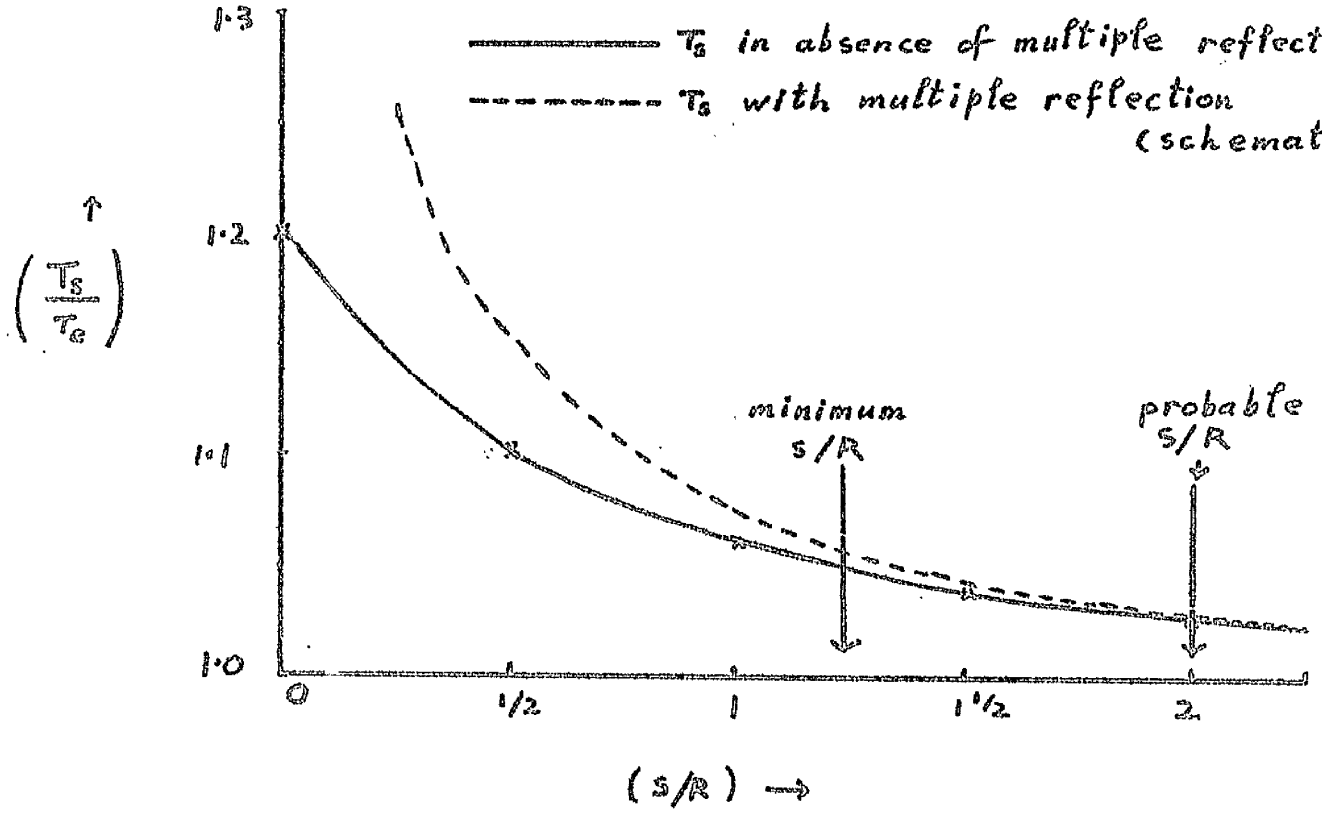

Temperature T_s at substellar points of identical components of a binary system. s represents the separation of the substellar points.

$T_e \equiv$ temperature in absence of reflection

$R \equiv$ radius of star

Note that when $s=0$, $T_s = 2^{\frac{1}{4}} T_e$ in the absence of multiple reflection

Figure 10

6. Dr. OVENDEN mentions in his paper that he found evidence (partly confirmed by PETRIE) of a third component. It is also possible that the 'third component' is in fact a gaseous stream. Such a stream might be expected to give rise to emission as well as absorption lines. BUTLER and THOMSON† have measured the equivalent widths of lines of a number of early type stars, including 57 Cygni. In the range 4100 - 6700 Å a few weak emissions are found, but these are stated in the paper to be interstellar: they may be circumstellar. Exceptions are, for instance, OII at $\lambda\lambda$4591, 4596; but other stars examined, of the same spectral type, also have these emission lines with similar strength. Therefore if a gaseous stream exists in the neighbourhood of each component it is unusual in that no emission lines are associated with it.

Another possibility is that a different sort of reflection altogether is involved. If T_s were high enough, corresponding to the temperature of an O-type star, then electron-scattering might be important in the region of the sub-stellar points. T_s refers to the effective temperature of the sub-stellar point of each star. In such a case

† Pub. Roy. Obs. Edin., Vol II, no. 6, 225, 1961.

photons incident on a star from its neighbour might be reflected by the free electrons without other interactions with the atmosphere, except for some change in energy due to Compton scattering. The spectrum of the star would then consist not only of lines inherent to the star, but also of another set of absorption lines, displaced relative to stronger lines, but softened by scattering and therefore fainter. In general the displacements of such lines would differ from those of lines formed by heating. This type of reflection (due to scattering rather than heating) is not considered here as 57 Cygni is not sufficiently hot for the process to be important, judging by the extreme faintness of the lines, even supposing that the 'third component' is due to this effect.

7. We may now ask what observable consequences are to be expected from the preliminary model of 57 Cygni.

The hypothesis is adopted throughout the remainder of the chapter that each small surface area of 57 Cygni can be treated as a minature stellar atmosphere with the same spectral type/effective temperature relationship as exists for main

sequence stars. The curves relating equivalent width, W, to spectral type, derived from main sequence stars, may then be applied to 57 Cygni. These W(spectral type) curves are usually gaussian (see figure 12), with half-widths which increase as T_{max} decreases, T_{max} being the effective temperature at which a given absorption line reaches maximum strength on the main sequence.

Neglect for the moment the effect of the Planck function and consider a sequence of absorption lines of decreasing T_{max}. Let T_e represent the effective temperature of the averted (non-illuminated) hemispheres. Then for $T_{max} > T_e$, the displacements will decrease as T_{max} decreases, leading to region A of the T_{max} / ρ diagram (figure 11). Region B is occupied by lines which have $T_{max} < T_e$, so that they are weaker over the inner hemisphere of each star. MgII is an example of this. As T_{max} falls further, the W(T) curve becomes flatter over the relevant temperature range, and this flatness may have the effect of causing the lines to tend back towards $\rho = 0$ (region C). Any lines appearing in region D would be anomalous if the Planck function had no effect.

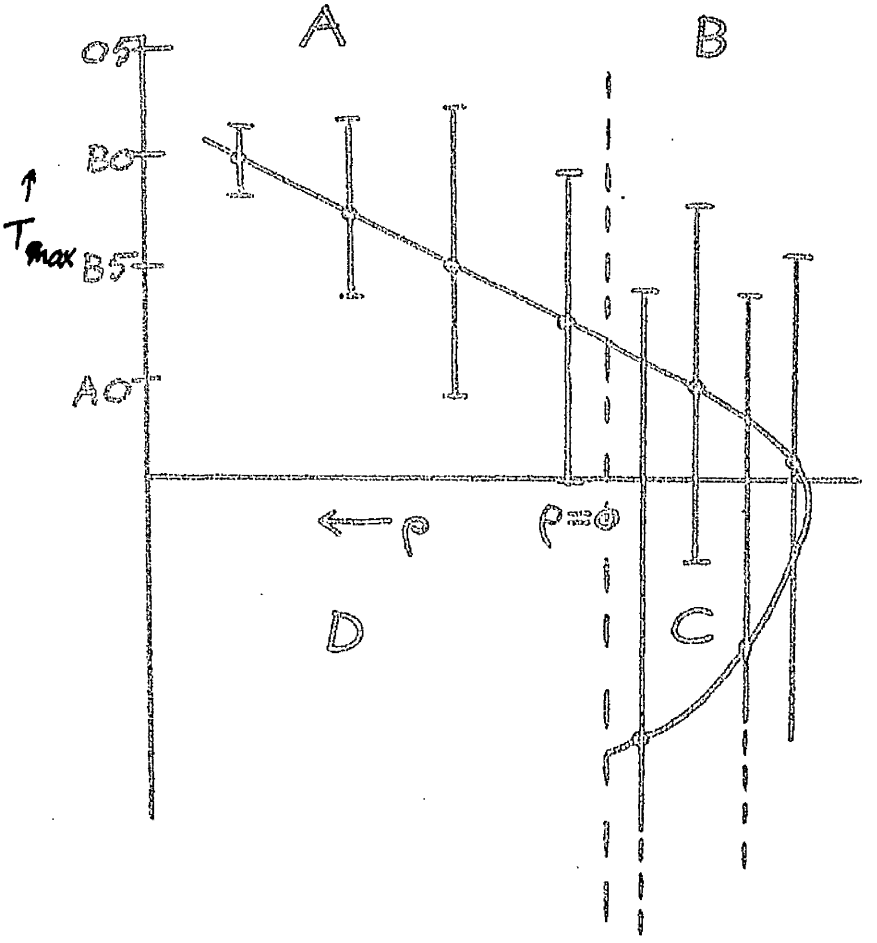

T_{max}/ρ diagram qualitatively expected (neglecting the influence of the Planck Function).

Figure 11

Consider now the influence of the Planck function. An absorption line which is highly sensitive to temperature will appear, on the stellar disc, only over a thin strip whose temperature lies within a narrow range about T_{max}. The value of displacements due to reflection is then obtained by a suitable averaging of velocity over the strip. As the coordinates of the strip depend only on the T_{max} distribution over the disc, the Planck function cannot enter into the expression for ρ. A sequence of such lines of various wavelengths will therefore show no correlation with wavelength arising as a consequence of $B_\lambda(T)$, and a diagram such as figure 6 should not be expected.

Likewise a sequence of lines completely insensitive to temperature, and which would all lie on $\rho = 0$ in the absence of a wavelength effect, is subject to the full influence of the effect, as the lines appear over the whole star.

The observed ρ/λ diagram is at least consistent, at first glance, with the above remarks. Nevertheless one or two discrepancies become apparent on closer examination of the observed diagrams. In the first place NII, which is anomalous in terms of the S/ρ

diagram, is not so in the ρ/λ diagram. But NII is the most highly sensitive of the absorption lines observed and should therefore be unaffected by the wavelength correlation, so that it can only be a coincidence that it lies where it does in figure 6; and the abnormal position of NII in figure 3 remains unexplained. Consider, furthermore, a gradient defined in the ρ/λ diagram by drawing the best straight line through absorption lines with similar W(spectral type) curves. Three such gradients, for instance, are defined by the OII lines, the sequence ($H\gamma$, $H\delta$, $H\epsilon$), and the best line through the multiplets of HeI(^1D). According to the ideas of the previous paragraphs the slopes of these lines should decrease with increasing T_{max}, and yet there is no evidence of this: lines so formed are more or less parallel.

In conclusion, the model adopted appears to represent the observations quite well qualitatively, although there seem to be one or two disturbing features in the ρ/λ diagram.

The Formula for ρ

8. If the absorption lines of 57 Cygni had been

only slightly displaced by reflection, it might have been necessary to consider any asymmetries in the line profiles which might arise. It would also have been necessary to consider more closely the relationship between the setting of a cross-wire on a line, and the expression for the line's displacement. However the effect is so large that this problem does not arise. The intensitometer tracings gave indications of asymmetric line profiles in the case of one or two lines. Tracings of the CII line taken from several spectrograms are shown in figure 13. However throughout the present work I shall use a mean, appropriately weighted, and assume that this mean is compatible with the corresponding cross-wire setting on the absorption line. The other obvious expression for a line displacement is a centroid, which is less convenient to handle mathematically and is not used.

In accordance with the argument in OVENDEN's paper, we shall weight the velocity at any point of the star with the energy removed from the continuum at that point. This is $W(T)\,R(T)$.

The equivalent width of a line will in general vary over the disc, the variation depending on unknowns such as the departure from thermodynamic

equilibrium in the reflecting atmosphere. The distribution of temperature over the disc will vary not only because of the reflection effect but also because of limb-darkening. The latter is convoluted with reflection. MILNE† (1926) showed that the radiation emitted by each part of the reflecting atmosphere can be separated into a 'non-reflected' and a 'reflected' component; this arises from the linear nature of the transfer equation, so that particular solutions can be superposed. According to MILNE the reflected radiation is strongly limb-darkened, while the unreflected component has a limb-darkening coefficient which is unaffected by reflection.

Suppose B_1, B_2 represent the Planck functions of the non-reflected and the reflected components of radiation respectively. Let $d\sigma_-$ and $d\sigma_+$ represent elements of area on the outer and inner hemispheres respectively (of either component), and let $B'_{1,2}$ be the value of $B_{1,2}$ at the centre of the stellar disc. Suppose Θ is the usual limb-darkening angle. Then

$$\rho = \frac{\iint_{\Sigma_{+,-}} VWB_1'(1-u+u\cos\Theta)\cos\Theta\, d\sigma_{+,-} + \iint_{\Sigma_+} VWB_2' \cos^2\Theta\, d\sigma_+}{\iint_{\Sigma_{+,-}} WB_1'(1-u+u\cos\Theta)\cos\Theta\, d\sigma_{+,-} + \iint_{\Sigma_+} WB_2' \cos^2\Theta\, d\sigma_+}$$

† M. N. 87 . 43

where the domains of integration are over the respective hemispheres. It should be noted that MILNE's analysis is valid only in the case when the illuminating flux is in the form of a parallel beam.

As a first approach to the problem, I decided to see whether or not the T_{max}/ρ and ρ/λ diagrams of the model would agree, to within an order of magnitude, with the observed diagrams of 57 Cygni. Limb-darkening is then a refinement which can be neglected and I took the reflected and non-reflected components of radiation to be undarkened. In the nodes, the isotherms will appear as straight lines parallel to the y-axis (figure 15), a configuration which arises due to the symmetry of temperature about the sub-stellar point. The star is here taken to be of unit radius, and the x-axis has, as origin, the centre of the disc and, as direction, the line joining the stellar centres. The radial velocity V of any point is then given by $V = \omega x$, where ω is the angular velocity of rotation about the y-axis. There is no loss of generality in taking the stellar rotation to be about the y-axis, as ω_x broadens but does not displace a line, while ω_z has no effect on the

change or displacement of a line. ω is taken to be uniform. Then the formula for ρ reduces to

$$\rho = \frac{\omega \int_{-1}^{1} x \sqrt{(1-x^2)}\, W(T)\, B_\lambda(T)\, dx}{\int_{-1}^{1} \sqrt{(1-x^2)}\, W(T)\, B_\lambda(T)\, dx} \qquad (3)$$

9. An empirical knowledge of the function W(T) is necessary in order to make use of (3). The temperature referred to here is colour temperature, as this is the argument of the continuum intensity $B_\lambda(T)$. A few authors have published W(spectral type) data, the most extensive being due to WILLIAMS† (1938) and to RUDNICK* (1938). Diagrams following WILLIAMS are reproduced in figure 12; those of RUDNICK are similar.

To use data such as that of WILLIAMS and RUDNICK we require a conversion from spectral type to colour temperature T_c. Such a conversion is shown in figure 14. The points O5, B0, B5 and so on have been taken from ALLEN's AQ and the curve has been formed by interpolation. Unfortunately it is then necessary to convert from the spectral classification system used by ALLEN to the systems used by other authors. There is some disagreement between the various systems of classification, amounting to an uncertainty of about one spectral sub-division.

† Ap. J. 83, 305. * Ap. J. 83, 433.

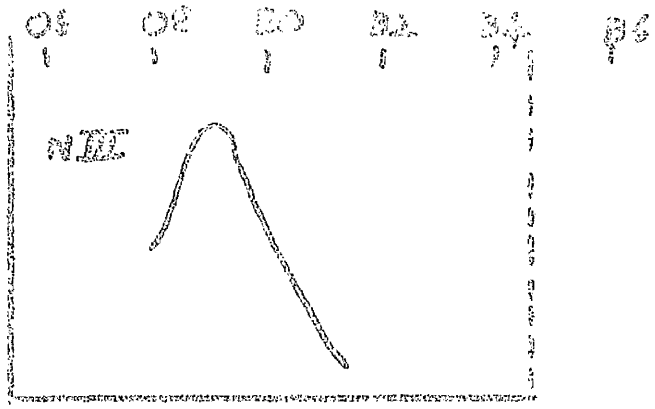

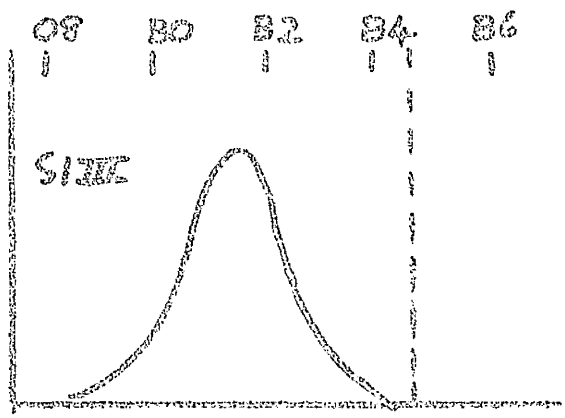

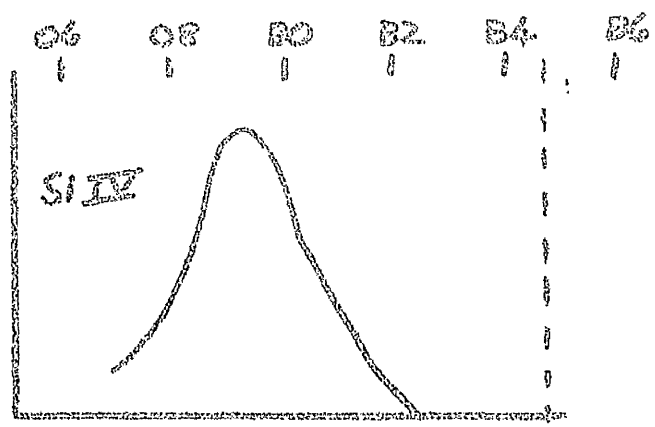

Figure 12

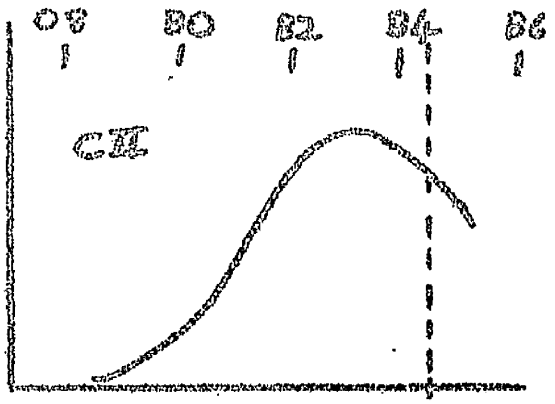

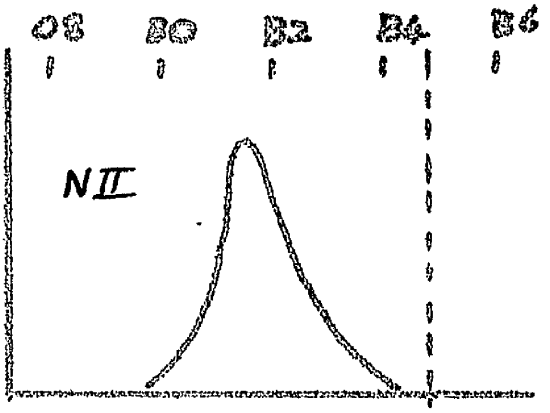

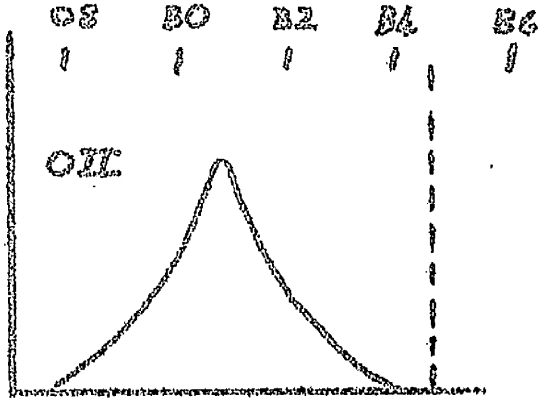

w (spectral type) curves after WILLIAMS.

Vertical scale arbitrary

Figure 12.

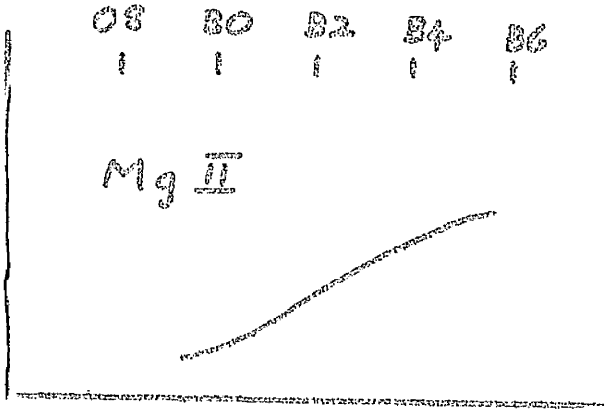

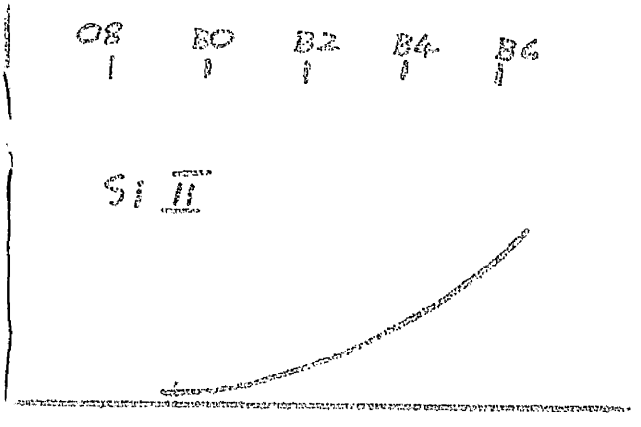

Figure 12.

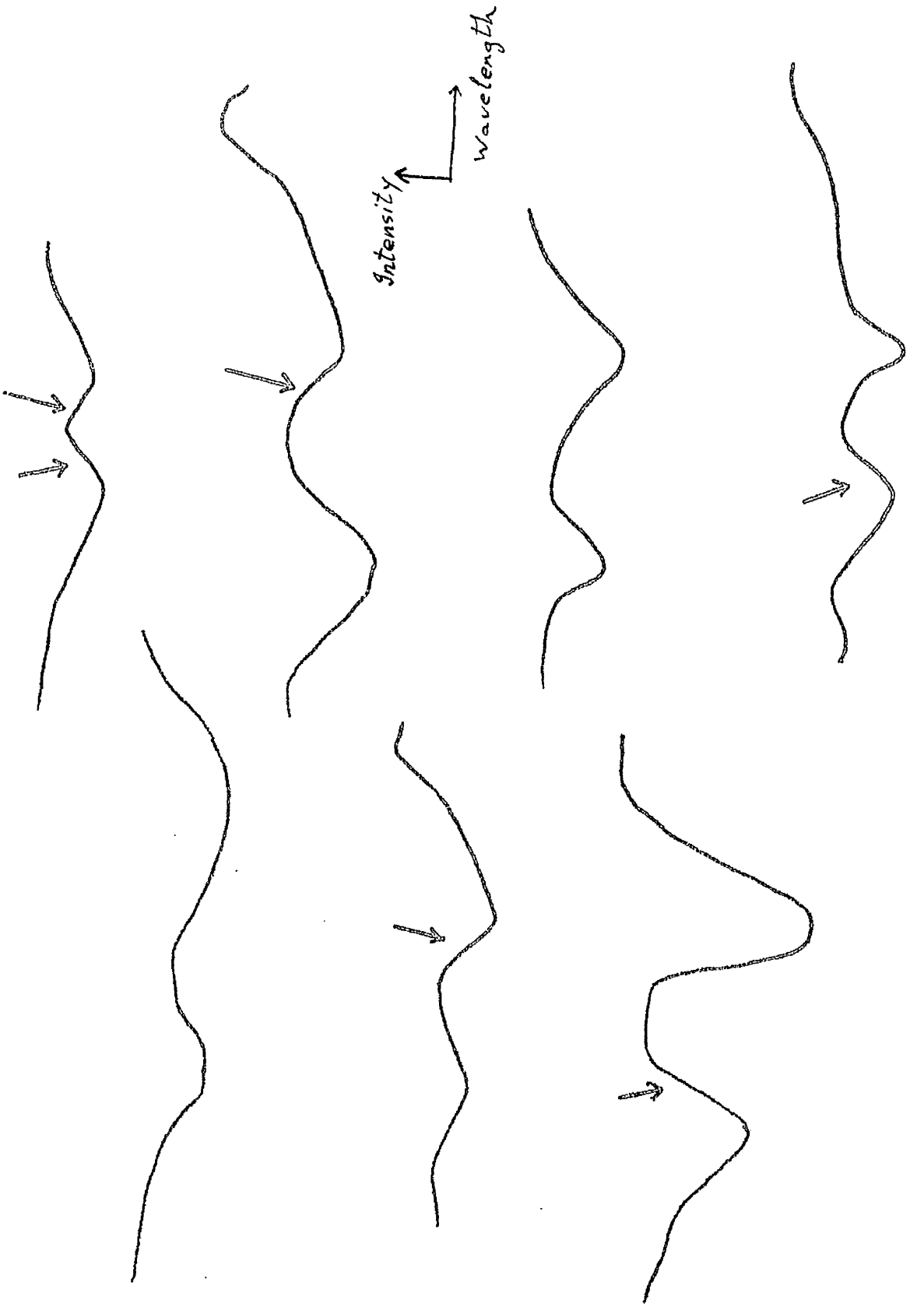

Intensitometer tracings of C II (smoothed).
There is slight evidence of asymmetry in the profiles.

Figure 13

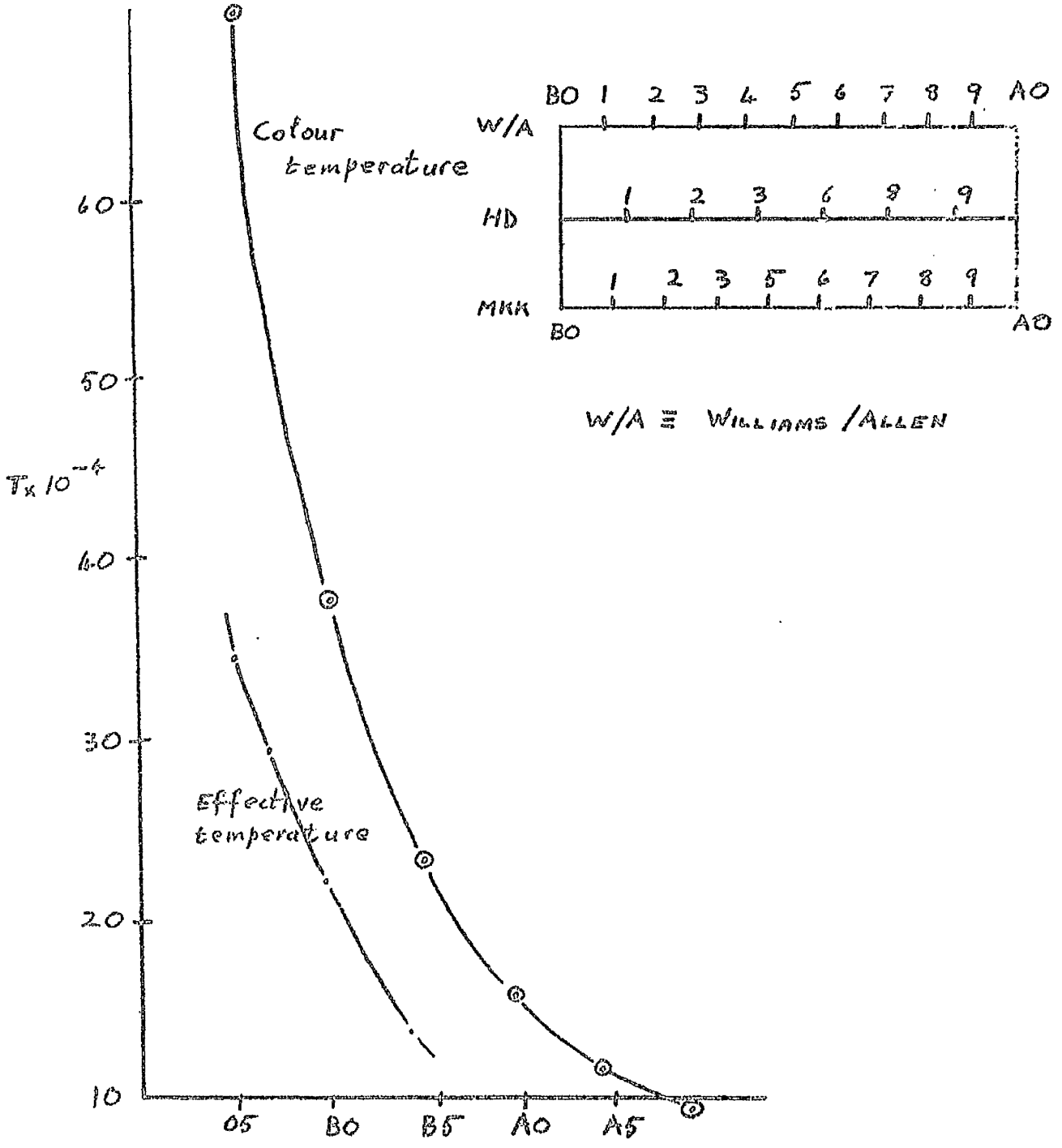

Conversion used between (T_{eff}, T_c) and WILLIAMS spectral type (supposed identical to ALLEN's, in AQ).

Inset allows a rough conversion between different systems of spectrum classification.

Figure 14

It is impossible to intercompare the various spectral classifications in detail: each involves consideration of variations of strengths of numerous lines and of comparisons of relative lines strengths. And different systems make use of different lines, even when, say, a particular star is being examined. The following notes briefly summarise some aspects, pertaining to B stars in particular, of the classification systems used in the subsequent analysis:-

1.	Allen	(Astrophysical Quantities) Data is supplied for O5, B0, B5.....and the required data for other spectral types is obtained by interpolation, assuming ten equal divisions of each type.
2.	Harvard System(HD)	B4, B6, and B7 are omitted.
3.	Yerkes System(MKK)	B4 is omitted. Luminosity classes I to V have been introduced.
4.	Victoria System	No sub-divisions are omitted, and large numbers of stars are found in classes B3 and B5.
5.	Williams	Williams adjusts his sub-divisions so that the number of stars increases smoothly with lateness of spectral type. No sub-divisions are omitted.

Since the equivalent widths of some lines vary from maximum strength to zero over two spectral sub-divisions, and since the above systems may well differ from each other by about one sub-division, the conversion between equivalent width and colour temperature by way of spectral type cannot be reliable if the data are taken from various authors. As far as possible, therefore, I chose to use that of WILLIAMS, as his system of classification seems to be the most significant physically, and in addition his data is smoothed, increasing its usefulness. It was necessary to supplement this by information from RUDNICK, in particular for the helium lines.

An Iterative Method

10. Theory From figure 14 and the discussion of § 5 it appears that the rise in effective temperature over the hemispheres of the component stars corresponds to a change in spectral type from 'ALLEN' type B4.5 to about B4.0, or only half a spectral sub-division. The change in equivalent width of the line is small over this range and a linear relationship

between colour temperature and equivalent widths holds. However in order to take account of any curvature of the W(T) curve over this range, which might be marginally significant, it was decided to represent W by a quadratic expression. For simplicity the temperature T_e on the outer hemispheres was taken equal to unity, and the equivalent width at any point expressed in terms of the difference in temperature between the point and that of the outer hemisphere: thus

$$W(T) = 1 + w_1 \Delta T + w_2 (\Delta T)^2$$

where $\Delta T = T - T_e$

The quantities (w_1, w_2) describing the variation of W over the range of temperature of interest, are easily calculated.

Figure 17 is derived from tables of the Planck function and covers the range of wavelength of the observed lines. The Planck function is also sensibly linear over the relevant range of temperature and wavelength and could be described with sufficient accuracy by a linear expression in T. However a quadratic term was once more included to take account of any curvature:

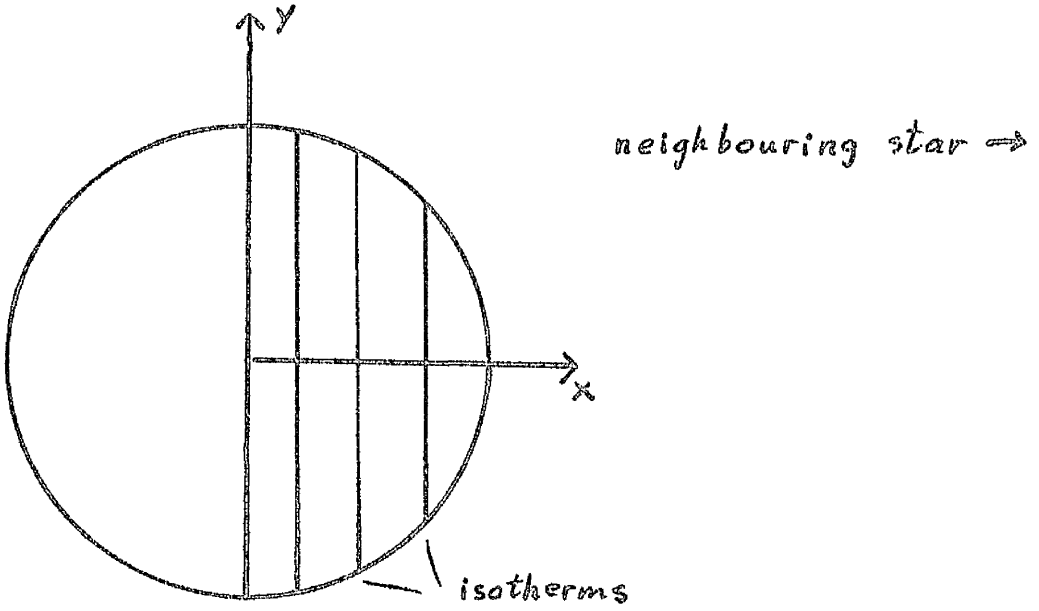

Configuration of isotherms with system in nodes

Figure 15

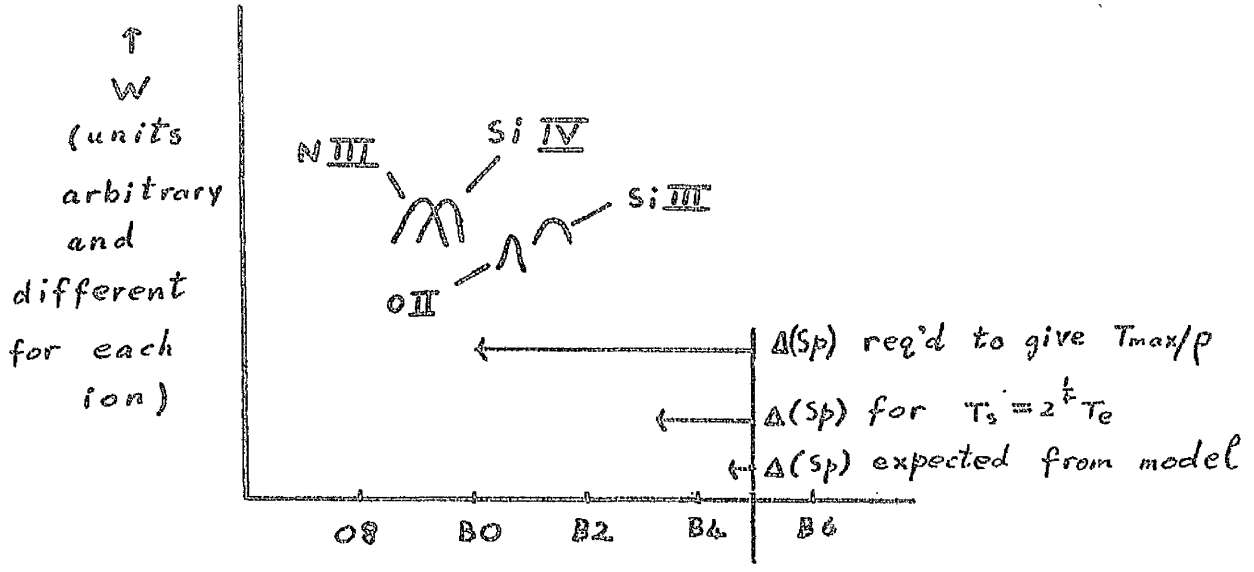

Δ(Sp) ≡ change in spectral type

Figure 16

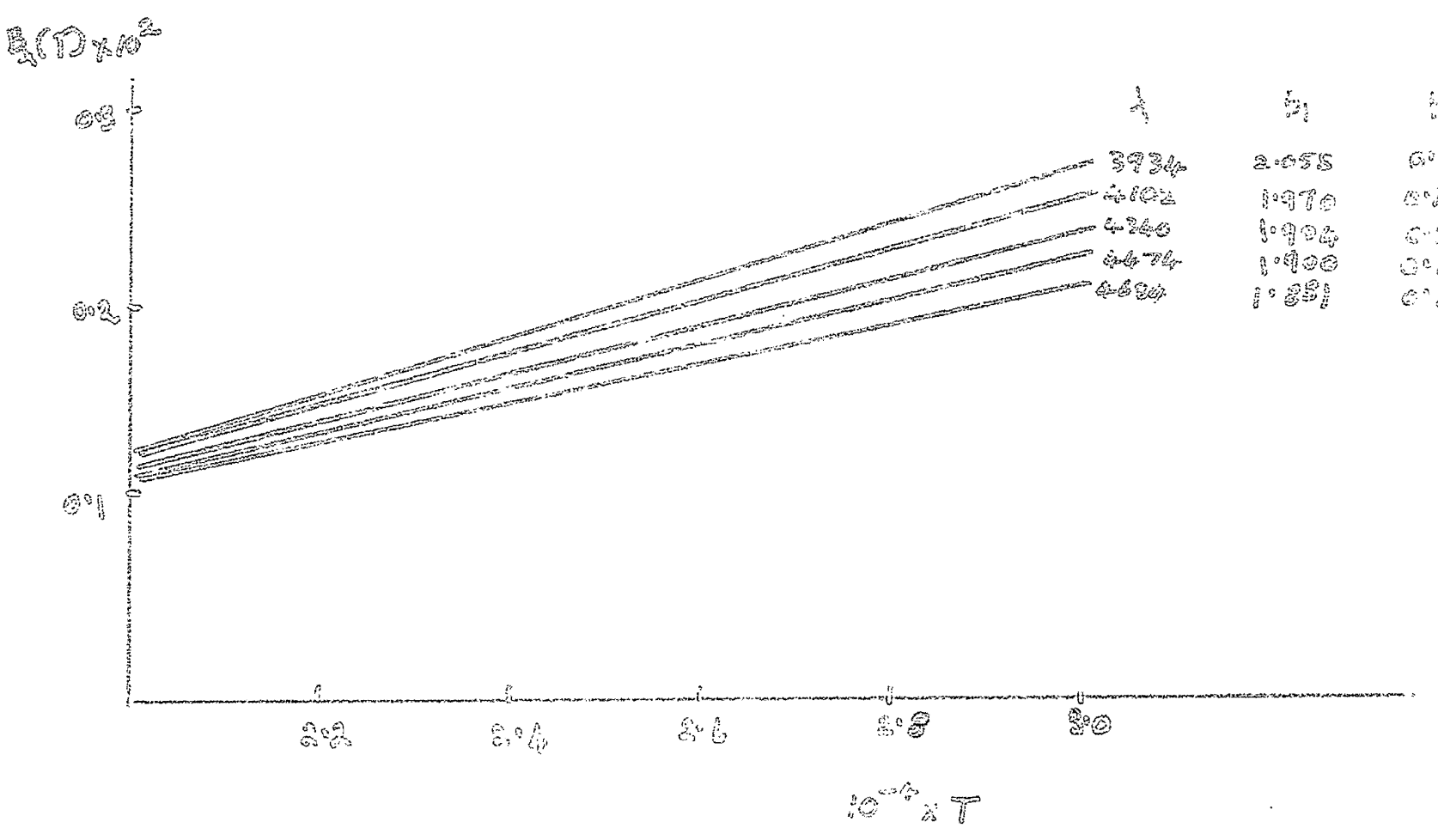

Figure 17

$$B_\lambda(T) = 1 + b_1(\Delta T) + b_2(\Delta T)^2.$$

$B_\lambda(T)$ is arbitrarily put equal to unity at temperature T_e. We are entitled to do this as it appears as a ratio in the expression for the displacement. b_1 and b_2 are tabulated for various wavelengths in figure 17. b_2 does not vary appreciably over the range $3934 < \lambda < 4684$ and is small compared with b_1. We have that

$$W(T)\, B_\lambda(T) = 1 + q_1\Delta T + q_2(\Delta T)^2 + q_3(\Delta T)^3 \qquad (4)$$

where
$$q_1 = w_1 + b_1$$
$$q_2 = w_2 + b_2 + w_1 b_1$$
$$q_3 = w_1 b_2 + w_2 b_1$$

As a first approach I decided to represent the temperature distribution over the inner hemisphere of the reflecting star by a cubic in x:

$$\Delta T = 0 \qquad \text{for} \quad -1 \leqslant x < 0$$
$$\Delta T = T_1 x + T_2 x^2 + T_3 x^3 \qquad \text{for} \quad 0 \leqslant x \leqslant 1$$

The coefficients (T_1, T_2, T_3) are kept arbitrary for the moment. The idea was to develop (3) analytically: the adoption of particular values for the T_i and (ω, K_0) would result in diagrams which could then be compared with observation. The comparison would result in an

improvement of the (T_1, ω, E_0) by iteration until the best cubic had been found. In the event two difficulties arose which led to the abandonment of the simple model so far adopted:-

We have, in the range $0 \leq x \leq 1$,

$$\begin{aligned} \Delta T &= T_1 x + T_2 x^2 + T_3 x^3 \\ (\Delta T)^2 &= j_0 x^2 + j_1 x^3 + j_2 x^4 + j_3 x^5 + j_4 x^6 \\ (\Delta T)^3 &= k_1 x^3 + k_2 x^4 + k_3 x^5 + k_4 x^6 + k_5 x^7 + k_6 x^8 + k_7 x^9 \end{aligned} \qquad (5)$$

where

$$j_0 = T_1^2 \qquad j_1 = 2T_1 T_2 \qquad j_2 = 2T_1 T_3 + T_2^2$$

$$j_3 = 2T_2 T_3 \qquad j_4 = T_3^2$$

$$k_1 = T_1^3 \qquad k_2 = 3T_1^2 T_2 \qquad k_3 = 3T_1(T_1 T_3 + T$$

$$k_4 = 6T_1 T_2 T_3 + T_2^3 \qquad k_5 = 3T_1 T_3^2 + 3T_2^2 T_3 \qquad k_6 = 3T_2 T_3^2$$

$$k_7 = T_3^3$$

Inserting the above in (4) we have

$$P = \omega \frac{N}{\frac{\pi}{2} + D} \qquad (6)$$

where

$$\begin{aligned} N = {} & [q_1 T_1] B(\tfrac{3}{2}, \tfrac{3}{2}) + [q_1 T_2 + q_2 j_0] B(2, \tfrac{3}{2}) \\ & + [q_1 T_3 + q_2 j_1 + q_3 k_1] B(\tfrac{5}{2}, \tfrac{3}{2}) + [q_2 j_2 + q_3 k_2] B(3, \tfrac{3}{2}) \\ & + [q_2 j_3 + q_3 k_3] B(\tfrac{7}{2}, \tfrac{3}{2}) + [q_2 j_4 + q_3 k_4] B(4, \tfrac{3}{2}) \\ & + [q_3 k_5] B(\tfrac{9}{2}, \tfrac{3}{2}) + [q_3 k_6] B(5, \tfrac{3}{2}) + [q_3 k_7] B(\tfrac{11}{2}, \tfrac{3}{2}) \end{aligned}$$

$$D = [q_1, r_1]\, B(1, \tfrac{3}{2}) + [q_2, r_2 + q_2 j_0]\, B(\tfrac{3}{2}, \tfrac{3}{2}) + [q_2, r_3 + q_2 j_1 + q_3 k_1]\, B(2,$$

$$+ [q_2 j_2 + q_3 k_2]\, B(\tfrac{5}{2}, \tfrac{3}{2}) + [q_2 j_3 + q_3 k_3]\, B(3, \tfrac{3}{2}) + [q_2 j_4 + q_3 k_4]\, B(\tfrac{7}{2}$$

$$+ [q_2, k_5]\, B(4, \tfrac{3}{2}) + [q_3 k_4]\, B(\tfrac{9}{2}, \tfrac{3}{2}) + [q_3 k_5]\, B(5, \tfrac{3}{2})$$

where $B(m,n) = 2\int_0^{\frac{\pi}{2}} \sin^{2m-1}\theta \cos^{2n-1}\theta\, d\theta$ on putting $x = \sin\theta$. The $B(m, \frac{3}{2}) = I_{2m-1}$ take the values

$I_1 = 0.33333$	$I_2 = 0.19635$
$I_3 = 0.13333$	$I_4 = 0.09817$
$I_5 = 0.07619$	$I_6 = 0.06136$
$I_7 = 0.05079$	$I_8 = 0.04295$
$I_9 = 0.03694$	$I_{10} = 0.03221$

Given a value of ω (which has the dimensions of a velocity as the star has radius R = 1) and the quantities (q_1, q_2, q_3) for any line, then (6) expresses a relationship between the displacement of the line and the temperature distribution, represented by a cubic over the inner hemisphere. If the observed radial velocity V_{obs} in the nodes is composed of the orbital component, V_{orb}, and the component ρ due to the reflection effect,

$$V_{obs} = V_{orb} + \omega \overline{x}.$$

The systemic velocity is here neglected.

For assumed values of the parameters, an orbital velocity V_{calc} could be calculated, where

$$V_{calc} = (V_{orb})_0 + \omega \bar{x}$$

suffix zero referring to the first assumed values. We can then write

$$V_{obs} - V_{calc} = \Delta(V_{orb} + \omega \bar{x})$$

$$= \Delta V_{orb} + \omega \Delta \bar{x} + \bar{x} \Delta \omega$$

$$But \quad \Delta \bar{x} = \sum_{n=1}^{3} \frac{\partial \bar{x}}{\partial T_n} \Delta T_n$$

and finally

$$\Delta V_{orb} + \omega_0 \sum_{n=1}^{3} \frac{\partial \bar{x}}{\partial T_n} \Delta T_n + \bar{x} \Delta \omega = V_{obs} - [(V_{orb})_0 + \omega_0 \bar{x}]$$

If initial values of V_{orb}, ω, (T_1, T_2, T_3) are taken, then five lines are necessary to solve for $(\Delta V_{orb}, \Delta T, \Delta \omega)$. A least squares procedure using all the lines available would give the 'best' values of the various quantities consistent with the neglect of limb-darkening and prolateness, and with the cubic representation of temperature.

11. As initial values I took $T_1 = 0.1$, $T_2 = T_3 = 0$. This gives a 10% rise in effective temperature, and the conversion from effective temperature to spectral

type was made on the assumption that WILLIAMS spectral type is identical to that of ALLEN.

Then

$$\bar{x} = \frac{q_1 I_2 T_1 + q_2 I_3 T_1^2 + q_3 I_4 T_1^3}{\frac{\pi}{2} + q_1 I_1 T_1 + q_2 I_2 T_1^2 + q_3 I_3 T_1^3} \qquad (7)$$

Expressions for $\frac{\partial \bar{x}}{\partial T_1}$ were derived but are not reproduced here as they were not made use of.

The coefficients (w_1, w_2) of the expansion (4) for W may be found either by directly fitting the quadratic on to the W(T) graphs of figure 12, or by a Taylor expansion about T_c, assuming that the curves are gaussian.

These values were easily derived for absorption lines such as MgII, CII and the hydrogen and helium lines, as they are visible in normal stars of Harvard type B3. The corresponding $\bar{x}$ were all extremely small, being generally in the region of 0.02. The spread in displacement of these lines amounts to about 30 km/sec on the T_{max}/ρ diagram of each star (see figure 3 of chapter 1). Since $\rho = \omega \bar{x}$, then for lines designated 1 and 2,

$$\rho_1 - \rho_2 = \omega(\bar{x}_1 - \bar{x}_2)$$

$$\therefore \quad \omega = \frac{\rho_1 - \rho_2}{\bar{x}_1 - \bar{x}_2}$$

Taking $\rho_1 - \rho_2 = 30$ km/sec., $\bar{x}_1 - \bar{x}_2 = 0.02$, the necessary projected equatorial velocity of rotation of each component turns out to be ~1,500 km/sec., which is absurd.

The extremely small values of $\bar{x}$ are in fact a necessary consequence of (7). The q's are quantities of order unity, the T_i's are small compared with unity and the product $q_i I_j T_k^6$ is therefore small compared with the $\frac{T}{\mu}$ in the denominator of the equation for $\bar{x}$. That the observed spread of ~30 km/sec. is due to the T_{max}/ρ correlation as such (and not the ρ/λ correlation with which it is convoluted) is obvious from the sequence He I(^{1}D), CII, He I(^{3}D), MgII, of figures 3a and 3b.

A further difficulty arises because we would not expect to observe NIII and SiIV at all on the stars; and the same probably applies to NII and OII. An extrapolation of the form shown:-

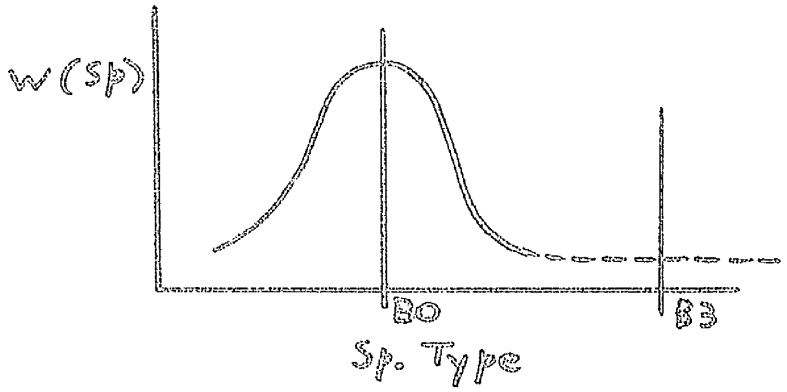

would ensure visibility of NIII. However we would then have $v_1 \neq v_2 \neq 0$ and therefore $\bar{v} \neq 0$.

The circumstances that NIII and SiIV are (i) visible, (ii) highly displaced, are therefore mutually exclusive in the context of the model used so far.

12. Discussion of the Difficulties. Variation (within a reasonable range) of the geometrical elements of the model, or of the stellar masses, has no effect of any consequence:-

A rise of, say, $1,000^{\circ}$, would strain the dimensions of the model, and $2,000^{\circ}$ can be regarded as being completely outside the permissible limits. $\Delta T = 2,000^{\circ}$ corresponds to a spectral change from B4.5 to B3, and it is clear from figure 12 that even this is inadequate to account for the visibility of NIII and SiIV. Furthermore, as the inclination $i = 38^{\circ}$ or so, the neighbourhood of the sub-stellar point of each star will be hidden from the observer over part of the orbital cycle. NIII being visible over the entire cycle, it cannot be confined to a small area around the hotspot, but must be visible over much of the inner surface of the stars.

Even for $\Delta T = 2,000^{\circ}$ the first difficulty, viz that the Γ of the hydrogen and helium and other lines are very small, remains.

If the star is of a somewhat earlier spectral type than we have been adopting, it might be that NIII would appear at the hotspot. The argument concerning the visibility at all phases of NIII still applies, however. 57 Cygni would have to be of type B1 or so before a large ρ and an always visible NIII would result; and at type B1 lines such as OII would have zero displacement. Apart from which all authors agree fairly well amongst themselves concerning the type of 57 Cygni. B1 or so must be completely ruled out.

The basic difficulty is that the expected heating of each star by the other is so small that very little change in the spectral characteristics of the atmospheres should be expected over the surfaces. Hence only very small reflection displacements should be observed.

The qualitative picture behind the prediction of a T_{max}/ρ diagram is that of a series of strips on the star, each containing an absorption line. The closer the strip to the sub-stellar point, the higher the T_{max} of the line it contains: the

'spread' of V about T_{max} does not affect the general trend. The implication is that the temperature rise over the reflecting star must be sufficiently great to 'contain' the T_{max}, even of lines such as SiIV and NIII. In turn (figure 16) this suggests that if we abandon the restriction that $T_s \leq 2^{\frac{1}{4}} T_e$ and consider much higher ranges of temperature to be permissible, a more satisfactory diagram would be produced.

13. In order to test whether a large temperature variation would give rise to the observed diagram, some numerical models were constructed. The assumption of a quadratic variation of equivalent width with temperature had to be dropped, the representation

$$W(T) = W_0 e^{-k^2 (T_{max} - T)^2} \qquad (3)$$

being more appropriate. The integrals which result are intractable analytically and a numerical approach was adopted. It was considered sufficient at this stage to assume some function T(x) and, using the W(spectral type) graphs and tables of the Planck function, to find T for the lines and compare with observation. The possibility of a more sophisticated approach was considered (for instance the method of

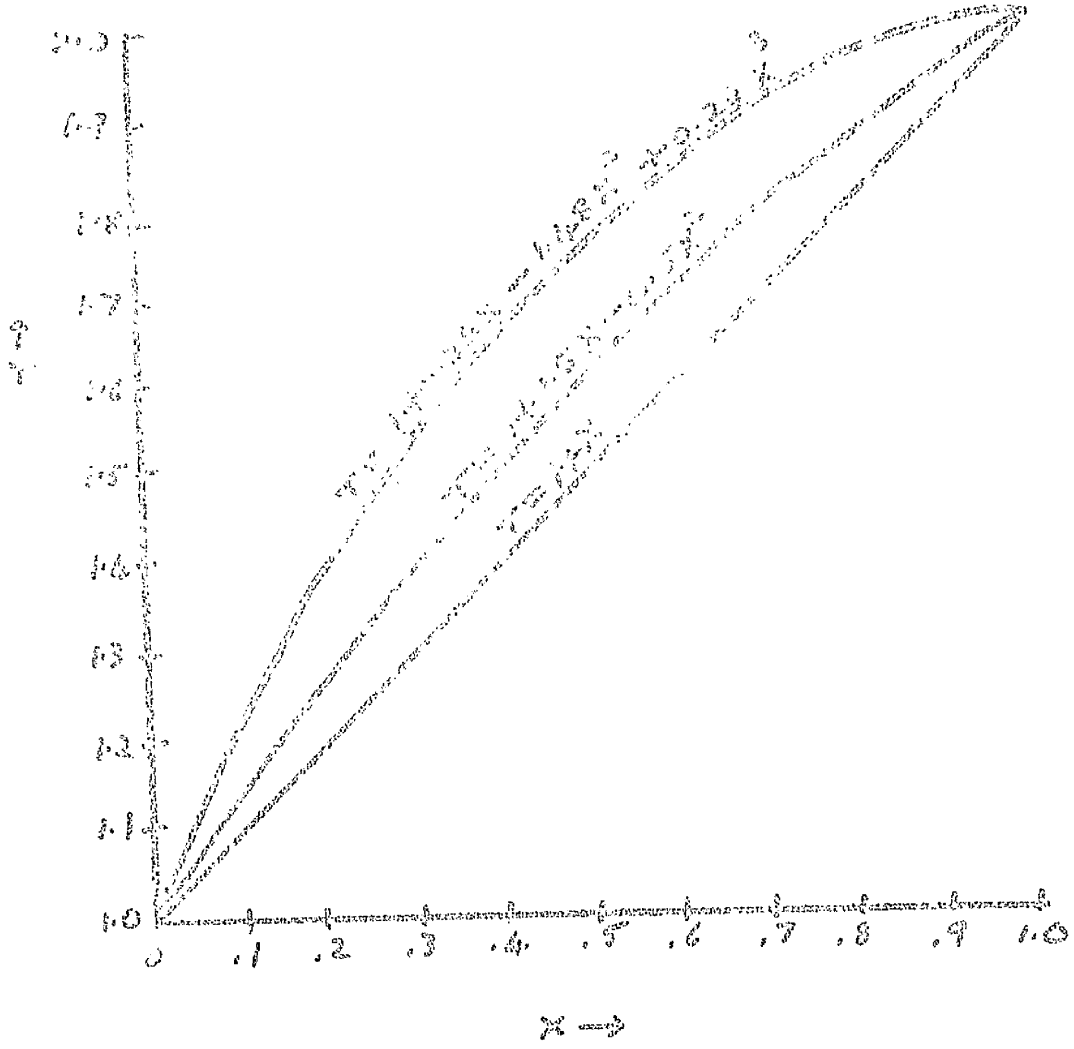

Figure 18

steepest descents could be used to evaluate (3) with (8) for the more sensitive lines, that is, for large h) but it was decided to follow the method outlined above in order to be sure of orders of magnitude and the like before embarking on more laborious calculations. It turns out that a second unexpected feature arose, as a consequence of which the model had to be modified further, and in the event no more complicated approach than the one above is justifiable.

The colour temperature at the sub-stellar point was chosen to be double that of the far hemisphere. Fortunately a formula exists which is well adapted to the present problem:- BRONWIN's formula states that, for a function whose twelfth differences are negligible,

$$\int_{-1}^{1} f(x)(1-x^2)^{-\frac{1}{2}}\,dx = \frac{\pi}{6}\{ f(\cos 15^\circ) + f(\cos 45^\circ) + f(\cos 75^\circ) + f(\cos -15^\circ) + f(\cos -45^\circ) + f(\cos -75^\circ)$$

where
$\cos 15^\circ = 0.965\ 926$
$\cos 45^\circ = 0.707\ 107$
$\cos 75^\circ = 0.258\ 819$

In the numerator we put $f_1(x) = x(1-x^2)\ W(x)\ B_\lambda(x)$, while in the denominator, $f_2(x) = (1-x^2)\ W(x)\ B_\lambda(x)$.

Three of the various temperature distributions which were tried are plotted in figure 18. Two corresponding T_{max}/ρ diagrams are shown in figures 19 and 20. There is agreement with the qualitative expectations and with the diagrams obtained from the observations of 57 Cygni.

Regard T_s for the moment as a parameter which can be varied at will. For $T_s \neq T_e$, the absorption lines in the T_{max}/ρ diagram lie close to $\rho = 0$. As T_s increases, the lines will begin to sort themselves out, but NIII, SiIV, OII and NII will not be visible. For NIII and SiIV in particular to appear, T_s must correspond to at least type BO.

If the proportional displacement of a line, $\bar{x}$, corresponds roughly to the x-coordinate at which the star has colour temperature $T = T_{max}$, it can be seen that as T_s increases further, the lines will then tend to move back towards $\rho = 0$:-

Let the effective temperature distribution take the form

$$T = 1 + (T_s - 1)\ x$$

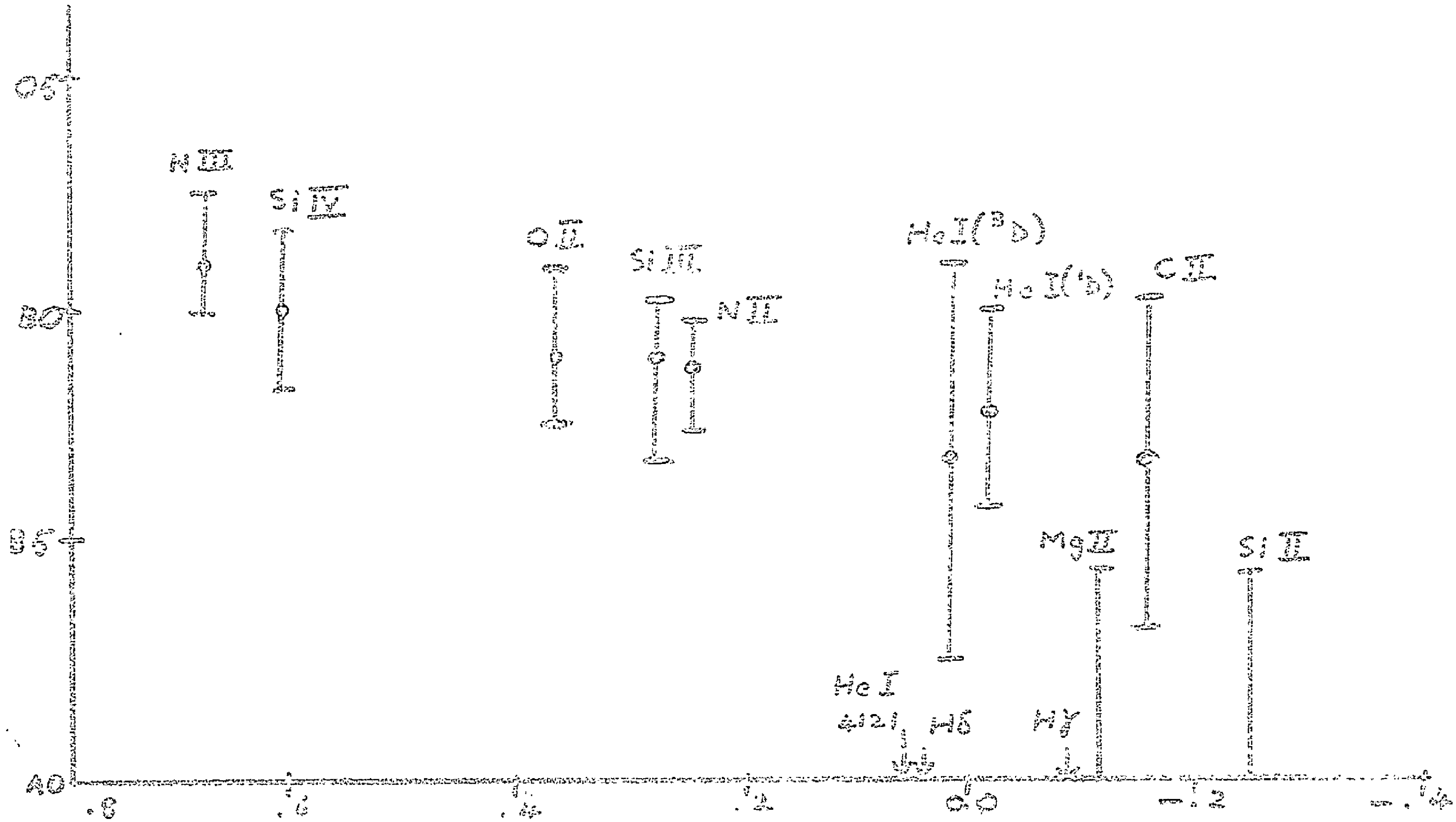

T_{max}/ρ diagram for $T = 1 + 1.5x - 0.5x^2$

Figure 19

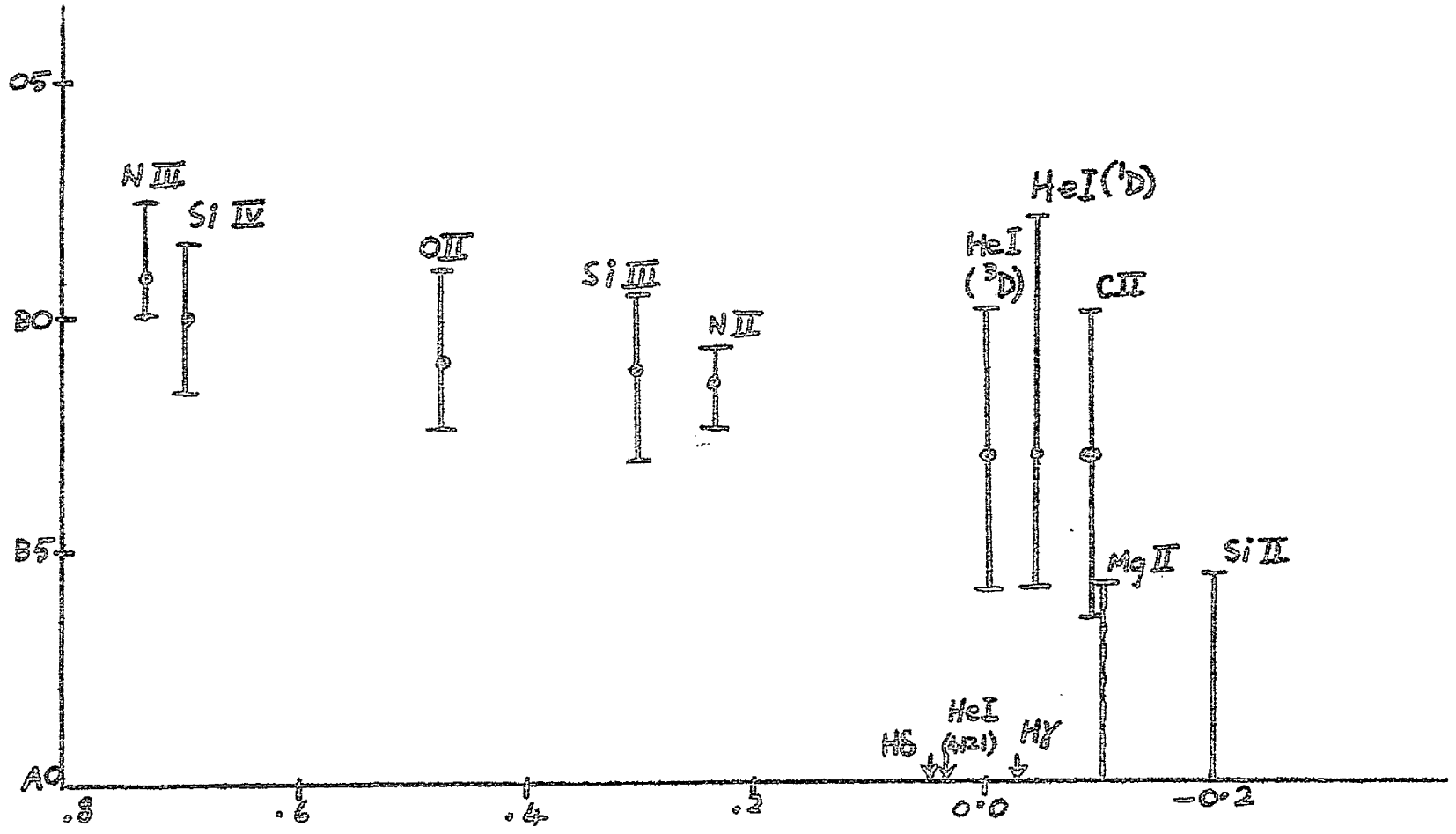

T_{max}/ρ diegram for $T = 1+x$

Figure 20

over the inner hemisphere. Then

$$T'_{max} = 1 + (T_s - 1)\,\bar{x}$$

provided that $T_s \gg T'_{max}$, hence

$$\bar{x} \doteq \frac{T'_{max} - 1}{T_s - 1}$$

T'_{max} is the effective temperature corresponding to the colour temperature T_{max}. Take $T'_{max} = 20{,}000^0$, corresponding to a line with maximum strength at B1 (e.g. OII). Then from the table below

T_s	$\bar{x}$
$20{,}000^0$	1
30,000	1/3
40,000	1/5
50,000	1/7

and from the observations it is clear that a temperature T_s much higher than $30{,}000^0$ is unacceptable as the displacements of the OII lines would then be too small. This corresponds to about O8.

In conclusion, the T_{max}/ρ diagrams of 57 Cygni are accountable if the temperature is taken to rise smoothly from $T = 15{,}000^0$ (B4.5)

to $22{,}000^{\circ} \leq T_s \leq 30{,}000^{\circ}$ (B0 to O8 at the sub-stellar point).

14. A Further Difficulty. A plot of the ρ/λ diagrams corresponding to the three T(x) distributions reveals no indication of any wavelength correlation:- e.g. figure 21 .

15. The fact that temperature distributions with $T_s \leqslant 2^{\frac{1}{4}} T_e$ fail by at least two orders of magnitude to duplicate the observed ρ/λ diagram, indicates that the Planck function explanation is insufficient. (See also §B2 of chapter II). Some major effect must occur on 57 Cygni which has not been allowed for.

As

(i) $T_s \gg 2^{\frac{1}{4}} T_e$

(ii) the observed ρ/λ correlation is much greater than that expected,

it is clear that the physics of the reflection effect adopted so far is inadequate to account for the observations of 57 Cygni, and I decided to abandon the attempt to find an accurate T(x) distribution.

Some speculations as to the possible causes

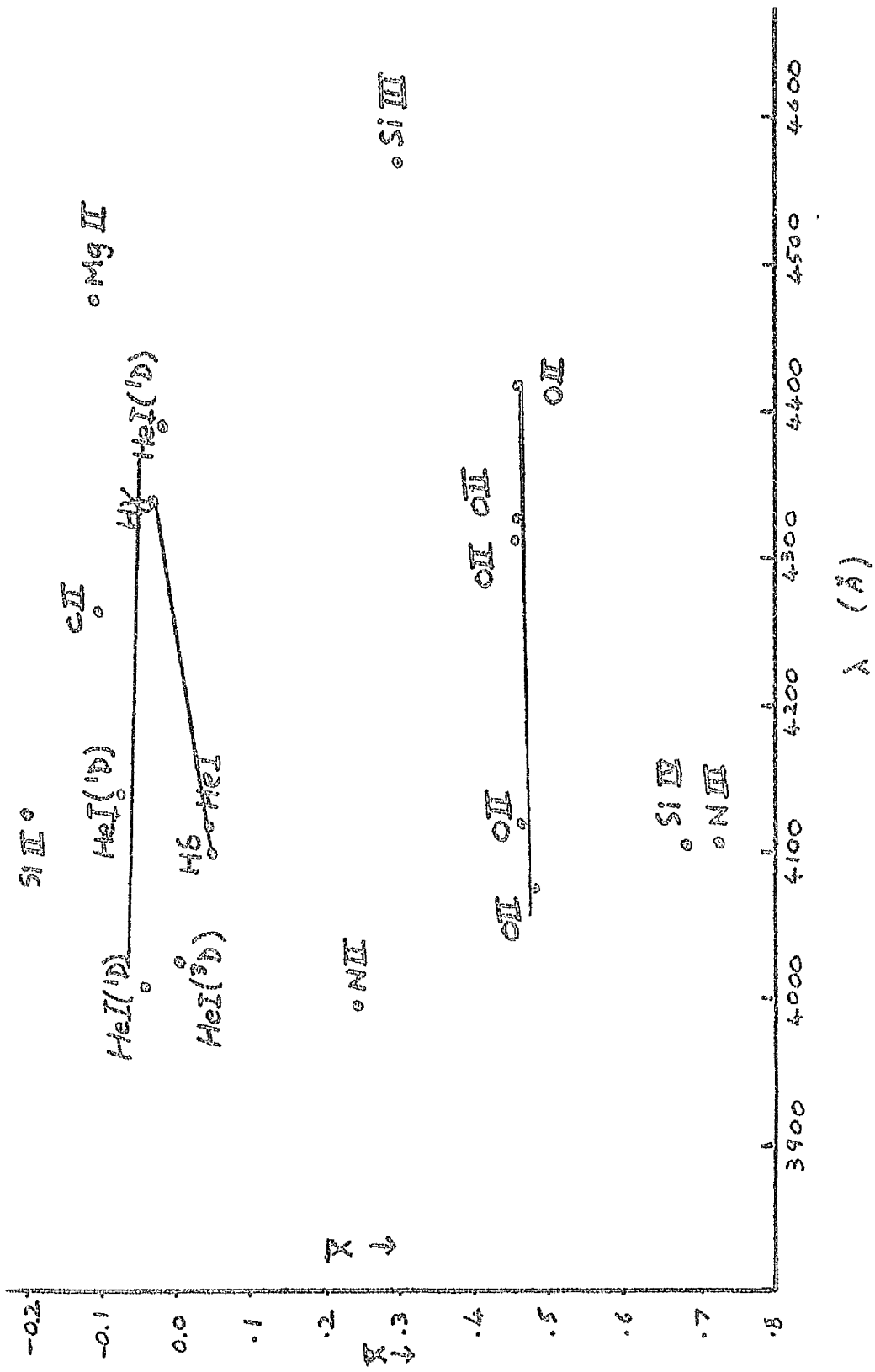
ρ/λ (or x̄/λ) diagram for τ = 1+x (0 ≤ x ≤ 1)
λ (Å)
3900
4000
4100
4200
4300
4400
4500
4600
-0.2
-0.1
0.0
.1
.2
.3
.4
.5
.6
.7
.8
x̄ →
Si II
Mg II
C II
He I(¹D)
He I(³D)
Hδ
Hε
He I(¹D)
He I(³D)
N II
O II
O II
O II
O II
Si II
N III
Si III

Figure 21

of the difficulties above are described in chapter II.

Chapter II. FURTHER ANALYSIS AND INTERPRETATION

'----function
Is smother'd in surmise.'

SHAKESPEARE
(Macbeth)

A. THE TEMPERATURE DIFFICULTY

The result that $T_s \gg 2^{\frac{1}{4}} T_e$ is so surprising that is is as well to see whether this conclusion can be avoided. Two areas where error might arise are:-

(1) The data of RUDNICK and WILLIAMS might be unsuitable as a measure of the variation of line strength over the star.

(2) The conversion from spectral type to effective temperature might be inaccurate; for

example the temperature scale itself for early type stars may be erroneous. A perusal of the literature indicated that disagreement between authors is marked for early type stars, amounting to over $10{,}000^{\circ}$ (effective) for BO. It was decided to investigate this discrepancy.

1. The W(T) data. PISMIS[†] has shown that, statistically, the reflection effect in close binary systems is such that there is a heating of the inner surfaces of the stars: there is no evidence that in any system radiation is reflected without being considerably changed, in quality, by the atmosphere on which it is incident. To this extent, therefore, we may expect the W(T) data to be an appropriate measure of the variation of line strength with spectral type over the surfaces of the component stars.

The equivalent width of a line in a stellar atmosphere depends not only on temperature, but also on surface gravity g. It is only because g is a unique function of temperature along the early part of the main sequence that one can write $W(T, g_{ms}(T)) = W_{ms}(T)$, where suffix ms refers to the main sequence. The component stars of a close

† Ap. J. 104, 141, 1946.

system must be distorted by rotation and revolution to some extent, causing a variation of local gravity
system must be distorted by rotation and revolution
from point to point. Then at some point on the star, at which there is a temperature T, a given line will have equivalent width $W(T, g_s(T)) = W_s(T)$, where suffix s refers to the star. We would not expect $W_{ms}(T) = W_s(T)$ to hold in general, as $g_{ms}(T) \neq g_s(T)$ in general.

A variation of surface gravity must occur (i) over the surface of each component of 57 Cygni and also (ii) along the main sequence.

(i) For two polytropes of equal mass with $\omega_{rot} = \omega_{rev}$, the shape of each star is that of an ellipsoid with three unequal axes, the longest being directed towards the companion and the shortest being the polar axis, where the ratios are, according to LUYTEN (1938)†

polar:	$1 - \frac{2}{3}\epsilon$	$- \frac{1}{5}\zeta$
medium:	$1 + \frac{1}{3}\epsilon$	$- \frac{1}{5}\zeta$
longest:	$1 + \frac{1}{3}\epsilon$	$+ \frac{2}{5}\zeta$

To the fifth order in (R/a), we have $\epsilon = \left(\frac{R}{a}\right)^3 \Delta_2$, $\zeta = \frac{3}{7}\left(\frac{R}{a}\right)^3 \Delta_2$ and

$$\frac{\text{Longest diameter}}{\text{Polar diameter}} = \frac{1 + \frac{4}{3}\left(\frac{R}{a}\right)^3 \Delta_2}{1 - \frac{7}{6}\left(\frac{R}{a}\right)^3 \Delta_2}$$

† M.N. 98, 459.

Δ_2 is a constant related to the degree of the polytrope, and varies from 2.5 for a homogeneous star (n = 0) to 1.0 for a Roche model (n = 4).

Roche		Homogeneous	
s/R	longest/polar	s/R	longest/polar
0	1.37	0	2.16
½	1.17	½	1.49
1	1.10	1	1.26
1½	1.06	1½	1.15
2	1.04	2	1.10

(ii) Figure 22 demonstrates the change of surface gravity with spectral type for main sequence stars, derived from masses and radii tabulated in AQ.

Neglecting for simplicity the departure of the stars from the spherical shape, the surface g at the hotspots is 0.38 in solar units (corresponding to B4.5), whereas according to the previous simple model W(spectral type) data should correspond to not earlier than B3.5 and g = 0.32. The effect of an increase of $\frac{.38}{.32}$ = 20% in g on the equivalent widths of absorption lines should be considered.

The influence of gravity manifests itself

also in the difference in spectra of giant and dwarf stars and we may adapt the calculation used in discussing this effect (the absolute magnitude effect):-

If N_n = no of ionised atoms of an element in state n per unit volume,

N_o = no of (ionised + neutral) atoms of an element in state n per unit volume,

then

$$\frac{N_n}{N_o} = \frac{n^2 e^{-\frac{W_n}{kT}}}{1 + \frac{1}{N_e} G(T)}$$

where N_e = no of electrons per unit volume, and

$$G(T) = \frac{(2\pi m k T)^{3/2}}{h^3} \; 2 \frac{g_{ion}}{g_{neut}} e^{-W_i/kT}$$

where (g_i, g_n) are appropriate statistical weights.

Let g_{57} = surface gravity at a point on 57 Cygni corresponding to a particular temperature T;

g_{ms} = surface gravity on a star on the main sequence corresponding to the same temperature.

Then

$$\frac{N_n(g_{57})}{N_n(g_{ms})} = \frac{1 + \frac{1}{N_e(g_{ms})} G(T)}{1 + \frac{1}{N_e(g_{57})} G(T)}$$

and since $P_e = N_e kT$,

$$\frac{N_e(g_{57})}{N_e(g_{ms})} = \frac{P_e(g_{57})}{P_e(g_{ms})}$$

P_e is the electron pressure.

If we suppose that 57 Cygni is at a high enough temperature for all the hydrogen to be ionised, then since hydrogen is presumably the predominant element, the electron pressure is half the gas pressure and we may write

$$\frac{N_e(g_{57})}{N_e(g_{ms})} = \frac{P(g_{57})}{P(g_{ms})}$$

where P is the total gas pressure.

Since

$$\frac{dP}{d\tau} = \frac{g}{\kappa}$$

$\bar{\kappa}$ being a mean absorption coefficient, we have $P \doteq g\bar{\tau}/\bar{\kappa}$ supposing that $\bar{\kappa}$ does not vary greatly throughout the region in which absorption lines are formed. $\bar{\tau}$ is a mean optical depth. Then we may write, approximately,

$$\frac{N_e(g_{57})}{N_e(g_{ms})} = \frac{g_{57}}{g_{ms}}$$

Hence

$$\frac{N_n(g_{57})}{N_n(g_{ms})} \doteq \frac{1 + \frac{g_{57}}{g_{ms}} \frac{G(T)}{N_e(g_{57})}}{1 + \frac{G(T)}{N_e(g_{57})}}$$

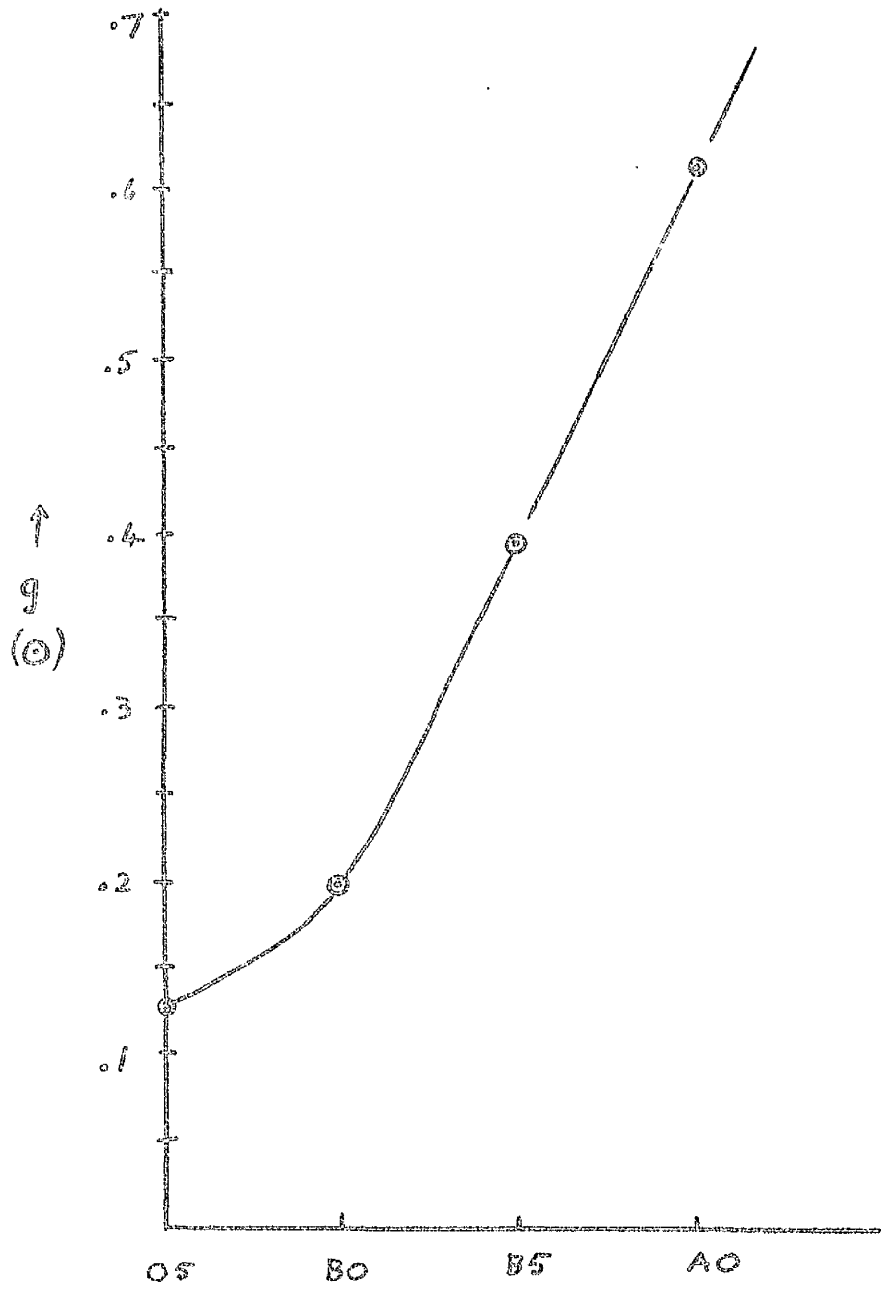

Surface gravity against spectral type for main-sequence stars.

Figure 22

If we take $W \propto N_n$, then

$$\frac{W(g_{57}, T)}{W(g_{ms}, T)} \leq \frac{g_{57}}{g_{ms}}$$

Applying this to the sub-stellar points, we have

$$\frac{W(g_{57}, T_s)}{W(g_{ms}, T_s)} \leq \frac{0.38}{0.32} = 1.19$$

It follows that the use of the W(T) data leads to an underestimate of the strength of absorption lines around the sub-stellar points, but that the increase is likely to be less than 20%. This effect corresponds to a slight change in the value of W in the expression

$$W = 1 + \omega_1 \Delta T$$

and therefore does not appreciably change the conclusion of chapter I that the temperature rise is an order of magnitude greater than expected.

2. The Temperature Scale. Four types of temperature are used here:-

1) excitation temperature, which occurs in Boltzmann's equation

2) ionisation temperature, which occurs in Saha's equation.

3) colour temperature, which occurs in Planck's law; that is, T_c would be derived for some wavelength range from the spectrophotometric gradient in the range.

4) effective temperature, which is defined by $L = 4\pi R^2 \sigma T_e^4$ where (L,R) are the luminosity and radius of the star, and is Stefan's constant.

The restriction that $T \leqslant 2^{\frac{1}{4}} T_e$ refers of course to effective temperature.

One of the earliest effective temperature scales for early type stars was introduced by KUIPER† (1938). For stars of type O and B, effective temperature was found from a theoretical study of the maxima of certain spectral series, discussed on the basis of the theory of the continuous absorption coefficient given by PANNEKOEK (1936). Taking surface gravity to be constant ($\log g = 4.4$) for main sequence stars, KUIPER derived the result summarised in figure 23.

A temperature scale proposed by KOPAL* in 1955 relied on three early type eclipsing systems for which parallaxes and radii were available:-

Aur A	$T_e = 10{,}700^{\circ} \pm 500^{\circ}$	Type A0
Per A	$T_e = 12{,}200^{\circ} \pm 500^{\circ}$	Type B8
μ' Sco A	$T_e = 16{,}600^{\circ} \pm 500^{\circ}$	Type B3

† Ap. J. 88, 429

* Ann. d'Ap. 18, 379.

The scale derived by KOPAL differs from that due to UNDERHILL† et.al., derived from model atmospheres, by about 10,000°. This discrepancy appears in the range B0 - B5 or so, which range depends considerably on the value of effective temperature deduced for μ' Sco A, whose parallax was derived by KAPTEYN in 1914 on the assumption that it is a member of the Scorpio-Centaurus Group. Using a more recent parallax for the group due to BERTIAU (1958), HARRISS* increases the deduced T_e for μ' Sco A by about 10,000°, eliminating the discrepancy between the empirically determined temperatures and those found from theoretical atmospheres. According to HARRISS, the star is of MKK type B1.5 V and has $T_e = 27,500°$.

Nevertheless the parallax of μ' Sco A remains uncertain, particularly as the existence of the Scorpio-Centaurus Group has recently been doubted. The MKK type B1.5, given by HARRISS, corresponds to about B1 on the HD system. This is such a large difference from the earlier estimate that the spectral type must also be regarded as uncertain. The binary has a period of $1^d.4463$ and must therefore be almost a contact system.

* Basic Astronomical Data, Vol III, p. 263 (1963). † Pub. D.A.O. X, 19, 1957.

It is likely that a spectroscopic reflection effect similar to that on 57 Cygni is found in the binary: this would account for the discrepancy between the estimates of the spectral type. At any rate, the system cannot be relied upon to provide an accurate plot on the spectral type/ effective temperature diagram.

In his compendium on the subject, HARRISS (1936) states that T_e(spectral type) was first obtained for the MKK system of classification by KEENAN and MORGAN (1951) using the temperature scales of KUIPER and of STEBBINS and WHITFORD (1945). HARRISS revises this in various ways taking, for example, B0 V to have a temperature of 30,000° rather than 25,000°. Some of his results are shown in figure 23.

STROM(1964)† has computed a grid of early type atmospheres using an IBM 7090, on the assumption of radiative, hydrostatic and local thermodynamic equilibria. The integrated flux in the models was constant to within a few parts perthousand. A photoelectric scanner was used to obtain spectrophotometric observations of a group of B-type stars in the Pleiades. The effective

† Smithsonian Institution, Special Report No. 167, 293.

temperatures were deduced (by comparing observed and calculated monochromatic fluxes) to within $\pm 500^{o}$. These observations, combined with the spectrophotometric data of OKE and BLESS, give a scale of effective temperature in good agreement with that of HARRISS, except at A0.

KOPYLOV† (1963) has determined the relationship between effective temperature and spectral type by reference to a considerable number of published atmospheric models. These were fitted on to a homogeneous spectral sequence of real stars by an analysis of the spectral characteristics of the models.

Independently, T_{eff}(spectral type) was found from models of the internal structures of stars on the zero-age main sequence (e.g. HOYLE* 1960).

MKK	T_{eff}	T_{ion}	T_{exc}	ex:ion	ex:eff	ion:eff
O8	39,200	33,000	29,500	.89	.75	.84
O9	35,300	29,500	26,700	.91	.76	.84
B0	31,400	25,700	24,200	.94	.77	.82
B1	27,300	22,500	21,600	.96	.79	.82
B2	23,700	20,000	19,500	.98	.82	.84
B3	20,200	17,200	17,200	1.00	.85	.85
B5	17,400	15,000	15,000	1.00	.86	.86
B6.5	15,000	13,000	13,500	1.04	.90	.87
B8	12,800	11,200	11,700	1.04	.91	.88
B9	10,750	9,800	9,800	1.00	.92	.91
A0	9,850	8,850	8,950	1.01	.91	.90

Table 5

† Astrophys. Obs. Crimea, 30, 69. * M.N. 120, 22.

From figure 23 it is evident that if we neglect the earlier results of KUIPER and KOPAL, agreement between authors is satisfactory, and the discrepancy of $10{,}000^{\circ}$ which applied to stars around B0 no longer appears. The rise in temperature due to the reflection effect on 57 Cygni should therefore correspond to a change of only about one half of one spectral sub-division, a conclusion which is strengthened by KOPYLOV's result that $T_{eff} > T_{ion} > T_{exc}$.

3. The existence of the large rise in temperature over the surfaces of the components, although completely at variance with the simple physical picture postulated by KOPAL and others, is accepted here as there seems to be no other way in which the behaviour and visibility of some of the absorption lines can be explained. As a final negative check on the reality of the effect it was decided to see whether the photometric consequences of such a large temperature variation are compatible with the observations.

4. <u>The Magnitude Variation</u>. 57 Cygni is listed in the catalogues as a 'suspected variable'.

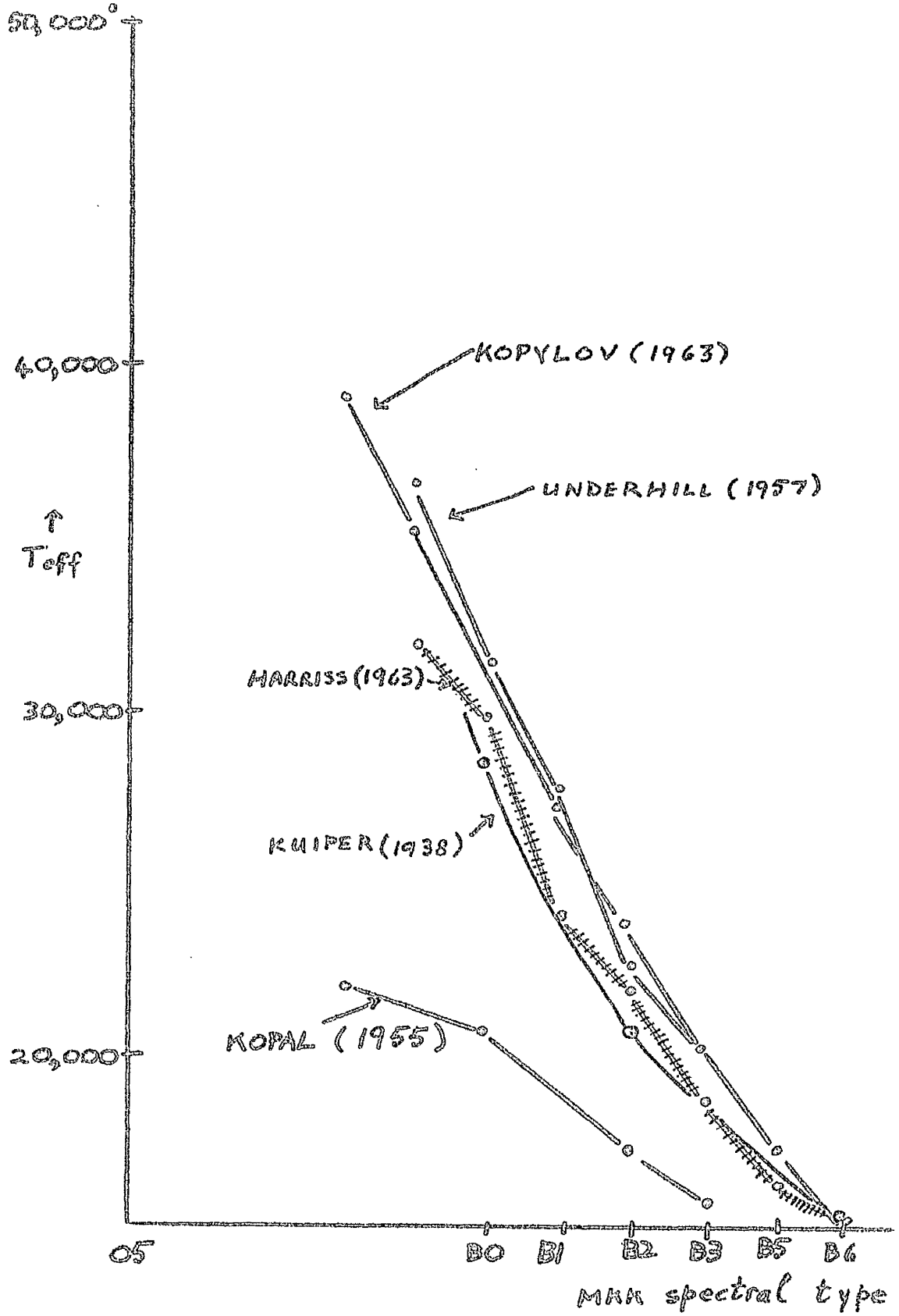

Effective temperature against spectral type

Figure 23

Dr. OVENDEN has observed the star photometrically in a number of wavelength ranges over a six-week period, but the observations have not at the time of writing been reduced. At present it can only be said that the variation of magnitude in the visual range over a cycle must be less than about $0^m.15$: thus $\Delta m_\lambda \leqslant 0^m.15$ in an obvious notation. The photometric consequences of the temperature variation must therefore be comparatively small if this explanation is to be accepted. This suggests that some constraint might be applied to the model.

In figure 24, C is the centre of the reflecting star and H is the sub-stellar point. P is an arbitrary point on the stellar surface. Then $\epsilon = O\hat{C}H$ is a measure of the phase of the system: if $\epsilon = 90^\circ$ the stars are in the nodes, while if ϵ takes its minimum value $(90^\circ - i)$, the stars posess only the systemic radial velocity. $\delta = P\hat{C}H$. It is to be expected that along the small circle defined by some given δ, the physical characteristics of the atmosphere will not change. In particular the monochromatic brightness J_λ of a unit area is constant and we may write $J_\lambda(\delta)$. In chapter V it is shown that the monochromatic brightness of

the entire system, subject to some assumptions, is given by

$$L_\lambda = \pi\left\{\frac{2}{3} + p + (q - p)\sin^2\epsilon\right\}$$

where

$$p = 2\int_{\delta=0}^{\frac{\pi}{2}} J_\lambda \sin\delta\cos^2\delta\, d\delta$$

$$q = \int_{\delta=0}^{\pi/2} J_\lambda \sin^3\delta\, d\delta$$

$(q - p)$ is usually a negative quantity. Minimum brightness therefore occurs when ϵ takes its maximum value, that is, in the nodes, while the system is brightest when $\epsilon = 90^\circ - i$. Therefore

$$\Delta m_\lambda = 2.5 \log_{10}\left(\frac{L_\lambda(max)}{L_\lambda(min)}\right)$$

$$\doteq \log_e\left(\frac{L_\lambda(max)}{L_\lambda(min)}\right)$$

$$= \frac{L_\lambda(max)}{L_\lambda(min)} - 1$$

for small magnitude changes.

$$\therefore \Delta m_\lambda = \frac{p - q}{\frac{2}{3} + q}\sin^2 i \qquad (1)$$

Equation (1) gives the variation in magnitude to be expected, given the inclination i and a prescribed variation of intensity $J_\lambda(\delta)$ over the stars. The procedure adopted was to assume some particular form for the temperature distribution, leaving some parameters unspecified, and test whether the requirement that $\Delta m_\lambda < 0^m.15$ could be satisfied for reasonable values of the parameters. The value of inclination adopted was 38°, so that $\sin i = 0.62$.

Distributions of the form $J_\lambda = 1 + j \cos^n\delta$, where (j,n) are constants, are shown below for $j = 1$ and various positive integers n (*fig. 25*).

Then

$$p = \tfrac{2}{3} + 2j \int_0^{\frac{\pi}{2}} \cos^{n+2}\delta \sin\delta\, d\delta = \tfrac{2}{3} + \frac{2j}{n+3}$$

$$q = \tfrac{2}{3} + j \int_0^{\pi/2} \cos^n\delta \sin^3\delta\, d\delta$$

$$\therefore \Delta m_\lambda = \frac{0.38j\left\{\int_0^{\pi/2} \cos^n\delta \sin^3\delta\, d\delta - \frac{2}{n+3}\right\}}{\frac{4}{3} + j\left\{\frac{1}{2}\int_0^{\frac{\pi}{2}} \cos^n\delta \sin^3\delta\, d\delta + \frac{1}{n+3}\right\}} \qquad (\sin^2 i = .38$$

for $n = 1$, $\Delta m_\lambda = \dfrac{3j \sin^2 i}{16 + 3j}$

$n = 2$, $\Delta m_\lambda = \dfrac{4j \sin^2 i}{20 + 2j}$

$n = 3$, $\Delta m_\lambda = \dfrac{3j \sin^2 i}{16 + j}$

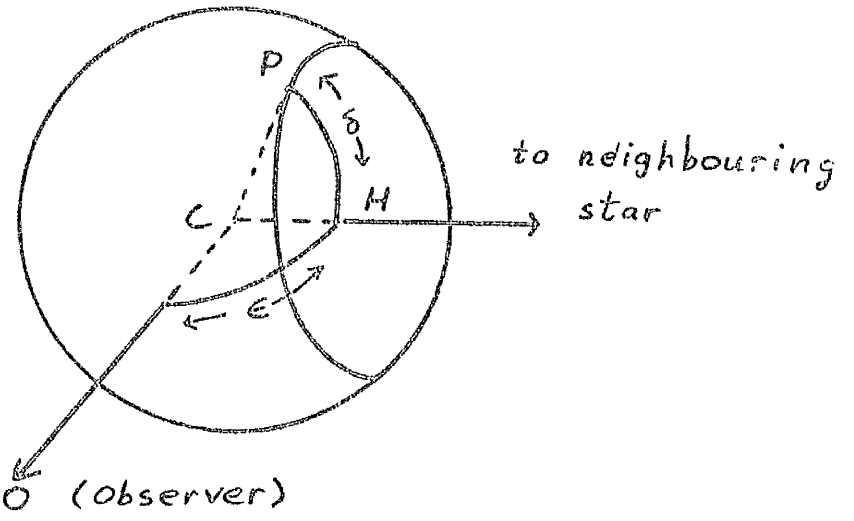

Figure 24

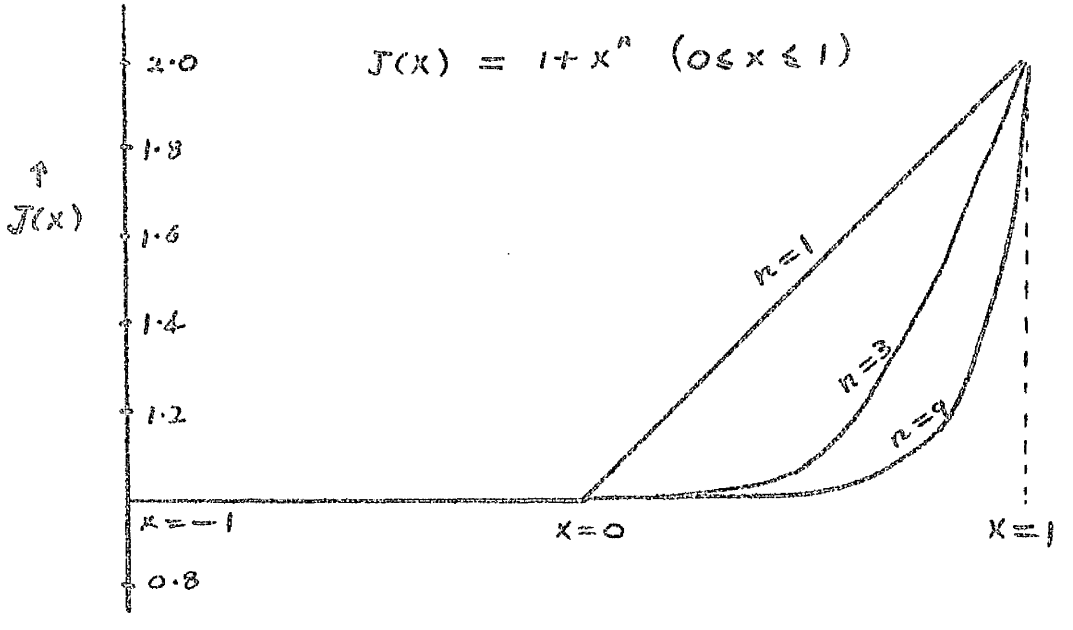

Figure 25

$$n = 4, \quad \Delta m_\lambda = \frac{24\, j \sin^2 i}{150 + 6j}$$

$$\vdots$$

$$n = 9, \quad \Delta m_\lambda = \frac{9\, j \sin^2 i}{80 + j}$$

(as $j \to \infty$, $\Delta m_\lambda \to n \sin^2 i$).

The T_{max}/P diagram can be explained if it is supposed that the temperature rises to $T_s = 2$ or so in terms of the effective temperature T_e over the outwards hemispheres. From tables of the Planck function we then have $B(T_s)/B(T_e) = 3$, which implies that $j = 2$. Then for

$$n = 1, \quad \Delta m_\lambda = 0.27 \sin^2 i$$

$$n = 2, \quad \Delta m_\lambda = 0.33 \sin^2 i$$

$$n = 3, \quad \Delta m_\lambda = 0.33 \sin^2 i$$

$$n = 4, \quad \Delta m_\lambda = 0.30 \sin^2 i$$

$$\vdots$$

$$n = 9, \quad \Delta m_\lambda = 0.22 \sin^2 i$$

In spite of a wide variety of forms of temperature distribution, the theoretical magnitude variation is small and for a reasonable value of inclination there is no conflict with the observation that 57 Cygni does not vary greatly in brightness. Thus for $i = 38^\circ$, $n = 1$, we have

$\Delta m_\lambda = 0^m.14$. If the real temperature distribution is convex downwards, the corresponding intensity distribution may be fitted approximately on to a distribution giving the form $J_\lambda(\delta) = B_\lambda(\delta) = 1 + jx^n$.

It remains to be found whether a temperature distribution which is concave downwards will also give a small magnitude variation. A distribution of this form might be represented approximately by a hot polar cap, the pole being the sub-stellar point. Thus for

$$B_\lambda(T) = W > 1, \text{ for } \quad 0 \leqslant \delta \leqslant \delta_0 \leqslant \frac{\pi}{2}$$

$$B_\lambda(T) = 1 \text{ otherwise,}$$

Since

$$W \int_{\delta=0}^{\delta_0} + \int_{\delta_0}^{\frac{\pi}{2}} = (W-1) \int_0^{\delta_0} + \int_0^{\frac{\pi}{2}}$$

then after reduction we find that

$$p - q = \frac{1}{3}(W - 1) \cos\delta_0 \left\{ 2 + \sin\delta_0 - 2\cos^2\delta_0 \right\}$$

$$q = \frac{2}{3} - \frac{1}{3}(W - 1)\left\{ 2(\cos\delta_0 - 1) + \sin\delta_0 \cos\delta_0 \right\}$$

$$\therefore \Delta m_\lambda = \frac{(W-1)\cos\delta_0 \left\{ 2 + \sin\delta_0 - 2\cos^2\delta_0 \right\}}{4 - (W-1)\left\{ 2(\cos\delta_0 - 1) + \sin\delta_0 \cos\delta_0 \right\}} \sin^2 i$$

For $\delta_0 = 0^0$, $\Delta m_\lambda = 0$,

$$\delta_0 = 30^\circ, \quad \Delta m_\lambda = \frac{0.866\,(W-1)}{4 - 0.165\,(W-1)} \sin^2 i$$

$$\delta_0 = 45^\circ, \quad \Delta m_\lambda = \frac{1.208\,(W-1)}{4 + 0.086\,(W-1)} \sin^2 i$$

$$\delta_0 = 60^\circ, \quad \Delta m_\lambda = \frac{1.183\,(W-1)}{4 + 0.567\,(W-1)} \sin^2 i$$

$$\delta_0 = 90^\circ, \quad \Delta m_\lambda = 0.$$

Again, for a reasonable value of the inclination and for W = 3, the magnitude variation is small.

The shape of the distribution has little effect on Δm_λ. However if it should be possible to isolate that part of Δm_λ due to the reflection effect, then it should be possible to find j or W within certain limits. In particular it should be possible to test the hypothesis that $T_s \gg 2^{\frac{1}{4}} T_e$.

The main conclusion of the present section is that a temperature distribution high enough to account for the spectroscopic observations need not conflict with the observation that $\Delta m_\lambda < 0^m.15$.

Possible Explanations

5. Circulation Currents. A vertical velocity V cm/sec on one star, produced by the heating

effect of the other, requires a net accession of energy of amount Vg ergs/sec/gm. (g being the local gravity), that is, $V\rho g$ ergs/c.c./sec. Now if E ergs/cm.^{2}/sec., of energy are emitted by the stellar surface, then as the stars are identical the amount incident on the neighbouring atmosphere is Ef, where $0 < f < 1$. In a uniform atmosphere of height h cm., the rate of deposition of energy in a cubic centimetre is Ef/h ergs/c.c./sec.

If a fraction p of this energy is converted into vertical motion,

$$V\rho g = \frac{Efp}{h}$$

Typically, $\rho = 10^{-9}$; $g = 10^{3}$; $h = 10^{9}$; $E = 10^{14}$; $f = 10^{-1}$

$$\therefore \quad \frac{V}{p} = 10^{12} \text{ cm./sec} \qquad 0 \leq p \leq 1$$

If a substantial fraction of the incident energy were converted to motion, the resulting velocities would be relativistic. p must be a negligibly small quantity, say 10^{-3} or less, as there is no evidence in the spectrum of velocities of 10^{3}km/sec. Nevertheless there is a plentiful supply of energy with which circulation currents could be maintained, and the circulation velocity might be, say, of the order

of 10 - 20 km/sec.

It can be shown that there must be circulation currents on the stars:-

From the equation of hydrostatic equilibrium grad $P = \rho$ grad Φ, it is a well-known result that temperature T (as well as P and ρ) is constant over a surface of constant potential Φ, i.e. $T = T(\Phi)$. However T varies due to the reflection effect over the surfaces of the components of 57 Cygni. Thus there arises a contradiction, as these surfaces are of constant potential. Hydrostatic equilibrium cannot hold in the atmospheres and there must be circulation.

By analogy with the HADLEY cells which occur in the terrestial atmosphere (and are caused by solar heating) it is likely that the circulation currents rise at the sub-stellar point, spread outwards and sink after they have radiated their excess energy:-

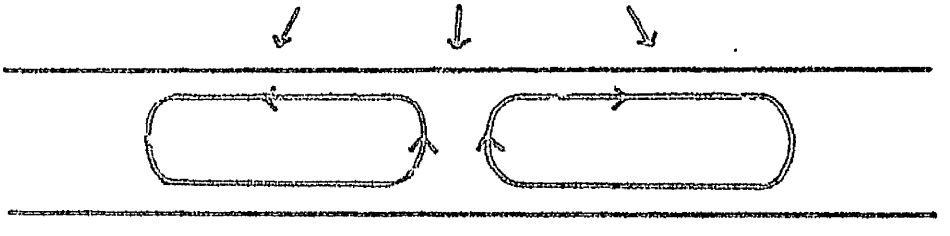

As the temperature immediately below the photosphere may reach 10^{6}°, it is at least possible that a supply of energy adequate to account for the observations might be obtained. The process can operate only if atmospheric material retains a temperature in excess of that of the surrounding for a 'sufficient' length of time, in the sense that an appreciable temperature excess must remain in the time taken for material to rise from the base to the top of the photosphere:-

In the photosphere, the transfer equation with a time-dependent factor has a term, additional to the usual terms, $\frac{1}{c}\frac{\partial I_\nu}{\partial t}$. The factor c in the denominator indicates that the characteristic time a photosphere will take to adjust to a changing radiation field is roughly the time taken by a photon to traverse the atmosphere.

The situation is different at the sub-photospheric level, where the mean free path is of the order of a centimetre (cf 10^{4} km in a B-type photosphere). At this level, the flow of heat across a unit area is $k(T, \rho)$ grad T, where $k(T, \rho)$ is a thermal conductivity depending in some way on the state of the gas. The rate of flow of heat into a unit

elementary volume is therefore

$$\text{div}\{\, k(T, \rho)\ \ \text{grad}\ T\}$$

But by definition this must equal minus the divergence of the radiative flux:

$$\text{div}\ \underset{\sim}{F} = -\ \text{div}\{k(T, \rho)\ \text{grad}\ T\}$$

$$\therefore\ \underset{\sim}{F} = -\ k(T, \rho)\ \text{grad}\ T$$

But the equation of point transfer, valid in sub-photospheric regions, is

$$\underset{\sim}{F} = -\ \frac{16\sigma}{3k_0} \cdot \frac{T^{3+\beta}}{\rho^{1+\alpha}} \cdot \ \text{grad}\ T$$

The thermal conductivity must therefore be given by

$$k(T, \rho) = \frac{16\sigma T^{3+\beta}}{3k_0 \rho^{1+\alpha}}$$

(An absorption coefficient of the form $\kappa = k_0 \rho^{\alpha} T^{-\beta}$ is assumed in the derivation of the transfer equation. σ represents Stefan's constant).

If H is the amount of heat/unit elementary volume of gas, then the rate of increase of H with time is given by

$$\frac{dH}{dt} = \frac{dH}{dT} \cdot \frac{dT}{dt} = \frac{d}{dT}\left(\frac{4\sigma}{c} T^4\right) \frac{dT}{dt}$$

$$= \frac{16\sigma}{c} T^3 \frac{dT}{dt}$$

Again, this equals - div F, by definition.

$$\therefore \frac{16\sigma}{c} T^3 \frac{\partial T}{\partial t} = \operatorname{div}\{K(T,\rho)\,\operatorname{grad} T\}$$

The diffusion equation is thus, finally,

$$T^3 \frac{\partial T}{\partial t} = \left(\frac{1}{3}\frac{c}{K_0}\right) \operatorname{div}\left\{\frac{T^{3+\beta}}{\rho^{1+\alpha}} \operatorname{grad} T\right\}$$

In an equilibrium atmosphere, $T^{3+\beta}/\rho^{1+\alpha} = A$, where A is a known constant. For small perturbations, the diffusion equation is therefore

$$T^3 \frac{\partial T}{\partial t} = \left(\frac{1}{3}\frac{Ac}{K_0}\right) \nabla^2 T$$

Neither equation can be handled analytically. Even the standard numerical techniques for dealing with diffusion equations (e.g. CRANK; Mathematics of Diffusion) are inapplicable. An order of magnitude estimate of the rate of cooling of a hot, rising stream of gas may, however be obtained.

If a mass of gas at temperature T_2 is surrounded by material at a lower temperature T_1, the characteristic cooling time t is given by $t = O\left(\frac{3\rho^2}{T^3} K_0 \frac{L^2}{c}\right)$

where L is the scale height of the region over which the temperature difference exists.

KRAMERS' absorption coefficient is $\kappa = \kappa_0 \rho^{\alpha} T^{-\beta}$ with $\alpha = 1$, $\beta = 3.5$, $\kappa_0 = 3.10^{24} Z(1+X)$ where Z is the proportion by mass of heavy elements (Z=0.03 typically) and X represents the hydrogen content of the atmosphere: X=0.71, say, hence $\kappa_0 = 1.5\ 10^{25}$.

$$\therefore t \sim 1.5\ 10^{13} (\rho L)^2 / T^{3.5}$$

Thus, in the sub-photospheric regions, a deviation from an equilibrium temperature distribution, even over 10^4 kms., would decay in a time of about a second, on taking $\rho \sim 10^{-8}$, $T \sim 4.10^4$, $L \sim 10^9$.

It follows that the circulation current is everywhere at an equilibrium temperature and that the suggested effect cannot operate. The same result holds a fortiori for an electron-scattering atmosphere.

Another consequence of this rapid damping in an unstable situation is that non-radial energy transfer due to circulation currents in the atmosphere of a reflecting star can be

neglected. Furthermore, a study of such currents need not involve consideration of the heat capacity of the atmospheric material. Finally a 'time-lag' of the reflected radiation, when the rotation of the reflecting star is not synchronous with its orbital period, should not be expected.

6. Gaseous Streams. An attempt was made, without success, to invoke the effects of circumstellar material. KOCH has suggested that the asymmetries in the light curves of some secondary components within eclipse can be explained as a consequence of the heating effect of outflowing matter from the primary, impinging on the secondary. KRUSZEWSKI† has shown that, when ejection of mass arises from non-synchronism, the various particle trajectories which arise tend to converge just before landing, resulting in a relatively localised 'hotspot'.

These results apply to stars for which $\omega_{rot} \neq \omega_{rev}$ and the secondary is about a tenth as massive as the primary; they cannot be applied to 57 Cygni. It is possible, however, that a similar effect operates in this system. In chapter III it is

† Acta Ast., 14, 241, 1964.

shown that the hotspots of the stars coincide with their respective sub-stellar points. Then any gaseous streams giving rise to atmospheric heating by collision are likely to interpenetrate. As the mean free path of an atom in the stream is much less than the dimension of a binary system, the streams cannot interpenetrate and the explanation seems unlikely.

7. Variation of Absorption Coefficient. Possibly the incident radiation modifies the absorption coefficient of the atmosphere in such a way as to expose the hotter layers below. The radiative flux $\mathcal{F}$ and the absorption coefficient κ are related by

$$\mathcal{F} \propto \frac{1}{\kappa} \operatorname{grad} T$$

and it could be argued that the atmosphere will adjust itself to a change in κ by altering its temperature gradient rather than its net flux. This question is considered further in the following section.

8. Secular Stability. The high-temperature lines are visible on both stars over all phases of 57 Cygni, including those phases during which the 'hot' hemisphere of one star is partially hidden from the observer. This implies that $T \gg 2^{\frac{1}{4}} T_e$ over an appreciable part of the stellar surfaces. Consequently the energy emitted over the inner hemisphere of each star must be considerably in excess of that over the averted hemisphere.

Comparing the luminosity L_i of the star with the luminosity L_o it would have in the absence of a temperature rise,

$$\frac{L_i}{L_o} = \frac{\iint T_i^4 \, dA}{\iint T_o^4 \, dA}$$

Suppose $T_i = T_o(1+\alpha x)$ (2)

α a constant.

Then

$$\frac{L_i}{L_o} = \frac{\int_{-1}^{0} \sqrt{(1-x^2)}\, dx + \int_{0}^{1} \sqrt{(1-x^2)}(1+\alpha x)^4 \, dx}{2\int_{-1}^{0} \sqrt{(1-x^2)}\, dx}$$

$$\therefore \frac{L_i}{L_0} = 1 + \frac{2}{\pi}\left[\frac{4}{3}\alpha + \frac{3\pi}{8}\alpha^2 + \frac{8}{15}\alpha^3 + \frac{\pi}{32}\alpha^4\right]$$

For example, for $\alpha = 1$, corresponding to a hotspot effective temperature twice that of the averted hemisphere,

$$\frac{L_i}{L_0} = 3.001$$

Consequently the component stars of 57 Cygni are radiating much more energy, measured roughly by L_i, than is being produced by the nuclear reactions of the interior, measured by L_0. The conclusion rests on the assumption that $T \gg 2^{\frac{1}{4}}T_e$ over much of the inner hemispheres, and does not depend on the adoption of any particular T(x) distribution such as (2) above.

Therefore either

(i) the interpretation so far adopted, viz. that the appearance and behaviour of the high excitation lines can only be due to very hot inner hemispheres, must be false,

or

(ii) the stars must be secularly unstable.

In the present section the alternative (ii) is discussed.

As the excess energy $(L_i - L_o)$ is comparable with the nuclear energy production L_o, and as the energy/second radiated by a contracting star is comparable with its rate of nuclear energy production when it reaches the main sequence then the components of 57 Cygni must be contracting in a time comparable with their classical KELVIN contraction time 5.10^7 M/L years, say 3.10^6 years. The evolution of these B-type stars must then be profoundly different, if we accept $T \gg 2^{\frac{1}{4}} T_e$, from the evolution of solitary early-type stars.

The implication of the above remarks is that a change in the surface conditions of a star, induced by a neighbour, can give rise to an emission of excess energy such that the star must contract to supply the deficiency.

This appears to contradict the VOGT-RUSSELL theorem, according to which a star of given mass and chemical composition has a uniquely determined structure. Peculiar circumstances arising in the atmosphere cannot therefore appreciably affect

the entire stellar structure; in particular the star cannot be made unstable by, say, a change in the surface absorption coefficient.

The basis of the VOGT-RUSSELL theorem is that we have a number of internal structure equations (hydrostatic equation, equation of state, etc.) and the same number of boundary conditions ($P = T = \rho = 0$ at the surface, for example). The structure must therefore be uniquely defined in the absence of degeneracies and the like. Certainly no change in the surface conditions is produced by a change in the atmospheric absorption coefficient.

However, it is supposed in the theorem that the rate of energy generation/gram, ϵ , depends only on the state of the gas: $\epsilon = \epsilon(\rho, T)$. If the star is contracting or expanding, energy released by gravitational contraction must be added to the nuclear energy source: $\epsilon = \epsilon_0(\rho, T) + f(\rho, T, v)$. f depends in some way on the velocity v of contraction of the gas. The equations contain an additional unknown and without some further hypothesis a unique solution is not possible.

As the VOGT-RUSSELL theorem presupposes stability ($f = 0$), it cannot be used to prove stability as otherwise a circular argument is involved. Hence the question of whether a secular instability can be produced by a change in surface conditions cannot be resolved by the VOGT-RUSSELL theorem. (An example of contractional instability caused by peculiar atmospheric conditions which do not change the surface conditions $T = 0$, etc, is provided by the circulation currents of § 5. If the heat capacity of a stellar atmosphere had turned out to be large, an upwelling of hot material from below would have given rise to gravitational collapse.)

In the absence of any general theorem stating the circumstances in which instability of a star will be produced by conditions prevailing in its atmosphere, the question of whether a high temperature (i.e. $T_s \gg 2^{\frac{1}{4}} T_e$) may be produced by virtue of incident radiation from the neighbour, should perhaps be left open.

However the effect is considered unlikely. The effect of an increased intensity of radiation is to increase κ, if the absorption is due to ionised hydrogen, and this is the reverse of what we require.

9. Deviation from a Classical Atmosphere. If the hypothesis of the previous section is rejected, then we require a mechanism which will produce a high excitation temperature in a medium whose effective temperature is low by comparison. This can only be achieved by a departure from local thermodynamic equilibrium, either in the sense of an excess of high-energy photons, or by collisional excitation corresponding to a high electron temperature ($T \sim 30{,}000^{\circ}$ atthe hotspots).

(i) High-energy Photons. In his 1926 paper, EDDINGTON remarked that 'The radiation from S_1 has a strategic advantage in that it attacks the atmosphere of S_2 from outside. The absorption for which it is responsible is the last to be imprinted on the spectrum of S_2, and cannot be blurred out by the subsequent experiences of the radiation.'

In the case where S_1 is a cool star, illuminated by a hot star S_2, the ionisation of the inner surface of S_1 will be determined by the energy of the photons incident from S_2. Absorption lines, formed at the top of the photosphere of S_1, will therefore correspond to an ionisation temperature close to the effective temperature of the hot star, although the

increase in the effective temperature of S_1 may be comparatively slight.

When S_1 and S_2 are identical, however, the argument clearly no longer applies, as the illuminating star is then no longer a source of photons whose mean energy is higher than that of the photons from the reflecting star.

An excess of energy at short wavelengths might be sufficient to cause an atmosphere at 15,000° to have some of the characteristics of one at 30,000°. If λ_m is the wavelength at which the Planck function takes its maximum value for some temperature T, then $\lambda_m T = 0.288$ cm.deg. Thus for T = 30,000°, $\lambda_m = 1{,}000$ Å. An appreciable excess of non-thermal emission in the region of 1,000 Å would thus be expected to give rise to lines such as SiIV and NIII.

An ultra-violet excess might be caused by a change in the atmospheric absorption coefficient induced by the incident radiation. If 10% or so increase in the radiation density were to produce such a drastic change in the atmosphere of a B4.5 star (WILLIAMS spectral type) we would expect stars of type B3.5 and earlier to show appreciable ultra-violet excesses, which is not the case. It seems

improbable that the continuous absorption coefficient is so sensitive to a small increase in the intensity of the radiation.

(ii) Excitation by Collisions. A kinetic temperature greater than the radiation temperature of the material arises in the solar chromosphere. If the absorption lines of 57 Cygni originate in a stellar chromosphere, the possibility then arises that its properties vary suitably over the surfaces.

According to Miss UNDERHILL (1965)†

'Any spectral feature in a stellar spectrum that is strong in the theoretical sense will give information about a stellar chromosphere because the strength and shape of a strong line will be governed by the particular conditions characterising the chromosphere rather than the conditions that evolve from applying the conditions of radiative and mechanical equilibrium of the gas and making the simplifying statement that the monochromatic emissivity is that appropriate to a gas in thermodynamic equilibrium at the local temperature.

'If you look at the spectra of O and B stars, you will find that the lines that are used for classification purposes, and which thus determine the spectral type,

† Smithsonian Institution, Special Report No. 174, 384.

are indeed the types of line that one would expect to be useful as criteria of the presence of a chromosphere.'

The kinetic temperature in the upper layers of the stars may therefore be greater than that expected from thermodynamic equilibrium. This heating must be caused by mechanical dissipation of energy in these layers, which energy is usually supposed to rise from the convection zone in the photosphere below. Theoretically a convective envelope is not to be expected in a B-type star, although the observations indicate that they exist (ibid)†.

The noise production from a convection zone is proportional to the fifth or sixth power of the turbulent velocity of the zone. An explanation along the lines suggested thus requires only a slight increase in the turbulence at the hotspots of the stars as compared with the averted hemispheres. This turbulence could arise directly as a consequence of the incident radiation or indirectly from the circulation currents over the inner hemispheres.

In a normal atmosphere, intrinsically weak lines such as NIII would be formed in the upper part

† Special Report No. 167, 232.

of the photosphere ($\bar{\tau}$ = 0.1 or less). The suggestion described above implies that they would arise in the inward-facing regions of the stellar chromospheres, along with strong lines such as $H\gamma$ which probably appear over the entire chromosphere.

It is difficult to evaluate this hypothesis. In the first place there is no theory of stellar chromospheres; secondly there is no theory concerning the influence of incident radiation (or surface currents) on the turbulent velocities in an atmosphere and as it is quite likely that the properties of this chromosphere will vary over the surface of each component of the binary, it is clear that a detailed interpretation of the T_{max}/ρ diagram may be very complex.

B. THE WAVELENGTH DIFFICULTY

1. If the temperature at which the equivalent width of a line reaches its maximum on the main sequence varies systematically with wavelength, a ρ/λ correlation would be introduced by virtue of the T_{max}/λ correlation. No such correlation exists as can be seen by plotting sensitivity of various lines against wavelength, and anyhow it would be expected that in the event of such a relationship existing, the numerical models would then show a ρ/λ correlation. The observed diagram must therefore correspond to some physical phenomenon occurring on the star.

2. It has been shown in §7 of chapter 1 that ρ/λ should be numerically largest for lines whose equivalent widths are completely independent of temperature, that is $W(T)$ = constant. For such a line, with the usual assumptions (no limb-darkening spherical stars, etc.) we have

$$\bar{x} = \frac{\int_{-1}^{1} x\sqrt{(1-x^2)}\, B_\lambda\{T(x)\}\,dx}{\int_{-1}^{1} \sqrt{(1-x^2)}\, B_\lambda\{T(x)\}\,dx}$$

As the Planck function is virtually linear in temperature over the range of temperature implied by the S/ρ diagram† we may put

$$B_\lambda(T) = 1 \qquad -1 \leqslant x < 0$$
$$B_\lambda(T) = 1 - b_\lambda + b_\lambda T \qquad 0 \leqslant x \leqslant 1$$

Then

$$\bar{x} = \frac{b_\lambda\left[\int_0^1 x\,T(x)\sqrt{(1-x^2)}\,dx - \frac{1}{3}\right]}{\frac{\pi}{2} + b_\lambda\left[\int_0^1 T(x)\sqrt{(1-x^2)}\,dx - \frac{\pi}{4}\right]}$$

For two insensitive lines at wavelengths λ_1 and λ_2

$$\bar{x}_{\lambda_2} - \bar{x}_{\lambda_1} = \frac{\left[\int_0^1 x\,T(x)\sqrt{(1-x^2)}\,dx - \frac{1}{3}\right](b_{\lambda_2} - b_{\lambda_1})}{\frac{\pi}{2} + b_\lambda\left[\int_0^1 T(x)\sqrt{(1-x^2)}\,dx - \frac{\pi}{4}\right]}$$

where in the denominator a mean value b_λ has been taken. This is justified as at

$\lambda_1 = 3934$ Å, $\quad b_{\lambda_1} = 2.078$
$\lambda_2 = 4684$ Å, $\quad b_{\lambda_2} = 1.849$.

† S ≡ sensitivity of absorption line to change in temperature. See Table 1. S/ρ is used occasionally and is interchangeable with T_{max}/ρ.

(λ_1, λ_2) covers the observed λ - range.

Now

$$\int_0^1 x\,\tau(x)\sqrt{(1-x^2)}\,dx \leqslant \tau_s \int_0^1 x\sqrt{(1-x^2)}\,dx = \frac{1}{3}\tau_s$$

and

$$\int_0^1 \tau(x)\sqrt{(1-x^2)}\,dx \geqslant \int_0^1 \sqrt{(1-x^2)}\,dx = \frac{\pi}{4}$$

$$\therefore \quad \bar{x}_{\lambda_2} - \bar{x}_{\lambda_1} < \frac{2}{3\pi}(b_{\lambda_2} - b_{\lambda_1})(\tau_s - 1)$$

$$= 0.049\,(\tau_s - 1)$$

$$\doteq \frac{1}{20}(\tau_s - 1)$$

$$\text{i.e.,} \quad \Delta\rho < \frac{1}{20} V_{eq} \sin i\,(\tau_s - 1)$$

As $\Delta\rho \geqslant 40$ km/sec from figure 6 of chapter 1, and as $\tau_s \leqslant 2$ or thereabouts, we require $V_{eq} \sin i = 800$ km/sec, which is absurd. The value of $\Delta\rho$ cannot be reduced, certainly not to the 5 km/sec or so necessary for the inequality to be reasonably satisfied; and τ_s cannot be increased by the amount necessary to resolve the contradiction, as temperatures of several hundred thousand degrees would then be involved. The conclusion is that the behaviour of the Planck function cannot be invoked to account for the observed ρ/λ diagram. This accounts for

the discrepancies pointed out in § 7 of chapter I.

Possible Explanation

3. Limb-Darkening. We may formally account for the ρ/λ diagram by introducing into the expression for $\bar{x}$ any parameter varying suitably with wavelength. Thus we may introduce a limb-darkening factor of the form $\sum_{n=0}^{\infty} a_n \mu^n$, where $\mu \equiv \cos\theta$, with suitable values for the coefficients a_n. If we suppose the star to be strongly darkened at the longest wavelengths and undarkened at the shortest wavelengths, this might account for the observations.

Suppose that in the range $3900 \leqslant \lambda \leqslant 4700$ (Å) we have

$$I_\lambda(0,\mu) = I_\lambda(0,0)(1-u_\lambda+u_\lambda\cos\theta)$$

Take $$u_\lambda = \frac{1}{800}(\lambda-3900)$$

Now $$K_\lambda = -\frac{1}{\rho}\frac{d\tau_\lambda}{dr}$$

$$= -\frac{1}{\rho}\frac{d\tau}{dr}\cdot\frac{dB_\lambda(\tau)}{d\tau}\cdot\frac{1}{B_\lambda(0)u_\lambda}$$

(since $B_\lambda(\tau_\lambda) = B_\lambda(0)(1-u_\lambda+u_\lambda\tau_\lambda)$)

$$\therefore K_\lambda \propto (\lambda-3900)^{-1}$$

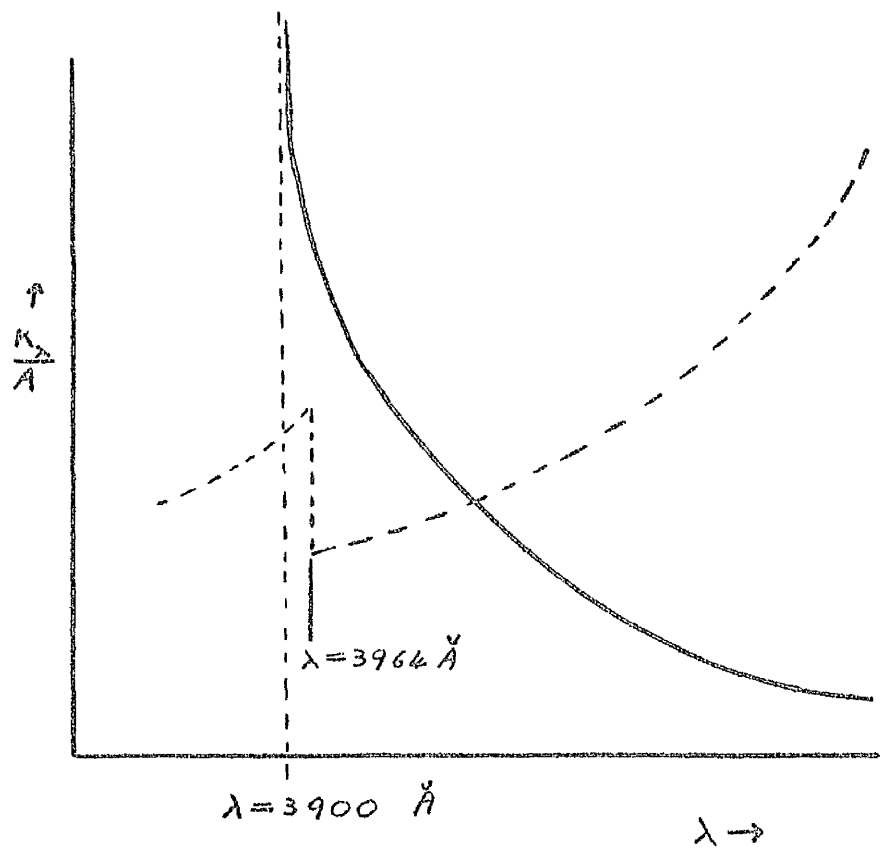

——— relative absorption coefficient required to account for the ρ/λ diagram.

– – – – – absorption coefficient due to hydrogen over the relevant (T, λ) range

Scale is arbitrary; representation is schematic.

Figure 26.

Figure 26 shows a plot of the required relative absorption coefficient against wavelength in the observed range. This is completely different from the absorption coefficient for hydrogen atoms in this range (AMBARTSUMIAN, Theoretical Astrophysics, p. 52) and we must conclude that the limb-darkening required to produce the ρ/λ diagram, apart from being inconsistent with that deduced from a study of eclipsing binaries, leads to an absorption coefficient completely different from that expected from theory.

4. A similar conclusion can be reached concerning the effect of monochromatic gravity-darkening. It is clear from a perusal of KOPAL's table of the coefficient b'_λ in $H_\lambda = b'_\lambda g$ (Z. KOPAL: Close Binary Systems, p. 173) that the variation of b'_λ over the observed wavelength range is too small and goes in the wrong direction.

5. Non-thermal Emission. Suppose, without any attempt at theoretical justification, that the temperature distribution over the star is taken to vary with wavelength: $T = T(\lambda, x)$. Since the larger displacements ρ are correlated with the

shorter wavelengths, we might expect to produce (T_{max}/ρ , ρ/λ) diagrams resembling those observed if, for given x, T increases as λ decreases. A number of attempts were made to reproduce the observed diagrams, the procedure being to assume a function $T(\lambda, x)$ and calculate the diagrams numerically. A slight correlation was generally obtained, but the resemblance to the observed diagrams was poor (A typical example is shown in figure 27).

Now take

$$W(T_1)\ B\ (T_2),\ \text{with}\ T_1 = T_1(x),\ T_2 = T_2(\lambda, x).$$

It must be formally possible to reproduce the observed diagrams as ρ is a function of two quantities: $\rho = \rho(T_{max}, \lambda)$, and we have two disposable functions (T_1, T_2). It is probable that a more satisfactory wavelength diagram could be produced if $T_2(x = 1)$ were taken sufficiently high at shorter wavelengths: but then the Planck function would cease to be a useful measure of such a large non-thermal emission. The possibility then arises that an emission sufficiently large to produce a satisfactory wavelength diagram would conflict with

Figure 27

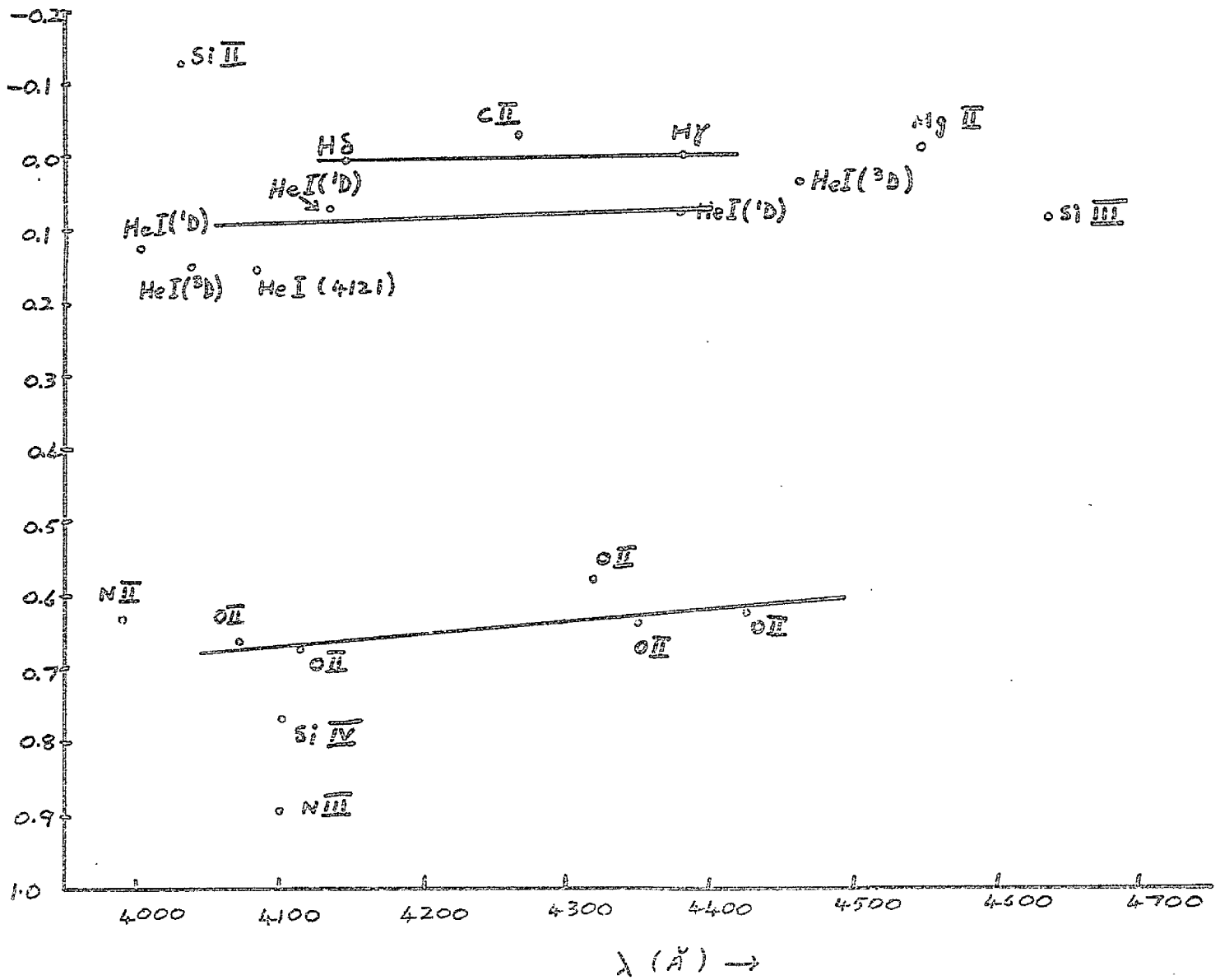

$(\bar{x}_\lambda, \lambda)$ or (ρ, λ) diagram for $T(\lambda, x) = 24{,}600\,[1 + 0{\cdot}6597.10^{-3}(4680 - \lambda)\,x]$ $(0 \leq x \leq$

the observation that 57 Cygni is only marginally variable:-

5.1 Constraints Imposed. The formula for Δm_λ may be used as before, except that the Planck function $B_\lambda(T)$ must now be replaced by the 'non-thermal' quantity $J_\lambda(\delta)$. As before, particular forms of distribution are taken, but with free parameters so that a wide range of real distributions may be approximately fitted on to the theoretical forms by a suitable choice of the parameters. There is now a further constraint to be applied to the model. Consistent with the requirement that $\Delta m_\lambda \leqslant 0^m.15$, we require to produce a difference of displacements of about 40 km/sec. between the temperature-insensitive lines at $\lambda_2 = 4600$ Å and at $\lambda_1 = 3900$ Å. The corresponding $\bar{x}_{\lambda_1} - \bar{x}_{\lambda_2}$ is 0.73 on the model of chapter 1. As there is no guarantee that the non-thermal emission has vanished at the longer wavelength, we cannot necessarily take $\bar{x}_{\lambda_2} = 0$. Any model with this emission is therefore required to give $\bar{x}_\lambda \geqslant 0.73$.

5.2 $J_\lambda = 1 + j_\lambda \cos^n \delta$. With this form of intensity

distributions over the inner hemispheres, we require $j_\lambda = 0$ at the longer wavelengths, and j_λ large at the shorter observed wavelengths. As before,

$$\Delta m_\lambda = \frac{\left\{ \int_0^{\frac{\pi}{2}} \cos^{n+2}\delta \sin^3\delta \, d\delta - \frac{2}{n+3} \right\} j_\lambda \sin^2 i}{\frac{4}{3} + j_\lambda \left\{ \frac{1}{2} \int_0^{\pi/2} \cos^2\delta \sin^3\delta \, d\delta + \frac{1}{n+3} \right\}}$$

The displacement from zero of a line in the nodes is given by $\rho_\lambda = V_{eq} \overline{x}_\lambda \sin i$, where

$$\overline{x}_\lambda = \frac{\int_{-1}^{1} x\sqrt{(1-x^2)}\,(1+j_\lambda' x^n)\,dx}{\int_{-1}^{1} \sqrt{(1-x^2)}\,(1+j_\lambda' x^n)\,dx} \qquad \begin{matrix} j_\lambda' = 0 & -1 \le x \\ j_\lambda' = j_\lambda & 0 \le x \end{matrix}$$

i.e. $$\overline{x}_\lambda = \frac{j_\lambda \int_0^1 x^{n+1}/\sqrt{(1-x^2)}\,dx}{\frac{\pi}{2} + j_\lambda \int_0^1 x^n/\sqrt{(1-x^2)}\,dx}$$

Strictly speaking the above form for $\overline{x}_\lambda$ should not be used in conjunction with that for Δm_λ as they have been derived under different assumptions. These assumptions concern only limb-darkening, however, which cannot have a large effect on the results derived below.

For $n = 1$, $$\overline{x}_\lambda = \frac{0.196\, j_\lambda}{\frac{\pi}{2} + 0.333\, j_\lambda}$$

For $n = 5$, $\bar{x}_\lambda = \dfrac{0.061\, j_\lambda}{\frac{\pi}{2} + 0.076 j_\lambda}$

For $n = 9$, $\bar{x}_\lambda = \dfrac{0.032\, j_\lambda}{\frac{\pi}{2} + 0.037 j_\lambda}$

$(\Delta m_\lambda, \bar{x}_\lambda)$ are plotted for various (n, j) in figure 28. It is of interest that a distribution with $n = 1$ is unacceptable as even if $j_\lambda \to \infty$ a sufficiently large $\bar{x}_\lambda$ cannot be reached, even apart from the fact that Δm_λ is then too large. The requirement that $\Delta m_\lambda \leqslant 0^m.15$ has been relaxed (see the shaded zone in the figure) as the visual range also encompasses wavelengths at which there will be little or no non-thermal emission. It is clear that a distribution of the form considered, convex downwards, can produce a sufficiently large displacement only at the price of too large a magnitude variation.

The situation cannot be improved by adopting a different orbital inclination. Suppose that at some point in the figure the situation is almost but not quite acceptable, both of the $(\Delta m_\lambda, \rho)$ being just outside the permissible zone. Then it can be seen that a change in i simultaneously increases or decreases $(\Delta m_\lambda, \rho)$, that is, it

improves one quantity but makes the other less acceptable.

5.3 'Hot-Spot' Model. In this model, as before we have $J_\lambda = W > 1$ for $0 \leq \delta \leq \delta_0 \leq \frac{\pi}{2}$, and otherwise $J_\lambda = 1$.

Then $\left(\ell \overset{def}{=} \cos\delta_0 \right)$

$$\bar{I}_\lambda = \frac{\frac{1}{3}(W-1)(1-\ell^2)^{3/2}}{\frac{\pi}{4}(1+W) + (1-W)\left\{\frac{\ell}{2}\sqrt{(1-\ell^2)} + \frac{1}{2}\sin^{-1}\ell\right\}}$$

Also,

$$\Delta m_\lambda = \frac{(W-1)\cos\delta_0\left\{2+\sin\delta_0-2\cos^2\delta_0\right\}}{4-(W-1)\left\{2(\cos\delta_0-1)+\sin\delta_0\cos\delta_0\right\}} \sin^2 i$$

For $\delta_0 = 0^0$, $\ell = 1$, $\bar{I}_\lambda = 0$.

For $\delta_0 = 30^0$, $\ell = \frac{\sqrt{3}}{2}$ $\bar{I}_\lambda = \frac{0.042(W-1)}{\frac{\pi}{2}+0.045W}$

For $\delta_0 = 45^0$, $\ell = \sqrt{\frac{1}{2}}$ $\bar{I}_\lambda = \frac{0.118(W-1)}{1.428+0.143W}$

For $\delta_0 = 60^0$, $\ell = \frac{1}{2}$ $\bar{I}_\lambda = \frac{0.217(W-1)}{1.264+0.306W}$

For $\delta_0 = 90^0$, $\ell = 0$ $\bar{I}_\lambda = 0.424\left(\frac{W-1}{W+1}\right)$

The corresponding plot is shown in figure 29.

As before, a Δm_λ of $0^m.3$ or $0^m.4$ is taken to be acceptable. Once more all models of this sort (with $i = 38^\circ$) are found to be inconsistent with the observations. The situation is different, however, in that for $\delta_0 = 90^\circ$ there is no change in the brightness of the system as it revolves. Thus by a different choice of inclination or equatorial velocity V_{eq} it is possible to decrease the acceptable $\bar{x}_\lambda$ while still retaining an acceptable Δm_λ.

A permissible value of $\bar{x}_\lambda$ is 0.35 or less, Since $\rho_\lambda = V_{eq} \sin i . \bar{x}_\lambda$, it is necessary to double $V_{eq} \sin i$ if a sufficiently small $\bar{x}_\lambda$ is to be produced. This cannot be done by a change in sin i (= .62 for 38°), and must therefore be largely achieved by increasing V_{eq} appreciably. There are three main objections to this idea:-

(i) M.HACK (1960)† has shown that statistically at least, binary systems with periods of less than about ten days have $\omega_{rot} = \omega_{rev}$. As no large change in the relative dimensions of the model adopted can be contemplated, this implies that the value of V_{eq} chosen, based on the assumption of synchronous rotation, must be approximately correct.

(ii) HOWARD and SLETTEBAK (Ap.J. 121, 102, 1955). agree with HACK's conclusion more or less. However for two of the systems examined by them, it appears that $\omega_{rot} < \omega_{rev}$,

† Proc. International School of Physics, Course XXVIII. p.452.

57 Cygni being one of the two exceptions. They point out that the reflection effect might distort the absorption line profiles, and that their conclusion can only be tentative in the case of 57 Cygni. Nevertheless the lines measured by them were presumably strong lines such as Hγ and MgII whose profiles are probably not greatly distorted by reflection; so that an increase in the adopted value of V_{eq} by a factor of 2 seems to be ruled out. Furthermore we require $\omega_{rot} > \omega_{rev}$, contrary to HOWARD and SLETTEBAK's conclusion for 57 Cygni.

(iii) 'Tidal drag' should tend to equalise the periods of rotation and revolution, equality being achieved in a time of order 10^6 years for a system such as 57 Cygni.

The above points are not conclusive however. In the first place the restriction that $\Delta m_\lambda < 0^m.3$ or $0^m.4$ is only rough. Prolateness, which also has a sin 2ϵ form, has the opposite effect bolometrically to that of reflection, the coefficients of sin 2ϵ having different signs: it is not impossible that a Δm_λ of about $0^m.7$ would be acceptable. Furthermore the dynamical argument refers to a mean angular velocity throughout the body of the star, and

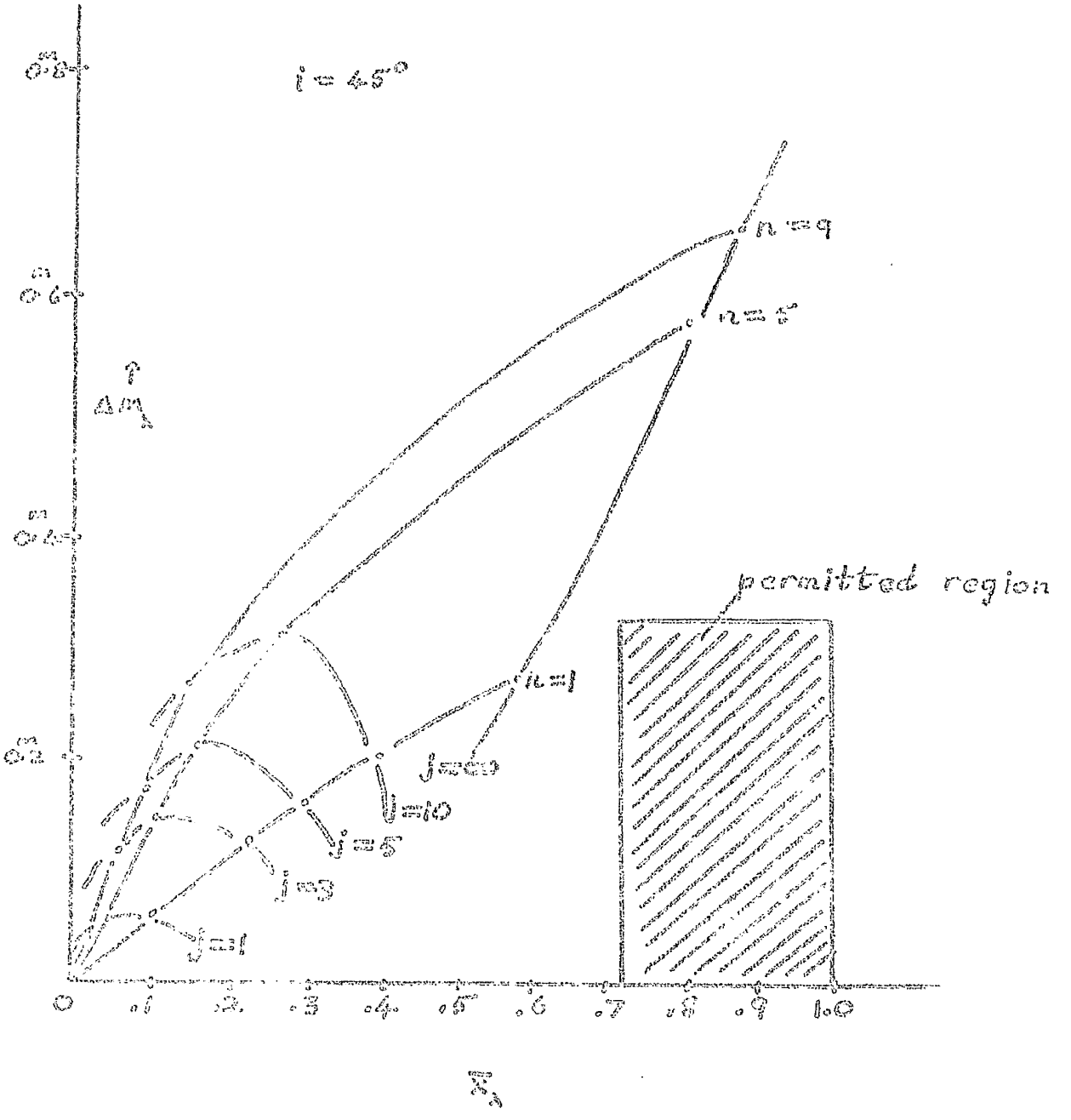

$(\Delta m_\lambda, \bar{x}_\lambda)$ for intensity distributions whose form is $I_\lambda = 1 + jx^n$ in the range $0 \leq x \leq 1$.

57 Cygni must lie within the shaded region.

Figure 28

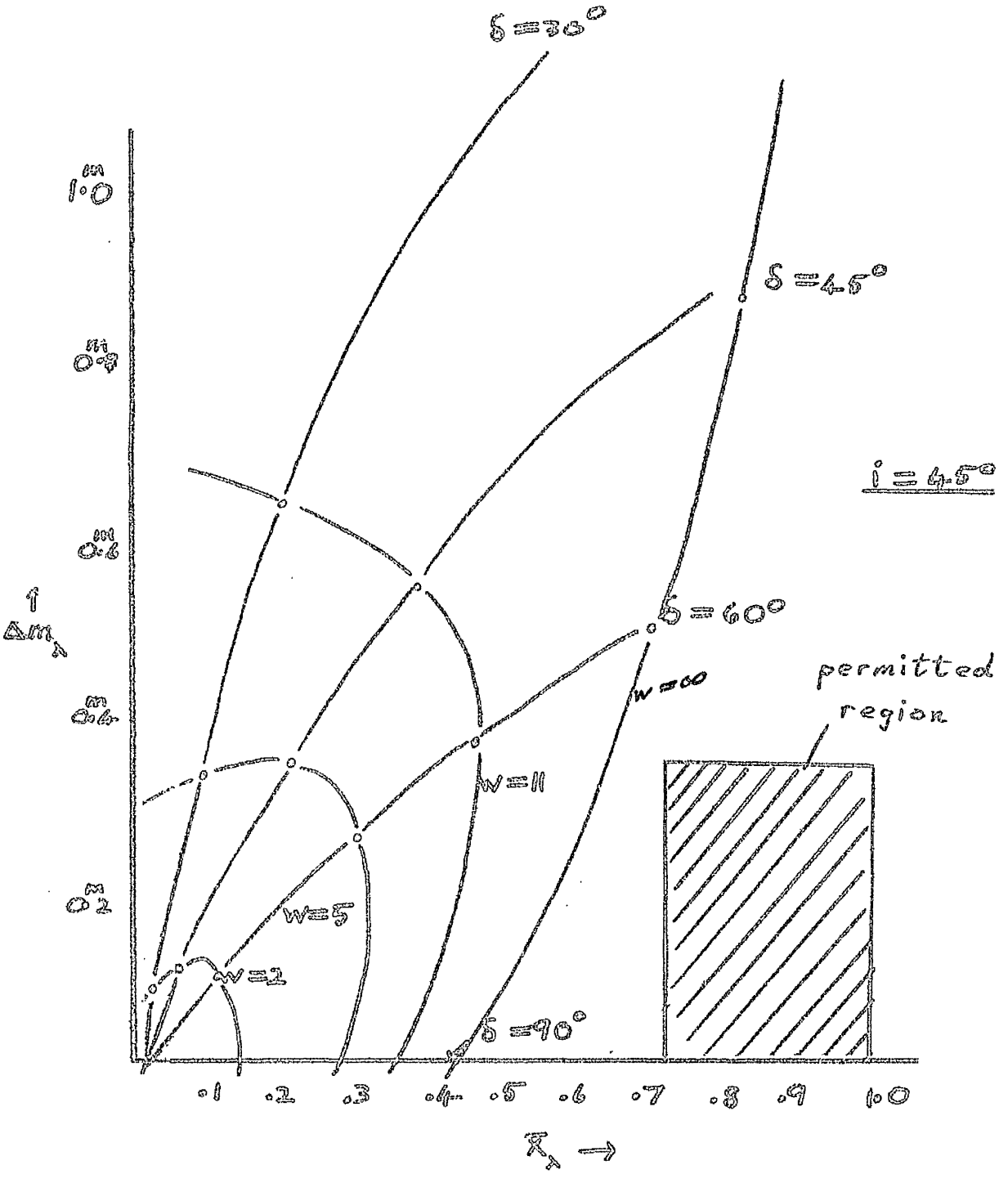

$(\Delta m_\lambda, \bar{x}_\lambda)$ for hotspot model.

Figure 29

states nothing about the velocity in the photosphere which might be different. Nevertheless a rather improbable combination of circumstances has to be postulated, and the conclusion of the present section is that it is unlikely that even a 'hotspot' distribution can be made to satisfy the observations.

5.4 Energy Requirements. The surface area of the 'Polar cap' of the hotspot model is given by

$$A = 2\pi \int_{x_0}^{a} y \sqrt{\left(1 + \left[dy/dx\right]^2\right)}\, dx$$

where a represents the stellar radius. Since $y = \sqrt{(a^2 - x^2)}$

$A = 2\pi a(a - \ell)$. For a star of unit radius,

$$\frac{\text{excess energy}}{\text{stellar energy}} = \frac{2\pi(w-1)(1-\ell)}{4\pi} = \frac{1}{2}(w-1)(1-\ell)$$

By 'excess energy' here is meant the energy emitted/sec., by the star in excess of the energy emitted by a normal B5V star, the latter being referred to above as 'stellar energy'. From the factor 4π in the denominator, representing the stellar energy, it is clear that the energy/cm^2/sec. emitted from the outwards facing hemisphere has

been taken as the unit of energy.

Figure 30 demonstrates the relationship between ΔE, the energy excess in terms of the total 'normally' emitted from the star(i.e. twice the emission from the outwards facing hemisphere), and $\bar{x}_\lambda$. As δ_o must be in the region of 90^o if Δm_λ is to remain small, the bulk of the energy emitted by the star must be in the form of non-thermal emission, on the hotspot model.

5.5 The result of the previous section suggests that <u>any</u> continuum intensity distribution giving the necessary $\bar{x}_\lambda = .75$ will require a large excess energy, and this is found to be so:-

To simplify the equation we put $J_\lambda(\delta) = 1 + f(\delta)$ and consider the change ΔL_λ in luminosity corresponding to Δm_λ. Then

$$\bar{x}_\lambda = \frac{\int_0^{\frac{\pi}{2}} \sin\delta \cos^2\delta \, f(\delta)\, d\delta}{\frac{\pi}{2} + \int_0^{\frac{\pi}{2}} \cos^3\delta \, f(\delta)\, d\delta}$$

$$\Delta L_\lambda = \int_0^{\frac{\pi}{2}} \sin\delta \cos^2\delta \, f(\delta)\, d\delta - \frac{1}{2}\int_0^{\frac{\pi}{2}} \sin^3\delta \, f(\delta)\, d\delta$$

Then $$\int_0^{\frac{\pi}{2}} \sin^3\delta\, f(\delta)\, d\delta = \left[\pi + 2\int_0^{\frac{\pi}{2}} \cos^2\delta\, f(\delta)\, d\delta\right]\overline{X}_\lambda - 2\Delta L_\lambda$$

As we must have $f(\delta) \geq 0$, $\int_0^{\frac{\pi}{2}} \cos^2\delta\, f(\delta) \geq 0$ and therefore

$$\int_0^{\frac{\pi}{2}} \sin^3\delta\, f(\delta)\, d\delta \geq \pi\overline{X}_\lambda - 2\Delta L_\lambda$$

Defining the excess of energy from each star over what it would have in the absence of reflection to be ΔE_λ, we then have

$$\Delta E_\lambda = \frac{2\pi\int_0^{\frac{\pi}{2}} f(\delta)\sin\delta\, d\delta}{4\pi} = \frac{1}{2}\int_0^{\frac{\pi}{2}} f(\delta)\sin\delta\, d\delta$$

But $$\int_0^{\frac{\pi}{2}} f(\delta)\sin\delta\, d\delta \geq \int_0^{\frac{\pi}{2}} f(\delta)\sin^3\delta\, d\delta$$

$$\therefore\ \Delta E_\lambda > \frac{\pi}{2}\overline{X}_\lambda - \Delta L_\lambda$$

The ΔL_λ corresponding to $\Delta m_\lambda \leq 0^m.15$ is 0.06.

$$\therefore \Delta E_\lambda > 1.57 \times 0.73 - 0.06 = 1.12.$$

At the very least, no matter how we choose the function $J_\lambda(\delta)$, the continuum emission from each star must be double that expected from a B5 V star over the wavelength range, say, 3900 - 4200 Å. This result has essentially been obtained by comparing the inward and outward facing hemispheres of each star.

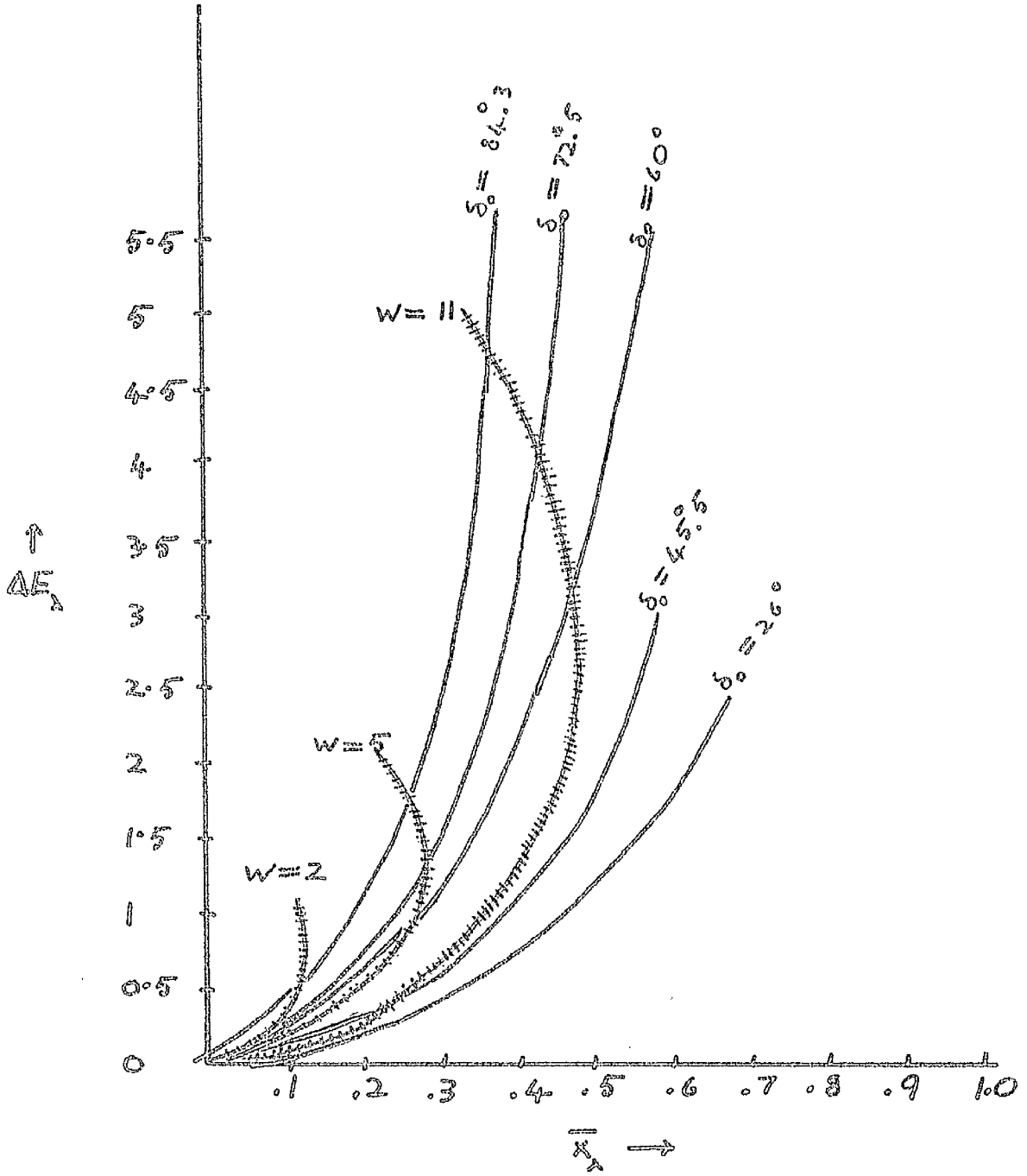

'Excess' energy emitted by star at wavelength λ in terms of $\overline{x}_\lambda$; hotspot model.

Figure 30

5.6. The hypothesis that the ρ/λ diagram can be accounted for by a suitable distribution of non-thermal continuum emission, varying suitably with wavelength, over the inner faces of the stars, should probably be rejected:-

(i) A small magnitude variation over the visual and photometric ranges can only be achieved by adopting an improbable distribution of energy namely one in which the inner hemispheres are uniformly bright (hotspot model with $\delta_0 = 90^0$). Even a small deviation from this model results in a large increase in Δm_λ.

(ii) Such a distribution, if adopted, results in a value of $\overline{\kappa}_\lambda$ which is too low by a factor of two. The discrepancy can be removed only by an increase in the adopted value of the equatorial velocity of rotation. It has already been shown that the required increase is unlikely.

(iii) The rate of energy generation necessary to give the observed ρ/λ diagram exceeds the thermal emission by a factor of at least three over a range of several hundred Angstrom units, and probably more.

(iv) Even if an 'explanation' of this sort were acceptable from a phenomenological point of view, it

is difficult to see what physical process could give rise to such intense emission, and such a distribution.

6. Radiation Dilution. The principle of detailed balancing holds that transitions between any two energy levels in an atom occur with equal frequency in either direction. This holds in a state of thermodynamic equilibrium. If the principle holds in any two states, it must also hold for any closed circuit of transitions, for example A and B below (ROSSELAND 1936).

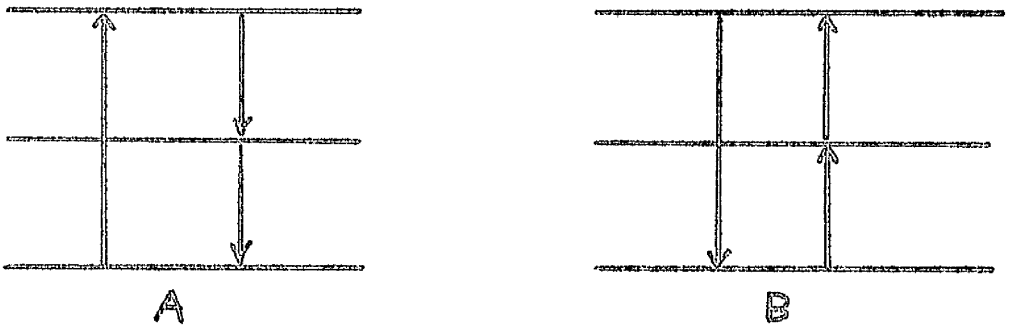

Fluorescense arises when radiation whose spectral distribution corresponds to some temperature interacts with material at a lower temperature. Relative to the equilibrium situation there is then an excess of high-energy photons, as a consequence of which cycles of Type A operate more frequently

than type B. The effect will be to weaken long-wavelength lines, while strengthening the short-wavelength lines. There is evidence of fluorescence in early-type stars, and the question arises whether dilute radiation from one component falling on the other will cause additional fluorescence sufficient to account for the ρ/λ diagram.

Let $n(\nu)$ represent the number of photons of energy ν in a unit volume of material in thermodynamic equilibrium. Then at frequencies ν_1 and ν_2 we may define

$$\alpha = \frac{n(\nu_1)}{n(\nu_2)}$$

According to the above ideas, fluorescence will occur only if the addition of energy from an external source increases the number of high-energy photons capable of performing cycle A relative to the number of low-energy photons which may perform cycle B.

Suppose now that $pn(\nu_1)$, $qn(\nu_2)$ photons of energy (ν_1, ν_2) are added to the volume from an external source of illumination. The ratio of the numbers of photons at energies (ν_1, ν_2) is now

$$\beta = \frac{n(\nu_1) + p\,n(\nu_1)}{n(\nu_2) + q\,n(\nu_2)} = \alpha\left(\frac{1+p}{1+q}\right)$$

In the case of 57 Cygni, the illuminating and reflecting sources are identical. Thus the ratio of the number densities of photons from the illuminating source with energies (ν_1, ν_2) is α, i.e., p=q. Hence $\alpha = \beta$. According to the above remarks, fluorescence depends on an excess of high-energy photons from an external source, i.e., $\beta \neq \alpha$. Fluorescence will not therefore be caused by the mutual illumination of the components of 57 Cygni.

The argument above appears to be contrary to the usual point of view, which is that fluorescence must arise in a medium exposed to dilute temperature radiation. It may be re-expressed qualitatively as follows. Consider a medium in thermodynamic equilibrium. Let it now be exposed to photons from an external source whose energy density is not so great as to appreciably increase the temperature (The latter condition is not essential but it simplifies the argument).

Analogously to the tendency towards equipartition of energy between the molecules of a gas, incoming photons will gain or lose energy in such a way as to reach an energy distribution corresponding to equilibrium at the temperature T of the medium.

If the incoming photons correspond to a higher temperature, they must tend to be converted to greater numbers of lower-energy photons (cycle A). Conversely, dilute radiation corresponding to a lower temperature must be converted to fewer photons of higher energy (cycle B).

If this argument is valid, it is not sufficient for incoming radiation to be dilute: the mean energy of the photons must also be greater than that corresponding to the equilibrium temperature. Differential fluorescence over the surfaces of 57 Cygni should not therefore arise.

The possibility of an intense emission in the ultra-violet over the inner hemispheres was considered earlier. This could formally account for the T_{max}/ρ correlation. If such an emission exists it will give rise to fluorescence in the ambient atmosphere, and a ρ/λ correlation is then much more likely.

One phenomenon would thus give rise to the two correlations, which is an attractive feature of the idea . I have been told by Dr. OVENDEN that evidence exists, largely unpublished, indicating that the inner hemispheres of some close binaries

are bluer than their averted hemispheres, to a greater extent than the heating would imply. Some published evidence of this exists: e.g. HURUHATA et al.† have shown that intense ultra-violet emission extending into the blue is found over the inner surfaces of the close eclipsing binary U Pegasi, which they attempt to explain in terms of flare-like activity around the sub-stellar points.

7. The displacement due to reflection of a line involves (i) the continuum emission
(ii) the intrinsic line strength
(iii) the velocity field

We have seen that (a) a large non-thermal emission in the visible range could explain the ρ/λ correlation but would conflict with the small variability of the star.

(b) radiation dilution cannot account for the ρ/λ correlation unless an intense UV emission of unexplained origin arises over the inner surfaces.

The remaining possibility is a suitable modification of the velocity field adopted so far. If a differential rotation with height exists in

† Ann. Tokyo Ast. Obs., Vol V, no. 1, 1957.

the atmospheres of the stars, we require to correlate the wavelength of an absorption line with the mean height at which it is formed. But no obvious correlation exists.

Chapter III THE GENERAL SOLUTION

Introduction

1. So far the problem has been to find a temperature T(x) satisfying equations of the form

$$\overline{x}_i = \frac{\int_{-1}^{1} x\sqrt{(1-x^2)}\, J_i(\lambda, x)\, dx}{\int_{-1}^{1} \sqrt{(1-x^2)}\, J_i(\lambda, x)\, dx} \qquad (1)$$

$$i = 1, 2, \ldots\ldots\ldots n$$

where the $\overline{x}_i$ are given by observation, i referring to the i - th spectral line, and there are n lines. The $J(\lambda, x)$ are related to the temperature T(x).

As it stands the set (1) cannot be solved uniquely, although a best solution can be found in the least-square sense.

If the chromospheric origin of the lines, suggested in chapter II, is correct, a different temperature distribution $T_i(x)$ will apply to each

absorption line as they form at different levels. Thus we have $W_i(T_i(x))$ for the i th line, with no obvious connection between the various $T_i(x)$. The temperature distribution $T_i(x)$ for the i th absorption line must then be found from that line alone, without relating it to the other absorption lines.

On the other hand, if $T_s \gg 2^{\frac{1}{4}} T_e$ over much of the stellar surfaces, that is if the stars were secularly unstable, then the 'best' solution would be meaningful. However, this hypothesis was considered to be unlikely.

A unique solution, or even a 'best' solution, for $T_j(x)$ cannot be obtained from figures of the form 3(a) and 3(b) alone. But if we were to follow the stars throughout a revolution, the continually changing aspect of the visible discs as 'seen' by the spectrograph might be expected to give a unique solution even if only a single absorption line was observed. We might also hope to find in principle the genuine orbital elements of the system, including the orbital inclination, as well as the magnitude and direction of the stellar rotations.

The present chapter thus describes an attempt to use the entire velocity curve of each line. As the lines are now considered separately there is no need to assume any form of interdependence of the J_i and the quantity to be found is simply $J_i(x)$ for a given i.

The Orientation of the Poles of Rotation

2. Statistical studies of line broadening in spectroscopic systems have suggested to some authors, for example M.HACK† (1960) that if a system has a period of less than about ten days, the periods of rotation and revolution coincide; while more widely separated binary components tend to have shorter rotation times relative to their periods. The implication of this is that in systems with P < ten days or so the axes of rotation and revolution will usually be parallel in space. An examination of the velocity curves tends to bear out this conclusion in the case of 57 Cygni:-

An observed velocity curve can be regarded as being composed of a reflection-free, 'standard' velocity curve, plus a curve due to reflection alone. As the eccentricity of the system is small we may write approximately $V = K_0 \cos(v+\omega)$ for the

† Proc International School of Physics. Course XXVIII, p.452.

standard part, neglecting a systemic velocity which has no influence on the subsequent discussion. An inspection of the velocity curves in M.W.OVENDEN's paper (see figure 4 of chapter *I*) reveals that to a high degree of approximation there is simply a scaling up or down of the curve; this is also in evidence for the other lines from an examination of the tabulated elements. The term due to reflection must therefore take the form $-D_i \cos(v+\omega)$, D_i a constant for the i th line considered. It is obvious by comparing, say, MgII and NIII that D_i may be comparable with K_o.

Suppose now, without attempting theoretical justification, that the reflection term can take the form $-D_i \cos(v+\omega-v_o)$, v_o a constant.

Then $$V_i = (K_o - D_i \cos v_o)\cos(v+\omega) - D_i \sin v_o \sin(v+\omega) \quad (2)$$

$$\therefore \frac{\partial V_i}{\partial v} = -\left(K_o - D_i \cos v_o\right)\sin(v+\omega) - D_i \sin v_o \cos(v+\omega)$$

$$= 0 \text{ for maximum velocity}$$

$$v_{max} = \tan^{-1}\left\{\frac{D_i \sin v_o}{D_i \cos v_o - K_o}\right\} \quad (3)$$

where V_{max} is the true anomaly corresponding to the maximum velocity. Also when $V = 0$,

$$V_{zero} = \tan^{-1}\left\{\frac{K_0 - D_1 \cos V_0}{D_1 \sin V_0}\right\}$$

In general, therefore, when $v_0 \neq 0$, different absorption lines will reach their greatest displacements at different times, and likewise for zero displacement, as V_{max} and V_{zero} now depend on D_1 which varies considerably from line to line. Also, the sine term in (2) introduces a skewness into the velocity curve, which would give rise to a spurious eccentricity if naively interpreted.

It will now be shown that necessary (but not sufficient) conditions for $v_0 = 0$ are that

(i) the pole of axial rotation lies on the great circle defined by the pole of orbital revolution and the observer

(ii) there is no 'time-lag': the reflected radiation has symmetry about the line joining the stellar centres.

The necessity of the first circumstance can be seen from figure 3/ . In position A the star has its systemic velocity and axis «‹' satisfies condition (*i*). Then from the indicated symmetry of the rotational velocity and the lines of equal

absorption (isosorbs) it is obvious that the reflection term must be zero. If the axis is in position $\rho\rho'$ there is no such symmetry and there will be a non-zero reflection term. The case $\alpha\alpha'$ is consistent, and that of $\beta\beta'$ is inconsistent, with a reflection term which is simply a multiple of the standard velocity $K_0\cos(v+\omega)$.

Position B represents the instant when the isosorbs and the velocity contours are symmetrical with respect to each other in the $\beta\beta'$ case. Then the reflection term is zero, which is consistent with the form $-D_1\cos(v+\omega-v_0)$ and is inconsistent with the form $-D_1\cos(v+\omega)$, the standard velocity then being of the form $-D_1\cos(v+\omega-v_0)$.

The upshot of this argument is that the necessity of (i) has been demonstrated. Condition (ii) follows immediately from a similar argument.

The great circle on which the rotation pole must lie includes the physically significant pole of revolution; if the rotation pole lies elsewhere on the circle this can only be a coincidence as the position of the observer in space is random. Since both stars satisfy conditions (i) and (ii) it seems very likely that the axes of rotation and

revolution are parallel in space.

4. In figure 34, S_1 represents the star under consideration, S_2 being the illuminating star. Sx, the x-axis, is the projection (on to the plane perpendicular to the observer's line of sight) of the line joining the stellar centres, Sy being the y-axis. P represents the pole of rotation of S_1; the other symbols are self-explanatory. In view of the preceding discussion the poles of rotation and revolution are taken to coincide, so that $PK = i$ and $\angle\Omega P = 90^\circ$.

Only ω_y, the y-component of the angular rotation of S_2, contributes to the reflection effect; $\omega_y = \omega \cos Py$ and we thus require to find how Py varies with v. From triangle PyK,

$$\cos Py = \sin i \cos \hat{K} = \sin i \cos Qy.$$

As $K\Omega = \Omega P = 90^\circ$, KPQ is a great circle with Ω as a pole, hence $Q\Omega = 90^\circ$. But $xy = 90^\circ$. Hence $Qy = \angle\Omega x$ and

$$\cos Py = \sin i \cos(\angle\Omega x).$$

From triangle $S_2\Omega x$, using the four-parts formula,

$$\tan(\angle\Omega x) = \tan(v+\omega) \cos i.$$

It follows that

$$\omega_y = \omega \sin i \cos\left\{\tan^{-1}\left(\tan(v+\omega) \cos i\right)\right\} \quad (4)$$

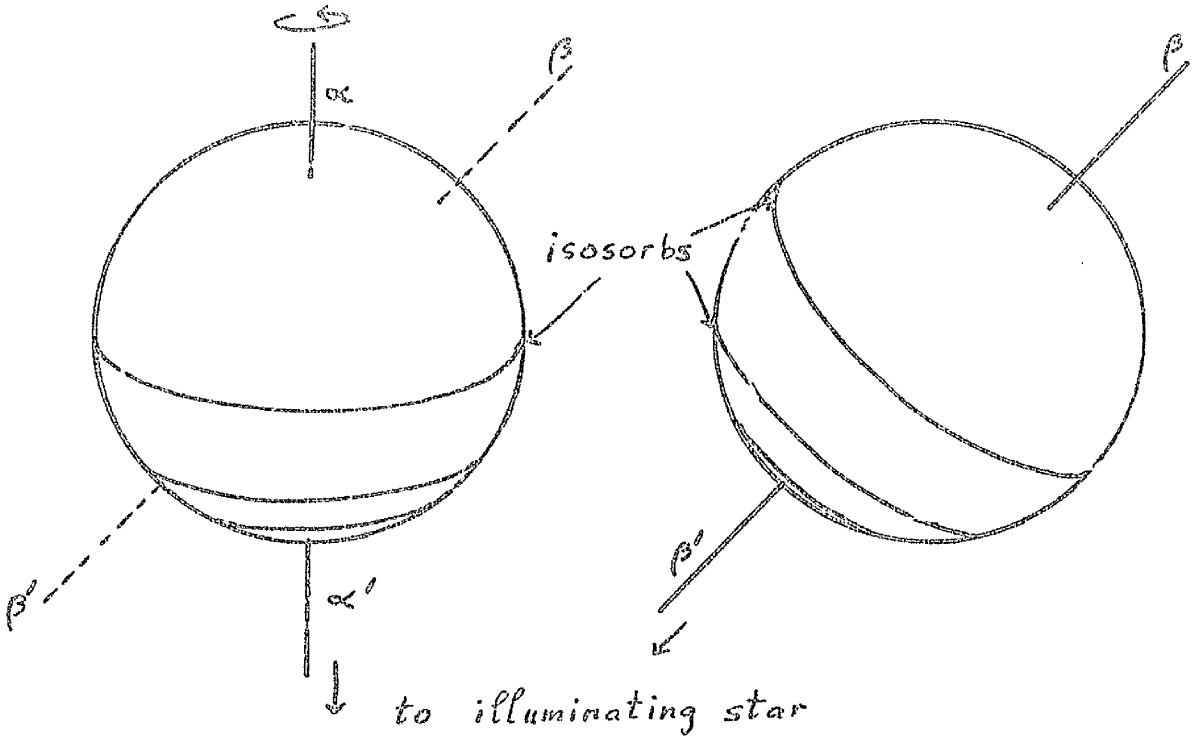

Figure 31

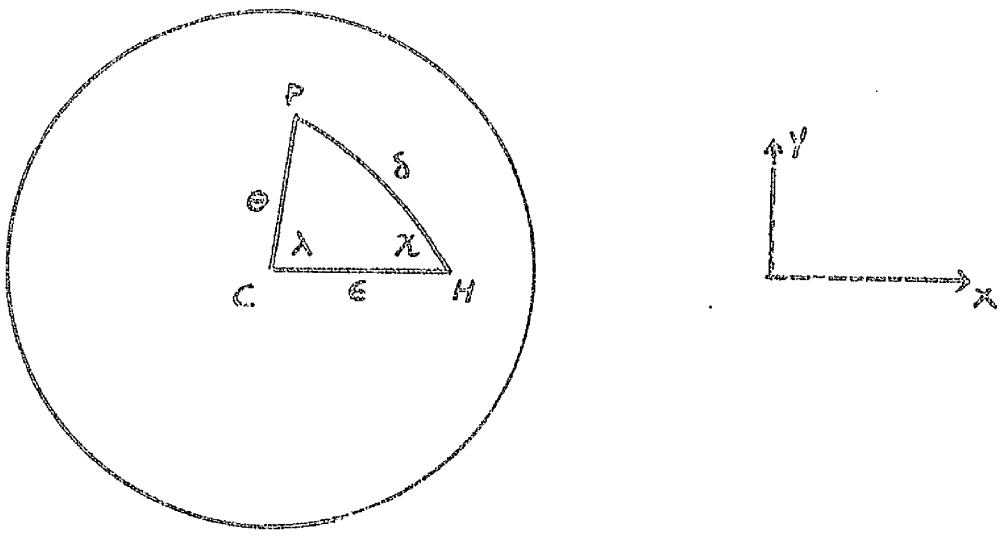

Figure 32

The Question of Solvability

5. Substitution of numerical values reveals that over a wide range of inclination i, the expression (4) may be replaced by

$$\omega_y = \omega \sin i \cos(v + \omega)$$

with an error of only a few percent. In particular the above expression is adequate over the range $30^\circ \leqslant i \leqslant 45^\circ$ within which 57 Cygni must lie. But ω_y appears as a multiplier in the expression for the reflection, the other factor being a function of the intensity distribution $J_i(x)$. The reflection term is therefore approximately of the form $-\mathcal{Q}(J_i) \cos(v + \omega)$. But we have seen that to a high degree of approximation the reflection terms of the absorption lines of 57 Cygni are of the form $-D_i \cos(v + \omega)$, D_i a constant.

While this re-affirms the conclusions that the axes of rotation and revolution are probably parallel in space and that there is no time-lag involved in the reflection effect, the conclusion must also be drawn that $\mathcal{Q}(J_i) = D_i$, a constant. The implication of this is that the variation with phase

of the reflection term is due almost entirely to the changing value of ω_y and is little affected by the changing aspect of the reflecting hemisphere. In turn this suggests that no more information about $J_i(x)$ can be obtained from the study of an entire velocity curve than can be got by examining the curve at any one phase, for example in the nodes.

$\mathfrak{L}(J_i)$ depends on J_i in the same way that K_i depends on J_i in the nodes case: of all possible functions J_i the observations enable us to select an infinity of functions as possible distributions but give no further information.

This can be seen another way if we plot the elements against the semi-amplitude K_0, as in figure 33. The vertical lines on the right of the diagrams represent typical standard deviations, and it is obvious that by and large the spread of the elements is within that which would be expected if no systematic distortion of the curves existed; this again implies that each velocity curve is obtainable from any other by an appropriate change of the vertical scale, and that we have $-D_i \cos(v+\omega)$. The tendency for elements from lines

with smaller K to show a greater spread is presumably due to their greater standard deviations, lines with small K being weaker and more difficult to measure.

(The single exception to this rule is the systemic velocity γ, which shows a distinct slope when plotted against K. There seems to be no way in which a reflection effect could produce a spurious γ, and the cause of the slope must lie in some physical process not yet discussed. It follows that in addition to the S/ρ and ρ/λ diagrams there exists a third correlation, the γ/ρ diagram, whose explanation cannot be found in terms of our model so far. Discussion of the new diagram is deferred until a later section).

In spite of the low sensitivity of the curves to the intensity distributions, a general solution might still be worth trying. Firstly, a very rough answer might still be obtained from such deviations from a mere vertical scaling as may exist. Secondly it is conceivable that not every distribution would give rise to a $-D_i \cos(v+\omega)$ form of answer: a general solution would narrow down the range of possible J_i to those whose precise shape is undiscoverable from the velocity curves, and it is at

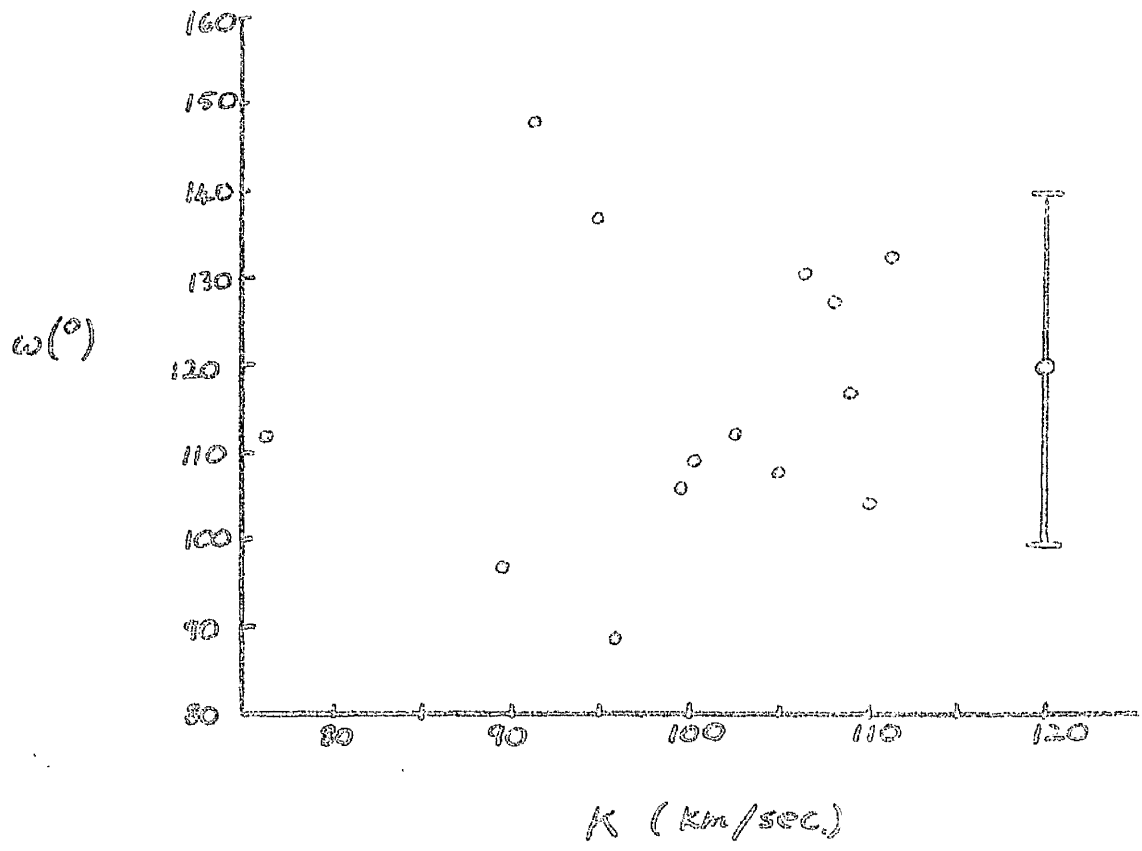

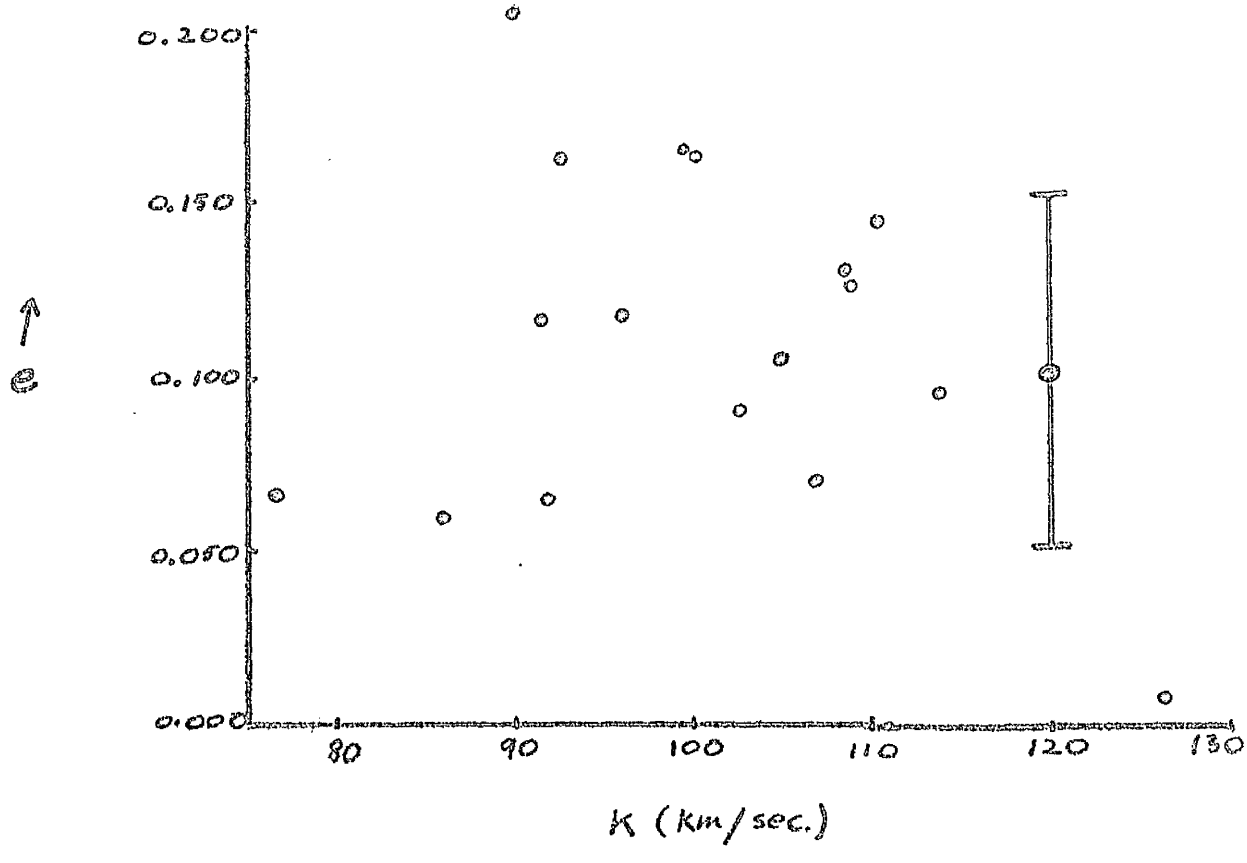

Figure 33. (ω, e) against K for star 1.

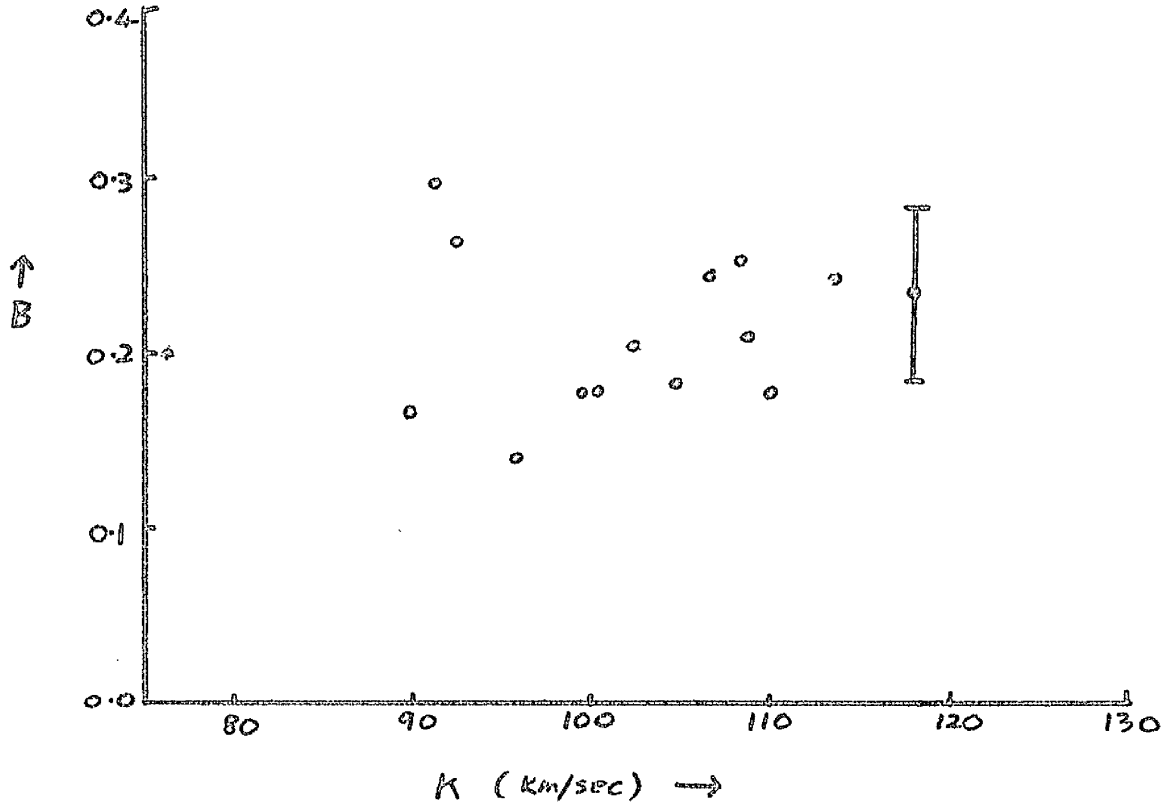

Figure 33

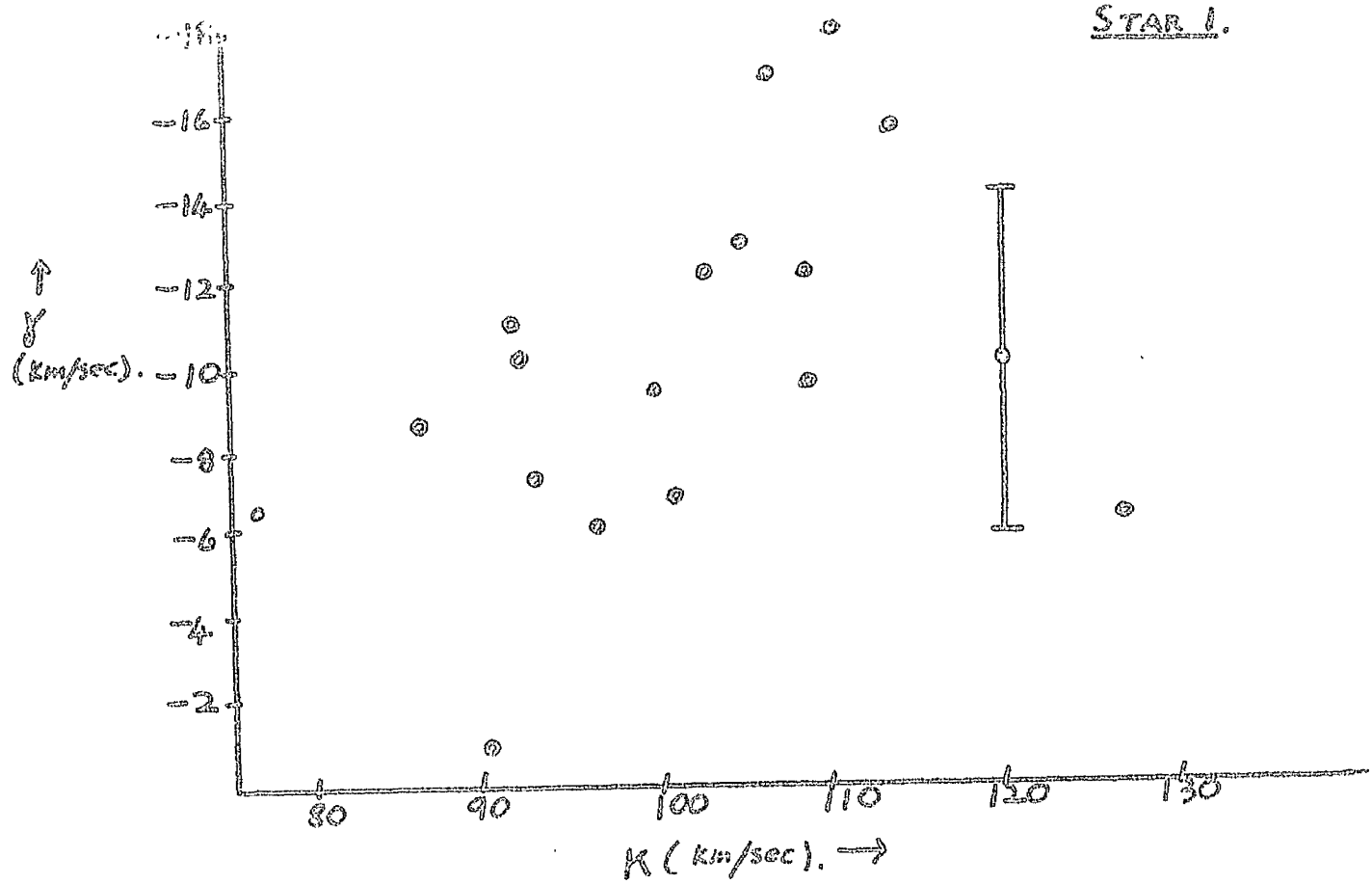

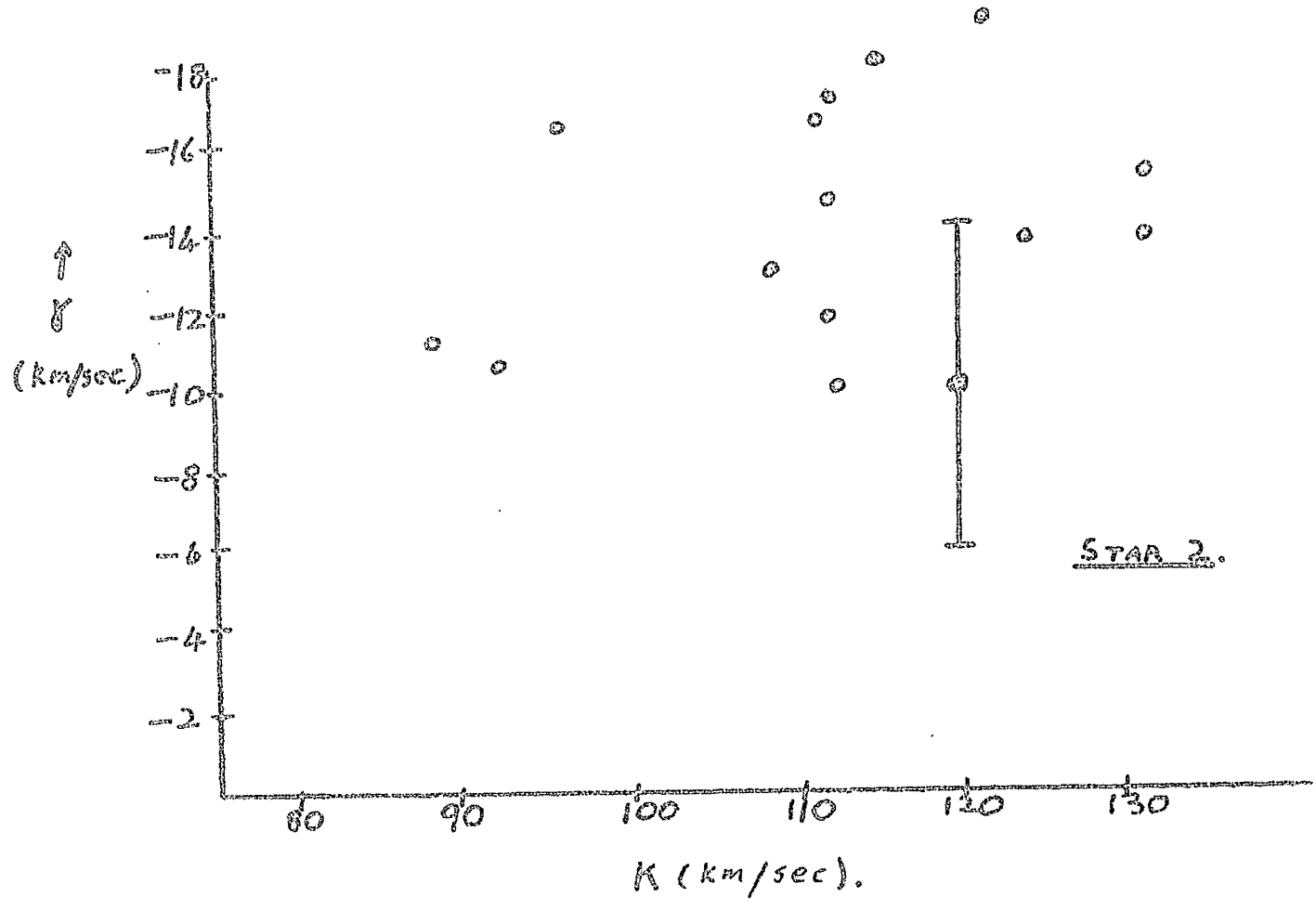

Figure 33 γ/K for stars 1 and 2.

least possible that the narrowing-down would be considerable. In the light of these possibilities a general solution was attempted.

The General Solution

6. The problem is to find $J_i(\delta)$ for the i th absorption line from the expression

$$\rho_i = \frac{\iint_\Sigma V J_i(\delta)\, d\sigma}{\iint_\Sigma J_i(\delta)\, d\sigma} \qquad (5)$$

where V is the radial velocity at each point on the stellar surface, $d\sigma$ is an elementary area on the star projected onto the observer's celestial sphere, Σ represents the visible disc over which the integration is to be carried, δ is a single parameter on which J depends (J being supposed symmetrical about the sub-stellar point) and ρ_i is the distortion due to the reflection effect at any phase, measured in units of velocity.

As all the velocity curves are closely represented by equations of standard form, it is not possible to decide which curve is the reflectionless one, if any, and I assumed a 'true' curve

with elements

K_o = 130 km/sec:	e = 0.125;
γ = -15 km/sec:	ω = 2.0944;
τ = 0.6182 ;	n = 2.2009;

n = $2\pi/P$ and (e, ω, τ) are average values for all the lines. The Large value for K_o was chosen before the model for 57 Cygni, presented in chapter I was derived. Re-computation with the improved K_o (= 110km/sec) is not worth while. An equatorial velocity of 70 km/sec in a direct sense was assumed. This is less than the V_{eq} given by HOWARD and SLETTEBAK, but I was not aware of their paper at the time; and re-computation was once more not considered worth while.

$$\rho_i = \gamma + K_o[\cos(\nu+\omega)+e\cos\omega] - \gamma_m - K_m[\cos(\nu_m+\omega_m)+e_m\cos\omega_m]$$

where suffix m refers to the (measured) velocity curve of the i the line.

7. An Integral Equation Formulation. Consider the surface of the star as seen by the observer (figure 32). Let C represent the centre of the apparent disc, H the sub-stellar point. Then CH (= ϵ) measured over the spherical stellar surface, is a

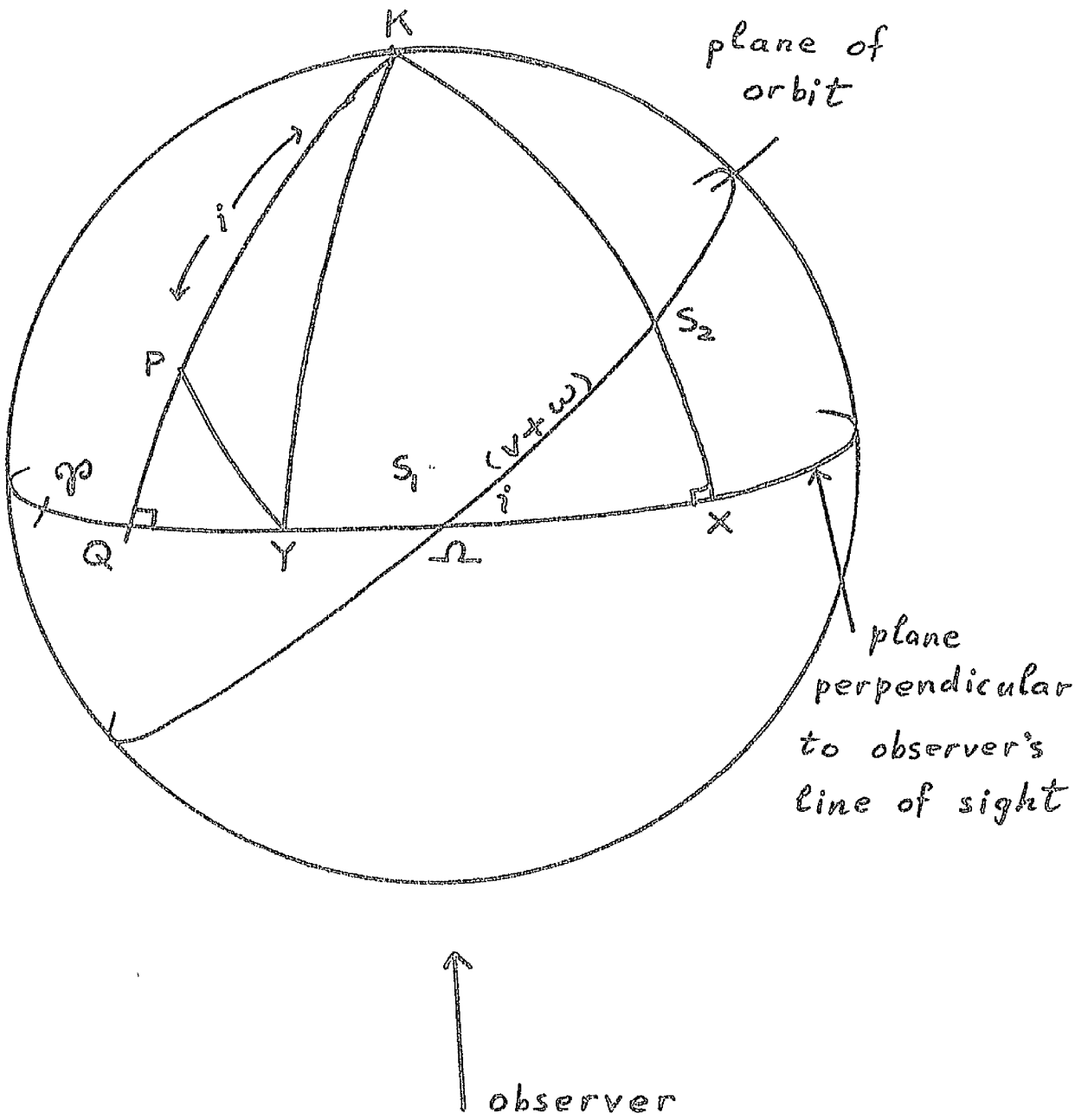
K
plane of orbit
i
P
S2
(v+ω)
S1
i
φ
Q
Y
Ω
X
plane perpendicular to observer's line of sight
observer

Figure 34.

measure of the phase of the system; if $\epsilon = 90^{\circ}$ the stars are in the nodes, while if ϵ has its minimum value the stars possess only the systemic velocity. The co-ordinates of an arbitrary point P are (δ, χ), where δ is measured over the stellar surface from H and $\chi = \hat{PHC}$ in the spherical triangle. Alternatively we may measure the position of P by (θ, λ) as shown where θ is measured over the surface.

Sphericity has been assumed, and consequently there is no gravity darkening. Limb-darkening will also be neglected although this is less obviously justified. But as it is questionable whether any answer at all will be obtainable at this stage of the presentation, it can be regarded as a refinement to be included only if the undarkened case yields significant results.

We have $d\sigma = dx\,dy = \frac{\partial(x,y)}{\partial(\delta,\chi)} d\delta\, d\chi = \sin\delta \cos\theta\, d\delta\, d\chi$. (An elementary area on the sphere has $d\sigma' = \sin\delta\, d\delta\, d\chi$ and we require its projection on the observer's celestial sphere; hence the $\cos\theta$ factor). There are two prevailing regimes, one when $|\epsilon| \leqslant \frac{\pi}{2}$ and the other when $|\epsilon| > \frac{\pi}{2}$. Different limits of integration correspond to these two regimes, and if $\chi_m(\delta, t)$ is the value of χ at time t when P is on the stellar limb, we have

$$\rho_i(t) = \frac{\left\{ \int_{\delta=0}^{\frac{\pi}{2}-\epsilon(t)} \int_{\chi=0}^{2\pi} + 2 \int_{\delta=\frac{\pi}{2}-\epsilon(t)}^{\pi-\epsilon(t)} \int_{\chi=0}^{\chi_m(\delta,t)} \right\} V(\delta,\chi,t)\, J_i(\delta) \sin\delta\cos\Theta \, d\delta\, d\chi}{\left\{ \int_{\delta=0}^{\frac{\pi}{2}-\epsilon(t)} \int_{\chi=0}^{2\pi} + 2 \int_{\delta=\frac{\pi}{2}-\epsilon(t)}^{\pi-\epsilon(t)} \int_{\chi=0}^{\chi_m(\delta,t)} \right\} J_i(\delta) \sin\delta\cos\Theta \, d\delta\, d\chi}$$

for $|\epsilon| \leq \frac{\pi}{2}$

and

$$\rho_i(t) = \frac{\left\{ 2 \int_{\delta=\frac{\pi}{2}-\epsilon(t)}^{\pi-\epsilon(t)} \int_{\chi=0}^{\chi_m(\delta,t)} + \int_{\delta=\pi-\epsilon(t)}^{\pi} \int_{\chi=0}^{2\pi} \right\} V(\delta,\chi,t)\, J_i(\delta) \sin\delta\cos\Theta \, d\delta\, d\chi}{\left\{ 2 \int_{\delta=\frac{\pi}{2}-\epsilon(t)}^{\pi-\epsilon(t)} \int_{\chi=0}^{\chi_m(\delta,t)} + \int_{\delta=\pi-\epsilon(t)}^{\pi} \int_{\chi=0}^{2\pi} \right\} J_i(\delta) \sin\delta\cos\Theta \, d\delta\, d\chi}$$

$|\epsilon| > \frac{\pi}{2}$

It only remains to give an explicit expression for $V(\delta, \chi, t)$. We have seen that the symmetry of J_i about H implies that the only component of ω which contributes to the reflection effect is ω_y measured in an inertial frame. Hence

$$V = (\omega_y R)x = \omega_y R \sin\Theta \cos\lambda$$

$$= \omega_y R(\cos\delta \sin\epsilon - \sin\delta \cos\epsilon \cos\chi)$$

If the star has unit radius, R = 1 and we must let ω take the dimensions of a velocity. Then ω = 70 km/sec in (4).

From the cosine formula,

$$\cos\Theta = \cos\delta \cos\epsilon + \sin\delta \sin\epsilon \cos\chi$$

Then, e.g., $\rho_i(t) =$

$$\omega_y \frac{\left\{\int_{\delta=0}^{\frac{\pi}{2}-\epsilon}\int_{\chi=0}^{2\pi} + 2\int_{\delta=\frac{\pi}{2}-\epsilon}^{\pi-\epsilon}\int_{\chi=0}^{\chi_m}\right\}(\cos\delta\sin\epsilon - \sin\delta\cos\epsilon\cos\chi)(\cos\delta\cos\epsilon + \sin\delta\sin\epsilon\cos\chi)\sin\delta\, J_i(\delta)\,d\delta\,d\chi}{\left\{\int_{\delta=0}^{\frac{\pi}{2}-\epsilon}\int_{\chi=0}^{2\pi} + 2\int_{\delta=\frac{\pi}{2}-\epsilon}^{\pi-\epsilon}\int_{\chi=0}^{\chi_m}\right\}(\cos\delta\cos\epsilon + \sin\delta\sin\epsilon\cos\chi)\sin\delta\, J_i(\delta)\,d\delta\,d\chi}$$

for $|\epsilon| \leq \frac{\pi}{2}$

where the unknown is $J_i(\delta)$.

In a system of finite eccentricity we should strictly write $J_i(\delta, t)$, as the temperature at any point (δ, χ) on the inner hemisphere of the star will vary in general with the distance of the illuminating star from that point. The eccentricity is small and the effect is neglected below. In any case a unique solution for $J_i(\delta, t)$ is impossible without some further physical hypothesis.

The occurence of the unknown under an integral sign suggests that the above expression might be reducible to an integral equation of standard form. It turns out that this can be done, but the solution of the resulting equation by the usual method involves intractable algebra:-

Suppose that the integration over χ has been performed, giving integrands of $K^*(\delta, t)\, J_i(\delta)$ and $K_*(\delta, t)\, J_i(\delta)$ in numerator and denominator respectively. Then

$$\rho_i(t) = \frac{\omega_y \int_{\delta=0}^{\delta'(t)} K^*(\delta,t)\, J_i(\delta)\, d\delta}{\int_{\delta=0}^{\delta'(d)} K_*(\delta,t)\, J_i(\delta)\, d\delta}$$

$$\therefore \int_{\delta=0}^{\delta'(t)} \left\{ \frac{\rho_i(t)}{\omega_y} K_*(\delta,t) - K^*(\delta,t) \right\} J_i(\delta)\, d\delta = 0$$

(where the inclination i should not be confused with the suffix i).

If we replace the time-dependent upper limit by its maximum value π, we obtain a homogeneous Fredholm integral equation of the first type with a discontinuous kernel:

$$\int_{\delta=0}^{\pi} K(\delta,t)\, J_i(\delta)\, d\delta = 0 \qquad (6)$$

where if $|\epsilon| \leqslant \frac{\pi}{2}$

$$K(\delta,t) = \begin{cases} \omega_y^{-1}\rho_i(t) K_*(\delta,t) - K^*(\delta,t) & \text{where } 0 \leqslant \delta \leqslant \epsilon \\ \omega_y^{-1}\rho_i(t) L_*(\delta,t) - L^*(\delta,t) & \text{where } \epsilon < \delta \leqslant \pi-\epsilon \\ 0 & \text{where } \pi-\epsilon < \delta \leqslant \pi \end{cases}$$

and if $|\epsilon| > \frac{\pi}{2}$

$$K(\delta,t) = \begin{cases} 0 & \text{where } 0 \leqslant \delta \leqslant \epsilon \\ \omega_y^{-1}\rho_i(t) L_*(\delta,t) - L^*(\delta,t) & \text{where } \epsilon < \delta \leqslant \pi-\epsilon \\ \omega_y^{-1}\rho_i(t) K_*(\delta,t) - K^*(\delta,t) & \text{where } \pi-\epsilon < \delta \leqslant \pi \end{cases}$$

The integration over χ yields

$$K^{*}(\delta,t) = \pi \sin\delta\,(2\cos^2\delta - \sin^2\delta)\sin\epsilon\cos\epsilon$$

$$K_{*}(\delta,t) = 2\pi \sin\delta\cos\delta\cos\epsilon$$

$$K_{*}(\delta,t) = 2\pi \sin\delta\cos\delta\cos\epsilon$$

$$L^{*}(\delta,t) = \sin\delta\{\chi_m \cos^2\delta \sin\epsilon\cos\epsilon + (\sin^2\epsilon - \cos^2\epsilon)\sin\delta\cos\delta\sin\chi_m - \sin^2\delta\sin\epsilon\cos\epsilon(\tfrac{1}{2}\chi_m + \tfrac{1}{4}\sin 2\chi_m)\}$$

$$L_{*}(\delta,t) = \sin\delta\{\chi_m \cos\delta\cos\epsilon + \sin\delta\sin\epsilon\sin\chi_m\}$$

$$\chi_m = \cos^{-1}\left(-\frac{\cot\delta}{\cot\epsilon}\right)$$

The literature contains virtually nothing on the subject of integral equations of the first type. I considered, however, that the equation might be solved by converting it to an inhomogeneous equation of the second type by putting $J_i(\delta) = 1 + f_i(\delta)$, regarding $f_i(\delta)$ as the function to be determined and differentiating (6) with respect to time:

$$\int_{\delta=0}^{\pi} \frac{\partial K}{\partial t}(t,\delta) f_i^{*}(\delta)\,d\delta + K(t,\pi) f_i^{*}(\pi)$$

$$= -\int_{\delta=0}^{\pi} \frac{\partial K}{\partial t}(t,\delta)\,d\delta - K(t,\pi) \qquad (7)$$

This is of the form

$$u(x) = f(x) + \lambda \int_a^b K(x,\delta)\, u(\delta)\, d\delta$$

which is generally solved by the Liouville-Neumann method: If

$$D(\lambda) \equiv 1 - \lambda \int_a^b K(\delta,\delta)\, d\delta + \frac{\lambda^2}{2!} \int_a^b \int_a^b \begin{vmatrix} K(\delta_1,\delta_1) & K(\delta_1,\delta_2) \\ K(\delta_2,\delta_1) & K(\delta_2,\delta_2) \end{vmatrix} d\delta_1\, d\delta_2 - \frac{\lambda^3}{3!} \int_a^b \int_a^b \int_a^b \begin{vmatrix} K(\delta_1,\delta_1) & \cdots & K(\delta_1,\delta_3) \\ \vdots & & \vdots \\ K(\delta_3,\delta_1) & & K(\delta_3,\delta_3) \end{vmatrix} d\delta_1\, d\delta_2\, d\delta_3 + \cdots\cdots$$

and

$$D(x,y;\lambda) \equiv \lambda K(x,y) - \frac{\lambda^2}{2!} \int_a^b \begin{vmatrix} K(x,y) & K(x,\delta) \\ K(\delta,y) & K(\delta,\delta) \end{vmatrix} d\delta + \frac{\lambda^3}{3!} \int_a^b \int_a^b \begin{vmatrix} K(x,y) & K(x,\delta_1) & K(x,\delta_2) \\ K(\delta_1,y) & K(\delta_1,\delta_1) & K(\delta_1,\delta_2) \\ K(\delta_2,y) & K(\delta_2,\delta_1) & K(\delta_2,\delta_2) \end{vmatrix} d\delta_1\, d\delta_2 - \cdots\cdots$$

then provided that $D(\lambda) \neq 0$, the unique and continuous solution for $u(x)$ is

$$u(x) = f(x) + \frac{1}{D(\lambda)} \int_a^b f(\delta)\, D(x, \delta; \lambda)\, d\delta$$

Inspection of the kernel in the present problem makes it clear that the algebra involved in solving by the standard method would be prohibitive.

An equation of the type(7) has a unique, non-zero solution if and only if $D(\lambda) \neq 0$. By inspection, $f_1(\delta) = -1$ is a solution of (7) which must therefore be the unique solution if $D(\lambda) \neq 0$. As this solution is physically untenable then $D(\lambda)$ must be zero and the method does not in any case apply.

Given that we must have $D(\lambda) = 0$, it follows from the Liouville-Neumann theory that either (7) must have no solutions at all or it has an infinite number. But an inspection of (5) reveals that $J_1(\delta)$ is arbitrary to the extent of a multiplying constant. Whether there is a single or a multiple infinity of solutions in the context of the Liouville-Neumann theory can only be

determined by further intractable algebra. Physically it is to be expected that to each $\rho_i(t)$ there will correspond a $J_i(\delta)$ unique apart from an arbitrary constant.

8. A Numerical Approach. A more practible approach would be to approximate (6) or (7) by a set of simultaneous linear equations. The integral over δ could be replaced by a sum of the integrand evaluated at $\delta = 0, \delta_1, \delta_2, \ldots \delta_{n-1}$, where $\delta_{n-1} = \pi$. On inserting specific values $\epsilon_0, \epsilon_1, \epsilon_2, \ldots \epsilon_{n-1}$ of phase angle we would have n equations for the n unknowns $J_i(\delta_0)$, $J_i(\delta_1)$, $J_i(\delta_2)$, $\ldots\ldots J_i(\delta_{n-2})$, $J_i(\pi)$. Presumably some optimum n exists which represents a compromise between a loss of information due to under-representation of $J_i(\delta)$, and an excess of $J_i(\delta)$ to whose values little weight can be given. This approach would be feasible on an electronic computer for large n, while if only a few lines were being considered and the optimum n was, say, 5 or less, computation by hand would suffice.

If we had assumed $J_i(\delta_0,e)$, $J_i(\delta_1,e)$, $J_i(\delta_2,e)$, $\ldots J_i(\pi,e)$ as the finite eccentricity of the system strictly

speaking implies, on taking n phase angles we would have a set of n equations involving the n^2 unknowns

$$J_i(\delta_r, \epsilon_s) \qquad \begin{matrix} r = 0,1,2,\ldots\ldots n-1; \\ s = 0,1,2,\ldots\ldots n-1; \end{matrix}$$

We then always have more unknowns than equations, and by considering the situation as $n \to \infty$ we arrive at a heuristic argument justifying the earlier assertion that a unique solution is impossible without some hypothesis prescribing the variation of J_i with time.

9. An Analytical Approach. The method which was actually used in tackling the general solution involves changing the limits of integration from (δ, χ) to (λ, θ) and expressing the intensity as a polynomial in $\cos\delta$. The unknowns then become the coefficients of the polynomial. This is a natural extension of the nodes case, where we have $x = \cos\delta$ and

$$J_i(x) = j_0 + j_1 x + j_2 x^2 + \ldots\ldots\ldots$$

and the problem is to determine the j's from the observations.

Both the integral equation and the purely

numerical methods have the advantage that it is simple to introduce the assumption that over the outer hemisphere of the reflecting star the intensity $J_f(\delta)$ is constant. In the former case one introduces another discontinuity of the kernel at $\delta = \frac{\pi}{2}$, with $J_f = 1$, say, in the kernel when $\delta \geq \frac{\pi}{2}$; while in the numerical case the accuracy of representation of J_f obtainable from the observations is increased.

The following analysis does not possess this advantage, but this is of no consequence in application to 57 Cygni. There is probably little to choose between the numerical and analytical procedures from the point of view of simplicity, and the only justification for applying the analytical method to 57 Cygni is that this was the method which was first thought of.

We shall therefore represent the intensity distribution by a truncated series of the form

$$J_f(\cos\delta) = j_0 + j_1 \cos\delta + j_2 \cos^2\delta + \ldots\ldots + j_{10}\cos^{10}\delta \quad (8)$$

Other series are conceivable, such as a Fourier series or a sum involving Legendre or Tschebyscheff polynomials. However, any of these series is equivalent to any other, as an expansion of (say)

$P_r(\cos\delta)$ and an appropriate re-arrangement of the terms is always possible. Only if the orthogonality properties of (say) $P_r(\cos\delta)$ or $\cos(r\delta)$ resulted in a simplification of the integration would such an expansion be worth while, and it was found by trial that (8) was easily the most straightforward representation.

The degree of the polynomial was chosen as a compromise between the desirability of representing the intensity distribution by as many terms as possible in order to handle any sharp peaks or discontinuities in gradient which could arise, and the labour involved in deriving the terms.

In equation(5) we have

$$V = \omega_y \sin\theta \cos\lambda$$

$$d\sigma = \sin\theta \cos\lambda \, d\theta \, d\lambda$$

Therefore

$$\rho_i(t) = \omega_y \frac{\int_{\theta=0}^{\frac{\pi}{2}} \int_{\lambda=0}^{2\pi} \sin\theta \cos\lambda \, J_i(\delta) \sin\theta \cos\theta \, d\theta \, d\lambda}{\int_{\theta=0}^{\frac{\pi}{2}} \int_{\lambda=0}^{2\pi} J_i(\delta) \sin\theta \cos\theta \, d\theta \, d\lambda} \qquad (9)$$

Since $\cos\delta = \cos\Theta\cos\epsilon + \sin\Theta\sin\epsilon\cos\lambda$, the double integration in (9) is easily performed as we only have B-functions to evaluate. We have

$$\rho_i(t) = \frac{\omega_y \sum_{n=0}^{10} f_n j_n}{\sum_{n=0}^{10} g_n j_n} \qquad (10)$$

where (f_r, g_r) are known functions of phase (and hence time). Removing a factor π which cancels out of all terms, we find

$f_0 = 0$

$f_1 = \frac{1}{4}\sin\epsilon$

$f_2 = \frac{4}{15}\sin\epsilon\cos\epsilon$

$f_3 = \frac{1}{4}\sin\epsilon\cos^2\epsilon + \frac{1}{8}\sin^3\epsilon$

$f_4 = \frac{8}{35}\sin\epsilon\cos\epsilon$

$f_5 = \frac{5}{24}\sin\epsilon\cos^4\epsilon + \frac{5}{16}\sin^3\epsilon\cos^2\epsilon + \frac{5}{64}\sin^5\epsilon$

$f_6 = \frac{12}{63}\sin\epsilon\cos^5\epsilon + \frac{8}{21}\sin^3\epsilon\cos^3\epsilon + \frac{12}{63}\sin^5\epsilon\cos\epsilon$

$f_7 = \frac{7}{20}\sin\epsilon\cos^6\epsilon + \frac{7}{16}\sin^3\epsilon\cos^4\epsilon + \frac{21}{64}\sin^5\epsilon\cos^2\epsilon + \frac{7}{128}\sin^7\epsilon$

$f_8 =$ $f_7 = \frac{7}{40}\sin\epsilon\cos^6\epsilon + \frac{7}{16}\sin^3\epsilon\cos^4\epsilon + \frac{21}{64}\sin^5\epsilon\cos^2\epsilon + \frac{7}{128}\sin^7\epsilon$

$f_9 =$ $f_8 = \frac{16}{99}\sin\epsilon\cos^7\epsilon + \frac{16}{35}\sin^3\epsilon\cos^5\epsilon + \frac{16}{35}\sin^5\epsilon\cos^3\epsilon + \frac{16}{99}\sin^7\epsilon\cos\epsilon$

$f_9 = \frac{9}{60}\sin\epsilon\cos^8\epsilon + \frac{21}{40}\sin^3\epsilon\cos^6\epsilon + \frac{21}{32}\sin^5\epsilon\cos^4\epsilon + \frac{21}{64}\sin^7\epsilon\cos^2\epsilon$

512

$f_{10} = \frac{20}{143}\sin\epsilon\cos^9\epsilon + \frac{80}{143}\sin^3\epsilon\cos^7\epsilon + \frac{840}{1001}\sin^5\epsilon\cos^5\epsilon + \frac{80}{143}\sin^7\epsilon\cos^3\epsilon$

$+ \frac{1260}{9009}\sin^9\epsilon\cos\epsilon$

$$g_0 = 1$$

$$g_1 = \tfrac{2}{3}\cos\epsilon$$

$$g_2 = \tfrac{1}{2}\cos^2\epsilon + \tfrac{1}{4}\sin^2\epsilon$$

$$g_3 = \tfrac{2}{5}\cos^3\epsilon + \tfrac{2}{5}\sin^2\epsilon\cos\epsilon$$

$$g_4 = \tfrac{1}{3}\cos^4\epsilon + \tfrac{1}{2}\sin^2\epsilon\cos^2\epsilon + \tfrac{1}{8}\sin^4\epsilon$$

$$g_5 = \tfrac{2}{7}\cos^5\epsilon + \tfrac{4}{7}\sin^2\epsilon\cos^3\epsilon + \tfrac{2}{7}\sin^4\epsilon\cos\epsilon$$

$$g_6 = \tfrac{1}{4}\cos^6\epsilon + \tfrac{5}{8}\sin^2\epsilon\cos^4\epsilon + \tfrac{15}{32}\sin^4\epsilon\cos^2\epsilon + \tfrac{5}{64}\sin^6\epsilon$$

$$g_7 = \tfrac{2}{9}\cos^7\epsilon + \tfrac{3}{5}\sin^2\epsilon\cos^5\epsilon + \tfrac{3}{5}\sin^4\epsilon\cos^3\epsilon + \tfrac{2}{9}\sin^6\epsilon\cos\epsilon$$

$$g_8 = \tfrac{1}{5}\cos^8\epsilon + \tfrac{7}{10}\sin^2\epsilon\cos^6\epsilon + \tfrac{7}{8}\sin^4\epsilon\cos^4\epsilon + \tfrac{7}{16}\sin^6\epsilon\cos^2\epsilon + \tfrac{7}{128}\sin^8\epsilon$$

$$g_9 = \tfrac{2}{11}\cos^9\epsilon + \tfrac{8}{11}\sin^2\epsilon\cos^7\epsilon + \tfrac{12}{11}\sin^4\epsilon\cos^5\epsilon + \tfrac{8}{11}\sin^6\epsilon\cos^3\epsilon + \tfrac{2}{11}\sin^8\epsilon\cos\epsilon$$

$$g_{10} = \tfrac{1}{6}\cos^{10}\epsilon + \tfrac{3}{4}\sin^2\epsilon\cos^8\epsilon + \tfrac{21}{16}\sin^4\epsilon\cos^6\epsilon + \tfrac{105}{96}\sin^6\epsilon\cos^4\epsilon + \tfrac{105}{256}\sin^8\epsilon\cos^2\epsilon + \tfrac{21}{512}\sin^{10}\epsilon$$

In figure 34, since ϵ is the angle between the observer's line of sight and SS_2, we have $S_2x = \epsilon - 90^0$. Then since

$$\sin S_2x = \sin(v+\omega)\sin i$$

we have

$$\cos\epsilon = -\sin(v+\omega)\sin i$$

$$\sin\epsilon = +\sqrt{(1-\cos^2\epsilon)}$$

the positive sign being required as angles measured over a sphere are always $\leq 180^0$. The f's and g's may now be found in terms of the true anomaly and hence time t. As the eccentricities concerned are all of order 0.1, it was considered sufficient to solve

for the true anomaly in terms of time by the truncated series:

$$v = M + (2e - \tfrac{1}{4}e^3)\sin M + \tfrac{5}{4}e^2 \sin 2M + \tfrac{13}{12}e^3 \sin 3M$$

with $M = n\,(t - \tau)$.

The question arises as to whether ω is to be taken as a positive or a negative quantity. With the elements chosen to represent the 'true' orbit, we see that a line such as NIII must be displaced along the positive x-axis, i.e., $\Sigma f_i j_i / \Sigma g_i j_i$ is positive. But for NIII, ρ_{Nm} is also positive in the region of the ascending node ($v + \omega = 0^0$). Thus (10) implies that, when $v + \omega = 0^0$, ω should be such that ω_y is positive which, as (4) indicates, means that ω must be taken positive for direct rotation, negative for rotation retrograde with respect to an inertial frame.

Equation (10) becomes

$$\sum_{n=0}^{10} [\rho_n g_n - \omega_y f_n] j_n = 0 \qquad (11)$$

To solve this set it was necessary to arbitrarily specify one of the j_n's and j_1 was taken equal to unity. This is consistent with the earlier remark that $J_i(\cos \delta)$ is arbitrary to the extent of a

multiplying constant. Ten equally spaced values of time were therefore taken, $(\rho_i, \omega, f_r, g_r)$ calculated for those times, the set (11) was solved, and the distribution $J(\cos\delta)$ calculated for $\cos\delta$ in the range -1 (0.1)1. This was done on an electronic computer for a number of lines, with various combinations of 'true' K_0 and i. A typical result is shown in figure 35. The results cannot correspond to real $J_i(\delta)$ distributions.

10. The algebra and the computer programme were checked thoroughly and no error was revealed. In addition the programme was extended to calculate the velocity curve corresponding to some $J_i(\delta)$ distribution. The distributions derived in the first place were found to give the velocity curves from which they originally came; thus $V_i(t) \rightleftharpoons J_i(\delta)$.

The possibility was considered that the real distribution might be over-represented by the tenth degree polynomial. Thus in a sense the coefficients of the polynomial might not be subject to sufficient constraint, and a polynomial of lower degree, or which was required to fit more points on the velocity curve, might give a better representation of the

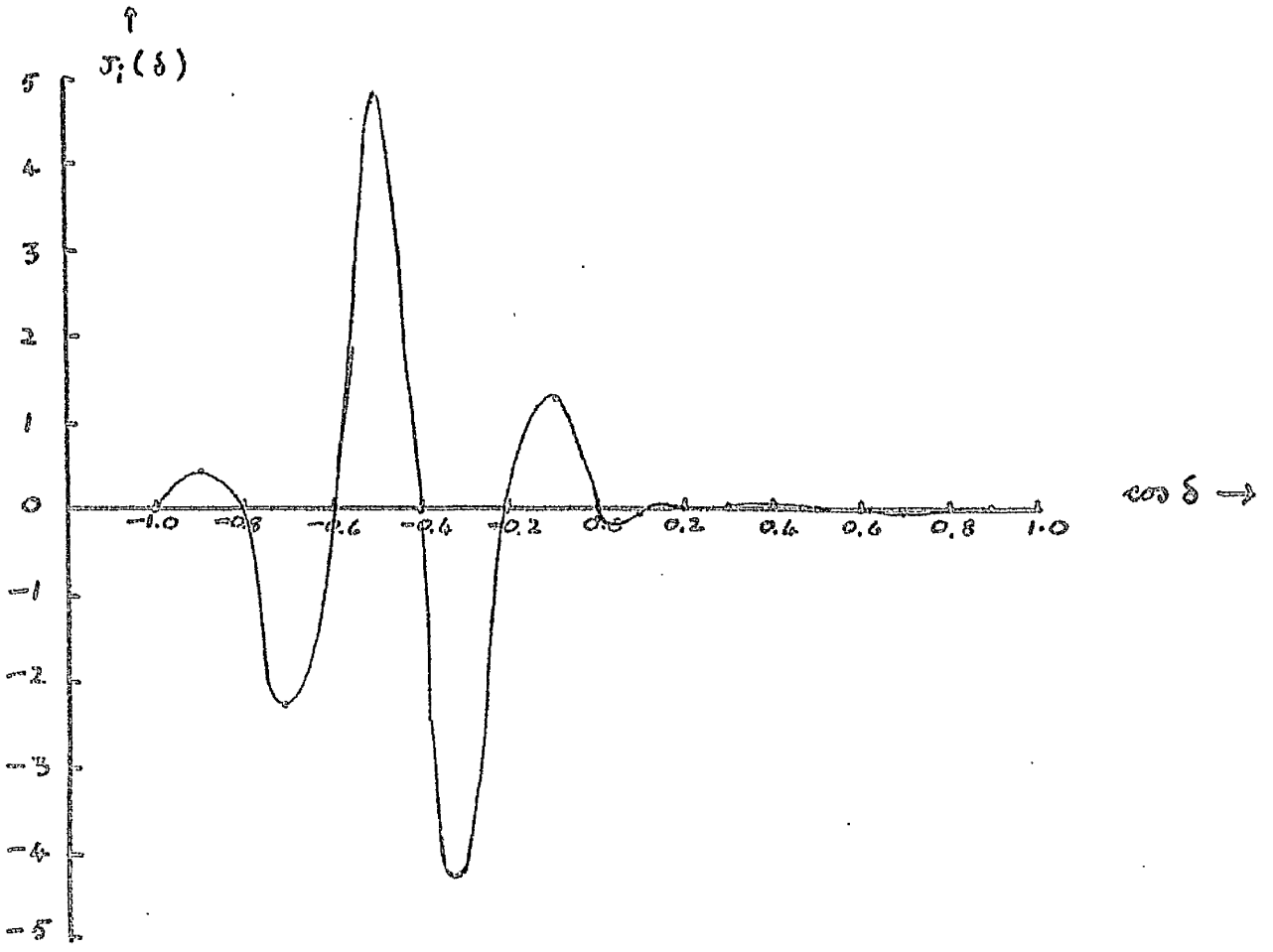

$J_i(\delta)$ for N III. V_{eq} = 180 km/sec, otherwise adopted elements are as stated in the text. Note that a negative $J_i(\delta)$ is meaningless.

Figure 35

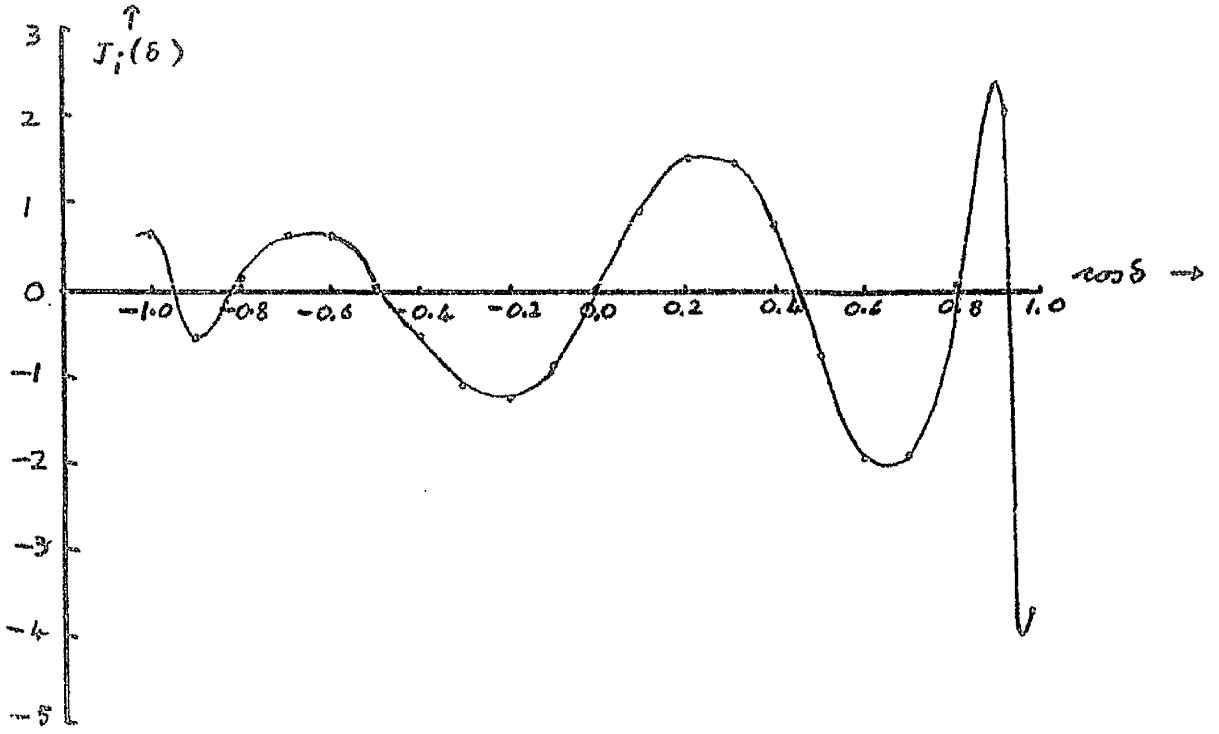

$J_i(S)$ for N III : 10^{th} degree polynomial ; least-squares operation on 50 points.

Figure 36

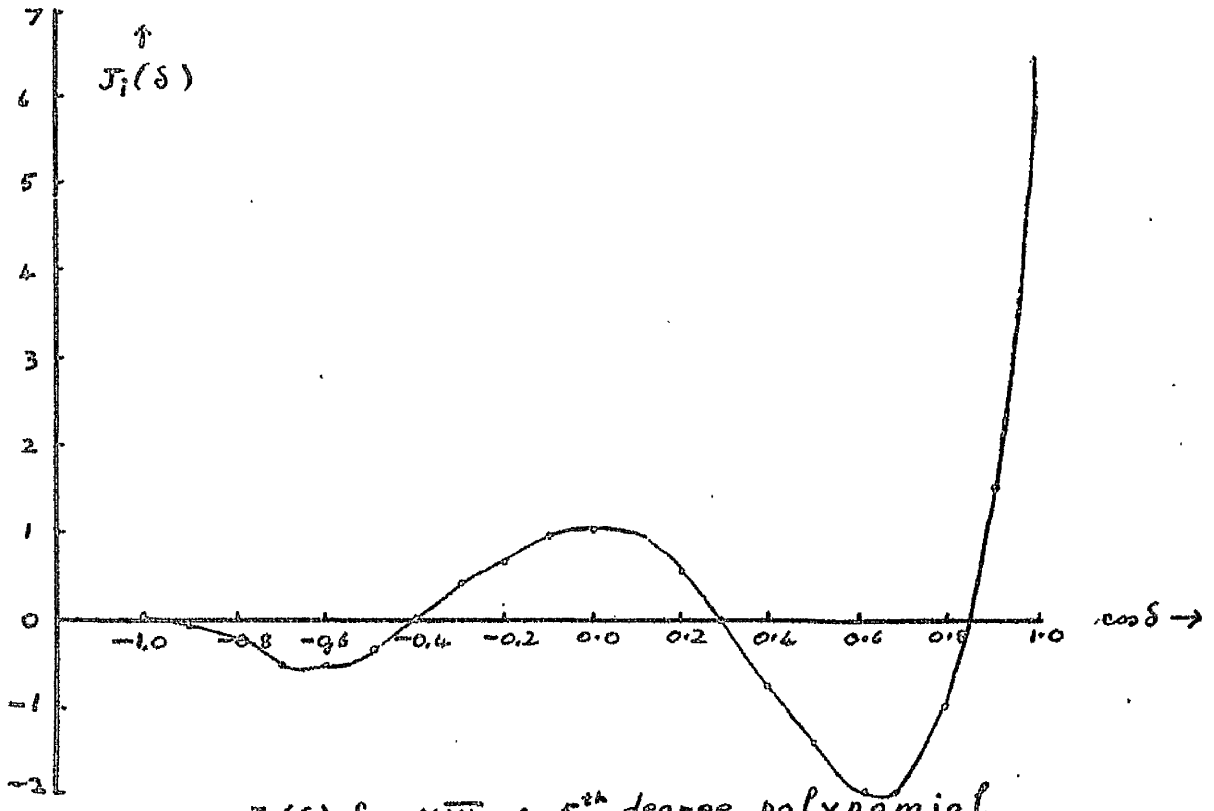

$J_i(S)$ for N III : 5^{th} degree polynomial

Figure 37

$J_i(\delta)$ curve.

A fifth degree polynomial was taken and applied to the observations of NIII (figure 37). Also for NIII, a tenth degree polynomial representation was required to fit 50 equally spaced points on the velocity curve as well as possible, that is, using a least squares analysis. (figure 36) Evidently the oscillations of the curves cannot be accounted for in this way.

Finally, the conclusion was reached that the $J_i(\delta)$ distributions for the various lines on 57 Cygni are such that $\mathcal{D}_i(\epsilon) = D_i$, that is that the oscillations occur because the distributions are undiscoverable from the observed velocity curves. Presumably a slight change in some parameters, such as the values of time taken, would produce a large change in the distributions, such as a shift in the phase of the waves.

11. Circulation Currents. It has been shown in § 5 of chapter II that atmospheric material must stream away from the sub-stellar points. This streaming arises because of a horizontal pressure gradient. If the density ρ of material at some

physical depth in the atmosphere does not vary over either star, this pressure gradient is given by

$$\Delta P = \rho \frac{R}{\mu} \Delta T$$

where R is the gas constant and the molecular weight $\mu = \frac{1}{2}$. ΔP is also the change in the internal energy of unit volume of gas whose temperature changes by ΔT. If this change in energy, which arises as the volume moves away from the sub-stellar point is converted to energy of motion, then

$$\tfrac{1}{2} \rho V^2 = \Delta P$$

and we find

$$V = 0.18 \, (\Delta T)^{\frac{1}{2}}$$

when V is measured in km/sec.

If ΔT is a typical change in surface temperature arising from the reflection effect, V may represent a typical velocity of streaming. In fact V is likely to be an upper limit. In photospheric regions, $\Delta T \simeq 500^{\circ}$ and $\therefore V \simeq 4$ km/sec. In the chromosphere, according to the previous ideas, we may have $\Delta T \simeq 10{,}000^{\circ}$ and thus $V \simeq 20$ km/sec. If absorption lines are formed in a chromosphere, evidence of a velocity of streaming of this order should be observable in the velocity curves.

The velocity curves of the γ/ρ correlation may arise as a consequence of such a streaming. Lines which are highly distorted by reflection show the largest spurious γ, implying that the circulation velocity is highest around the sub-stellar points. This is qualitatively in agreement with one's expectations from the equation of continuity.

P A R T II

Bolometric Reflection Effect

Chapter IV KOPAL'S BOLOMETRIC THEORY

1. Introduction. The effect of reflection on the light curves of eclipsing systems in particular was not treated under realistic physical conditions until 1954. Before then the radiation incident on a reflecting star was considered to be either parallel in space, or to emanate from a point of light at a finite distance (SEN,† 1948). In 1954, KOPAL extended the simpler picture to include the case of a spherical illuminating source.

The problem can be divided into three main parts namely:-

1) To find the bolometric intensity distribution $J(\delta)$ over the surface of each star.

2) To convert this to a monochromatic intensity distribution $J_\lambda(\delta)$ in some discrete wavelength range.

3) To convert this, in turn, to a monochromatic magnitude variation $m_\lambda(\epsilon)$ with phase ϵ of the system.

These three parts are convoluted in KOPAL's approach.

† Proc. u.s. Acad. Sci., 34, 311.

Mainly, his concern is with the following problem, which for convenience is referred to later as KOPAL's problem:-

> Given two spherical stars with arbitrary radii, luminosities, limb-darkening and separation. To find the consequent bolometric magnitude variation with phase, on the assumptions that the albedo of each star is unity (in EDDINGTON's terminology) and that LAMBERT's cosine law of reflection applies.

KOPAL's theory is reviewed in the first part of the present chapter. In the course of examination of the theory a number of algebraic errors were found and the work was repeated with corrected algebra; in the event the final answer is unchanged. The second part of the chapter consists of a discussion of the theory from a conceptual point of view.

Review of KOPAL's Theory

2. If (a_1, a_2) represent the radii of the component stars and R the separation of their centres, the tidal distortion is of the order of $(a/R)^3$, and since the reflection effect is of order $(a/R)^2$, then distortion terms will not enter into the reflection effect unless terms of

order $(a/R)^5$ and higher are employed. The assumption of sphericity therefore implies that terms of order higher than $(a/R)^4$, which is terms of order higher than $(a/R)^4$, which is ar. taken to include $(a, a_2/R^2)^2$, will not appear. g star, also described as the primary by KOPAL.

The amount $\mathcal{L}$ of the secondary's light reflected by the primary in the direction of the observer is given by

$$\mathcal{L} = \int\int_C J(\phi, \eta) \cos\gamma \, d\sigma,$$

where $J(\phi, \eta)$ denotes the intensity of radiation reflected from a point P with coordinates (ϕ, η) not yet defined, γ is an angle of foreshortening, and the domain C of integration extends over the visible hemisphere. Evaluation of $J(\phi, \eta)$ is possible provided that the flux incident at (ϕ, η) is known and that the physics of the transfer of the radiation is also understood. The latter problem is by-passed by KOPAL when he adopts LAMBERT's law and considers mainly bolometric radiation.

3. <u>The Fully-Illuminated Zone</u>. In figure 38,

P is an arbitrary point on the reflecting star O_1, β denotes the angle O_2PQ between the lengths ρ, ρ' defined in the diagram and $\omega = \hat{QPQ'}$. ξ is the angle between ρ' and the normal at P.

Then

$$\cos\xi = \cos\alpha\cos\rho + \sin\alpha\sin\rho\cos\omega$$

Let the distribution of brightness $I(\theta')$ over the apparent disc of the secondary component (suffix 2) be given by

$$I(\theta') = I(0)\left\{1-u+u\cos\theta'\right\}$$

Then KOPAL states that the intensity of light reflected at P is given by

$$J(\varphi, \eta) = I(0)\left\{(1-u)J_1 + uJ_2\right\}$$

where

$$J_n = \frac{1}{\pi}\int\int \frac{\cos\xi\cos^n\theta'}{\rho'^2}\, ds_2 \qquad (1)$$

with $ds_2 = a_2^2\sin\theta\, d\theta d\omega$

$$= a_2(\rho'/\rho)\, d\rho' d\omega .$$

The derivation of (1) has involved LAMBERT's law, i.e., the assumption that the reflected radiation is distributed isotropically.

After a straightforward reduction, carrying the integration over

$$\rho - a_2 \leq \rho \leq (\rho^2 - a_2^2)^{\frac{1}{2}}$$

$$0 \leq \omega \leq 2\pi$$

it is found that

$$J_1 = \frac{a_2^2}{\rho^2} \cos\alpha$$

while similarly,

$$J_2 = \frac{2}{3}\frac{a_2^2}{\rho^2} \cos\alpha$$

Thus finally

$$J(\phi, \eta) = \frac{L_2 \cos\alpha}{\pi \rho^2}$$

where $$L_2 = \pi a_2^2 I(0)\left\{1 - \tfrac{1}{3}u\right\}$$

represents the apparent luminosity of the secondary component.

Since the integration has been carried over $0 \leq \omega \leq 2\pi$, the above expression for $J(\phi, \eta)$ applies only in the fully-illuminated zone of the reflecting star. In this zone, the amount of light reflected at any point is exactly the same as if the illuminating star were a point with the same distance, direction and apparent luminosity as the real star (a result which arises as a particular

case of a more general theorem established in chapter V). It should be noted, however, that the effect of secondary reflection has so far been neglected. Secondary reflection arises when the brightness distribution, due to reflection, over the disc of the illuminating star is taken into account.

4. The Penumbral Zone. In this region the secondary component is partially eclipsed by the horizon of the observer at P. KOPAL now writes

$$I'(q,\gamma) = I(0)\left\{(1-u)\,J_1' + J_2'\,u\right\}$$

where

$$\pi J_n' = 2a_2^2 \int_{|-\chi|}^{\cos^{-1}\left(\frac{a_2}{\rho}\right)} \int_{0}^{\cos^{-1}\left(\frac{\sin\chi}{\sin\Theta}\right)} \frac{\cos\xi\,\cos^n\theta'\,\sin\Theta\;.\;d\Theta\,d\omega}{\rho'^2} \qquad (2)$$

χ is a geometrical 'depth of eclipse' and is given by $\widehat{HO_2P}$

To check the limits of integration, consider figure 39 .

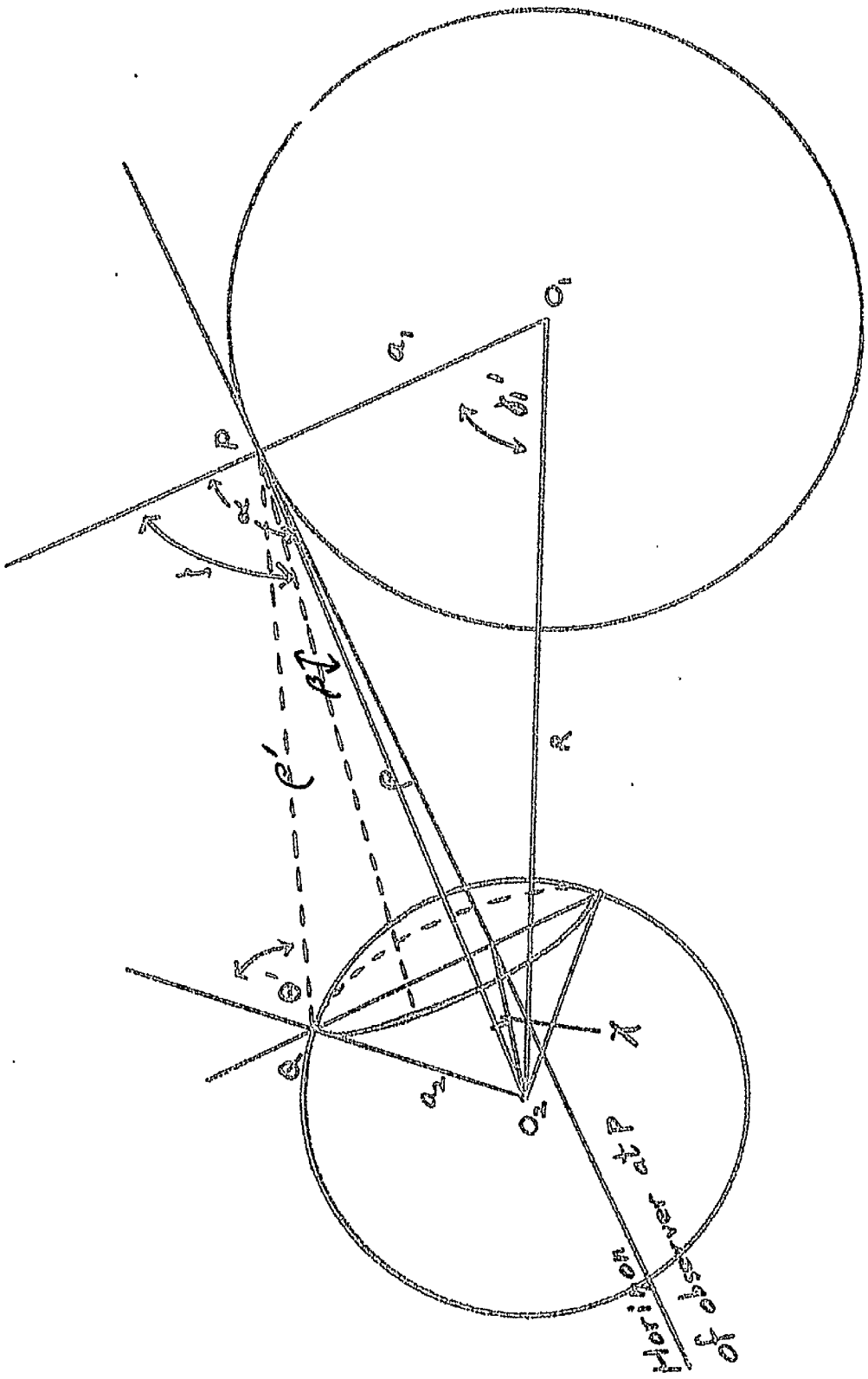

Figure 38

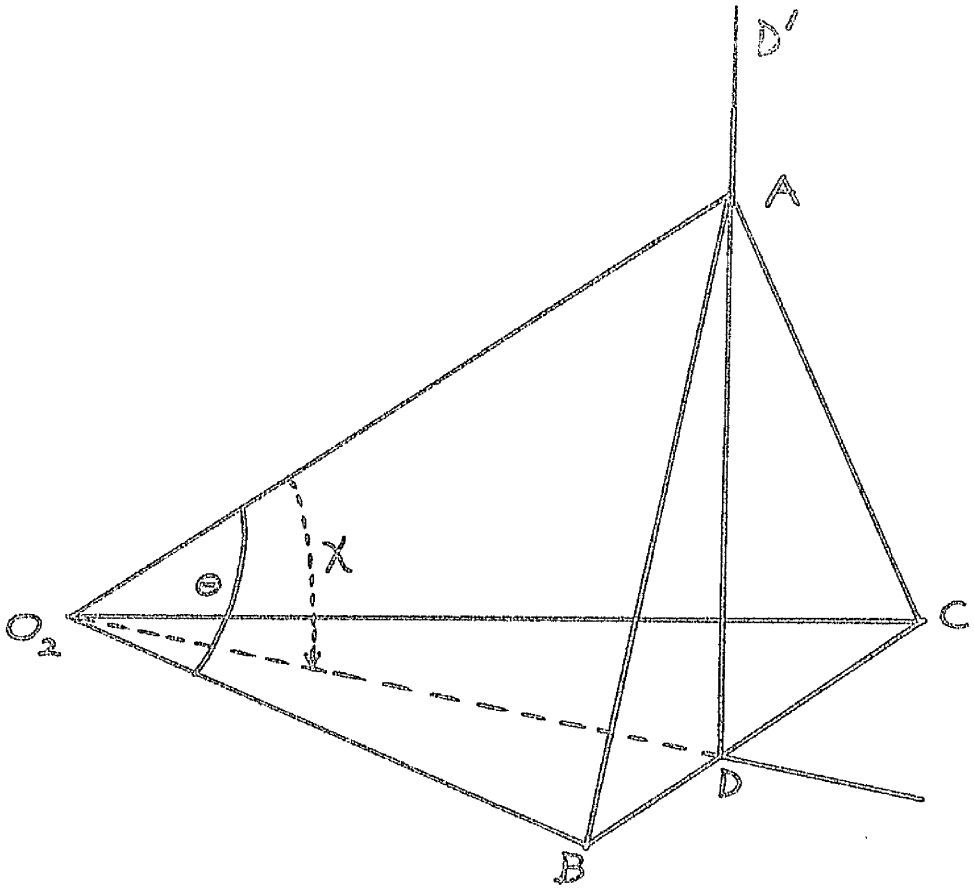

Figure 39

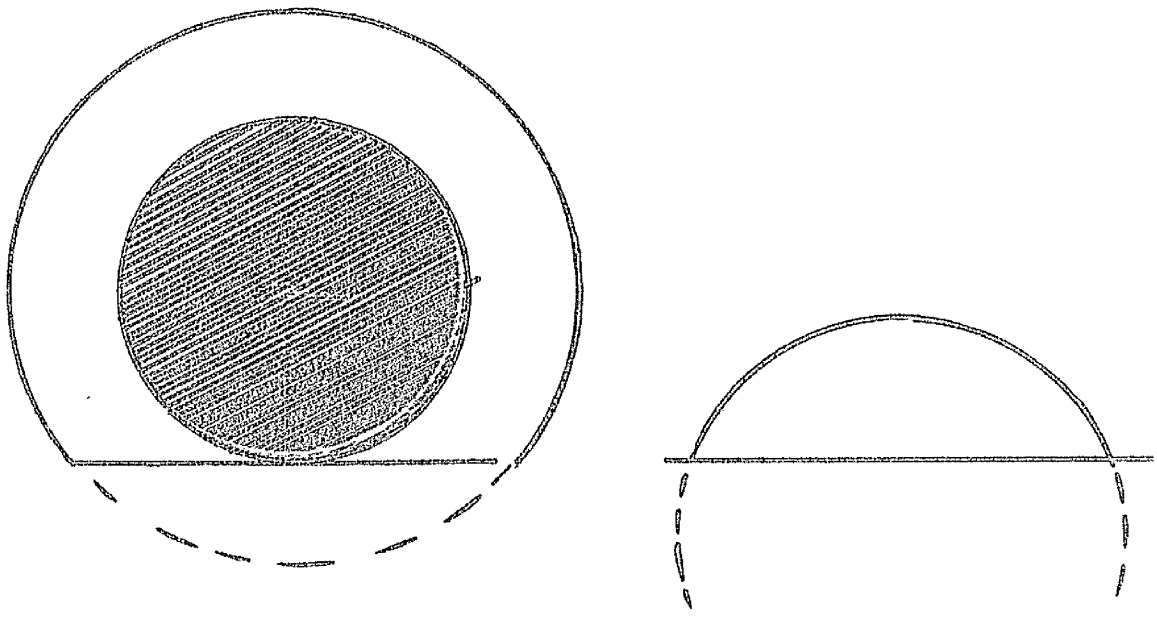

Figure 40

BC represents the horizon of the observer at P. Then

$$\sin\chi = \frac{AD}{O_2A} \qquad \sin\ = \frac{AB}{O_2A} \qquad -\cos\omega = \frac{AD}{AB}$$

$$\therefore \sin\chi = -\cos\omega \sin\Theta$$

$$\therefore \omega = \cos^{-1}\left(\frac{\sin\chi}{\sin\Theta}\right)$$

When the centre of the illuminating star is below the horizon, ω will always be less than 90^0 and we must have $\omega = \cos^{-1}(+k^2)$. Similarly when O_2 appears above the horizon, we require $\omega = \cos^{-1}(-k^2)$. We may take

$$\omega = \cos^{-1}\left(\frac{-\sin\chi}{\sin\Theta}\right)$$

or

$$\omega = \cos^{-1}\left(\frac{+\sin\chi}{\sin\Theta}\right) \qquad (3)$$

as we please, provided that a sign convention for χ is taken such as to satisfy the conditions above.

In both his 1954 paper and his book (Close Binary Systems) KOPAL takes an upper limit of integration

$$\omega = \cos^{-1}\left(+\frac{-\sin\chi}{\sin\Theta}\right)$$ Since we require

$$\omega = \cos^{-1}(-k^2)$$

when O_2 is above the horizon, χ must then be taken

negative. Similarly we require χ positive when O_2 is below the horizon. In his book, KOPAL states that 'We shall, moreover, reckon so that its upper limit corresponds to the beginning of the eclipse'. Evidently one is not entitled to use such a sign convention for χ if (3) is to be adopted. The opposite convention for χ is adopted in his paper, and this leads to different formulae for various quantities, although the final result is the same.

In figure 40(a), when O_2 is above the horizon, the limits of integration are

$$\int_0^{|\chi|}\int_0^{2\pi} + 2\int_{|\chi|}^{\cos^{-1}(a_2/\rho)}\int_0^{\cos^{-1}(+\sin\chi/\sin\Theta)} \tag{4}$$

while when O_2 is below the horizon, we have

$$2\int_{|\chi|}^{\cos^{-1}(a_2/\rho)}\int_0^{\cos^{-1}(+\sin\chi/\sin\Theta)} \tag{5}$$

KOPAL has apparently overlooked the shaded region in figure 40(a).

Since $\cos\zeta = \cos\alpha\cos\beta + \sin\alpha\sin\beta\cos\omega$,

$$J_n' = M_n\cos\alpha + N_n\sin\alpha .$$

In the case where O_2 is above the horizon,

$$\pi M_n = a_2^2 \left[2\pi \int_0^{|\chi|} \frac{\cos\beta \cos^n\theta' \sin\theta}{\rho'^2} \cdot d\theta \right.$$

$$\left. + \int_{|\chi|}^{\cos^{-1}(a_2/\rho)} + 2 \frac{\cos\beta \cos^{-1}\left(\frac{\sin\chi}{\sin\theta}\right) \sin\theta \cos^n\theta'}{\rho'^2} \cdot d\theta \right]$$

on using (4). Also

$$\pi N_n = 2a_2^2 \int_{|\chi|}^{\cos^{-1}(a_2/\rho)} \sin\beta \sin\theta (\sin^2\theta - \sin^2\chi)^{\frac{1}{2}} \cos\theta \cos^n\theta' \, d\theta$$

KOPAL states that 'If, however, only terms of the lowest order are to be retained, we may evidently set

$$\sin\beta \simeq \frac{a_2}{\rho} \sin\theta$$

$$\cos\beta \simeq 1$$

$$\cos\theta' \simeq \cos\theta$$

$$\rho' \simeq \rho \text{ !}$$

Then

$$M_1 = \frac{2a_2^2}{\pi\rho^2} \left[2\pi \int_0^{|\chi|} \sin\theta\cos\theta \, d\theta + 2\int_{|\chi|}^{\frac{\pi}{2}} \sin\theta \cos^{-1}\left(\frac{\sin\chi}{\sin\theta}\right) \cos\theta d \right.$$

$$N_1 = \frac{2a_2^3}{\pi\rho^3} \int_{|\chi|}^{\frac{\pi}{2}} \sin\theta \, (\sin^2\theta - \sin^2\chi)^{\frac{1}{2}} \cos\theta \, d\theta$$

(The corresponding expression for M_1 given by KOPAL is

$$M_1 = \frac{2a_2^2}{\pi\rho^2}\int_{-|\chi|}^{\frac{\pi}{2}} \cos^{-1}\left(\frac{\sin\chi}{\sin\theta}\right)\sin\theta\cos\theta\,d\theta$$

Which is meaningless for $\theta<\chi$).

These reduce to

$$M_1 = \left(\frac{a_2}{\rho}\right)^2\left\{\frac{1}{2} - \frac{\chi + \sin\chi\cos\chi}{\pi}\right\}$$

$$N_1 = \frac{2a_2^3}{3\pi\rho^3}\cos^3\chi$$

in the absence of limb-darkening.

It is of interest that the expression for M_1 is the same whether or not the centre of the illuminating star is above the horizon. It is because of this that KOPAL's omission did not lead to error.

From triangle HO_2P (figure 4-1),

$$\frac{\sin\left[\frac{\pi}{2} - (\alpha - \chi)\right]}{\rho} = \frac{\sin\left(\frac{\pi}{2} - \alpha\right)}{a_2}$$

$$\therefore \cos(\alpha - \chi) = \frac{\rho}{a_2}\cos\alpha$$

and since $\alpha \simeq \frac{\pi}{2}$

$$\sin\chi = -\frac{\rho\cos\alpha}{a_2} \qquad \therefore \cos\alpha = -\frac{a_2}{\rho}\sin\chi$$

$$\sin\alpha \neq 1$$

These equations are satisfied when O_2 is above or below the horizon.

Define $x = +\sin\chi$. Then

$$J_1' = \left(\frac{a_2}{\rho}\right)^2\left(\frac{1}{2} - \frac{\chi + \sin\chi\cos\chi}{\pi}\right)\left(-\frac{a_2}{\rho}x\right) + \frac{2a_2^3}{3\pi\rho^3}\cos^3\chi \qquad (6)$$

$$= \left(\frac{a_2}{\rho}\right)^3 x\left(\frac{\sin^{-1}x + x(1-x^2)^{\frac{1}{2}}}{\pi} - \frac{1}{2}\right) + \frac{2a_2^3}{3\pi\rho^3}(1-x^2)^{3/2} \qquad (7)$$

Similarly we find

$$J_2' = \frac{a_2^3}{\rho^3}\left\{\frac{x}{6}(1-x)(x^2+x-2) + \frac{1}{8}(1-x^2)^2\right\}$$

Both forms agree with those in KOPAL's paper.

Since

$$\left.\begin{aligned}
\sin^{-1}x &= x + \tfrac{1}{6}x^3 + \cdots\cdots\cdots\cdots \\
(1-x^2)^{\frac{1}{2}} &= 1 - \tfrac{1}{2}x^2 + \tfrac{3}{16}x^4 + \cdots\cdots\cdots \\
(1-x^2)^{3/2} &= 1 - \tfrac{3}{2}x^2 + \tfrac{3}{8}x^4 - \cdots\cdots\cdots
\end{aligned}\right\} \qquad (8)$$

Recalling that $J'(\phi, \eta) = I(0)\left\{(1-u)J_1' + uJ_2'\right\}$, and inserting (8) into (6) and (7), we find that to $O(x^4)$,

$$\mathcal{J}^u = \frac{a_2 L_2}{\pi R^3}\left\{\frac{2}{3\pi} - \frac{x}{2} + \frac{x^2}{\pi} - \frac{x^4}{12\pi} + \ldots\right\} \quad (9)$$

Where we have made use of the fact that $L_2 = \pi a_2^2 I(0)\,(1-\tfrac{1}{3}u)$, and also ρ has been taken equal to R. Superscript u refers to undarkened radiation. (9) differs from the corresponding equation (81) in KOPAL's paper: he has a $+\frac{1}{3}x$ term. As $\mathcal{J}^u$ represents the light reflected from a square centimetre of the primary when the source is an undarkened, partially set star, we should have $\mathcal{J}^u = 0$ when $x = 1$, this corresponding to $\sin\chi = \frac{\pi}{2}$. This check is satisfied in the case of $\mathcal{J}^u$ above but not for KOPAL's $\mathcal{J}^u$, which must therefore be erroneous.

Likewise,

$$\mathcal{J}^b = \frac{a_2 L_2}{\pi R^3}\left\{\frac{3}{16} - \frac{x}{2} + \frac{3x^2}{8} - \frac{x^4}{16}\right\} \quad (10)$$

Again, when x=1, $\mathcal{J}^b = 0$ as required, and once more KOPAL's $\mathcal{J}^b$ fails to satisfy the check.

For an arbitrarily limb-darkened irradiating star, the intensity $\mathcal{J}'$ of radiation reflected from unit area in the penumbral zone is given by

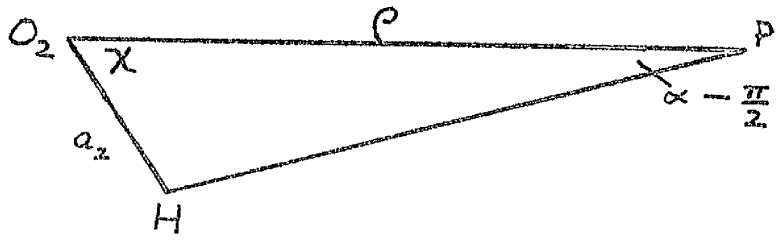

Figure 41

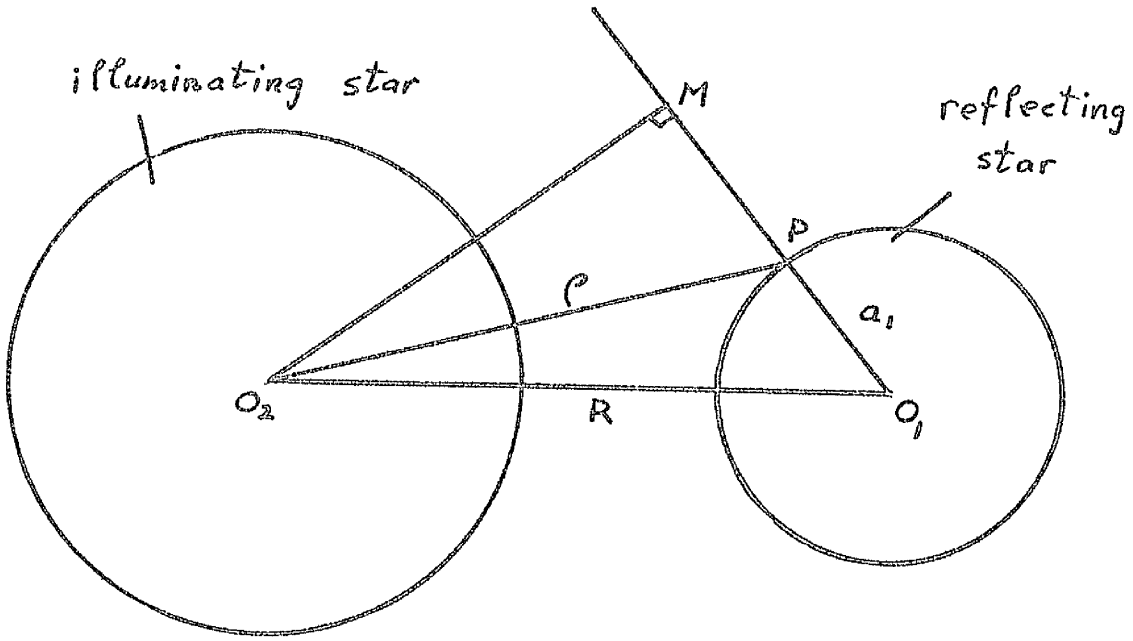

Figure 42

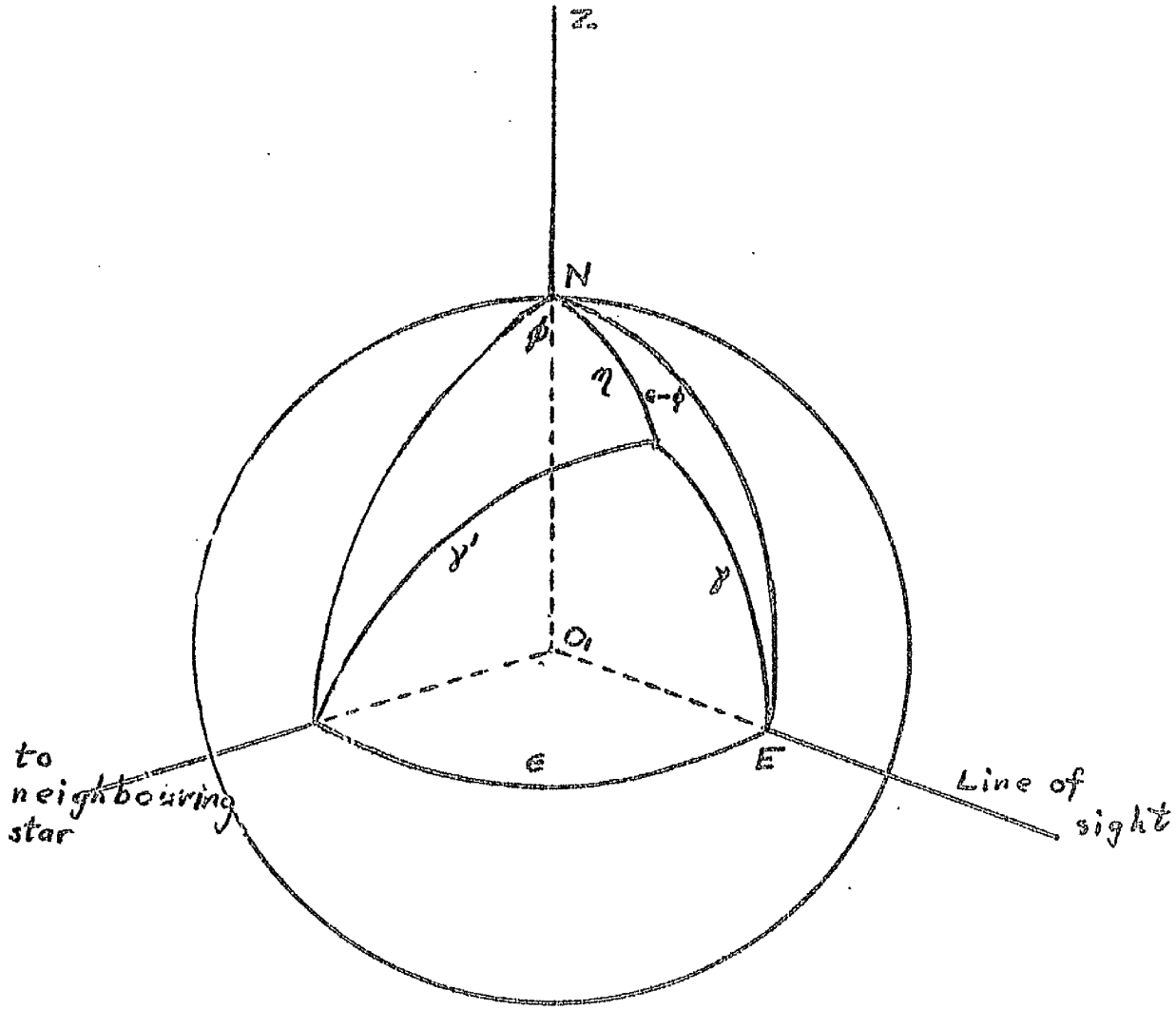

Geometry of the Reflection Effect, after KOPAL

Figure 43

$$S'(\varphi,\eta) = \frac{3}{3-u}(1-u)\,S''(\varphi,\eta) + \frac{2u}{3-u}\,S^{p}(\varphi,\eta)$$

5. The amount of the secondary's light reflected from the primary component into the line of sight has been given as

$$\mathcal{L} = \int\int_{c} S \cos\gamma \, d\sigma_1$$

where S has now been found in terms of $x \equiv \sin\chi$, the depth of eclipse. The integration of this equation constitutes the final part of the solution of KOPAL's problem. From triangle NPE in figure 43,

$\cos\gamma = \sin\eta\cos(\epsilon - \varphi)$

$\therefore d\sigma_1 = a_1^2 \sin\eta \, d\eta \, d\varphi$

The various quantities are defined in figure 34. Phase ϵ takes its minimum value when the intensity of radiation reflected from the primary towards the external observer is a maximum.

$$\cos\epsilon = -\sin(v+\omega)\sin i$$

KOPAL now introduces the integral operator K(x) defined by

$$K(x)\{---\} = \int_{\epsilon-\frac{\pi}{2}}^{\cos^{-1}x} \int_{\sin^{-1}\left(\frac{x}{\cos\phi}\right)}^{\pi-\sin^{-1}\left(\frac{x}{\cos\phi}\right)} --- \cos\gamma \, d\sigma,$$

The inner tangent cone to the stars has semi-angle η_1 given by

$$\sin\eta_1 = \frac{a_1+a_2}{R} \qquad \text{(figure 44)}$$

and within this cone, i.e. within the fully-illuminated zone,

$$\eta_1 \leqslant \eta \leqslant \pi - \eta_1$$

Similarly, the boundary between the penumbral zone and the non-illuminated part of the reflecting star described by $\eta = \eta_2$ where

$$\sin\eta_2 = \frac{a_1-a_2}{R}$$

Therefore in the range $\eta_1 \leqslant \epsilon \leqslant \pi-\eta_1$ the fully-lit zone is delimited by an application of the operator $K(\sin\eta_0)$: while the penumbral zone should be delimited by an application of $K(\sin\eta_2) - K(\sin\eta_1)$.

Outside this range of phase, the K-operator

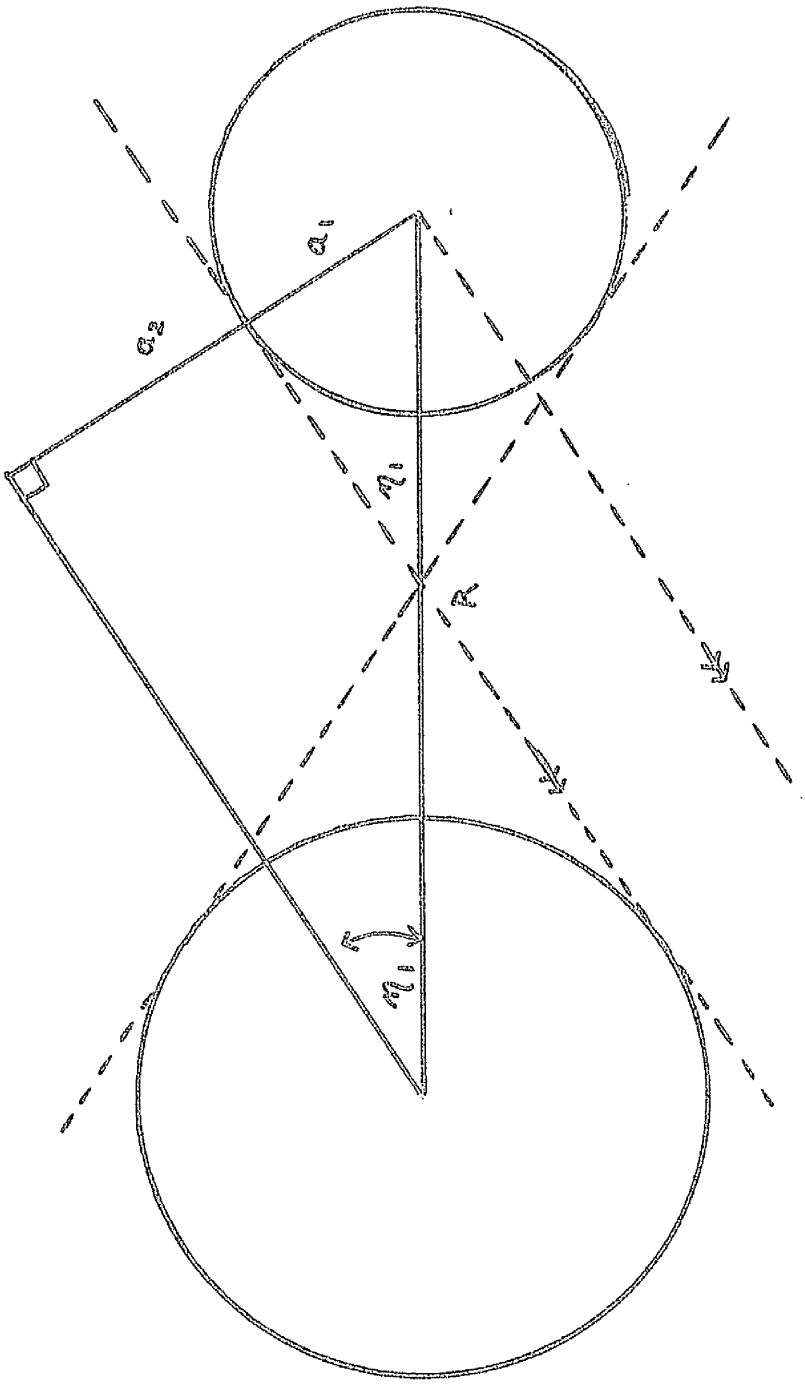

Figure 44

must be modified in a manner depending on the phase and relative radii of the stars. For example in the range $\pi - \eta_1 \leq \alpha \leq \pi + \eta_1$ the fully illuminated zone disappears from view and the integral operator must therefore vanish. However the modifications need not concern us.

In order to apply the operator, x is related to $\mu = \cos\gamma' = \cos\phi \sin\eta$. From figure 42,

$$\mu = \frac{O_1M}{R} = \frac{O_1P - MP}{R} = \frac{a_1 + \rho\cos\alpha}{R}$$

But $\rho \simeq R$ according to KOPAL

$$\therefore \frac{R}{a_2}\cos\alpha = \frac{R\mu - a_1}{a_2}$$

$$\therefore x = \frac{a_1 - R\mu}{a_2}$$

KOPAL has $-x = \frac{a_1 - R\mu}{a_2}$

His expansions in x of J'', J^D are correct if x is replaced by -x. Reversal of sign also corrects his $x(\mu)$ equation. Thus these errors cancel out when the integration over μ is performed, and in the absence of further errors his final result will be correct.

For the fully illuminated zone,

$$I(\rho,\eta) = \frac{L_2 \cos\alpha}{\pi\rho^2}$$

$$= \frac{L_2}{\pi} \frac{a_1 - R\mu}{(R^2 + a_1^2 - 2a_1R)^{3/2}}$$

$$= \frac{L_2}{\pi R^2}\left\{P_1(\mu) + \frac{2a_1}{R}P_2(\mu) + \frac{3a_1^2}{R^2}P_3(\mu) + \ldots\right\}$$

$$\mathcal{L}_1(a_1,a_2,\epsilon) = K(\sin\eta_1)\left\{P_1(\mu) + \frac{2a_1}{R}P_2(\mu) + \ldots\ldots\right\}\frac{L_2}{\pi R^2}$$

where $\mathcal{L}_1$ represents the amount of light reflected by the primary from the fully illuminated zone along the observer's line of sight. The actual integration is laborious. KOPAL finds eventually that for any phase angle ϵ within the range $\eta_1 \leqslant \epsilon \leqslant \pi - \eta_1$,

$$\mathcal{L}_1(a_1, a_2, \epsilon) = L_2\left\{\frac{2}{3}\left(\frac{a_1}{R}\right)^2 \frac{(\pi-\epsilon)\cos\epsilon + \sin\epsilon}{\pi}\right.$$

$$+\frac{1}{8}\left(\frac{a_1}{R}\right)^3(3\cos^2\epsilon + 2\cos\epsilon - 1)$$

$$+\left(\frac{a_1}{R}\right)^4 \frac{\sin\epsilon\cos^2\epsilon}{\pi} - \frac{a_1^2a_2^2}{R^4}\frac{\sin\epsilon}{\pi}$$

$$\left. + \ldots\ldots\right\} \qquad (11)$$

Outside this range the modified K-operator must be used. Further integration produces the result that within the range $-\eta_1 \leqslant \epsilon \leqslant \eta_1$,

$$\mathcal{L}_1(a_1, a_2, \epsilon) = L_2 \frac{a_1^2}{R^2}\left\{\frac{2}{3} + \frac{a_1 + a_2}{2R} + \ldots\right\}\cos\epsilon \qquad (12)$$

while for all other phases the reflection effect is negligible.

In the penumbral zone,

$$\mathcal{L}_2(a_1, a_2, \epsilon) = \frac{3(1-u)}{3-u}\mathcal{L}_2^{U} + \frac{2}{3-u}\mathcal{L}_2^{D}$$

$$\mathcal{L}_2^{U,D} = \left\{K(\sin\eta_2) - K(\sin\eta_1)\right\}\left\{J^{U,D}(\phi, \eta)\right\}$$

The expansion (9), (10) for $J^{U,D}$ in x are converted to expansions in μ :

$$J^{U}(\phi, \eta) = \frac{a_2 L_2}{\pi R^3}\sum_{n=0}^{\infty} C_n^{U}\left(\frac{R\mu}{a_2}\right)^n$$

and similarly for J^{D}.

Now it can be shown that

$$K(\xi)(\mu^n) = K(0)\{\mu^n\} - \frac{2a_1^2}{n+1}\xi^n \sin\epsilon + \ldots\ldots$$

whence

whence

$$\left\{K(\sin\eta_2) - K(\sin\eta_1)\right\} J^{U,D}(\phi,\eta)$$

$$= 2\,\frac{L_2}{\pi}\,\frac{a_1^2 a_2}{R^3}\sum_{n=0}^{\infty}\frac{C_n^{U,D}}{n+1}\left(\frac{R}{a_2}\right)^n\left(\sin^{n+1}\eta_1 - \sin^{n+1}\eta_2\right)\sin\epsilon$$

$$= \frac{2}{\pi}\left(\frac{a_1 a_2}{R^2}\right)^2 L_2 \sin\epsilon \sum_{n=0}^{\infty}\frac{C_n^{U,D}}{n+1}\left\{\left(\frac{a_1+a_2}{a_2}\right)^{n+1} - \left(\frac{a_1-a_2}{a_2}\right)^{n+1}\right\}$$

where all the C_n^D 's for $n > 4$ are identically zero. Inserting the coefficients C_n the summation reduces to $2/\pi$ and 0.6 for an undarkened and completely darkened irradiating source respectively (not $1/\pi$ and 0.3 as stated by KOPAL). However, the final expressions are given correctly by KOPAL as

$$\mathcal{L}_2^U = \left(\frac{2a_1 a_2}{\pi R^2}\right)^2 L_2 \sin\epsilon + \cdots$$

$$\mathcal{L}_2^D = \frac{6}{5\pi}\left(\frac{a_1 a_2}{R^2}\right)^2 L_2 \sin\epsilon + \cdots$$

Thus for an arbitrarily limb-darkened source,

$$\mathcal{L}_2 = \frac{12}{5}\left\{\frac{a_1 a_2}{\pi R^2}\right\}^2\left\{\frac{5+(\pi-5)u}{3-u}\right\} L_2 \sin\epsilon + \cdots$$

for any phase angle within the range

$$\sin^{-1}\frac{a_1+a_2}{R} \leqslant \epsilon \leqslant \pi - \sin^{-1}\frac{a_1+a_2}{R}$$

The total amount of light reflected from the primary is $\mathcal{L} = \mathcal{L}_1 + \mathcal{L}_2$. No expression for the penumbral light is given within the range

$$-\sin^{-1}\left(\frac{a_1+a_2}{R}\right) \leqslant \epsilon \leqslant +\sin^{-1}\left(\frac{a_1+a_2}{R}\right) \qquad (13)$$

KOPAL finally expands the phase law in a Fourier cosine series, and in ascending powers of $\cos\epsilon$. Thus, for example,

$$\mathcal{L}(a_1, a_2, \epsilon) = L_2 \sum_{n=0}^{\infty} C_n \cos^n \epsilon$$

with

$$C_0 = \frac{2}{3\pi}\left(\frac{a_1}{R}\right)^2 - \frac{1}{8}\left(\frac{a_1}{R}\right)^3 - \frac{k}{\pi}\left(\frac{a_1 a_2}{R^2}\right)^2 + \cdots$$

$$C_1 = \frac{1}{3}\left(\frac{a_1}{R}\right)^2 + \frac{1}{4}\left(\frac{a_1}{R}\right)^3 + \cdots$$

$$C_2 = \frac{1}{3\pi}\left(\frac{a_1}{R}\right)^2 + \frac{3}{8}\left(\frac{a_1}{R}\right)^3 + \frac{1}{\pi}\left(\frac{a_1}{R}\right)^4 + \frac{k}{2\pi}\left(\frac{a_1 a_2}{R^2}\right)^2 + \cdots$$

$$C_3 = 0$$

$$C_4 = \frac{1}{36\pi}\left(\frac{a_1}{R}\right)^2 - \frac{1}{2\pi}\left(\frac{a_1}{R}\right)^4 + \frac{k}{8\pi}\left(\frac{a_1 a_2}{R^2}\right)^2 + \cdots$$

with $k = 1 - \frac{12}{5\pi}\,\frac{5+(\pi-5)u}{3-u}$

6. <u>Secondary Reflection.</u> KOPAL states that 'The symbol L_2 ..... has been used to denote the fractional luminosity of the illuminating component

as seen from the reflecting star -- that is its intrinsic luminosity augmented by that part of the primary's light which will be reflected from it back in the direction of the radius vector (corresponding to $\epsilon = 0$)'.

The symbol L_2 must be replaced by $(L_2)_0$, representing the intrinsic luminosity of component 2, plus $(L_1)_0 \left(\frac{a_2}{R}\right)^2 \left\{\frac{2}{3} + \frac{a_1 + a_2}{2R} + \ldots\right\}$ from (12). That is,

$$L_2 = (L_2)_0 + (L_1)_0 \left\{\frac{2}{3}\left(\frac{a_2}{R}\right)^2 + \frac{1}{2}\left(\frac{a_2}{R}\right)^3 + \frac{1}{2}\left(\frac{a_1 a_2^2}{R^3}\right) + \ldots\right\} \quad (14)$$

7. Finally, an attempt is made to convert from bolometric to monochromatic radiation.

The luminosity $(L_2)_\lambda$ of the irradiating component in an effective wavelength λ is given by

$$(L_2)_\lambda = \left(\frac{J_\lambda}{J_b}\right)_2 L_2$$

where J_b, J_λ denote the surface brightness of the secondary in total and discrete light:

$$L_2 = \pi a_2^2 J_b \qquad (L_2)_\lambda = \pi a_2^2 J_\lambda$$

A known fraction $\mathcal{L} = q(\epsilon) L_2$ of the secondary's light is intercepted and reflected by the primary. Thus

$$\mathcal{L}_\lambda = \left(\frac{J_\lambda}{J_b}\right)_1 \mathcal{L} = q(\epsilon)\left(\frac{J_\lambda}{J_b}\right)_1 L_2$$

Eliminating L_2 :

$$\mathcal{L}_\lambda = f\, q(e)\,(L_2)_\lambda$$

where

$$f = \left(\frac{J_2}{J_1}\right)_b \left(\frac{J_1}{J_2}\right)_\lambda$$

represents the luminous-efficiency factor to be applied to the bolometric radiation reflected along the observer's line of sight.

If the stars radiate like black bodies

$$\left.\begin{aligned} \left(\frac{J_1}{J_2}\right)_b &= \left(\frac{T_1}{T_2}\right)^4 \\ \text{while} \quad \left(\frac{J_1}{J_2}\right)_\lambda &= \frac{e^{\frac{c_2}{\lambda T_2}} - 1}{e^{\frac{c_2}{\lambda T_1}} - 1} \end{aligned}\right\} \qquad (15)$$

where $T_{1,2}$ denote the mean effective temperatures of the illuminated hemispheres of the two stars. 'It should be stressed that these will <u>not</u> be identical with the proper effective temperatures of their averted (dark) hemispheres, because of the heating effect of incident radiation.....'

Discussion and Critique of the Theory

8. KOPAL states that 'the expressions for the

flux and limits of integration could, in fact, be used to study the reflection of light from two spheres in actual contact, or from a sphere illuminated by an infinite wall - in both of which cases there would be no fully illuminated zone, but only a penumbral zone (extending, in the latter case, over the entire surface of the reflecting sphere). Such extreme cases would, however, be of little or no astrophysical interest, since two stars brought so close together could not possibly retain spherical shape , and their mutual distortion would render the geometry of our preceding sections in exact.' Thus the solution is carried through to terms of the order of $(a/R)^4$, since the effect of rotational or tidal distortion of the primary component would influence the amount of light reflected from it through a term of $O(a/R)^5$.

However, the important point would seem to be that, although the error in the calculated reflection effect may be larger for close systems than for well-separated ones, the proportional error remains small. Typically, a light variation of about $0^m.05$ may be produced. The reflection effect is of order $(a/R)^2$, and as the influence of distortion

on the effect is of order $(a/R)^5$, the relative error, introduced by neglect of distortion, is of order $(a/R)^3$, which may be 10% typically. A theoretical reflection effect for contact systems should thus be systematically in error (by virtue of the neglect of distortion) by about $0^m.005$; a quantity which will be much less for systems separated by, say, a stellar radius, due to the third power dependence of distortion on separation.

It follows that a theory of the reflection effect which neglects tidal and rotational distortion is nevertheless a useful one to have, even for very close systems, as the error introduced will probably be only a few per cent. A 'useful' theory in the present context is one which can be used to draw meaningful conclusions from observational data.

9. It is fundamental to KOPAL's work that the effects of the penumbral regions and secondary reflection are so small that they may be dealt with only to the lowest order of approximation. In order to test this surmise a rough attempt was made to estimate the relative importance of the fully-lit

and penumbral zones.

Consider the reflecting star in a system with $i=0^{\circ}$ at full phase (neglecting the fact that it would then in reality be eclipsed.) Let (I_p, I_F) represent the relative intensities of the penumbral and fully illuminated regions respectively, as seen by the external observer. Then the star appears to the distant observer as a disc with concentric annuli of various brightnesses. Neglecting limb-darkening,

$$I_p = 2\pi \int_{\Theta_0}^{\pi/2} f_p(\Theta) \sin\Theta \, d\Theta$$

$$I_F = 2\pi \int_{0}^{\Theta_0} f_F(\Theta) \sin\Theta \, d\Theta$$

where Θ is the limb-darkening angle and Θ_0 represents the boundary between the zones (figure 45). $f_p(\Theta)$, $f_F(\Theta)$, are functions describing the intensity of radiation incident on points with angle Θ. To estimate the relative importance of the two zones, a mean intensity of reflected radiation from each region should be derived. Suppose that the intensity of radiation (incident on unit area of the reflecting star) is proportional to the cosine of the

zenith distance of the secondary and is independent of the distance of the area from the secondary. These assumptions probably underestimate the importance of the penumbra, as from a zenith distance of 90^0 the incident intensity is taken to be zero, whereas it is in fact finite. Then

$$\frac{I_p}{I_F} = \frac{\int_{\Theta_0}^{\frac{\pi}{2}} A(\Theta) \sin\Theta \cos\Theta' \, d\Theta}{\int_0^{\Theta_0} \sin\Theta \cos\Theta' \, d\Theta}$$

$A(\Theta)$ represents that fraction of the secondary's disc which is uneclipsed to an observer in the penumbral region. Close to $\Theta = \Theta_0$, $A(\Theta) \doteqdot 1$, while for $\Theta' \simeq \Theta = \frac{\pi}{2}$, $A(\Theta) = \frac{1}{2}$. Probably no large error is introduced if we suppose that a mean value $\bar{A}$ is about $\frac{3}{4}$; only a rough estimate of I_p/I_F is required. Adopting KOPAL's approximation that $\cos\Theta \doteqdot \cos\Theta'$, we find $I_p/I_F = \bar{A} \cot^2\Theta_0 = \frac{3}{4}\cot^2\Theta_0$

with $\cot\Theta_0 = (a_1 + a_2)/R$.

ϵ_0	$(a_1+a_2)/R$	I_P/I_F
0	1.00	∞
30	0.87	$2\frac{1}{4}$
45	0.72	$\frac{3}{4}$
60	0.50	$\frac{1}{4}$
90	0.00	0

It is clear from the above table that for close binary systems in general the penumbral regions cannot be treated in the lowest order of approximation if KOPAL's problem is to be solved at all accurately. For example in the case of 57 Cygni the radiation from the penumbra may be about a quarter of that from the fully illuminated zone, while for a system the separation of whose sub-stellar points is about a radius, the radiation from the penumbra is about 70% of that from the fully lit zone at the phase $\epsilon = 0$. Furthermore this phase gives the minimum value of I_P/I_F; other phases would result in a larger ratio.

10. Even for well-separated systems for which an accurate calculation of the effects of penumbral

and secondary reflection terms is not necessary, the percentage error in these terms introduced by virtue of KOPAL's approximations may be quite large:-

(i) If we take account of secondary reflection it is no longer true that the brightness distribution over the secondary is given by $I(\theta') = I(0)\{1-u+u\cos\theta\}$, as the isophotes of the reflected radiation are symmetrical about the line joining the stellar centres rather than the line joining the observer P and the centre O_2. The procedure of simply replacing $(L_2)_0$ by L_2 (from (14)) is therefore not justified, and a systematic error in the calculated value of $f(\rho, q)$ must be produced. It is difficult to judge the order of magnitude of the effect, but at any rate KOPAL has not shown that his approach is sufficient in the sense that all terms of $O(a_1 a_2/R^2)^2$ or lower have been included.

(ii) The influence of the penumbra on the $\Delta m(\epsilon)$ curve is neglected by KOPAL for all phase angles such that the fully illuminated zone is not eclipsed by the limb of the reflecting star (see (13)). This means that the penumbra is

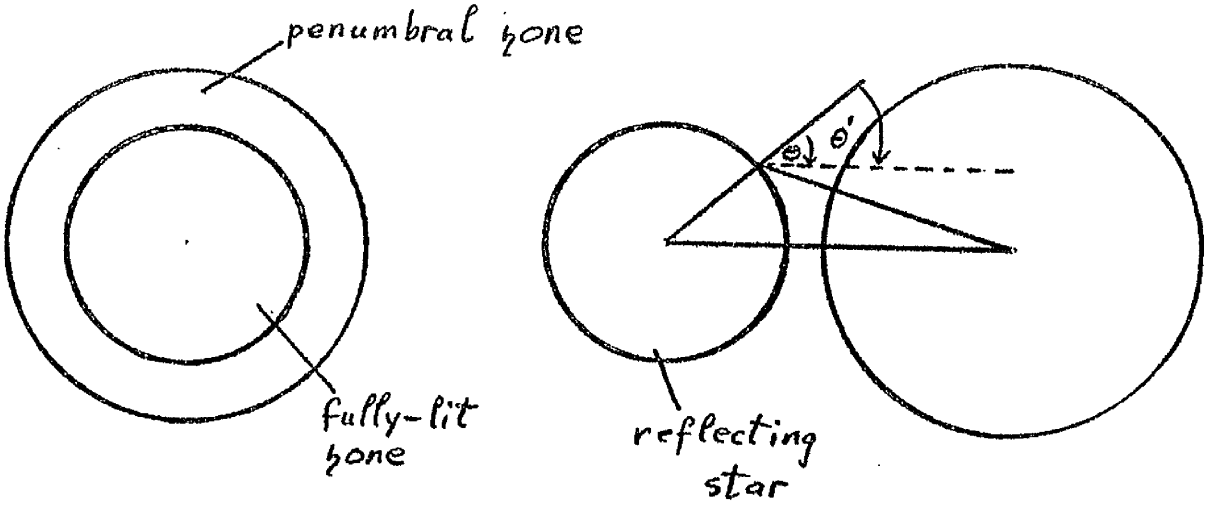

Figure 45

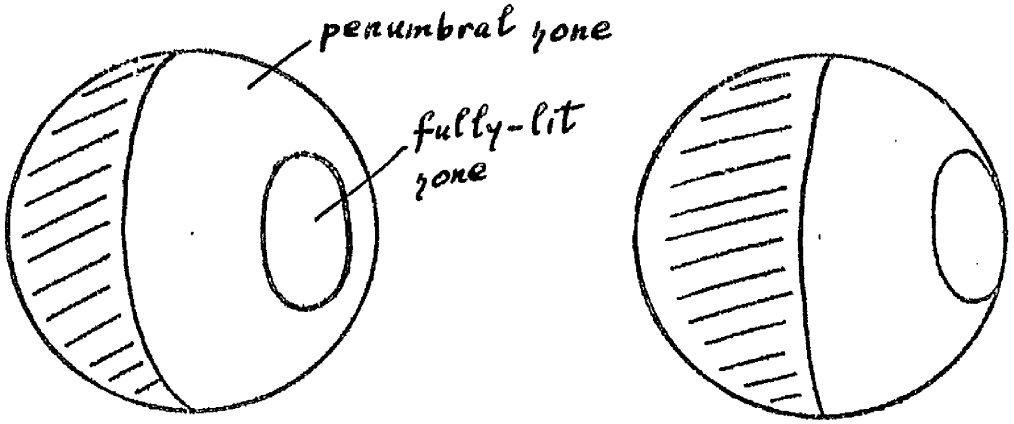

Figure 46

neglected in the configuration shown in figure 4c(a), but not in 4c(b).

No justification for this omission is given by KOPAL.

11. We have seen that the approximate treatment of the effects due to the finite radius of the illuminating component is open to question, not only because the penumbral zone is more important for close systems than KOPAL surmised, but also because his approximations are inadequate. It will now be argued that even if the treatment had been adequate to $O(a/R)^4$, it is doubtful whether realistic application to a close system could have been made.

The concept of 'an order of magnitude' is used by KOPAL and by the earlier workers such as TAKEDA. Its usefulness in the present context is open to some doubt, however. To illustrate this, consider a function L of some variable x, and expand L as a power series in x:

$$L = L_0 + L_1 x + L_2 x^2 + \text{terms of higher order} \quad (16)$$

If L is to be evaluated to, say, the order of x^2, the

implication is that the error committed by the omission of L_3x^3, L_4x^4, ..., lies within a fairly well-defined range which is small compared with L. For example if x = 0.1 and the coefficients L_i are comparable in magnitude, then by evaluating L to $O(x^2)$ a 1% accuracy may be expected. Suppose however, that x = 0.5, say. Then there is no longer any guarantee that $(L_3x^3 + L_4x^4 + ...)$ is a small quantity compared with L; it is likely that the sum of the terms omitted is a large, numerically, as L_2x^2, and even conceivable that $L_3x^3 > L_2x^2$.

It follows that to evaluate the bolometric reflection effect to $O(a/R)^4$ when $a/R \simeq 0.3$ or more, say, is a meaningless procedure, as the error committed by the omission of the higher order terms is likely to be fully as large as the $(a/R)^4$ terms, so that no significance can be attached to the latter. The expansion of KOPAL's phase law in ascending powers of cos e illustrates this point. The series for the coefficients C_n do not converge rapidly for realistic values of a/R, if they converge at all. A similar criticism can of course be levelled at the earlier theories

of the bolometric effect. Thus the applicability of KOPAL's theory is questionable, apart from the errors of approximation already discussed.

It follows that any attempt to extend the theory of the reflection effect by the addition of terms of successively higher order is likely to be laborious and of dubious validity.

11. The theme of the previous section may be further illustrated by considering multiple reflections in a very close system. Consider two identical stars with flux F_o ergs/cm^2/sec in the absence of reflection. Let the flux around the sub-stellar points be represented by F. Then if the stars are sufficiently close the area HH′ at the hot-spot of one star is illuminated by a disc of solid angle Ω and surface flux F. The flux from a square centimetre of HH′ is therefore $F_o + \frac{\Omega}{2\pi}F$, since a proportion $\frac{\Omega}{2\pi}$ of the radiation from KK′ is intercepted by HH′. Thus as the stars are identical

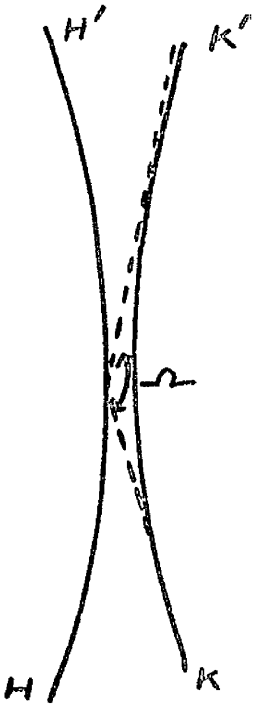

$$F = F_o + \frac{\Omega}{2\pi}F$$

$$F = \frac{F_o}{1 - \frac{\Omega}{2\pi}}$$

As the stars tend to touch, $\Omega \to 2\pi$ and $F \to \infty$. In effect this means that radiation from the interior is 'reflected' many times in the region of the sub-stellar points of a contact system. The implication is that convergence of (16) is slow at the hotspots of a close system, and breaks down when the stars are in contact. Thus at the sub-stellar points, when $x \equiv a/R$ is close to half, it is no longer true to say that all L_i are comparable: beyond some term we must have $L_{i+1}/L_i \simeq 2$; the derivation of a few terms of $O(a/R)^n$ cannot be expected to yield an accurate result for the intensity distribution of close or contact binary systems in the region of the sub-stellar points.

12. In order to compare theory with observation it is necessary to convert a bolometric distribution to a photometric one in some discrete wavelength range. The fact that no such conversion procedure is given detracts from the usefulness of KOPAL's theory. The quantities (T_1, T_2) in (15) denote the mean effective temperatures of the illuminated hemispheres of the stars. However no way in which the mean temperatures could be calculated is

indicated. It might be hoped that, given the bolometric distribution, it would be possible to convert to the photometric one, so that $\Delta m_{\lambda}(\epsilon)$ could then be calculated, but it turns out that the mathematics involved in the derivation of $J(\phi, \eta)$ is so convoluted with that involved in the conversion $J(\phi, \eta) \rightarrow \Delta m(\epsilon)$, that this is not a practical proposition.

13. Summary. (1) The neglect of tidal distortion would not invalidate any reflection effect theory even for very close and possibly contact systems.

(2) The importance of the penumbral zone and of multiple reflection are underestimated by KOPAL and in any case his approximations are inadequate.

(3) Any approach to reflection effect theory based on the idea of deducing and adding individual terms of various 'orders of magnitude' is unlikely to be valid for close systems, due to the slow convergence of series of the form (16).

(4) There seems to be no way in which a conversion from bolometric to photometric reflection could be made in KOPAL's theory, so that the theory cannot be accurately compared with observation.

Chapter V. BOLOMETRIC REFLECTION IN CLOSE SYSTEMS

Lead we not here a jolly life
Betwixt the shine and shade?

SIR HENRY TAYLOR

(Philip van Artevelde, Pt.II).

1. Introduction. The present chapter largely consists of the treatment of KOPAL's problem from a different point of view.

The question may be asked to what degree of accuracy it is desirable to solve the problem. In the first place, it is possible that the physics of real binaries does not bear a close resemblance to that adopted in the problem. For example HOSOKAWA† (1959) finds that the theoretical reflection effect for Algol predicts too large an amplitude for the $\Delta m_\lambda(\epsilon)$ curve by a factor of about two; and the possibility exists that $T_s \gg 2^{\frac{1}{4}} T_e$ for 57 Cygni,

† Sendai Astr. Raportoj, 10, 207.

suggesting that the solution of KOPAL's problem would have little relevance to the observed $\Delta m_\lambda(\epsilon)$ curves.

According to STRUVE and HUANG, gaseous streams are evident in nearly all systems with periods between two and five days; it is likely that these streams obscure the effects of reflection to some extent, and in fact the 'asymmetric' coefficients (A_3, A_4) in the Fourier expansion of the light curve outside eclipse are often comparable with the symmetric ones (A_1, A_2):-

$$l = A_0 + A_1 \cos\epsilon + A_2 \cos 2\epsilon + A_3 \sin\epsilon + A_4 \sin 2\epsilon$$

The asymmetric coefficients are usually attributed to gaseous material between and around the component stars.

However, a list of thirty close systems which are comparatively unaffected by streams has been compiled by HOSOKAWA† (1957); and there are probably many more which fail to satisfy various selection criteria used by him. All these binaries have large reflection coefficients. The observations of some of these systems are in reasonable

† Sendai Astr. Raportoj, 52, 208.

agreement with theoretical expectations, although most show systematic departures from the reflection theory used. The departures are significant but in most cases are not order of magnitude, indicating that for these systems the reflection theory, although not satisfactory, is not based on grossly erroneous physics. For HOSOKAWA's stars an accurate theory is called for.

It is usually considered that the A, term above is due to reflection, the A_2 term arising from the mutual distortion of the components. It remains to be seen whether in a realistic treatment of the reflection effect this result still holds; if not then estimates of the ellipticity of close stars must be systematically in error.

The solution of KOPAL's problem therefore seems worthwhile, although probably not to the limits of accuracy obtainable with a photoelectric photometer. An accuracy of $\sim 0^{m}.005$ or better is probably attainable with the method described later.

2. The problem can be regarded as that of solving a partial differential equation, the transfer equation, subject to appropriate boundary

conditions. In the absence of circumstellar absorption or emission, the transfer equation reduces to simply $dI/ds = 0$. Thus the intensity of radiation from any area is constant along any path length s. No integration need then be performed over distance and the problem now involves only two independent variables. (Although of course, relative dimensions are still involved). The result is a simplification of the algebra by about an order of magnitude, as a consequence of which a satisfactory treatment of the penumbral regions and of multiple reflections can be obtained.

3. Integral Equation Formulation. The distribution of intensity $J(\delta)$ over the reflecting star depends on that over the secondary, which in turn, due to the multiple reflections which become appreciable in close systems, depends on that over the reflecting star. An integral equation formulation is thereby suggested. It turns out that an equation of the form

$$J(\delta) = \int_A \int_B \int_\Gamma \int_\Delta J(\delta)\, F(A,B,\Gamma,\Delta)\, dA\, dB\, d\Gamma\, d\Delta$$

+ a constant

arises, where the kernel $F(A,B,\Gamma,\Delta)$ possesses several discontinuities in slope and is complicated. If $J(\delta)$ were expanded as a polynomial in $\cos\delta$, one would then have to solve n equations for the unknowns $j_1,\ldots\ldots j_n$ (j_0 being regarded as known). n would have to be large to accurately allow for the two discontinuities in slope along both borders of the penumbra, and the flatness of the $J(\delta)$ curve over the unlit part of the star. solution of the simultaneous equations would probably have to be done by electronic computer. The labour involved in evaluating

$$\int\int\int\int \cos^r\delta \; F(A,B,\Gamma,\Delta)\, dA\, dB\, d\Gamma\, d\Delta$$

analytically when r is greater than 3 or 4 is very considerable.

Given that an integral equation formulation arises, even formally, then any solution of KOPAL's problem must involve either an iteration procedure or the solution of a set of simultaneous linear equations: an explicit formula for $J(\delta)$ or $\Delta m(\epsilon)$ can no longer be expected. It is only because he evaluated secondary reflection to the lowest order

of approximation that KOPAL was able to derive an analytical expression.

4. Quadratic Representation. Let the intensity distribution over star 1 be represented by

$$J'(\delta) = j'_0 + j'_1 \cos\delta + j'_2 \cos^2\delta$$

This is inadequate to give $\Delta m(\epsilon)$ accurately, but may be ample in a calculation of $J(\delta)$, which calculation involves the as yet unknown $J(\delta)$. The point is that a rough representation of one distribution may be sufficient in a calculation to find an accurate representation of the other distribution.

The procedure therefore is to assume some plausible numbers (j'_1, j'_2), calculate an accurate $J'(\delta)$ distribution, represent this by an approximate $J'^2(\delta) = \sum_{r=0}^{2} j'^2_r \cos^r\delta$ and use the approximate $J'^2(\delta)$ to derive an accurate $J'^3(\delta)$, new (j'_1, j'_2) being found; and so on. Two or three iterations should suffice. The limitation of this approach is that for the closest systems, where multiple reflections are particularly important, a quadratic representation

may not be sufficiently accurate, while to extend the method to a cubic is impracticable because of the prolixity of the algebra.

This approach was developed but is not presented here as it is superseded by the method described below. The algebra was long and tedious, and the application of the method to practical cases appeared to be longer than that below.

5. The symbolism used is that of chapter IV as far as possible.

Since, we have seen, the brightness of an extended area per unit solid angle is independent of distance from the observer, then the energy/second incident on any unit area of the primary equals

(i) the intensity $J(\delta)$ at any point P on the illuminating star, multiplied by

(ii) the cosine of the zenith distance, $\cos\zeta$ at that point on the illuminating star, multiplied by

(iii) the limb-darkening factor $f(\theta')$ at that point, multiplied by

(iv) the area $\sin\rho\, d\rho\, d\omega$ surrounding the point,

integrated over the visible disc of the illuminating star.

$$-j'_o + J'(\delta) = \int_{\omega} \int_{\beta} f(\theta') \cos\zeta \; J^2(\delta) \sin\beta \; d\beta \; d\omega \qquad (1)$$

As a corresponding expression exists for $J^2(\delta)$ in terms of $J'(\delta)$, a completely numerical approach to the solution of $J'(\delta)$, $J^2(\delta)$ becomes practicable. The method below is best described as semi-numerical.

The Approach Adopted

6. Suppose that a square centimetre of the surface of the reflecting star is illuminated by a body of arbitrary shape but uniform surface brightness. The body is seen in projection on the observer's celestial sphere as an area of some shape, the intensity of radiation being constant over the area. Then the flux on the square centimetre is given by the intensity of each part of the irradiating area, weighted with the corresponding cos ζ (ζ the zenith distance), integrated over the visible area:-

$$L = \int_{A} \int \cos\zeta \; dA$$

where we have put the intensity equal to unity.

$$dA = \sin\beta \, d\beta \, d\omega$$

$$\cos\zeta = \cos\zeta_0 \cos\beta + \sin\zeta_0 \sin\beta \cos\omega$$

β is now measured from the centroid of the arbitrary area; ζ_0 represents the zenith distance of this centroid.

$$\therefore \; L = \cos\zeta_0 \int_{\omega=0}^{2\pi} \int_{\beta=0}^{\beta_1(\omega)} \sin\beta \cos\beta \, d\beta \, d\omega + \sin\zeta_0 \int_{\omega=0}^{2\pi} \int_{\beta=0}^{\beta_1(\omega)} \sin^2\beta \cos\omega \, d\beta \, d\omega$$

$$= I \cos\zeta_0 + J \sin\zeta_0$$

$$J = \frac{1}{8} \int_{\omega=0}^{2\pi} \left[\beta_1(\omega) - \frac{1}{2} \sin\{2\beta_1(\omega)\} \right] \cos\omega \, d\omega$$

We now postulate that $\beta_1(\omega) = \beta_1(\pi - \omega)$. But $\cos\omega = -\cos(\pi - \omega)$. The integrand above is then an odd function and the integral over 2π is zero.

$$\therefore \; L = I \cos\zeta_0$$

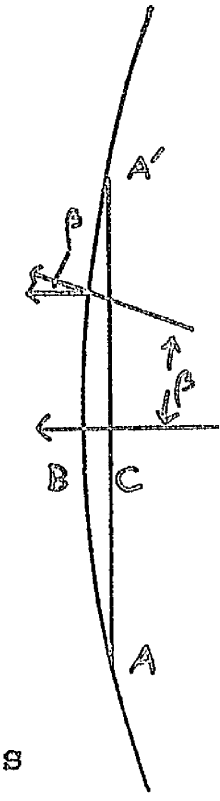

Consider the area ACA′ which forms the plane base of the segment ABA′. To each element of area $\sin\beta \, d\beta \, d\omega$ on the surface of the sphere, there corresponds an element on the segment of area $\sin\beta \cos\beta \, d\beta \, d\omega$. The area of the plane segment is

therefore given by

$$\int_{\omega=0}^{2\pi} \int_{\beta=0}^{\beta_1(\omega)} \sin\beta \cos\beta \, d\beta \, d\omega$$

where the radius of the celestial sphere is taken equal to unity.

Thus I is to be interpreted as the area of a plane figure whose perimeter is defined by $\beta_1(\omega)$.

Hence the flux from any uniformly bright area symmetrical about two orthogonal axes can be immediately found without integration: it is the product of area, intensity and cos ζ_0.

The method described in the following pages consists of approximating the irradiating source by a set of areas, each of uniform brightness, and summing the contributions from the areas. The requirement that $\beta_1(\omega) = \beta_1(\pi - \omega)$ if integration is to be avoided can always be met in principle, since an arbitrary area can be regarded as being composed of a sum of areas satisfying this condition.

7. Within the fully-illuminated zone of the irradiating star, the distribution $J(\delta)$ is represented by a set of concentric polar caps

(centre the sub-stellar point) of various brightnesses To an observer in the fully-illuminated zone of the reflecting star, each cap appears in projection as an ellipse of uniform brightness due to the adoption of LAMBERT's law for reflected radiation.

8. The Fully Illuminated Zone. In this region, as the observer above and the polar caps of the illuminating star are within the inner tangent cone common to the stars, the caps are not eclipsed, either by the observer's horizon or by the disc of the illuminating star:-

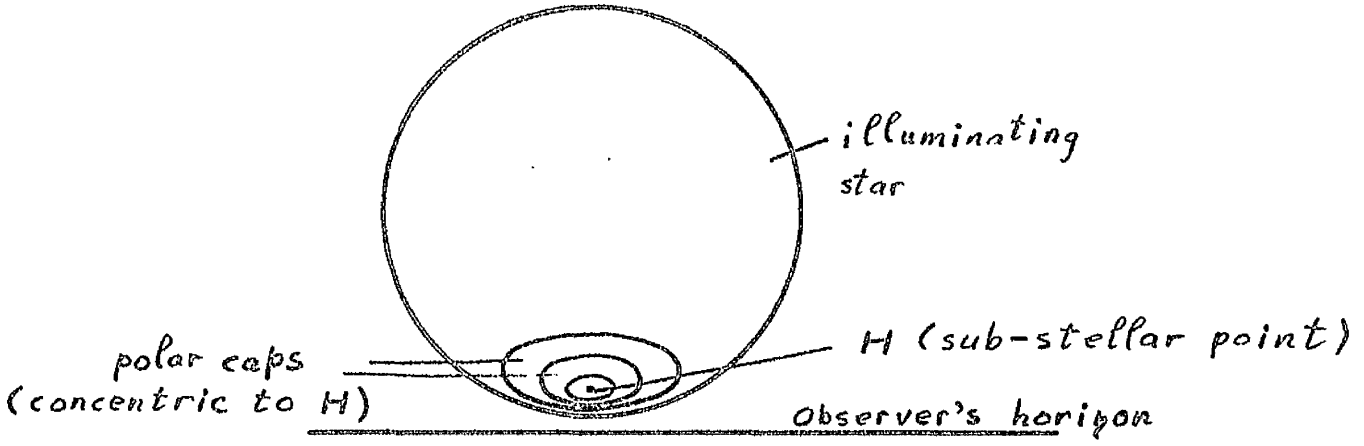

Neglecting for the moment multiple reflections from the penumbral zone of the irradiating star, the intensity distribution $J(\delta)$ at any point of star 1 is given by the intensity j_o^l of emission from the stellar atmosphere, plus that of the radiation

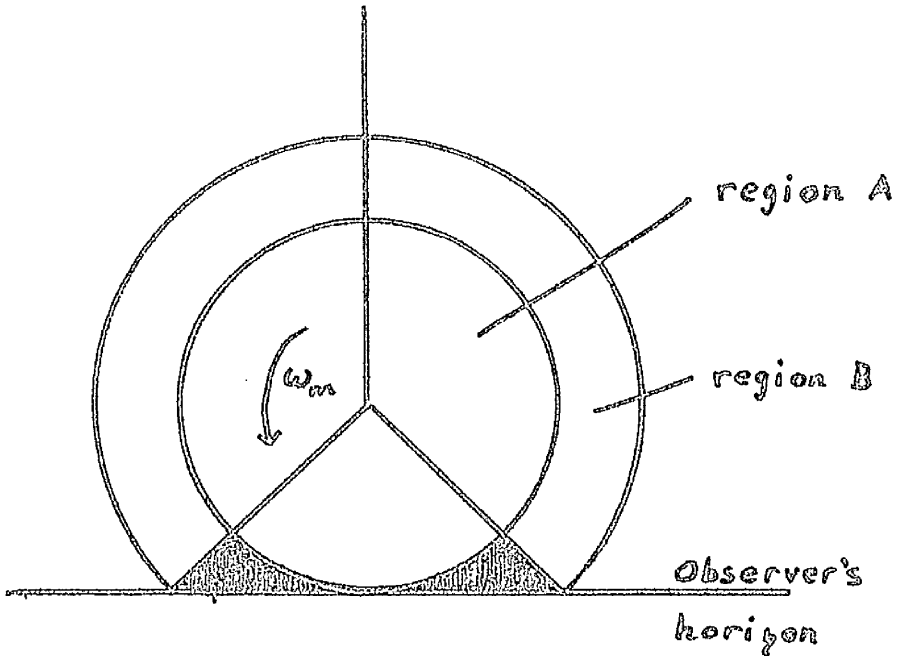

Figure 47

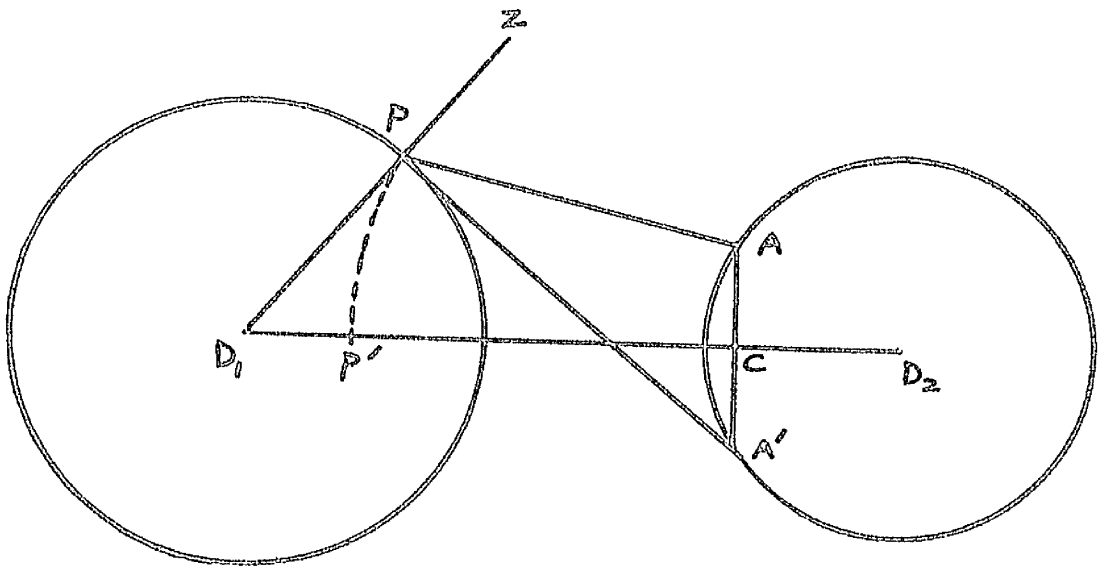

Figure 48

incident from an arbitrarily limb-darkened illuminating disc, plus the intensity due to the set of the polar caps representing the effect of multiple reflections. Thus

$$J(\delta') = j_o' + \frac{\pi a_2^2}{\rho^2}\left(1 - \tfrac{1}{3}u\right)\cos\alpha + \sum_i \pi a_i b_i \cos\xi_i j_i \qquad (2)$$

where (a_i, b_i) represent respectively the semi-major and semi-minor axes of the i th ellipse corresponding to the i th polar cap, and ξ_i and j_i are the zenith distance of the centroid, and brightness. We have $a_i = \sin\beta_{max}$; $b_i = \sin\beta_{min}$, where the β's represent the maximum and minimum semi-angles of each ellipse as measured by the observer.

It is simplest to measure these angles on a diagram of the binary system drawn to scale:-

In figure 48, ACA' represents the base of a polar cap, P the observer. Then

$$\xi_o = \tfrac{1}{2}\left(\hat{ZPA} + \hat{ZPA'}\right)$$

$$b_i = \sin\left[\tfrac{1}{2}\left(\hat{ZPA'} - \hat{ZPA}\right)\right]$$

The semi-major axis a_i is found by measuring $\hat{APC}$ from some point P' which is the distance PC from the base,

and which is such that there is no foreshortening of AA': P' therefore lies on the axis D_1D_2 as shown. $a_i = \sin[\angle AP'C]$

Measurement of three angles therefore gives the three quantities (a_i, b_i, ζ_i).

The procedure is to draw the system to scale, select a small number of polar caps and a representative set of points δ_i. To each point and to each cap, a set (a_i, b_i, ζ_i) can be found by measurement and the area $A_i = \pi a_i b_i \cos \zeta_i$ calculated. If the stars are not identical the procedure is repeated for star 2. Also required are (α, β_0) for the calculation of the expression

$$\pi \sin^2\beta_1 \cos\alpha \left(1 - \tfrac{1}{3}u\right)$$

and these can be immediately measured for each observer. Values of j_i^2 are assumed, $J(\delta')$ calculated for the various points, the j_i' giving the best representation of $J(\delta')$ are found, giving an improved $J(\delta^2)$, and so on. Alternatively a set of simultaneous linear equations may be derived as described later, the solution of which gives the j_r.

It is clear that measurements of the various angles by protractor is sufficiently accurate, as

a small uncertainty in the radius of either star, which uncertainty always exists, generally produces a probable error of more than a degree in the measured angles, while an angle can easily be measured by protractor to within $\frac{1}{2}^{0}$. For the sake of completeness, however, a routine was obtained which enables the calculation of (a_i, b_i, ξ_i) to be carried out for a polar cap of given δ_i, observed from any part of the annulus of star 1 with coordinates δ', but as it was not used it is not given here. It might be used, for example, in a computer programme for the calculation of the bolometric reflection effect.

9. The Penumbral Zone. Multiple reflections in this zone are neglected for the moment.

Suppose, in figure 47, that in region B the upper limit of integration over ω is taken to be a constant ω_m, as shown. $\omega_m = \cos^{-1}(-\cot\alpha \cot\beta_1)$. This is equivalent to neglecting the shaded region in figure 47.

The integration over region B becomes

$$2\int_{\omega=0}^{\omega_m}\int_{\beta=\beta'}^{\beta_1}\cos\zeta\,\sin\beta\,d\beta\,d\omega$$

$$=2\int_{\omega=0}^{\omega_m}\int_{\beta=\beta'}^{\beta_1}(\cos\alpha\cos\beta+\sin\alpha\sin\beta\cos\omega)\sin\beta\,d\beta\,d\omega$$

$$=\omega_m\cos\alpha(\sin^2\beta_1-\sin^2\beta')$$
$$+\sin\alpha\sin\omega_m\left[(\beta_1-\beta')-\tfrac{1}{2}(\sin 2\beta_1-\sin 2\beta')\right]$$

on neglecting the limb-darkening of the irradiating star.

The proportional error introduced by this approximation is of the order of

$$\frac{\text{area of shaded region}}{\text{area of A+B}}\times\frac{\cos(\text{z.d. of centroid of shaded region})}{\cos(\text{z.d. of centroid of A+B})}$$

For every depth of eclipse the relative area of the omitted region $\sim$ 0.1 or less, while, as the area borders the observer's horizon, the cosine of a typical zenith distance is close to zero, and we may 'guesstimate' 0.1 for the second factor. To an adequate degree of accuracy, then, an analytical

expression for penumbral illumination exists when the sources is uniformly bright. (A 1% error will always be negligible due to the physical approximations of the model, and the limitations of the photometry).

A limb-darkening factor $1-u+u\cos\theta'$ introduces

$$\int\int \cos\zeta \sin\beta \cos\theta' \, d\beta \, d\omega$$

and since $\cos\theta' = \sqrt{(1-\frac{1}{k^2}\sin^2\beta)}$, terms of the form

$$\int \sin\beta \sqrt{(1-\frac{1}{k^2}\sin^2\beta)} \cos\beta \, d\beta$$

$$\int \sin^2\beta \sqrt{(1-\frac{1}{k^2}\sin^2\beta)} \, d\beta$$

arise. The first can be handled analytically, while the second reduces to an elliptic integral.

Finally, in the penumbral zone, we have

$$J(\delta) = (1-u)\,X + u\,Y$$

where X and Y may be tabulated in terms of (α, β_1). It was sufficient for the present purpose to tabulate X: it is given in graphical form in

figure 49, over the range used in the examples which follow.

10. Refinements. So far the effect of multiple reflections from the penumbral zones has been neglected. The polar cap representation may be extended to these zones.

A polar cap on the illuminating star may appear to an observer in the penumbra as a partially set ellipse:-

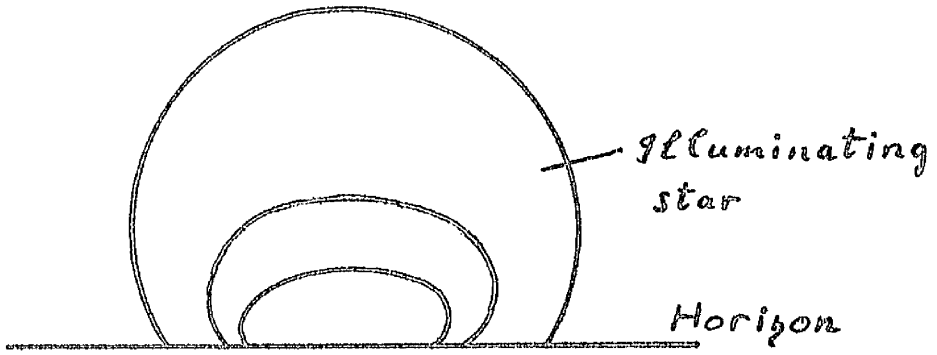

The dimensions, zenith distance and depth of eclipse can all be found by measurement with a protractor.

Consider a partially set disc with the same zenith distance and surface brightness, whose radius is the semi-minor axis of the ellipse. To each

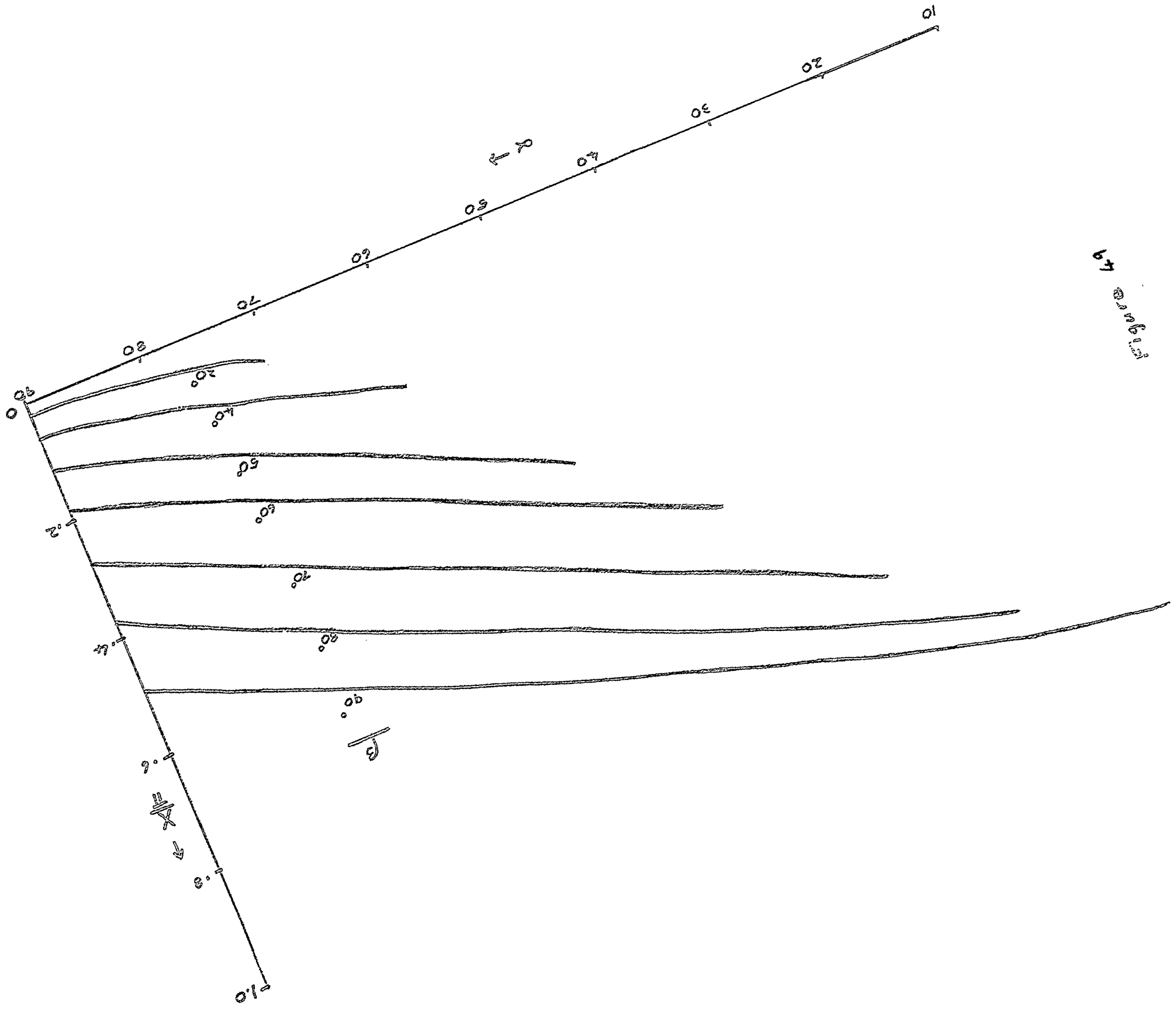

Figure 49

TABLE 6

β_1 \ α	10	20	30	40	50	60	70
30							.088
40						.209	.153
50					.420	.334	.254
60				.578	.496	.413	.335
70			.850	.693	.608	.524	.442
80		.915	.856	.787	.709	.620	.572
90	.990	.960	.909	.851	.787	.722	.684

Flux/cm^2 incident from illuminating star ($X/_{\pi}$)

(Zero limb-darkening: $u=0$)

horizontal strip of disc there corresponds a strip of ellipse of the same zenith distance and intensity, but with a width $1/\sqrt{(1-e^2)}$ times that of the disc, where e is the eccentricity of the ellipse. The flux from the polar cap is thus given by the flux from the partially set disc described, which is given in table 6 , multiplied by a_i/b_i .

An accurate treatment of multiple reflections in the penumbra of very close systems is difficult as large polar caps may then be involved. These will have projected areas delimited by rather complicated perimeters, for example:-

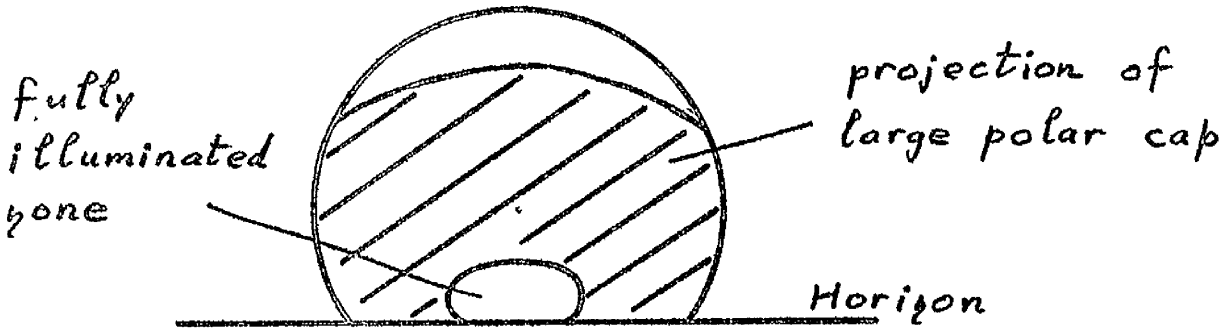

Possible approximations are to increase the effective value of j by some amount, or to approximate the shape by a rectangle whose dimensions are adjusted to minimise the error:-

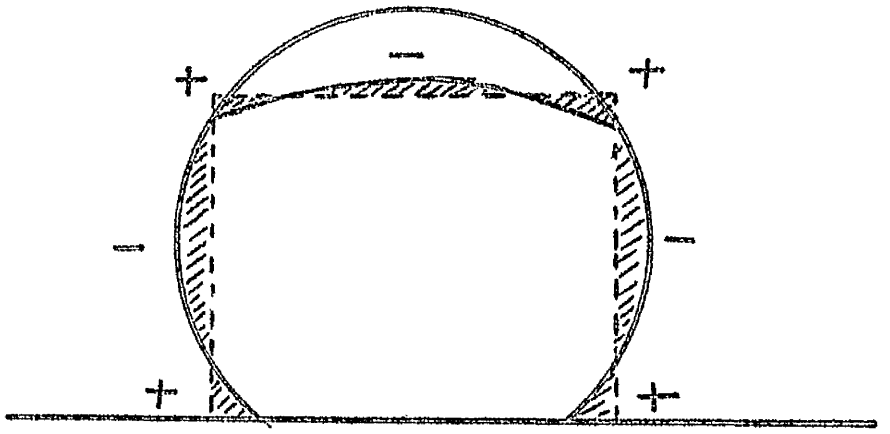

The errors in the diagram above are small and are alternately + and −, tending to cancel. The percentage error must be quite small and it is possible that even for contact systems it will suffice.

In the examples which follow I have not considered it worth while to take account of the influence, on the $J(\delta)$ curve, of multiple reflections from the illuminating penumbra. The neglect of these reflections is clearly below the uncertainty $\sim 0^{m}.01$ set by the limitations of the physics adopted.

$m(\epsilon)$, given $J(\delta)$.

11. Fourier Representation. If the intensity

distribution over a star in some wavelength range is represented by

$J_\lambda(\delta) = j_0 + j_1\cos\delta + j_2\cos^2\delta + \ldots\ldots + j_n\cos^n\delta$,

where the j_r are known from theory, the photometric luminosity of the star at any phase is

$$L_\lambda = \int\int_\Sigma J_\lambda(\delta)\, f(\theta)\, d\sigma$$

where the integration is carried over the visible disc and $f(\theta)$ is a function depending on limb-darkening. This expression is simply the denominator of the equation for the displacement of an absorption line at an arbitrary phase:-

$$\rho_i = \frac{\int\int v\, J_i(\delta)\, f(\theta)\, d\sigma}{\int\int J_i(\delta)\, f(\theta)\, d\sigma}$$

Thus if we neglect limb-darkening of both reflected and 'primary' radiation,

$$L_\lambda = \pi \sum_{r=0}^{n} j_r\, g_r(\epsilon)$$

where the $g_r(\epsilon)$ are the quantities defined in chapter III. (The factor π appears because it was removed from the $g_r(\epsilon)$). Arbitrary limb-darkening of both primary and reflected radiation could be taken into account by this method, as the integrations are performed over (λ, Θ) and are elementary. Once the $g_r(\epsilon)$ were tabulated, which could be done for all time, the labour involved in the conversion $J_\lambda(\delta) \rightarrow \Delta m_\lambda(\epsilon)$ is largely that of finding the coefficients j_r of best fit.

12. Representation by Strips. The approach adopted below had the disadvantage that the limb-darkening of the multiply reflected radiation must be neglected. However this was not considered to outweigh the saving in labour which results when computing $\Delta m_\lambda(\epsilon)$ by the present method. The effect of darkening on the light curve is probably very small and it has anyhow been neglected in the theory of the earlier sections.

The $J_\lambda(\delta)$ curve over any one star is represented by a histogram:-

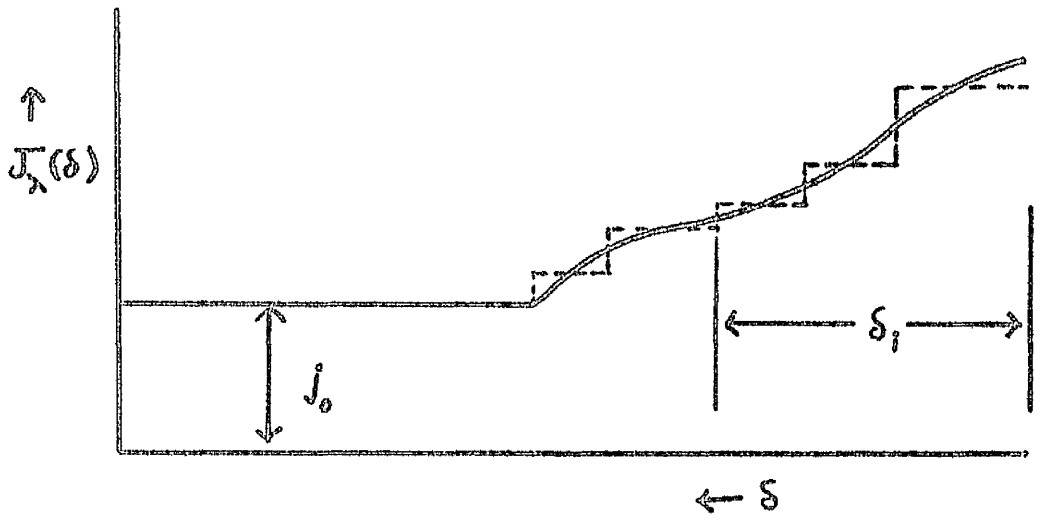

The curve can thus be considered to consist approximately of a series of concentric polar caps of various brightnesses whose centre is the sub-stellar point. If h is the 'height' of the (i+1)th step above that immediately below, and if a_{i+1} is the area of the (i+1)th cap projected on the observer's celestial sphere in terms of the area of the stellar disc as unity, then

$$L_\lambda = j_0 \left(1 - \tfrac{1}{3} u\right) + \sum a_r h_r$$

The problem is now to find $a_r(\delta_r, \epsilon)$.

Consider one polar cap. As the star rotates, the following five regimes may be distinguished.

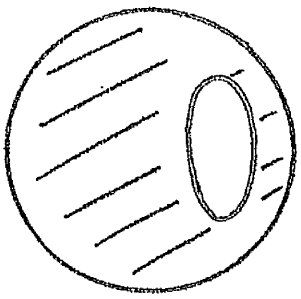

I

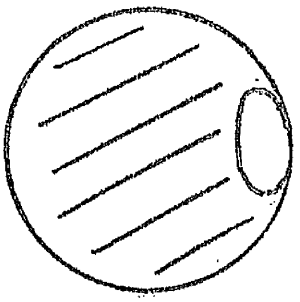

II

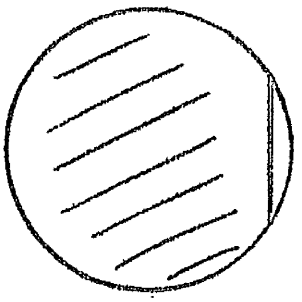

III

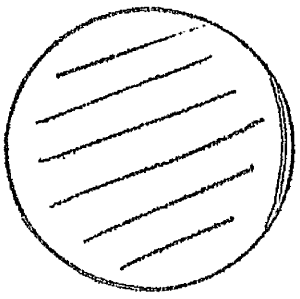

IV

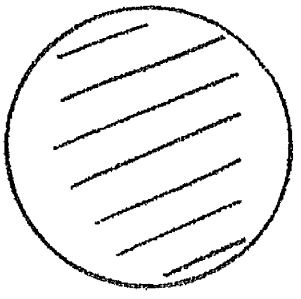

V

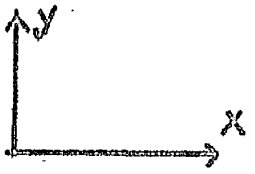

The radius of the cap is δ_0 measured at the centre of the star. The phase ϵ is measured from the centre of the disc, over the stellar surface, the centre of the cap. To find $m_\lambda(\epsilon)$ we require to find the projected area of the visible part of the cap.

Regime I

We have an ellipse whose semi-major axis

is $\sin\delta_o$, and whose semi-major axis is $\sin\delta_o \cos\epsilon$.
The area of the ellipse is $\pi ab = \pi \sin^2\delta_o \cos\epsilon$.
Due to the symmetry occurring in all cases we consider only the positive parts of the xy planes. $\therefore a_r(\delta_o, \epsilon) = \frac{\pi}{2}\sin^2\delta_o \cos\epsilon$ in this case.

Regime II

The projected cap may be divided up as follows:-

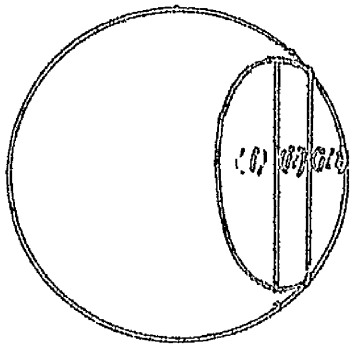

(i) is a half-ellipse, hence $A_{(i)} = \frac{\pi}{4}\sin^2\delta_o \cos\epsilon$
The area of (ii) is given by integrating between the two relevant straight lines:

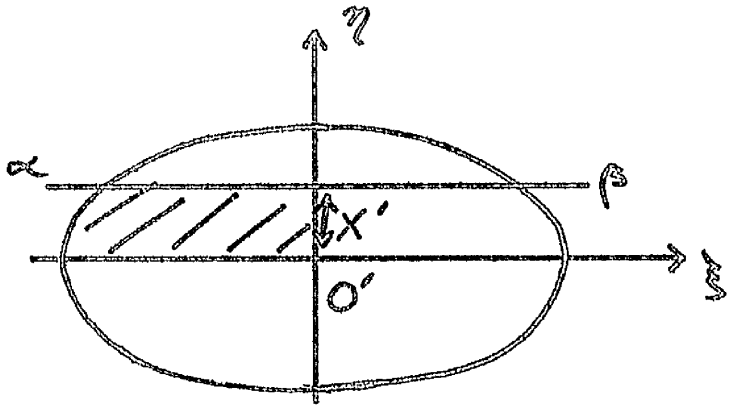

$$\frac{\xi^2}{\sin^2\delta_0} + \frac{\eta^2}{\sin^2\delta_0 \cos^2\epsilon} = 1$$

$$\therefore \xi = \frac{1}{\cos\epsilon} \sqrt{\left(\sin^2\delta_0 \cos^2\epsilon - \eta^2\right)}$$

Put $k = \sin\delta_0 \cos\epsilon$

$$\therefore A_{(ii)} = \frac{1}{2}\int_{\eta=0}^{x'} \xi \, d\eta$$

$$= \frac{1}{2\cos\epsilon} \int_0^{x'} \sqrt{\{k^2 - \eta^2\}}\, d\eta$$

$$= \frac{1}{2\cos\epsilon} \left[x' \sqrt{(k^2 - x'^2)} + k^2 \sin^{-1}\left(\frac{x'}{k}\right)\right]$$

where X' is the x-coordinate of the line $\propto\beta$ measured from the origin O' of the ellipse.

$A_{(iii)} = \frac{1}{2}(\propto - \sin\propto \cos\propto)$ where $\propto = \sin^{-1} Y$, Y being the y-coordinate of $\propto\beta$. This arises from the standard equation for the area of a segment of a circle. Hence

$$A_{\Pi} = \frac{\pi}{4} \sin^2\delta_0 \cos\epsilon + \frac{1}{2\cos\epsilon}\left[X'\sqrt{\{k^2 - X'^2\}} + k^2 \sin^{-1}\left(\frac{X'}{k}\right)\right]$$

$$+ \frac{1}{2}(\alpha - \sin\alpha\cos\alpha)$$

where $k = \sin\delta_0 \cos\epsilon$

$\alpha = \sin^{-1}Y$

and (X', Y) have not yet been calculated:-

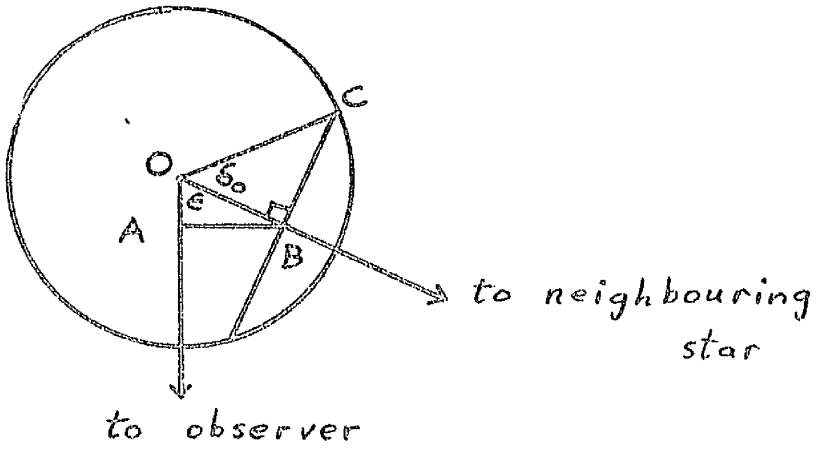

The x-coordinate of the centre of the ellipse is

$$AB = OB \sin\epsilon$$

$$= OC \cos\delta_0 \sin\epsilon$$

$$= \cos\delta_0 \sin\epsilon$$

Therefore the equation of the ellipse is

$$\frac{y^2}{\sin^2\delta_0} + \frac{(x - \sin\epsilon \cos\delta_0)^2}{k^2} = 1$$

The equation of the circle is $x^2 + y^2 = 1$ and we require the points of intersection. Substitution gives

$$X = \frac{\cos\delta_0}{\sin\epsilon}$$

$$Y = \sqrt{(1 - X^2)}$$

∴ the quantities required are

$$X' = \frac{\cos\delta_0}{\sin\epsilon} - \sin\epsilon\cos\delta_0 = \frac{\cos\delta_0 \cos^2\epsilon}{\sin\epsilon}$$

$$Y = \sqrt{(1 - X^2)}$$

Regime III

In the case $\epsilon = \frac{\pi}{2}$ $X = \cos\delta_0$, $Y = \sin\delta_0$

hence $\alpha = \delta_0$ and

$$A_{III} = \tfrac{1}{2}\left(\delta_0 - \sin\delta_0 \cos\delta_0\right)$$

Regime IV

The cap is now seen as the difference in areas of a segment of circle of base 2Y and a segment of ellipse as shown:

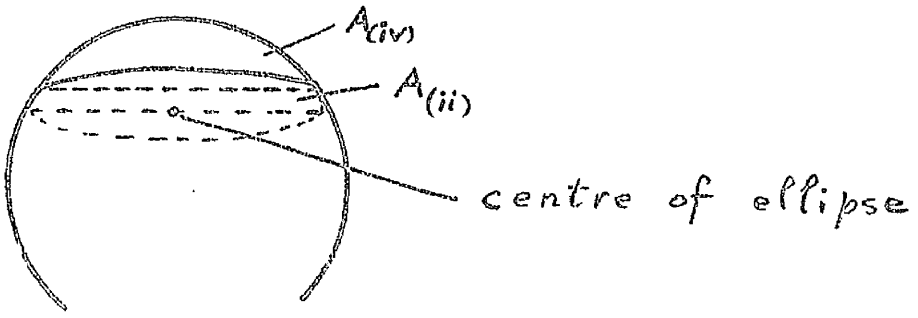

Area of segment of ellipse required

$$= \frac{\pi}{k}\sin^2\delta_0 \cos\epsilon - A_{(ii)}$$

$$= \frac{\pi}{2}\sin^2\delta_0 \cos\epsilon - \frac{1}{2\cos\epsilon}\left[X'\sqrt{\{K^2 - X'^2\}} + K^2 \sin^{-1}\left(\frac{X'}{K}\right)\right]$$

Thus

$$A_{IV} = \tfrac{1}{2}(\alpha - \sin\alpha\cos\alpha) - \frac{\pi}{4}\sin^2\delta_0\cos\epsilon + \frac{1}{2\cos\epsilon}\left[X'\sqrt{(K^2 - X'^2)} + K^2\sin^{-1}(X'/K)\right]$$

where (α, X, k) are defined as before.

TABLE 7

ϵ \ δ_o	10	20	30	40	50	60	70	80	90
30	0.041	0.160	0.340	0.562	0.798	1.020	1.215	1.410	1.465
40	0.036	0.140	0.300	0.498	0.706	0.963	1.148	1.259	1.387
50	0.030	0.118	0.252	0.418	0.597	0.812	0.998	1.141	1.290
60	0.024	0.092	0.196	0.332	0.484	0.664	0.860	1.013	1.178
70	0.016	0.062	0.139	0.244	0.378	0.531	0.724	0.885	1.054
80	0.008	0.036	0.080	0.170	0.281	0.417	0.581	0.750	0.922
90	0.002	0.013	0.046	0.098	0.190	0.307	0.450	0.613	0.785
100	0.000	0.004	0.012	0.056	0.121	0.213	0.325	0.484	0.648
110	0.000	0.000	0.005	0.022	0.062	0.129	0.220	0.363	0.516
120	0.000	0.000	0.000	0.006	0.022	0.074	0.122	0.251	0.392
130	0.000	0.000	0.000	0.000	0.005	0.054	0.048	0.161	0.280
140	0.000	0.000	0.000	0.000	0.000	0.061	0.018	0.091	0.183
150	0.000	0.000	0.000	0.000	0.000	0.000	0.013	0.090	0.105

Regime V

$$A_{\underline{V}} = 0.$$

The results for a polar cap of radius δ_o at some phase ϵ are given in table 7 .

13. Identical Stars. A general expression for the case where the stars have identical luminosities radii and intensity distributions in some discrete wavelength range can be given provided that it is supposed that the reflected radiation is completely limb-darkened, i.e. that $u_\lambda = 1$.

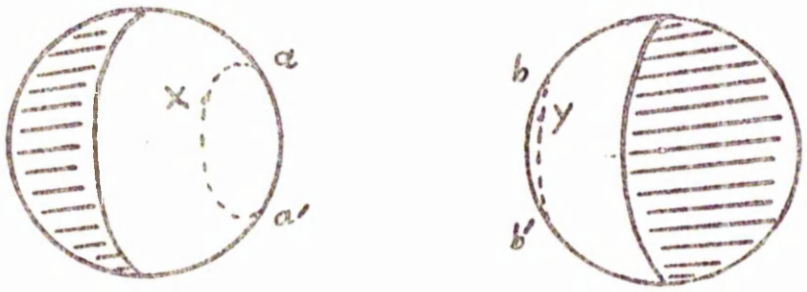

The shaded areas are the outer hemispheres with uniform unit intensity in the wavelength range considered. Compare the above system with the following:

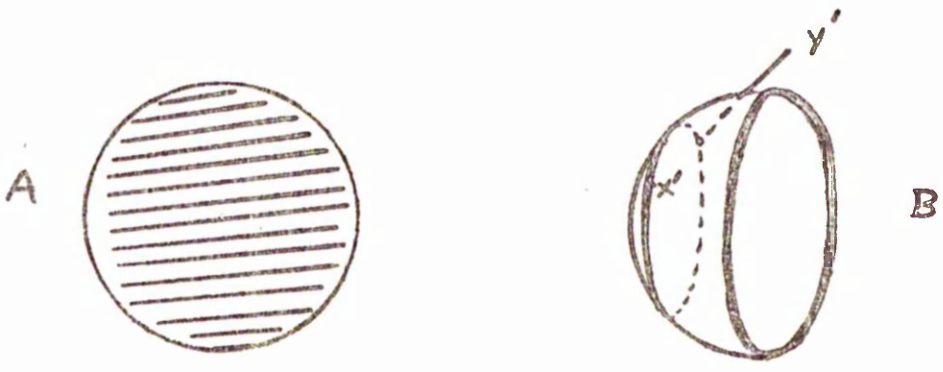

The shaded areas have been joined to give 'star' A. For a limb-darkening law dependent only on a power of cos Θ, there is a one to one correspondence between the small areas in the first system's averted hemispheres, and those of A. Integration over the averted hemispheres is therefore equivalent to integration over A.

From the geometry of the first system, the isophote aa' can be joined on to a corresponding isophote bb' to give an ellipse whose eccentricity depends only on the phase angle. This ellipse corresponds to one in B, which is a transparent hemisphere composed of the illuminated hemispheres of the binary system. B has phase angle ϵ.

A one to one correspondence must be established between each elementary area on B and each area on the illuminated hemispheres. Points (x,x') correspond in every way, but points (y,y') differ in that the limb-darkening angles are $(\Theta, \pi - \Theta)$, y' being on the far side of hemisphere B, although otherwise they are the same. An integration over B as it stands would mean that the intensity $J_\lambda(\delta)\cos\Theta$ over the far side of the hemisphere would take a negative value.

This difficulty may be overcome if we consider

the radiation to be strongly limb-darkened. Then there is a one to one correspondence as required The integration over the surface of the real stars may therefore be replaced in this case by a simpler integration over A and B.

We have

$$L_A = \int_{\theta=0}^{\frac{\pi}{2}} \int_{\lambda=0}^{2\pi} \sin\theta \cos\theta \, d\theta \, d\lambda$$

$$L_B = \int_{\delta=0}^{\frac{\pi}{2}} \int_{\chi=0}^{2\pi} J_\lambda(\delta) \sin\delta \cos^2\theta \, d\delta \, d\chi$$

(since intensity is J_λ, limb-darkening is $\cos\theta$, and elementary projected area is $\sin\delta \cos\theta \, d\delta \, d\theta$)

Now $\cos\theta = \cos\delta \cos\epsilon + \sin\delta \sin\epsilon \cos\chi$

and $$\int_{\chi=0}^{2\pi} \cos\chi \, d\chi = 0$$

$$\therefore L_B = \int_{\delta=0}^{\frac{\pi}{2}} \int_{\chi=0}^{2\pi} J_\lambda(\delta) \sin\delta \left(\cos^2\delta \cos^2\epsilon + \sin^2\delta \sin^2\epsilon \cos^2\chi\right) d\delta \, d\chi$$

$$L_\lambda = L_A + L_B = \tfrac{2}{3}\pi u + \pi p \cos^2\epsilon + \pi q \sin^2\epsilon$$

where $$p = 2\int_{\delta=0}^{\pi/2} J_\lambda \sin\delta \cos^2\delta \, d\delta$$

$$q = \int_{\delta=0}^{\pi/2} J_\lambda \sin^3\delta \, d\delta$$

i.e. $$L_\lambda = \pi\left\{\tfrac{2}{3} + p + (q-p)\sin^2\epsilon\right\}$$

In the absence of reflection $J_\lambda = 1$. Then $p = \frac{2}{3}$ and $q - p = 0$, hence $L_\lambda = \frac{4}{3}\pi$, for the luminosity of two separate, completely darkened spheres. The contribution to the total light due to the reflection alone is therefore $\pi\{p' + (q-p)\sin^2\epsilon\}$

where $$p' = 2\int_0^{\pi/2} (J_\lambda - 1)\sin\delta\cos^2\delta \, d\delta$$

Thus for two stars the radiation from which is arbitrarily limb-darkened apart from reflection,

$$L_\lambda = \pi\left\{2\left(1 - \tfrac{1}{3}u_\lambda\right) + p' + (q-p)\sin^2\epsilon\right\}$$

where u_λ is the limb-darkening coefficient of the unreflected radiation. Or,

$$L_\lambda = \pi\left\{\tfrac{2}{3}\left(2 - u_\lambda\right) + p + (q-p)\sin^2\epsilon\right\}$$

14. 57 Cygni. The method described above was applied to a system consisting of two identical stars whose centres are separated by three stellar radii. It was later realised that a separation of four radii would have been more appropriate as a representation of 57 Cygni, but the essential points are brought out below.

Each fully-illuminated zone was represented by four polar caps of radii $\delta_1 = 10^0, 20^0, 30^0, 40^0$. The flux/cm.^{2} from each star in the absence of reflection is designated by j_0 ; that from the cap of radius 40^0 by $(j_0 + j_4)$, that of radius 30^0 by $j_0 + j_4 + j_3$, and so on. It is a simple matter to apply (2) to various points $J(\delta)$, making the necessary measurements with a protractor as previously described. Points J(0), J(10), J(20), J(30), J(40) were taken. The total reflected fluxes from these points were found to be:-

$$J^*(0) = .250\, j_0' + .033\, j_1 + .095\, j_2 + .165\, j_3 + .250\, j_4$$
$$J^*(10) = .242\, j_0' + .026\, j_1 + .093\, j_2 + .147\, j_3 + .242\, j_4$$
$$J^*(20) = .200\, j_0' + .020\, j_1 + .063\, j_2 + .114\, j_3 + .177\, j_4$$
$$J^*(30) = .150\, j_0' + .012\, j_1 + .039\, j_2 + .074\, j_3 + .123\, j_4$$
$$J^*(40) = .095\, j_0' + .004\, j_1 + .019\, j_2 + .048\, j_3 + .074\, j_4$$

A factor π has been cancelled out of the equations. $j_o' = (1-\frac{1}{3}u)j_o$, and since units are arbitrary, j_o' may be taken equal to unity. As the stars are identical there is no need to use superscripts 1 and 2.

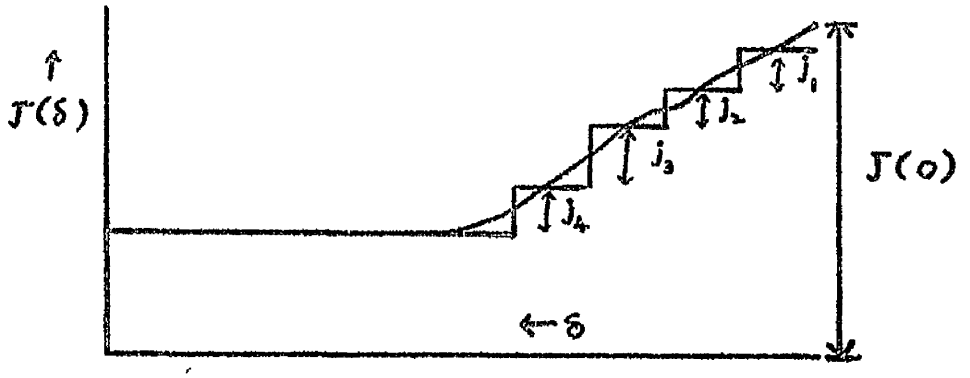

From the diagram above, j_1 may be roughly represented by $j_1 = \frac{1}{2}\{ J(0) - J(10)\}$. Similar expressions follow for j_2 , etc. Using as initial values of $J(\delta)$ the values given by $j_1 = j_2 = j_3 = j_4 = 0$, the values after one iteration are

	Initial	1st. Iteration
J(0)	1.250	1.263
J(10)	1.242	1.255
J(20)	1.200	1.209
J(30)	1.150	1.156
J(40)	1.095	1.098

No significant improvement follows from further iteration. The result is in figure 50. KOPAL's

×——————× $J(\delta)$ neglecting multiple reflection

o---------o $J(\delta)$ with Kopal's correction for multiple reflection

o-+-+-+-+-+-+-+-+-+-+-+-+-+-+-+-+-o $J(\delta)$ using theory of ch. V.

Penumbral intensity has been calculated neglecting limb-darkening of illuminating source.

Penumbral intensity after KOPAL has been obtained from the corrected formula for J^{ν}.

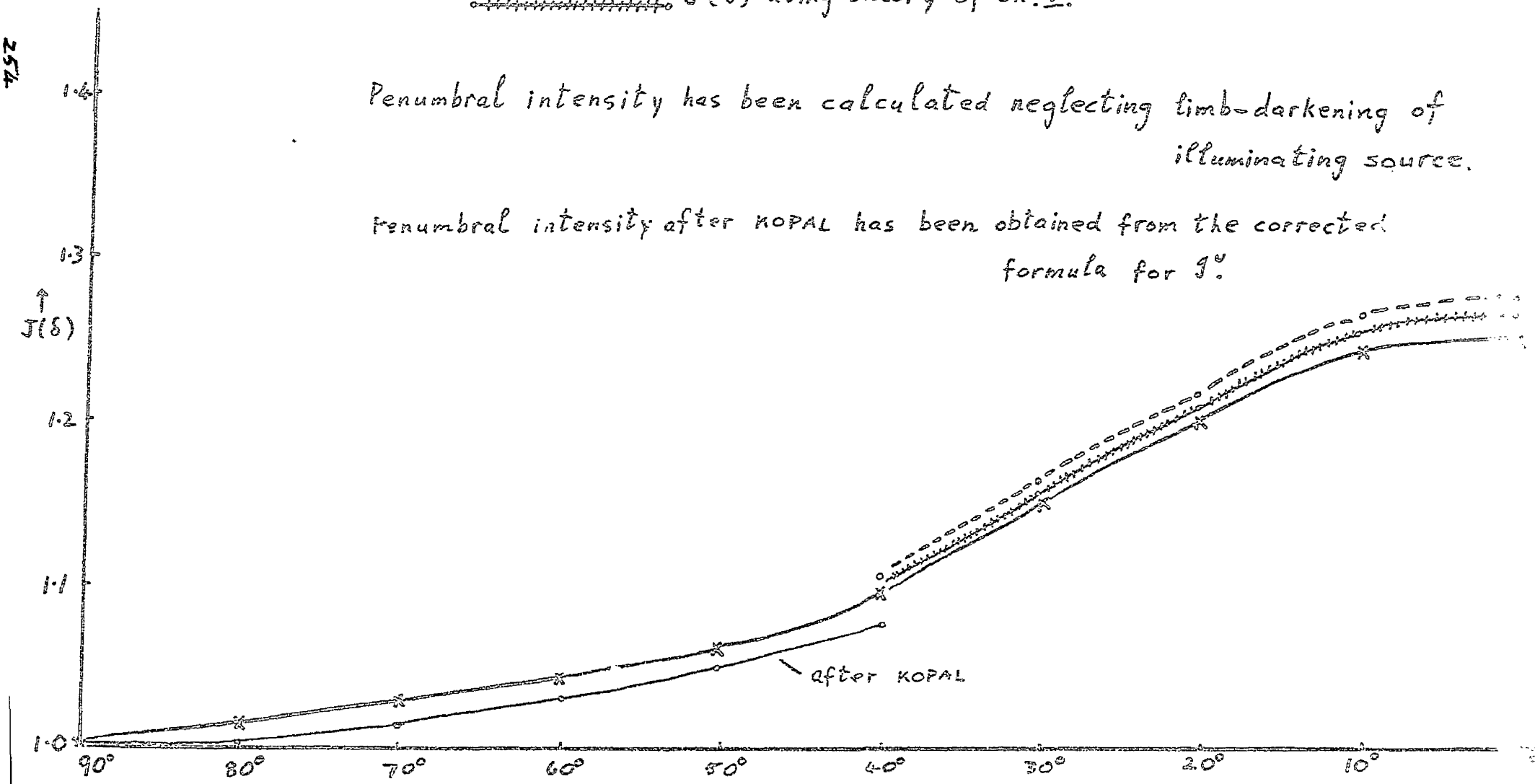

Figure 50

estimate of the effect of secondary reflection is obtained by multiplying the reflected radiation by the term in equation (14) of chapter IV, that is,

$$\frac{2}{3}\left(\frac{a_2}{R}\right)^2 + \frac{1}{2}\left(\frac{a_2}{R}\right)^3 + \frac{1}{2}\left(\frac{a_1 a_2^2}{R^5}\right) + \text{----}$$

His correction is seen to exaggerate the effect of secondary reflection by a factor which varies with δ but averages about two. Presumably in closer binaries his correction would underestimate multiple reflection as we have seen that $J(0) \to \infty$ as the separation tends to zero. It is to be expected that the importance of multiple reflections will increase rapidly as the separation diminishes.

The $J(\delta)$ distribution has been extended over the penumbral zone in figure 50, using figure 49. Multiple reflection has no effect of any consequence in this zone, in the present example. It is evident that the penumbral zone is fully as important as the fully-lit region, although the flux/cm^2 from it is less. This arises because its extent is greater. Thus from a strip of unit width and radius δ_0 measured from the hotspot, the flux is $J(\delta_0) \sin^2 \delta_0$. Comparing for example $\delta_0 = 30^0$ in the fully-lit zone, with $\delta_0 = 60^0$ in the penumbral, the reflected

radiation from the latter is found to be fully as important. The case of identical stars, furthermore is not one in which a penumbral zone will be most conspicuous.

15. Point Source. The poor convergence of the series used in past discussions of the reflection effect has been pointed out in chapter IV. By comparing the two solutions of a bolometric problem using the respective methods of chapters IV and V, it is possible to examine the error committed by the poor convergence. To this end the simplest problem will suffice: a point illuminating source.

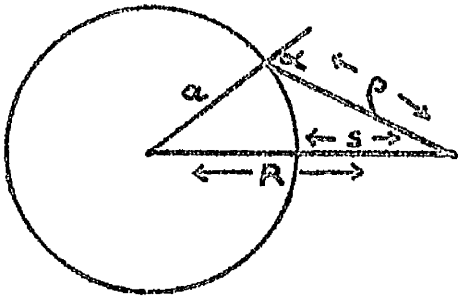

The configuration chosen was a/R = .636. The flux in the absence of reflection was taken equal to unity, and the luminosity of the irradiating source was chosen to be such that J(0) = 2. Then the luminosities of stars 1 and 2 are in the ratio $(a/s)^2 = 0.328 : 1$.

The series $\mathcal{L} = L_2 \sum_{n=0}^{\infty} C_n \cos^n \epsilon$ is used by KOPAL.

The formulae for the C_k' are given on page 200 of the thesis. In the present example we have

$C_0' = .110 + .016 + .012 + \_\_\_\_ = .138$

$C_1' = .135 + .065 + \_\_\_\_\_ = .200$

$C_2' = .024 + .048 + .045 + \_\_\_\_ = .117$

$C_3' = 0 = .000$

$C_4' = .001 - .008 + \_\_\_\_ = - .007$

Convergence is poor, as anticipated.

$\mathcal{L}$ represents the light reflected along the observer's line of sight. Then we require $1 + \mathcal{L} + L_2$, where $L_2 = 0.328$. The luminosity variation with ϵ is shown in figure 51, assuming the system to be inclined 60^0 to the observer's tangent plane.

The alternative procedure involved splitting the illuminated part of the star into polar caps with $\delta_j = 5^0, 10^0, 20^0, 30^0, 40^0$, Incident flux at any point, in terms of the (unit) incident flux reflected, at $\delta = 0^0$, is given by $(\frac{s}{r})^2 \cos\alpha$. Thus

$J''(0) = 1$

$J''(10) = .73$

$J''(20) = .40$

$J''(30) = .20$

$J''(40) = .05$

$J''(50) = .00$

r	δ_r	$\bar{J}_r$
1	40	.05
2	30	.15
3	20	.20
4	10	.33
5	5	.17

($J''(\delta)$ is reflected flux.)

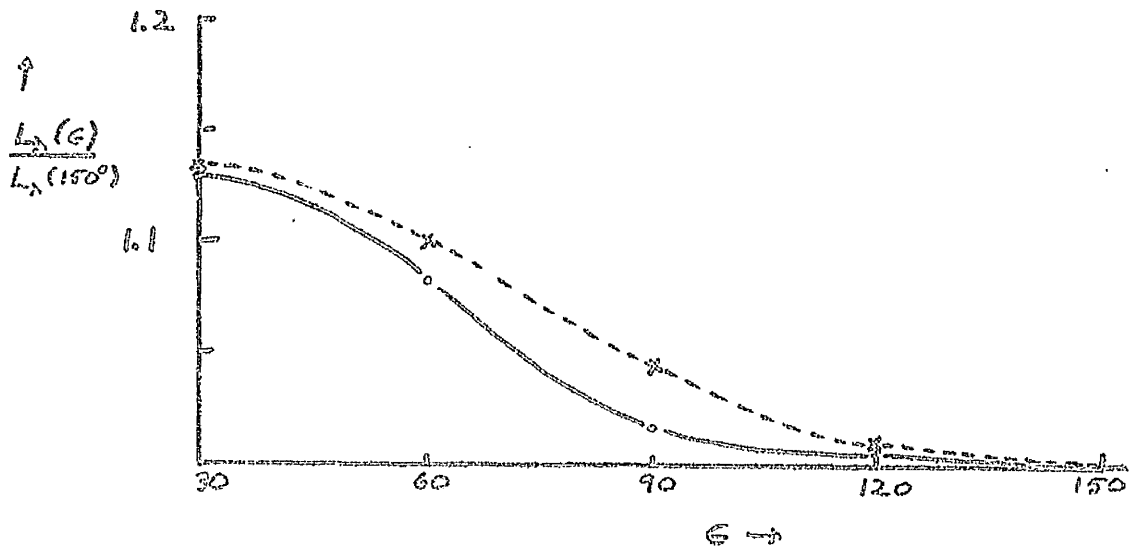

Luminosity variation on point source model

o——————o according to method in chapter V

x- - - - - - - - - x based on series expansion in chapter IV

Figure 51

and the light variation with phase is obtained with the help of table 7 . It is perhaps worth mentioning that the procedure is if anything less laborious than the first method. The result is also shown in figure 51.

Although the amplitudes of the light variation are in agreement in this particular case, there is a very large difference in the phase law. This may be taken to verify the opinion expressed in chapter IV that the addition of terms of increasing orders of magnitude is not a fruitful approach to reflection theory. This is particularly so as the addition of each term has involved laborious algebra (TAKEDA, SEN, KOPAL).

CONCLUDING REMARKS

Summary

1. The main conclusion of Part I is that the spectroscopic reflection effect, on 57 Cygni at least, cannot be explained in simple terms. This arises because the expected mutual heating of the stars is so small that there should be very little change in the strengths of the absorption lines over the stellar surfaces.

It was suggested that the properties of the chromospheres of the stars might be such as to account for the T_{max}/ρ diagrams, but I was unable to account for the ρ/λ correlation. Non-thermal visual emission was, however, shown not to be an acceptable explanation.

From the fact that each velocity curve can be transformed into any other by a change of vertical scale, we have that

(i) the mass-function cannot be taken as known. In particular, there is no reason to suppose that the mass-function derived from the strong absorption lines is significant. This was first pointed out in the paper by OVENDEN† (1963).

(ii) the ~~poles~~ axes of revolution and rotation are probably parallel in space.

(iii) the shapes of the velocity curves, apart from the vertical scaling, are insensitive to the intensity distributions $J_\lambda(\delta)$.

Some slight evidence for the existence of circulation currents was found.

It was shown in Part II that the bolometric theory of KOPAL, which is the only treatment of the effect under realistic conditions, contains several conceptual errors and is not in fact applicable to close systems. It is possible, however, by using a different approach to the problem, to treat the effect to an adequate accuracy for most close systems, possible exceptions being contact binaries.

Some Implications

2. Masses of O and B Stars. The analysis of 60 Cygni, published in 1954, indicated that the current theories of the spectroscopic reflection effect were inapplicable to the binary. In particular, the effect

† M.N. 126, 77.

is much larger on 60 Cygni than the work of KOPAL implied. The observations of 57 Cygni confirmed the existence of a large reflection effect which cannot be explained in simple terms. As both these systems appeared to be unexceptional before OVENDEN's analyses, it is very likely that the phenomenon they exhibit is widespread amongst close binaries. There are perhaps two reasons why the effect has hitherto been overlooked. In the first place, the effect is noticeable only by comparing velocity curves from strong lines with curves from lines which are weak and are therefore not normally measured. Secondly there is little deviation of a velocity curve from one of standard form, even when the reflection effect is large. An observer would presumably take this to mean that distorting influences are small. In this connection it should be noted that PEARCE (1939)† derived velocity curves for the components of 57 Cygni without discovering the various correlations.

A large reflection effect, whose existence has not been previously suspected, will give rise to systematic errors in the masses of stars. In particular, early-type stars whose masses are found exclusively from eclipsing and spectroscopic binaries,

† Publ. Am. Astr. Soc, 9, 268.

is much larger on 60 Cygni than the work of KOPAL implied. The observations of 57 Cygni confirmed the existence of a large reflection effect which cannot be explained in simple terms. As both these systems appeared to be unexceptional before OVENDEN's analysis, it is very likely that the phenomenon they exhibit is widespread amongst close binaries. There are perhaps two reasons why the effect has hitherto been overlooked. In the first place, the effect is noticeable only by comparing velocity curves from strong lines with curves from lines which are weak and are therefore not normally measured. Secondly there is little deviation of a velocity curve from one of standard form, even when the reflection effect is large. An observer would presumably take this to mean that distorting influences are small. In this connection it should be noted that PEARCE (1939) derived velocity curves for the components of 57 Cygni without discovering the various correlations.

A large reflection effect, whose existence has not been previously suspected, will give rise to systematic errors in the masses of stars. In particular, early-type stars whose masses are found anomalously from eclipsing and spectroscopic binaries,

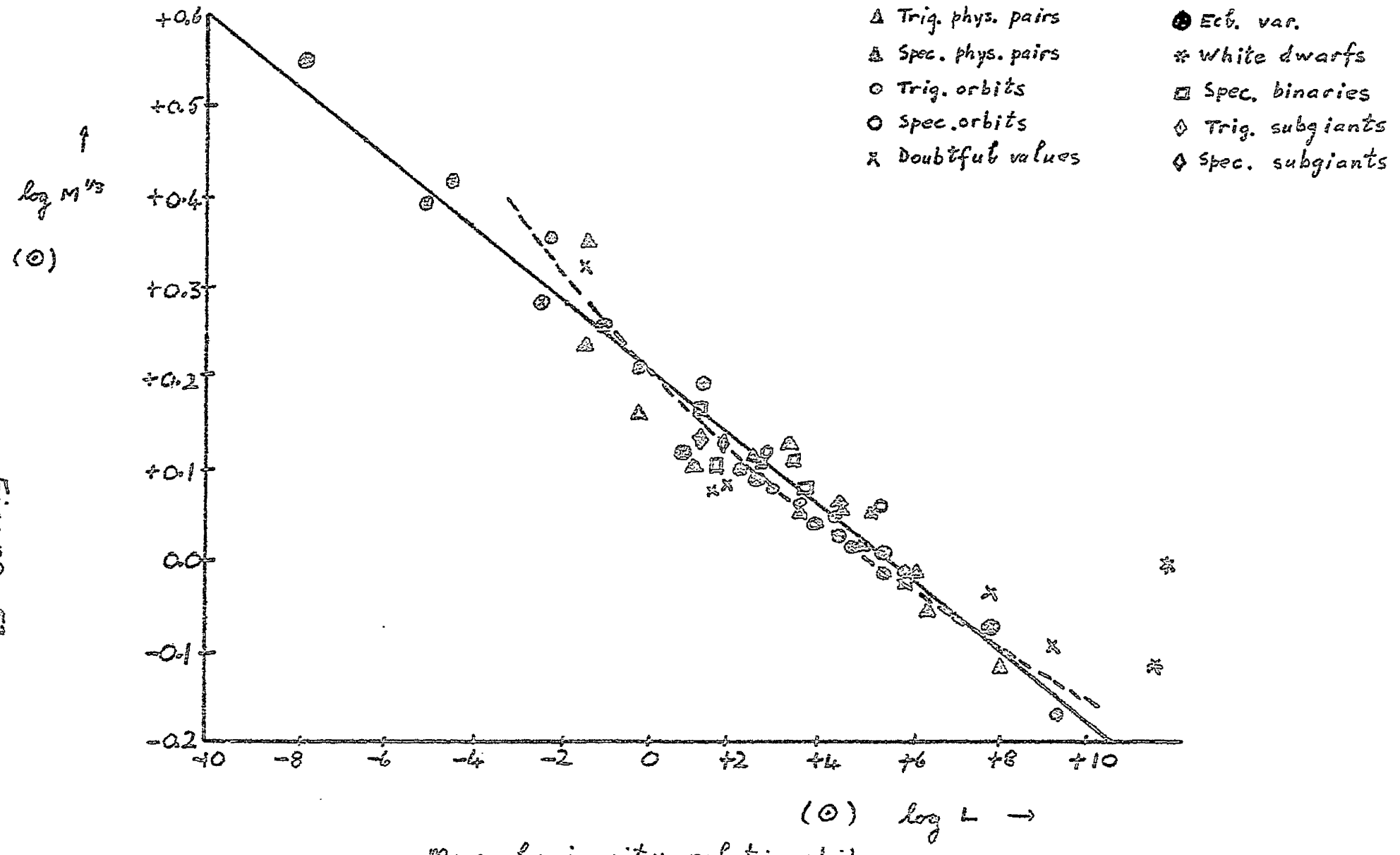

Figure 62

Mass-luminosity relationship

are quite likely to have calculated masses which are less than their actual masses. Figure 52, taken from the book by RUSSELL and MOORE, reveals an apparent discrepancy between EDDINGTON's theoretical mass/luminosity relationship, and the 'observed' relationship amongst more massive stars. The departure is consistent with the existence of a hitherto unsuspected spectroscopic reflection effect, but it must be admitted that the evidence is not very strong. A factor of about two may be involved.

If indeed the masses of O and B type stars are underestimated by a factor of two or so, some consequences of interest in stellar dynamics follow:-

It is well known that equipartition of energy exists amongst most Population I stars in the solar neighbourhood, the exception being stars of type O and B, which possess only about half the random energy of motion. (See table 8 , based upon the investigation by SEARES)

Spectral Type	Average Energy
B3	$1.95\ 10^{46}$
B8	1.62
A0	3.63
A2	3.72
F0	3.24
G0	4.07
K0	4.27
M0	3.55

TABLE 8

The time of relaxation of galactic stars is apparently about 10^{13} years, and a problem of stellar dynamics has been to find a mechanism which would give rise to a relaxation time greater than 10^{8} years and much less than 10^{10} years. The upper limit arises from the age of the Galaxy, the lower from the consideration that early-type stars with ages $< 10^{8}$ years have not yet attained equipartition of energy with other stars.

Given however, a doubling of the accepted masses of O and B stars, equipartition must exist amongst stars of all spectral type. The problem is then not to produce equipartition rapidly amongst existing stars, but rather to find a process which will give birth to stars, in groups in which equipartition of energy already exists.

A second consequence of the reflection effect is that the ages of early-type stars are at present overestimated. From the theoretical mass-luminosity (M-L) relationship, $L \propto M^{4}$. The age of an early-type star is $\tau \propto M/L \propto 1/M^{3}$. Thus a star of spectral class B, whose age has been previously taken as 5.10^{7} years, say, must now be taken to be $<10^{7}$ years. Some discrepancies between the expansion ages of AMBARTUSMIAN's stellar associations and their ages

deduced from $\tau \propto \frac{M}{L}$, may perhaps be resolved in this way. (For example 12 Lac and 16 Lac, members of the Lacerta association, have ages on the old scale an order of magnitude greater than that obtained from the expansion hypothesis: and similarly for 53 Ari, a member of the Orion association.)

The rate of conversion of interstellar material into stars is sensitive to the adopted masses. For O and B stars, the new turnover rate per star ($\propto \frac{1}{\tau}$) is about a factor 5-10 greater than the old rate, Thus the turnover rate per unit mass is a factor $\sim$ 10-20 greater than has been supposed, for early-type stars. The cycling of material between gas and the stars as a whole may consequently be significantly faster than was thought.

3. Masses of Close Binaries. It is amongst contact systems that gross deviations from the mass-luminosity relationship should appear to exist, due to reflection. Figure 53 is taken from KOPAL's 'Close Binary Systems', p. 494, and shows that large deviations indeed exist. In fact, if we ignore the W UMa systems, almost every contact component plotted in the figure is apparently under-massive.

(More massive stars appear, in the figure, to

approach the empirical M/L relationship more closely

But this may simply mean that the upper part of the relationship, derived exclusively from binaries for which no trigonometric parallaxes are available, is itself in error due to the reflection effect. There is thus some further slight evidence that the empirical mass-luminosity relationship underestimates the masses of the more luminous stars).

The R CMa stars, plotted in figure 53 , are remarkably under-massive for their spectra. The table below is taken from KOPAL's book.

Star	Period	Spectra	m_1	m_2
R CMa	1.136	F0+(gG9)	0.49	0.11
RW Gem	2.865	B5+F5	1.9	0.85
T LMi	3.020	A0+(gK0)	0.69	0.15
TU Mon	5.049	B5+A5	2.3	1.0
UU Oph	4.397	A0+(gG1)	0.84	0.24
XZ Sgr	3.276	A3+(gK1)	4.8	0.48
RZ Sct	15.190	B2+(F5)	0.47	0.20
S Vel	5.934	A5+K5	0.80	0.14

KOPAL states, of RZ Sct, that ' the mass of the primary component results as $m_1 = 0.42$; and that of the (F5) secondary, $m_2 = 0.20\ \odot$! The values of (radius

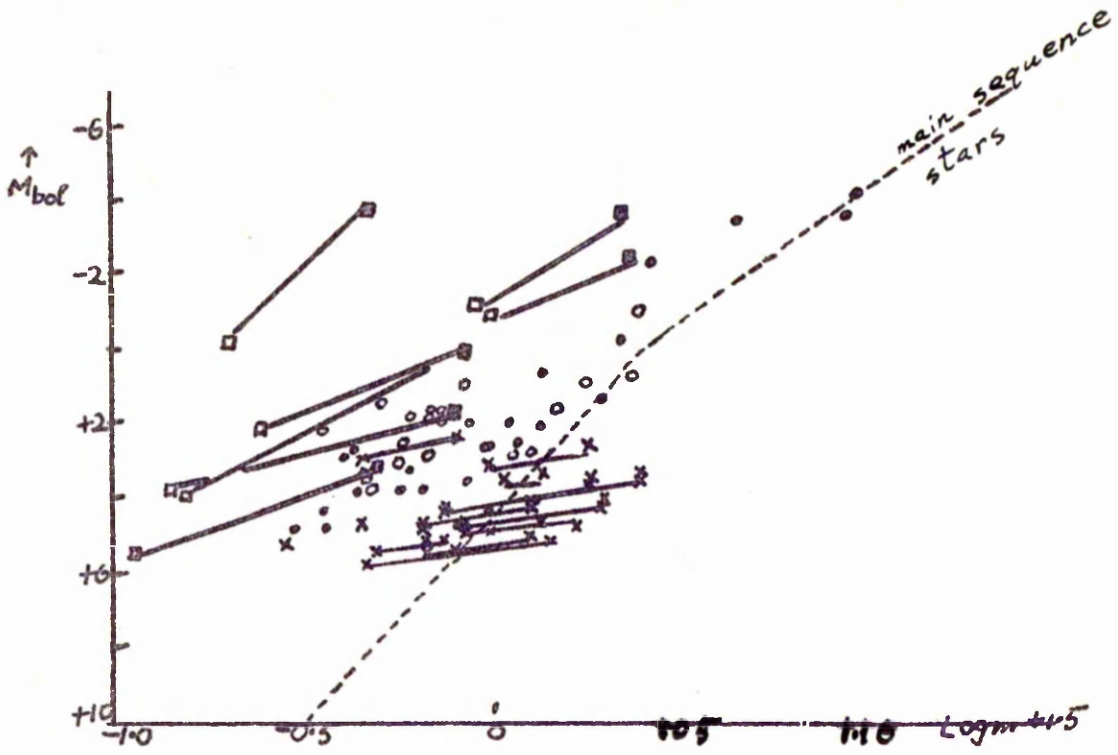

- secondary components at their Roche limits
- subgiant secondaries within their Roche limits
- primary components of R CMa systems
- secondary " " " "
- components of W UMa systems

Mass / luminosity diagram for components of contact binaries (after KOPAL)

Figure 53

and ~~mass~~ luminosity) are quite consistent with the B2 spectrum of RZ Set A, and would locate this star fairly well on the Main Sequence—the striking peculiarity is only the fact that the mass of this early B-star of -3.7 absolute bolometric magnitude appears to be less than one-half of that of the Sun !' He goes on to point out the severe energy difficulty involved, viz the maintenance of a high luminosity by such a small mass.

The explanation in terms of reflection is obvious. The relatively long period might seem to militate against this possibility in the case of RZ Set, but KOPAL points out later that R CMa stars appear to have rapid axial rotations. In particular, RZ Set A has an equatorial rotation speed of 50 km/sec., as against its (apparent !) orbital speed of 11 km/sec. Since $\rho = V_{eq} \bar{x}$, large reflection displacements might still result.

It is difficult to see why W UMa stars are apparently unaffected by the spectroscopic reflection effect.

4. Photometric Reflection. In the only paper devoted to the photometric reflection effect in one

system (Algol) it has been shown that an albedo of 0.5 is necessary to remove the discrepancy between theory and observation. (HOSOKAWA 1959).

A comparison between observed and theoretical reflection coefficients in thirty eclipsing binaries was made by HOSOKAWA (1959). A non-grey atmosphere was assumed. The author found that, for systems possessing a component of type earlier than B8, the observed luminous efficieney ratio E_2/E_1 was less than expected (suffix 2 referring to the cooler component). The theoretical expression for the reflection coefficient used by HOSOKAWA is due to RUSSELL and MERRILL† (1952). This expression was derived on the assumption that reflection from the penumbra is small; secondary reflection was overlooked by RUSSELL and MERRILL†; and they used series whose convergence is too slow to give accurate values for various coefficients.

The same general conclusion was reached by SOBIESKI, who solved the transfer equation for an irradiated atmosphere directly rather than by means of luminous efficiency factors (1965). Once more the bolometric theory used is unsatisfactory.

† Princeton Univ. Obs. Contrib. No. 26.

5. Observations of Close Binaries. It is clearly desirable to extend the empirical investigation of velocity curves (along the lines of that on 57 Cygni) to as many spectroscopic binary systems as possible.

Occasionally, spectroscopic binaries are observed with high eccentricities. As pointed out in chapter III, a pseudo-e will appear in a system if the axes of rotation and revolution are not parallel in space, and if there is an appreciable spectroscopic reflection effect. It would be of interest to examine whether the calculated eccentricities in such systems vary systematically from line to line. In this connection it should be noted that there exist binaries for which e, calculated from the photometric observations, is inconsistent with e derived from the velocity curve.

6. Observations of 57 Cygni Although the best curve through the ρ/λ diagram is a straight line, this line cannot continue indefinitely. A ρ/λ diagram extending over a wider range of wavelengths would presumably be represented by a non-linear curve

which might help in the interpretation of the diagram. For instance, measurement of even a single velocity curve short of the Balmer discontinuity (λ= 3684 Å) would be useful. A few high-resolution spectrograms at appropriate phases might be used to study the line profiles of the stronger lines. Absorption lines whose strength is different over the 'hot' and 'cold' hemispheres must appear asymmetrical at most phases.

The spread of the individual points about the mean velocity curve is rather large for NIII (figure 4) even considering the difficulty of measurement of the line. There is a suspicion of an intrinsic variability about the mean curve. This could be checked if sufficient high-dispersion spectrograms were available.

The reduction of the photometric observations of 57 Cygni will be of value in the interpretation of the phenomena occuring on the star. Evidence of a large reflection effect in the ultra-violet would tend to confirm the idea that non-thermal emission in this region gives rise, not only to the high excitation lines, but also to fluorescence and hence the ρ/λ diagram. Terms other than cos 2ϵ

in the light curves are probably not explicable as oblateness or reflection terms, and their occurrence would be of considerable interest.

7. Theory. (i) An understanding of the physics of line formation in a reflecting atmosphere is an outstanding requirement for the further development of the theory of the spectroscopic reflection effect. Line formation in a photosphere subject to incident radiation involves a theory of monochromatic reflection which became available for the parallel beam case in 1965. Absorption line formation in such simple conditions is insufficient to account for the observations of 57 Cygni, however. Further progress along these lines may have to await elucidation of the role of the chromosphere in line formation in early-type stars.

(ii) The work of HOSOKAWA and SOBIESKI should be repeated using the improved bolometric theory of chapter V. It is possible that the obs.-calc. discrepancies found in most systems examined by them will then disappear.

REFERENCES

Basic Papers

Bolometric Reflection Effect.

A.S.EDDINGTON	M.N. 86, 320, 1926
E.A.MILNE	M.N. 87, 43, 1926
H.K.SEN	Proc. U.S. Nat.Acad.Sci., 34, 311, 1948.
Z.KOPAL	M.N. 114, 101, 1954.

Photometric Reflection Effect

Y.HOSOKAWA	Sendai Astr.Reportoj, 52, 208, 1957
	ibid., 70, 207, 1959
S.SOBIESKI	Ap.J. Supp. No 109, 12, 263, 1965
	ibid., 109, 12, 276, 1965

Spectroscopic Reflection Effect

Z.KOPAL	Proc. Amer. Phil. Soc., 86, 351, 1954
M. KITAMURA	Pub. Astr. Soc. Japan, 5, 114, 1954
	ibid., 6, 217, 1954
A.H.BATTEN	M.N. 117, 521, 1957
M.W. OVENDEN	M.N. 126, 77, 1963.

Topics Subsidiary to the Reflection Effect

(i) The W(sp. Type) Data.

WILLIAMS	Ap.J. 83, 305, 1936
RUDNICK	Ap.J. 83, 433, 1936

(ii) Temperature Scale for Early-type Stars

KUIPER	Ap.J. 88, 429, 1938
KOPAL	Ann. D' Ap. 18, 379, 1955
UNDERHILL	Pub. D.A.O. x, 19, 1957
HARRISS	Basic Astronomical Data Vol III, (ed. by Strand), p. 263.
KOPYLOV	Astrophys. Obs. Crimea 30, 69, 1963
STROM	A.J. 69, 558, 1964